THE MECHANISM OF NEUROPATHY IN PERIPHERAL MYELIN PROTEIN 22 MUTANT MICE

Thesis submitted for the degree of Doctor of Philosophy in the Faculty of Science, University of London

ANDREA MARIE ROBERTSON

1999

Department of Clinical Neurosciences
Royal Free Campus
Royal Free and University College Medical School
University College London

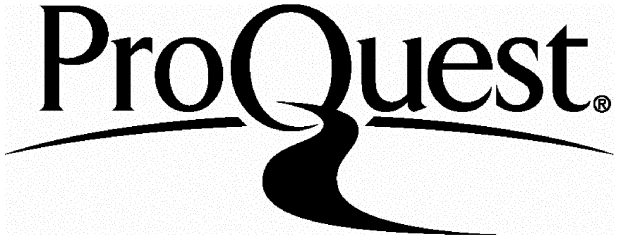

ABSTRACT

Mutations in the gene for peripheral myelin protein 22 (*PMP22*) are associated with peripheral neuropathy in mice and humans. PMP22 is produced mainly in Schwann cells in the peripheral nervous system where it is localised to compact myelin. The function of PMP22 is unclear but its low abundance makes it unlikely to be a structural myelin protein.

I have studied the peripheral nerves of two different mouse models with alterations in the *pmp22* gene. (1) The Trembler-J (Tr^J) mouse which has a point mutation [L16P] in the first transmembrane domain of PMP22. (2) *PMP22* overexpressing transgenic mice which have 7 (C22), 4 (C61) and 2 (C2) copies of the human *PMP22* gene in addition to the mouse *pmp22* gene.

In the nerves of adult Tr^J mice there was considerable evidence of abnormal Schwann cell-axon interactions. Abnormal features were reproduced in the early stages of regeneration following crush injury. This demonstrates that the abnormalities are a result of an intrinsic abnormality of Tr^J Schwann cells and not secondary changes related to demyelination. In the initial stages of postnatal development the number of axons that were singly ensheathed was the same in all the mutants examined, indicating that PMP22 does not function in the initial enclosure of groups of axons and subsequent separation of single axons. All strains examined had an increased proportion of fibres that were incompletely surrounded by Schwann cell cytoplasm indicating that this step is disrupted in PMP22 mutants. Increasing the number of copies of *PMP22* resulted in an increasing severity of phenotype. In C22 (7 copy) animals myelin formation was delayed or non-existent in many fibres whereas in C61 animals myelination initially appeared normal with abnormality appearing later in a small population of fibres. The C2 strain appeared relatively unaffected.

It is concluded that PMP22 functions in the initiation of myelination and most probably involves the ensheathment of the axon by the Schwann cell, and the extension of this cell along the axon. Abnormalities are most likely to result from defective interactions between the axon and the Schwann cell.

THESIS
WL 500
ROB

DECLARATION OF AUTHOR'S CONTRIBUTION

All the experimental work in this thesis was performed by the author. The majority of it has already been published.

ROBERTSON AM, HUXLEY C, KING RHM, THOMAS PK (1999) Development of early postnatal peripheral nerve abnormalities in Trembler-J and PMP22 transgenic mice. *Journal of Anatomy (in press)*

HUXLEY C, PASSAGE E, ROBERTSON AM, YOUL B, HUSTON S, MANSON A, SABERRAN-DJONIEDI S, FIGARELLA-BRANGER D, PELLISSIER JF, THOMAS PK, FONTES M (1998) Correlation between varying levels of PMP22 expression and the degree of demyelination and reduction in nerve conduction velocity in transgenic mice. *Human Molecular Genetics* 7, 449-458.

ROBERTSON AM, KING RHM, MUDDLE JR, THOMAS PK (1997) Abnormal Schwann cell/axon interactions in the Trembler-J mouse. *Journal of Anatomy* **190**, 423-432.

ROBERTSON AM, THOMAS PK (1997) Peripheral nerve response to crush injury in the Trembler-J mouse (Abstract) *Journal of Neurology* **244** (suppl 3):S140. (*Manuscript for a paper is in preparation*)

ACKNOWLEDGEMENTS

I would like to express my gratitude to Professor P.K. Thomas and Dr Rosalind King for their supervision and enthusiasm. I owe a great measure of thanks to them for the training, expert advice and support I have received over the last few years.

My special thanks go to Dr Clare Huxley for her collaboration; access to her transgenic animals and help with the mRNA techniques have added considerably to the depth of this thesis.

I appreciate the opportunity to work in this exciting field and would like to thank Prof A.H.V Schapira for allowing me to work his department and for the use of his facilities.

I would like to express my gratitude to other members of the department, both past and present, for their assistance, encouragement and discussion. Particular thanks go to John Muddle for the time he dedicated to writing programs specifically designed for this project and also to Michelle, Jane, Mei, Sophia and Peter for their day to day support in the lab.

The Trembler-J mice were maintained and bred in the CBU under the expert husbandry of Gavin Green whose help and sense of humour were much appreciated.

I would also like to thank my parents and other members of my family for their encouragement throughout my studies. Finally my thanks to Jonathan for his encouragement and patience throughout the 'writing up' period.

The financial support of the Wellcome and the Attenborough Trusts is greatly appreciated.

CONTENTS

INTRODUCTION

Chapter 2 Peripheral myelin protein 22 (PMP22)

Chapter 3 Genetically engineered PMP22 alterations

Chapter 4 Mutations affecting the human *PMP22* gene

MATERIALS AND METHODS

Chapter 6 Materials and Methods

RESULTS

Chapter 7 Results

List of Tables

List of Figures

Chapter 1 Trembler, Trembler-J and the new Trembler mice

1.1 DISCOVERY

The Trembler mouse. The Trembler (*Tr*) mutant first appeared in Falconer's colony in Edinburgh in 1946 (Falconer 1951). He reported a dominant gene producing spastic paralysis with convulsions in the young and generalised tremor in the adult. Braverman investigated the *Tr* mutant as a possible mouse model of neurological disorders (Braverman 1953). Examination of acetyl choline function in both the central and peripheral nervous systems, parathyroid function, electrocorticograms and histology of the CNS failed to find any explanation for the tremor. Peripheral nervous system abnormalities were not noted until 20 years later when Ayers and Anderson (1973) described hypomyelinated sciatic nerves and denervated skeletal muscle. Retarded myelin development and early onion bulb development in young animals are followed by hypomyelination, demyelination and well developed onion bulbs in adults.

The Trembler-J mouse. An independently occurring mutation was found in a colony of C57BL/6J mice in the Jackson Laboratory (Sidman et al. 1979). Using genetic, behavioural and morphological criteria Sidman et al (1979) judged it to be a mutation at the trembler locus and termed it Trembler-J (Tr^J). There has been very little literature published on the Tr^J mutation. It has been generally assumed to be an essentially similar but milder version of the *Tr* disorder. The literature presented here relates largely to the *Tr* model and is assumed also to apply generally to the Tr^J mutation. Investigations conducted specifically on the Tr^J mutation will be reviewed separately.

The new Trembler mutant. A spontaneous neurological mutant has recently been reported in a normal colony of an inbred strain of the gracile axonal dystrophy mouse (GAD/Ncnp) at the National Institute of Neuroscience, Japan (Suh et al. 1997). The most notable pathological feature of the new Trembler mutant (*Tr-Ncnp*) was the formation of giant vacuoles in the Schwann cell cytoplasm of sciatic nerves of homozygous animals. The Schwann cells of homozygotes failed to form myelin at any stage. Heterozygous animals showed normal myelination during the early postnatal stages, followed by segmental demyelination.

1.2 CLINICAL FEATURES

The Trembler mouse. The clinical features of the *Tr* mouse have been described by a number of investigators (Falconer 1951; Ayers & Anderson 1973; Henry et al. 1983). Affected animals develop an action tremor, 'convulsions', and a gait abnormality between postnatal days 10 to 14 (P10-P14). The tremor, which persists throughout the life of the animal is rapid and generalised, most obvious in the head and neck and disappears when the animal is at rest. Convulsions are reported as being frequent initially and easily induced by sensory stimuli. As the animals get older 'seizures' become less frequent and more difficult to evoke, usually ceasing completely by P40-P45 (Ayers & Anderson 1973).

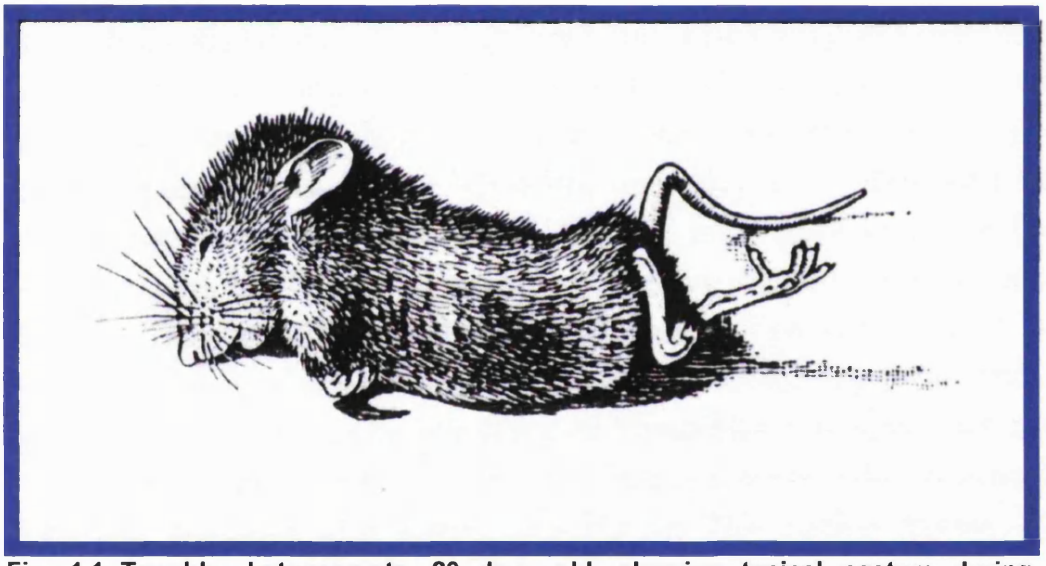

Fig. 1.1 Trembler heterozygote, 20 days old, showing typical posture during a convulsion. Drawn by Mr E.D. Roberts from a photograph. (Taken from Falconer 1951)

These 'convulsions' were later shown to represent neuromyotonia of peripheral nerve origin which appears to be related to PMP22 dosage (Toyka et al. 1997a). From an early age the limbs of *Tr* animals are held extended, making their gait awkward. When passively extended and flexed the joints are mobile but the limbs are weak (Henry et al. 1983). The gait abnormality consisted of extension at the knees and ankles and circumduction of the hind limbs at the hips (Henry et al. 1983). The original report by Falconer (Falconer 1951) of a non-progressive disorder has subsequently been disputed by Henry et al (1983) who described a gait abnormality that worsened throughout the lifespan of the animal.

When affected/affected and affected/normal *Tr* animals were mated (Henry et al. 1983; Falconer 1951) all animals could be designated as either affected or normal by P20. This was considered to indicate a dominant inheritance pattern (Falconer 1951). Animals homozygous for the *Tr* allele (gene symbol *Tr/Tr)* were behaviourally indistinguishable from heterozygous (*Tr /+)* animals (Henry & Sidman 1988). The oldest *Tr/Tr* mice examined appeared healthy at 1 year of age, although some *Tr/Tr* mice developed a more severe quadriparesis than was seen in *Tr/+* animals.

The Trembler-J mouse. Affected/normal matings of Tr^J animals yielded two distinct classes of progeny, normal and mildly affected. The mildly affected (putative Tr^J /+) were not distinguishable from their litter mates until P20-P25 in contrast to *Tr* mice which were identifiable by P20. They had a tremor with a smaller amplitude than *Tr*, no obvious seizures and a milder although similar gait abnormality that progressed only slightly with age (Henry et al. 1983). In contrast to *Tr* mice, affected/affected matings in the Tr^J produced three classes of progeny. In addition to normal and mildly affected animals one animal from each mating was severely affected. These animals were first distinguished by P5-P8 because they had grown much less than their litter mates. By P10 they had developed severely dystonic ineffective movements and were very poor in righting themselves and seemed certain to die before weaning. Such severely affected animals were presumed to be Tr^J homozygotes, Tr^J/Tr^J. On this basis Tr^J has been classified as a semidominant disorder.

The new Trembler mutant. The affected animals had a gait abnormality which appeared at P15-20 and progressed slightly with age. This was followed by motor and sensory ataxia, which remained throughout the life of the animal (Suh et al. 1997). Most animals survived for more than 1 year. Offspring of normal/affected matings were symptomatically indistinguishable from those from affected/affected matings. The segregation patterns of the *Tr-Ncnp* allele were followed by Southern blot analysis and could best be explained by simple autosomal dominant inheritance (Suh et al. 1997).

1.3 NORMAL DEVELOPMENT

The process of myelination has been described both qualitatively and quantitatively in a range of animal species including chicken (Geren 1954) and rat (Friede & Samorajski 1968; Peters & Muir 1959; Webster 1971; Fraher 1972). It has been divided into three phases.

Premyelination. The growth of small fetal fibres and the movement of these larger fibres to the periphery of each group (Friede & Samorajski 1968).

Fetal fibres can be identified by three features. They are small, arranged in bundles without intervening structures and are wrapped in a single, thin layer of Schwann cell cytoplasm

which often extends as long narrow processes between groups of fibres. In the rat, bundles of fetal fibres are most numerous during the first 2 weeks of life. Their number progressively decreased and by the fourth week they could no longer be found. A typical basement membrane surrounded the outer surface of each Schwann cell. Only axons at the periphery made contact with the Schwann cell plasma membrane, and none were completely enclosed by Schwann cell processes. As larger fibres appeared Schwann cell processes began to invade the central core of the axons (Peters & Muir 1959). Schwann cell processes then separated axons into large bundles that were subsequently subdivided as the Schwann cells multiplied rapidly.

Promyelination. Isolation of the enlarged fibres by individual Schwann cells

Promyelinated or intermediate myelinated fibres are thought to represent a transitional stage between the fetal and myelin forming fibres (Geren 1954; Friede & Samorajski 1968). Friede and Samorajski (1968) stated that promyelinated fibres differ from the fetal fibres in the large size of their axons and by the separation of axons from the fetal bundle into a 1:1 relationship with a Schwann cell (Friede & Samorajski 1968).

As the myelination process progresses these larger axons became more commonly found at the edge of the axon bundles. This suggests that axons destined to become myelinated are radially sorted within the longitudinal columns axons and Schwann cells (Webster et al. 1973). The sorting sequence involves axons to be myelinated being separated from the others by a thin layer of Schwann cell cytoplasm. The establishment of a 1:1 relationship with a single Schwann cell at the outer edge of the bundle occurs as Schwann cells divide. These daughter Schwann cells then become isolated from the family sheath before myelination begins (Webster et al. 1973). Promyelin fibres are present in great numbers during the first week of life in the rat, but diminish with progressive myelination (Friede & Samorajski 1968).

Myelination. The spiral growth and subsequent compaction of the Schwann cell around the axon to form a myelin sheath.

A flattened Schwann cell sheet becomes spiralled around the axon, the intervening extracellular space and the adjoining Schwann cell plasma membranes being referred to as the mesaxon. By obliteration of the cytoplasm and apposition of the cytoplasmic surfaces of the Schwann cell plasma membrane, the major dense line of myelin is formed. Further growth of the myelin sheet and apposition of the spiral layers occurs as the myelin sheath matures. The number of myelin lamellae present in the sheath rarely differs by more than two turns from the total number of rotations achieved by the Schwann cell (Low 1976a). Fibres containing more than two complete turns of the mesaxon without fusion and

formation of a myelin lamella are rarely seen (Friede & Samorajski 1968). It has been agreed that the Schwann cell, or part of its surface moves around the axon during the growth of the myelin spiral (Webster 1993). As the direction of rotation of the myelin spiral may not be the same between adjacent internodes, myelination cannot be the result of axonal rotation.

In terms of function the three most important dimensions of a myelinated nerve fibre are the axon diameter, and the thickness and length of the myelin segments. Generally elongation of myelin internodes parallels growth of that body part that contains the nerve fibres (Vizoso & Young 1948; Thomas 1955; Schlaepfer & Myers 1973). Although longer myelin sheaths are usually thicker and surround larger axons in mature nerves, developmental increases in axon calibre and myelin sheath thickness vary and do not necessarily parallel body growth throughout the peripheral nervous system. When axon diameters and myelin sheath thickness in motor and sensory fibres were compared, different growth patterns were found (Williams & Wendell-Smith 1971b). During myelination in the rabbit, myelin sheaths surrounding motor axons (nerve to the medial gastrocnemius) were thicker at each time interval (birth to 8 weeks) than those surrounding sensory axons (sural nerve). Many studies have shown that in most fibres up to a certain size, axon calibre, myelin sheath thickness and internodal length are related after growth patterns are established (Williams & Wendell-Smith 1971b; Hahn et al. 1987; Fraher 1978a; Fraher 1978b; Carlstedt 1980; Fraher et al. 1988). The minimum diameter of axons that Schwann cells began myelinating is thought to be about 1 μm (Duncan 1934; Matthews 1968). Axon diameter is not a major determinant of the onset of myelination, the sheath growth rate (in thickness or length) or the final area of compact myelin. The first fibres to be myelinated become the largest fibres in nerves with a bimodal distribution of fibres size (Williams & Wendell-Smith 1971b).

1.4 DEVELOPMENT OF MORPHOLOGICAL ABNORMALITIES

Postnatal days 3 to 7.

The Trembler mouse. As early as P3 abnormalities in *Tr* sciatic nerve were already becoming apparent. The process of myelin initiation appeared retarded and the small amount of myelin that had been formed was very thin. The abnormalities present at this early stage of development persisted into adult life. Despite having the same number of singly ensheathed axons as control animals (Ayers & Anderson 1976) there was a relative increase in the number of promyelinated fibres (Low 1976a; Ayers & Anderson 1975; Ayers & Anderson 1976) and a decreased number of myelinated fibres in *Tr* nerves (Ayers & Anderson 1976). Axons in *Tr* nerves were smaller than those in controls at all ages examined suggesting a delayed or slow axon growth rate (Ayers & Anderson 1976). Ayers and

Anderson (1975,1976) considered that the segregation of fetal fibres to promyelinated fibres in *Tr* sciatic nerve was delayed but this result was not supported by studies of other investigators (Low 1976a).

The number of myelinated fibres present in *Tr* nerves were decreased and where myelin is present it is very thin relative to the size of the axon (Ayers & Anderson 1975; Ayers & Anderson 1976; Low 1976a). The few larger myelinated fibres that are normally present in control nerves at P3 are absent from *Tr* nerve (Ayers & Anderson 1976). In most teased fibres from *Tr* nerve myelin was virtually absent and discontinuous along the length of the fibre. Nodes of Ranvier were not discernible and supernumerary Schwann cells were common (Low 1976a). Compact myelin formation was often incomplete and *Tr* animals could be identified from P2 onwards by the presence of large uncompacted spirals of Schwann cell membrane (Low 1976a; Ayers & Anderson 1975). In longitudinal section the nodes of Ranvier were frequently widened and covered only by a thin layer of Schwann cell cytoplasm or basement membrane (Ayers & Anderson 1975). In some instances axons were seen which were only partially covered by Schwann cell cytoplasm or basement membrane (Ayers & Anderson 1975). Some completely bare fibres were also seen (Ayers & Anderson 1975). Some internodes exhibited compaction only in the central region (Ayers & Anderson 1975). Schwann cells in the *Tr* mouse showed a high incidence of myelin degeneration products and in *Tr* nerves as early as P6 the number of Schwann cell nuclei was already increased relative to normal and Schwann cells were occasionally seen without axons (Ayers & Anderson 1976).

Postnatal day 7 to21.

The Trembler mouse. Although axon diameter had increased and myelin formation had progressed in *Tr* nerves, many myelin sheaths showed breakdown products (Ayers & Anderson 1975). Segmental demyelination was prominent and myelin sheaths were often uncompacted near the nodes of Ranvier (Ayers & Anderson 1973; Ayers & Anderson 1975). Myelin degeneration products were present within the Schwann cells, particularly in animals younger than one month, suggesting active demyelination in these nerves (Ayers & Anderson 1975; Ayers & Anderson 1976; Aguayo et al 1977, Bosse et al. 1994). Low (1976a) reported that between 7 and 14 days of age 3-5% of fibres were undergoing degeneration.

Some myelin appeared structurally normal but when examined at the ultrastructural level it was commonly only partially compacted or undergoing degeneration. Many axons were surrounded by large whorls of uncompacted Schwann cell cytoplasm which extended for the

length of the internode (Ayers & Anderson 1973). Schwann cells were retracted from the nodes of Ranvier and the normal interdigitation seen in control animals of this age was lacking (Ayers & Anderson 1975). Occasionally accumulations of degenerate mitochondria and membranous bodies were found within the axon localised at or near the nodes of Ranvier (Ayers & Anderson 1973). The fibre diameter spectrum from proximal, middle and distal levels of the sciatic nerve was examined and no difference was found between levels (Ayers & Anderson 1976). The number and size of cells in the dorsal root ganglia and spinal horn were normal in *Tr* mice younger than P23 (Ayers & Anderson 1976).

Many Schwann cells in developing *Tr* nerve appeared reactive (Ayers & Anderson 1975). The volume of cytoplasm and cytoplasmic organelle content was increased and frequently contained myelin debris. It has been suggested that the Schwann cells become reactive in the presence of myelin debris and undergo hypertrophy and hyperplasia resulting in the digestion of myelin debris and remyelination (Ayers & Anderson 1975). There was an increasing tendency for some axons to be surrounded by collapsed basement membrane, indicating that as Schwann cells become reactive they extended cytoplasmic processes and then withdrew them (Ayers & Anderson 1975). It was observed that Schwann cell cytoplasm extended into looped processes, and nuclei often appear lobed and show abnormal surface indentations similar to those observed in mild crush injury. The number of Schwann cell nuclei was increased and occasionally Schwann cells were not associated with axons (Ayers & Anderson 1975). Mitosis of Schwann cell nuclei was occasionally noted.

Fibroblasts were commonly found and the perineurium showed an increase in thickness (Ayers & Anderson 1973).

The Trembler-J mouse. Notterpeck et al (1997) examined the sciatic nerves of developing Tr^{J} animals and found that at P10 the histological appearance of normal and Tr^{J}/+ nerves was similar. However fibre measurement showed a difference in g ratio (+/+ = 0.47, Tr^{J} /+= 0.55) and a reduction in axon diameters in Tr^{J} animals (Notterpek et al. 1997). The number of Schwann cell nuclei was already increased by approximately 2 fold and there was an increased amount of extracellular connective tissue. A low frequency of fibres with abnormally thick myelin (tomacula) were seen along with myelin fragmentation indicative of active myelin breakdown.

Third postnatal week onward.

The Trembler mouse. From the third postnatal week onward in *Tr* mice there was an increasing incidence of abnormality. Large numbers of axons were covered only by basement membrane or by a thin rim of Schwann cell cytoplasm without myelin (Ayers & Anderson 1975). There was often a partial or complete additional layer of basement

membrane (Ayers & Anderson 1975). By 6 weeks of age onion bulb formation had begun (Ayers & Anderson 1976). Although a few fibres possess a normal myelin sheath most sheaths were very thin relative to axon diameter (Ayers & Anderson 1975).

1.5 MORPHOLOGICAL ABNORMALITIES IN ADULT MICE

The Trembler mouse. In adult Trembler nerves the majority of axons had no myelin with most fibres being surrounded by only 2-3 turns of uncompacted Schwann cell membrane (Ayers & Anderson 1973). There were fewer turns of myelin in *Tr* mice than in control mice at all ages and the myelin deficiency had become more pronounced with age (Low 1976a). In elderly *Tr* animals larger axons were associated with fewer myelin lamellae than smaller ones (Low 1976a). The myelinated fibre density in *Tr* animals always fell below control values (Henry et al. 1983; Low 1976b). Fibres that showed more advanced myelination often showed bizarre deformations and the internal and external mesaxons were often very complex (Ayers & Anderson 1973). In longitudinal section long lengths of axon were completely devoid of myelin (Ayers & Anderson 1973; Low 1976a). Approaching the node of Ranvier myelin often became uncompacted and looped. Uncompacted myelin was also found at random places along the internode. The total number of axons was normal in *Tr* nerves (Aguayo et al. 1977) but axonal area was decreased (Low 1976a; Ayers & Anderson 1976). The nerves of *Tr* animals had increased endoneurial and perineurial connective tissue (Henry et al. 1983; Ayers & Anderson 1973) when compared with controls yet the fascicular area was decreased (Henry et al. 1983). This was ascribed to a decrease in the volume usually occupied by myelin sheaths.

The mean Schwann cell density was increased in *Tr* nerves at all ages examined (Ayers & Anderson 1973; Low 1976a; Henry et al. 1983) and continued increasing throughout the animals' lifespan (Perkins et al. 1981b). The sciatic nerve of an adult *Tr* mouse contained 8.7 times more nuclei than controls (Low 1976b). Schwann cell cytoplasm often contained myelin debris (Ayers & Anderson 1973; Low 1976a; Henry et al. 1983). In longitudinal sections Schwann cell nuclei were seen more frequently than in control nerves indicating shortened internodes and not infrequently Schwann cell nuclei were situated within the node of Ranvier (Low 1976a; Low 1976b). *Tr* nerves of all ages contained more promyelin fibres than were found in control nerves (Henry et al. 1983).

In older *Tr* animals many fibres were surrounded by concentric layers of Schwann cell processes or basement membranes suggestive of ongoing cycles of de/remyelination (Ayers & Anderson 1973; Ayers & Anderson 1975; Low 1976a; Low 1976b; Low 1977). The evolution of 'onion bulb' formations in the *Tr* mouse was examined by Low (1977) who described the sequence of events leading to their formation. Following demyelination, which

was prominent between P7 and P28, Schwann cells divide. One Schwann cell surrounds the axon and begins remyelination while the supernumerary Schwann cell produced many processes which were confined within the limit of the original basement membrane. The processes initially appeared normal but the cytoplasm degenerated leaving behind empty membrane configurations. As more 'onion bulb' lamellae were added the outer lamellae became more degenerate than the central ones. 'Onion bulb' formations have been defined as myelinated or demyelinated axons surrounded by concentric arrays of Schwann cell processes or empty membrane configurations (Low 1977). They are thought to be produced by repeated cycles of demyelination and remyelination (Thomas & Lascelles 1967; Prineas 1971; Dyck 1975; Low 1977).

Anterior and posterior roots also showed hypomyelination and onion bulb formation with cytoplasmic extensions of Schwann cell cytoplasm being more pronounced and basement membrane deposition being less extensive than in the sciatic nerve (Ayers & Anderson 1973). Very thinly myelinated fibres were also found in the lumbosacral plexus and posterior roots, median nerve, posterior tibial nerve and the tail. There was also a relatively abrupt change from the severely hypomyelinated dorsal roots to well myelinated dorsal columns (Low 1976b). Dorsal ganglion cells appeared normal and their density and diameter distribution was found to be the same in *Tr* and control animals. The number of motor neurons in the ventral horn did not differ from that found in controls (Low 1976b).

Henry and Sidman (1988) examined the nerves of putative *Tr/Tr* animals and found that they have virtually no myelin in their PNS. In the sciatic nerves from *Tr/+* animals 28% of appropriately sized axons were surrounded by thin myelin (Henry & Sidman 1988). In contrast the nerves of *Tr/Tr* animals had at most 6 myelinated fibres. Fibres in both genotypes appeared to be blocked at the promyelin stage.

The Trembler-J mouse. The sciatic and vagus nerves of Tr^J mice showed a myelin deficiency that was milder than that seen in the nerves from similarly aged *Tr* animals. By P16 nearly all appropriately sized fibres had at least a thin myelin sheath. In contrast to *Tr* animals, where very large fibres were commonly unmyelinated, a thin myelin sheath was found on virtually all fibres in older Tr^J animals (Henry et al. 1983). The findings of thin myelin, small axons, increased extracellular matrix and increased number of Schwann cells have been confirmed in a recent study by Notterpek et al (1997).

The concentration of Schwann cells and fibroblasts was increased in nerves from Tr^J animals, but the increase in the amount of interstitial connective tissue was less than in *Tr* animals. Cervical sympathetic trunks appeared normal (Henry et al. 1983). There were virtually no onion bulbs in Tr^J animals.

The sciatic and vagus nerves of Tr^J/Tr^J homozygotes were also examined by Henry et al (1983). Tr^J/Tr^J animals had a very severe deficiency of peripheral myelination. Only a few dozen myelinated fibres were present in nerves which normally would have contained thousands. The abnormalities were qualitatively similar to each other and to the nerves of young *Tr* animals although they were much more pervasive in the nerves from putative Tr^J / Tr^J animals.

The new Trembler mutant Hypomyelination was obvious in the peripheral nervous system of both the hind and forelegs and the distal segments of the trigeminal nerves of the *Tr-Ncnp* mutants. Pathological alterations were not detected in the CNS.

***Tr-Ncnp/Tr-Ncnp* mice.** Nerves from homozygote *Tr-Ncnp/Tr-Ncnp* mice were completely devoid of myelin at all ages from P9 to 5 mo. Axons appeared to be at the promyelin stage (ensheathed but not myelinated). Electron microscope studies showed many swollen vacuolar structures of various sizes. These were located near the Golgi apparatus but were generated mostly from the swelling of rough endoplasmic reticulum in the Schwann cells and not from the Golgi apparatus. The vesicles localising around the stacks of the Golgi cisternae were empty inside and smaller than those derived from the endoplasmic reticulum. Occasionally Schwann cells with a dark nucleus and developed Golgi apparatus had a large population of free ribosomes (Suh et al. 1997). The collagen fibrils in the homozygous animals were less abundant in the intercellular spaces compared with heterozygotes. The sciatic nerve contained a number of pyknotic Schwann cell nuclei which stained darker than those in the normal mice. In adult homozygous mice apoptotic cells (detected by a variation of the TUNEL method) were sparsely distributed across the sciatic nerve and represented 7.9% of cell nuclei. In normal nerve no positive cells were seen.

***Tr-Ncnp/+* mice.** In the heterozygote, segmental demyelination was seen and the degree of myelination was variable even within a single internode. The compaction of myelin appeared normal. Collagen density was increased and basal lamina was seen irregularly surrounding the axons. The Schwann cells had a dark cytoplasm that contained a number of free polyribosomes, Golgi apparatus and mitochondria. The vacuoles in the Schwann cells were not as obvious as those in the homozygotes. Fragmented basal lamina surrounded the axons (Suh et al. 1997).

1.6 UNMYELINATED FIBRES

The Trembler mouse. The morphology of unmyelinated fibres is reported as being normal in the cervical sympathetic trunk and in the sciatic nerve of *Tr* mice (Ayers & Anderson 1973; Perkins et al. 1981b; Henry et al. 1983). Unmyelinated fibre density and size distribution in *Tr* sciatic nerves did not differ from that of controls (Low 1976a). In animals injected with [^{3}H] thymidine, which labels actively dividing cells, no labelled Schwann cells were found in unmyelinated fibres. (Perkins et al. 1981b). In unmyelinated nerves, such as the cervical sympathetic trunk (CST), the total number of Schwann cell nuclei in cross section was not significantly different from that found in controls (Perkins et al. 1981b). When phenotypically normal Schwann cells from the CST are transplanted into the sural nerve of normal animals they show typical *Tr* morphology (Perkins et al. 1981a) suggesting that the *Tr* mutation only affects Schwann cells when they are challenged to myelinate.

The Trembler-J mouse. In both homozygous and heterozygous Tr^J the cervical sympathetic trunk was ultrastructurally normal with the exception that small numbers of larger myelinated fibres normally present in control animals were in the promyelin state in Tr^J animals (Henry et al. 1983).

1.7 CONDUCTION VELOCITIES.

Electrophysiological studies were undertaken on the sciatic nerve, median nerve and the dorsal nerve of the tail in *Tr* and control mice by Low and McLeod (1975). The amplitude of the evoked muscle action potential, terminal latency and motor conduction velocity (MCV) recorded from the sciatic, median and dorsal nerve of the tail of the *Tr* mice fell outside the control range in every case. The distal motor latencies of in all nerves of the *Tr* mice were increased and the MCVs were less than 10m/s. In control mice the MCV increases with age until 4 months but the MCV in *Tr* mice was less than 10m/s as early as P6 and did not increase with age (Low & McLeod 1975).

1.8 FAST AXOPLASMIC TRANSPORT .

Fast axoplasmic transport was measured in *Tr* sciatic nerves after the injection of [^{3}H] leucine into the lumbosacral spinal cord region by Boegman et al (1977). There was no difference in the measurements from *Tr* and control animals, indicating that axoplasmic flow is unaffected by demyelination (Boegman et al. 1977).

1.9 SCHWANN CELL PROLIFERATION

During rodent ontogenesis, Schwann cells in peripheral nerves migrate along the axons and begin the process of ensheathment (Peters & Muir 1959; Speidel 1964). Schwann cells then divide intensely from the end of gestation until the first days of postnatal development (Peters & Muir 1959; Asbury 1967; Terry et al. 1974). The high rate of Schwann cell proliferation decreases and rapidly stops totally during the process of myelination (Peters & Muir 1959; Asbury 1967).

The Trembler mouse. Perkins et al (1981b) found abnormal persistence of postnatal Schwann cell proliferation in nerves of the *Tr* mouse. Schwann cell populations were greater in *Tr* than control nerves at all ages studied. Cross sections of L4 ventral roots at P10 contained twice as many Schwann cell nuclei in *Tr* than in controls. The difference increased to five fold by the time *Tr* animals were one month old and increased again to ten fold at 4 months of age. Beyond this time their numbers remained stable suggesting that additions to the Schwann cell population by mitotic division were balanced by losses due to Schwann cell death.

The density of Schwann cell nuclei in control animals nuclei decreased gradually from 1 Schwann cell /10 axons at P3 to 1/35 axons at P300. The fall in density in control animals corresponded to the elongation of the internodes. In *Tr* nerve the number of Schwann cells increased regularly from day 4 to day 300. Taking changes in body length in account Koenig et al (1991) calculated that the mean axonal length covered by a Schwann cell would decrease by a factor of three between P6 and P60 (Koenig et al. 1991).

When unmyelinated nerve segments of normal appearance from *Tr* mice are transplanted into myelinated nerves of unaffected animals, the regenerated grafts show characteristic *Tr* abnormalities of Schwann cell multiplication and myelination (Perkins et al. 1981a). As persistent Schwann cell multiplication was not seen in the intact unmyelinated nerves of *Tr* mice, but develops in the segments that form myelin, the authors postulated that the proliferative abnormality of *Tr* Schwann cells was related to the disorder of myelination but was probably not a primary manifestation of the disorder.

The Trembler-J mouse. In young animals the number of Schwann cells in the peroneal nerve were similar in *Tr/?*, +/+, Tr^J/+, and Tr^J / Tr^J animals (Henry et al. 1983). Schwann cell numbers tended to decline in older Tr^J animals but not in *Tr*.

1.10 IDENTIFICATION OF A PRIMARY SCHWANN CELL LESION IN THE TREMBLER MOUSE

In normal nerve axons influence Schwann cell proliferation (Wood & Bunge 1975; Aguayo et al. 1976c) and myelin formation (Friede & Samorajski 1967; Aguayo et al. 1976a; Aguayo et al. 1976b; Weinberg & Spencer 1976). The interdependence of Schwann cell and axon has led to suggestions that in certain neuropathies an axon abnormality may be responsible for the failure of the Schwann cell to maintain myelin.

Several authors have postulated that the *Tr* mutation results from a primary lesion of the Schwann cell. Ayers and Anderson (1975) considered that the presence of axons with normal morphology suggested a primary Schwann cell change. On the basis of several pieces of evidence Low (1976a) also concluded that primary Schwann cell alteration was the most likely. (1) Cell bodies in *Tr* animals are normal in appearance and numbers. (2) Normal fine structure of axons persists well into adulthood whereas hypomyelination and demyelination commence at an early stage in development. (3) A relatively abrupt transition from severely hypomyelinated anterior and posterior roots to well-myelinated central fibres when axons pass from the Schwann cell domain into the oligodendrocyte domain. (4) The middle and distal levels of *Tr* nerve are similarly affected (Ayers & Anderson 1976; Low 1976a).

1.11 NERVE GRAFT EXPERIMENTS IN THE TREMBLER MOUSE

Aguayo confirmed the *Tr* mutation as being a primary lesion of the Schwann cell in an elegant series of nerve grafting experiments (Aguayo et al. 1977). These consisted of transplanting segments of donor sciatic nerve into the midthigh of recipient animals. Schwann cells which originated from the donor nerve ensheath and myelinate axons arising from nerve cells of the host. Aguayo's experiments consisted of one of three graft paradigms, Normal to normal (N-N-N), Trembler to normal (N-T-N), and normal to Trembler (T-N-T). In all experiments, as regenerating axons grew into the grafts the morphological features of the donor nerve were fully reproduced by the donor Schwann cells. In N-T-N regenerated nerves, the widespread hypomyelination and absence of myelin, which are hallmarks of the *Tr* neuropathy, were duplicated in the grafts and contrasted abruptly with the normal myelin in the recipient nerve. Both the percentage of single axons with diameters greater than 1μm that were surrounded by Schwann cells without myelin and the myelin lamellae/axonal circumference ratios were normal for regenerated nerves in the N-N-N experiments and in the proximal and distal stumps of the N-T-N nerves. In the grafted segments of the N-T-N nerves the proportion of fibres with no myelin was markedly increased, and myelin lamellae/axonal circumference ratios were only one third of those in

normal grafts (Aguayo et al. 1979). The manifestations of the *Tr* gene are fully expressed by the transplanted Schwann cells and their daughter cells. These experiments proved unequivocally that the *Tr* mutation is due to a primary disorder of Schwann cells. Schwann cells in the *Tr* mutant are incapable of producing the quantities of myelin needed to ensheath axons normally and are unable to sustain the myelin that is formed. There was no indication from T-N-T experiments that axonally mediated or general systemic factors were involved in the pathogenesis of the neuropathy.

Pollard and McLeod (1980) inserted sciatic nerve grafts from normal animals into *Tr* mice. Within the normally myelinated graft that resulted, the mean axon area was significantly greater than within the proximal segment. Electrophysiological studies found that the mean conduction velocity across the demyelinated *Tr* nerve in the proximal segment was 2.6 m/s, the mean value across the graft was 31.3 m/s, a value 75% that of normal mice.

1.12 LOCALISATION OF THE TREMBLER AND TREMBLER-J GENE ABNORMALITIES TO THE PMP22 GENE

Based upon classical genetics, *Tr* and Tr^J were suggested to be allelic mutations leading to a similar phenotype (Falconer 1951). The *Tr* mutation was mapped to chromosome 11 (Davisson & Roderick 1978). During the early 1990s, descriptions of a new myelin protein, peripheral myelin protein 22 (PMP22), were being published (Welcher et al. 1991; Manfioletti et al. 1990; De León et al. 1994; Spreyer et al. 1991). The *pmp22* gene was localised to chromosome 11 in the mouse, (Suter et al. 1992) residing 4.4 ± 2.1 cM distal to the *Csfgm* and 2.2 ± 1.5 cM proximal to the *Myhs* restriction fragment length polymorphisim loci (Suter et al. 1992). *pmp22* cDNA from behaviourally and histologically characterised *Tr/+* mice was isolated and cloned (Suter et al. 1992). Two classes of cDNA were found, the first representing the wild type allele. In the second population of cDNAs, a nucleotide exchange was detected within the PMP22 coding region. The detected mutation from guanine (G) to adenine (A) leads to the substitution of an aspartic acid residue with a glycine in the PMP22 protein at amino acid position 150 (Suter et al. 1992). The results of gene mapping studies determined that *pmp22* is localised 4.4cM distal to the RFLM locus *Csfgm* and 2.2cM proximal to the locus *Myhs* (Suter et al. 1992). The localisation of *pmp22* between *Csfgm* and *Myhs* is consistent with its identity with *Tr*, which appears to be ≈ 4.4 cM distal to *Csfgm* and ≈ 2.2cM proximal to *Myhs*. Thus *pmp22* maps to the region where the *Tr* mutation resides. A point mutation in the Tr^J mouse was also found within the *pmp22* gene (Suter et al. 1992) supporting evidence that PMP22 was the candidate gene in these two murine neuropathies. The transition mutation from thymine (T) to cystine (C) in Tr^J translates into a nonconservative amino acid exchange from proline to leucine substitution at

position 16 of the PMP22 polypeptide. The predicted effect of a mutation in the PMP22 protein was consistent with the phenotypes of the *Tr* and *Tr^{J}* mutants. The PMP22 protein was expressed predominantly by Schwann cells of the PNS and was not detectable in the CNS (Snipes et al. 1992). PMP22 protein localised in the compact peripheral myelin sheath; this is consistent with the markedly reduced myelination in the PNS but no known abnormality in the CNS.

The distal half of mouse chromosome 11 shares exclusive conserved synteny with human chromosome 17. It appears that the order of genes has been conserved between human chromosome 17p and their homologues on mouse chromosome 11. *Myhs* has been localised to 17p12-17p13 in humans. Since *pmp22* has been localised proximal to *Myhs* in the mouse, Suter (Suter et al. 1992) predicted that if the human homologue of *pmp22* mapped to chromosome 17 it would reside on 17p11-p12 (Suter et al. 1992). This location in conjunction with its involvement with *Tr* and *Tr^{J}*, identified *PMP22* as the candidate gene to be affected in Charcot-Marie-Tooth disease 1A (CMT1A).

The new Trembler mutant. *pmp22* cDNA from clinically affected and control mice was cloned and sequenced (Suh et al. 1997). Two PCR products of different sizes were identified in the sciatic nerve of normal (742 base pairs) and affected mice (601 base pairs). Sequence analysis of the two PCR products showed that the smaller product lacks a 141bp sequence within the *pmp22* coding region. The *Tr-Ncnp* allele was shown to have a deletion of a region containing the whole of exon IV in the *pmp22* gene. This corresponds to the loss of the whole of the second and part of the third proposed transmembrane domains (Suh et al. 1997).

1.13 PMP22 PROTEIN AND GENE EXPRESSION IN TREMBLER MICE

Gene expression. Steady state levels of mRNAs encoding PMP22, PO, MBP, LP, MAG and CNP were examined P8 and P15 wildtype, *Tr*/+ and *Tr/Tr* nerves (Bascles et al. 1992). Northern blot analysis showed that the expression of all myelin protein genes were affected in the *Tr* mutation. *pmp22* mRNA was the most markedly decreased of all mRNA species examined. The amount of *pmp22* mRNA in the sciatic nerve of homozygous *Tr* mice is lower than that of heterozygous mice (5% and 10% of normal respectively). The mutation of the *pmp22* gene in the *Tr* results in a modified level of expression level of the gene in addition to an amino acid substitution in the protein. P_0, and *MBP* genes were also poorly expressed in the mutant nerves. But *MAG* and *PLP* gene expression was only slightly affected and the level of expression of the *CNP* gene was almost normal. Bascles et al (1992) suggested that the mutated protein may not be incorporated into the myelin membrane leading to its accumulation in the Schwann cell cytoplasm and that such an accumulation

could trigger a feedback repression of the *pmp22* gene. Bascles et al (1994) investigated steady state levels of mRNA encoding myelin protein genes in P8 *Tr* and normal brains a time which precedes the onset of clinical symptoms. They measured a two to four fold increase for *MBP* and *PLP* mRNAs in *Tr* samples but no such increase in the mRNA level of *MAG* (Bascles et al. 1994).

Protein expression. The nerves of adult *Tr* mice showed a 40% increase in the concentration of MAG when compared with age matched controls (Inuzuka et al. 1985). By contrast the concentrations of P_0 and MBP were decreased by 27 and 20% respectively. P_2 was also greatly reduced as was the specific activity of CNP. MAG in *Tr* nerves appeared to have a higher than normal Mr in the sciatic nerve but a normal Mr in the brain. The maintenance of high levels of MAG despite the severe deficit of myelin is consistent with the immunocytochemical localisation of MAG in the periaxonal Schwann cell membranes, Schmidt-Lanterman incisures, terminal loops at the node of Ranvier and the outer mesaxon and its absence from compact myelin.

The sciatic nerves of severely affected Tr^J/Tr^J mice contained nearly undetectable amounts of P_0, MBP and essentially no PMP22 (Notterpek et al. 1997). In adult $Tr^J/+$ mice the levels of P_0, MBP and PMP22 were severely reduced. In P18 $Tr^J/+$ animals the level of PMP22 expression is apparently reduced when compared with P_0 and MBP (Notterpek et al. 1997).

1.14 ALTERATIONS EXPRESSED IN CULTURES FROM TREMBLER MICE

Myelinating cultures. Organotypic cultures of dorsal root ganglia from embryonic control mice were substantially myelinated after 6 weeks in culture (Mithen et al. 1982). They typically developed several consecutive myelinated internodes averaging 80-200μm in length. *Tr* cultures had either no myelin or very small amounts of abnormally thin and short myelin segments (20-60 μm) and unusually long nodal regions. Ultrastructurally *Tr* cultures resembled adult *Tr* nerve. Myelin was commonly uncompacted, fibres were surrounded by redundant basal lamina and the amount of endoneurial and perineurial collagen was increased (Mithen et al. 1982). Abnormally short internodes were also seen when Schwann cells were cultured in the absence of fibroblasts. This confirmed Aguayo's experiments showing that the primary abnormality was in the Schwann cell (Aguayo et al. 1977).

Cultured Schwann cells. When Schwann cell cultures were prepared from the nerves of P15 *Tr* animals they were found to divide less often than control Schwann cells. After 10 days in culture the density of normal Schwann cells had increased 32 fold compared with only 10 fold in *Tr* Schwann cell cultures. In cultures obtained from P1 or P4 animals there

was no difference in the proliferation rates. The authors suggested that the increased proliferation in control cultures might result from an increased amount of mitogen provided by degrading myelin from the nerve segments used for culture. In normal mice the sciatic nerve contained 3 fold more myelin at P15 than it did at P4 whereas in *Tr* mice the amount of myelin present at the two ages was the same. Both *Tr* and control Schwann cells elicited a dose dependant proliferative response to myelin enriched fractions from both *Tr* and control animals. At high concentrations the proportion of labelled nuclei was almost identical in *Tr* and control derived Schwann cells. However at low concentration proliferation was 2 fold higher in Schwann cells derived from *Tr* animals suggesting that either *Tr* Schwann cells are more sensitive to low levels of myelin enriched fraction or their receptor numbers are increased.

1.15 EFFECTS OF TREMBLER SERUM ON CULTURED CELLS

Schwann cells. *Tr* Schwann cells in vitro proliferate at a lower rate than normal Schwann cells whereas in vivo the reverse is true suggesting that the mitogenic factor present in the mutant sciatic nerve is absent from culture dishes (Do Thi et al. 1993). When both *Tr* and control cultures were treated with *Tr* serum Schwann cells in both cultures divided rapidly producing a growth response curve similar to that seen with other mitogens. The serum of normal animals did not modify the proliferation of normal or *Tr* Schwann cells (Do Thi et al. 1993).

Oligodendrocytes. *Tr* serum has two effects on oligodendrocytes. It elicits a mitogenic response from oligodendrocytes in culture increasing their relative abundance 10 fold (Hantaz-Ambroise et al. 1988). Secondly *Tr* serum prevents differentiation .After two weeks in culture with *Tr* serum oligodendrocytes were either undifferentiated or degenerated. In control serum they differentiated normally. Both these effects of *Tr* serum were negated by the addition of laminin. When anti-laminin antiserum was added to control medium, differentiation of oligdendrocytes ceased completely but it did not trigger the increase in oligodendrocyte number caused by *Tr* serum, indicating that the *Tr* serum induced effects cannot be completely explained by modification, synthesis and/or expression of laminin. In the prescence of anti-laminin antibodies, *Tr* serum lost its mitogenic activity.

Neurites. In the presence of *Tr* serum the outgrowth of rat spinal cord neurons in culture was increased two fold when compared with those cultured with control serum. Neurite outgrowth was characterised by an increase in both the number of primary neurites emerging from the cell body as well as by an increase in the peripheral branching of neurites. As the *Tr* mutant is characterised by hypomyelination and the production of excess basal lamina, antibodies to basal laminal components were added to the culture medium. Neurite

outgrowth was reduced by the presence of antibodies against heparan sulphate proteoglycan and abolished by anti-laminin antibodies. The effect of *Tr* serum on neurite outgrowth decreased when the number of non-neuronal cells in the culture was reduced suggesting that the mutant serum did not act directly on neurons but through the intermediary action of non-neuronal cells.

Chapter 2 Peripheral Myelin Protein 22 (PMP-22)

2.1 ISOLATION

Peripheral myelin protein 22 (PMP22) is the name proposed by Snipes et al (1992) for the proteins and cDNAs that had previously been designated SR13, CD25, gas3, and PASII (Welcher et al. 1991; Spreyer et al. 1991; Kitamura et al. 1976; Manfioletti et al. 1990).

SR13 and CD25. The rat *Pmp22* gene was cloned independently in two laboratories by the screening of cDNA libraries constructed from regenerating nerve (Welcher et al. 1991; Spreyer et al. 1991). Two different cDNA clones were described, CD25 (Spreyer et al. 1991) and SR13 (Welcher et al. 1991), which encode for the same protein. *Pmp22* was found to be strongly expressed in normal sciatic nerve and down regulated in the initial phases after sciatic nerve injury. SR13/CD25 was shown to be a myelin protein on the three following pieces of evidence (Welcher et al. 1991). First the SR13 mRNA showed a similar time course of down regulation after sciatic nerve injury as observed for the mRNAs encoding the classical myelin proteins, protein zero (P_0) and myelin basic protein (MBP). Secondly, the recombinant SR13 encoded protein expressed in a transformed cell line was specifically recognised by an antiserum raised against preparations of purified peripheral nerve myelin. Thirdly, SR13 antibodies localised the SR13 protein to the myelin sheath of the sciatic nerve.

gas-3. *gas-3* was first isolated from serum starved 3T3 mouse fibroblasts (Manfioletti et al. 1990). The *gas-3* mRNA belongs to a group of genes whose expression is specifically associated with the quiescent cell state (Schneider et al. 1988). Their transcripts have been isolated from a variety of cell lines including 3T3 mouse fibroblasts and Chinese hamster ovary cells. These mRNAs have been hypothesised to be involved in regulation of general cell growth. In-vitro translation studies established that the protein product is a transmembrane glycoprotein (Manfioletti et al. 1990).

PAS-II. *PAS-II*, isolated from bovine peripheral myelin (Kitamura et al. 1976), shares a sequence homology of >80% with SR13. It has been isolated from purified myelin of various

species and shows the same developmental pattern of expression in the chicken sciatic nerve as other myelin proteins.

2.2 SEQUENCE COMPARISONS

A comparison of the reported *Pmp22* cDNA sequences of CD25, SR13 and *gas3* (Welcher et al. 1991; Spreyer et al. 1991; Manfioletti et al. 1990) revealed a very high degree of homology (>94%) of the entire protein coding sequences and the 3'UTR.

Pmp22/SR13 cDNA was found to encode a protein of 160 amino acid residues with a predicted molecular weight of 18kDa and four putative membrane spanning domains (Welcher et al. 1991). The N-terminal sequence possessed the characteristics of a signal peptide with one consensus site for N-linked glycosylation. The deduced *Pmp22/gas3* cDNA sequence consisted of 1817 nucleotides and coded for 144 amino acids (Manfioletti et al. 1990). From hydrophobicity plots, it was deduced that the sequences from amino acids 2-31, 65-91 and 96-119 represented three potential membrane spanning domains. One potential glycosylation site was present at residue 41.

When compared with the amino acid sequence for *Pmp22*/CD25, *gas3* showed only 5 single amino acid exchanges, (Glu30, Arg 35, Ser79, Val 101 and Asp 128) up to Ala 135 (Welcher et al. 1991). Beyond that point an additional T in nucleotide position 613 of the *CD25* produced a frame shift that interrupted the amino acid homology for the entire C terminus and extended the C terminus of the Schwann cell protein for 16 amino acids beyond that of *gas3* introducing an additional putative transmembrane domain. This frame shift was later reported to be a sequencing error and the *gas3* mouse protein sequence found have an amino acid identity of 97.5% with rat *Pmp22* (Suter et al. 1992). **(Fig. 2.1)**

2.3 TRANSLATION

Using metabolic labelling and immunoprecipitation De León et al. (1994) determined that cultured Schwann cells produce *Pmp22*/SR13. The N-linked glycoslyated form arises from an 18 kDa precursor which can also be detected in sciatic nerve. The inhibition of glycosylation by tunicamycin resulted in the immunoprecipition of an 18kDa protein

The *gas3/Pmp22* protein product translated in vitro (Manfioletti et al. 1990) also had an apparent molecular size of 18kDa which was increased to 22 kDa when translation was performed in the presence of the glycosylating agent dog pancreatic microsomes (DPM). When the *gas3/Pmp22* product was synthesised in the presence of DPM the product was found only in the detergent phase, suggesting that it is an integral membrane product (Manfioletti et al. 1990). Treatment of the microsomally translated product with proteinase K

did not change its apparent mobility with respect to the untreated control suggesting that the signal sequence responsible for translocation into the endoplasmic reticulum is not cleaved. The nature of the N-linked glycosylated side chains may not be identical in PMP22 from cultured Schwann cells, sciatic nerve and purified myelin (Pareek et al. 1993). An antibody to a peptide containing a consensus site for N-linked glycosylation (peptide 1) recognised PMP22 in metabolically labelled segments of sciatic nerve but not in cultured Schwann cells. In cultured Schwann cells a second protein was detected (48kDa) which was distinct from but immunologically related to PMP22 and unaffected by forskolin.

A nuclear run on experiment was performed to assess whether or not transcriptional regulation is responsible for the decreased expression of *gas3*/*Pmp22* RNA after serum addition (Manfioletti et al. 1990). Nuclei collected at various times after the addition of fetal calf serum synthesised *gas3*/*Pmp22* RNA at the same level after growth induction. Manfioletti et al (1990) concluded that *gas3* is probably regulated at the post-transcriptional level.

The stability of *Pmp22* mRNA was examined in cultured cells using RNA polymerase (actinomycin D) and protein synthesis (cycloheximide) inhibitors (Manfioletti et al. 1990), neither altered the stability of *Pmp22* RNA. The addition of serum to the cultures resulted in a decrease in mRNA stability which was abolished in the presence of actinomycin D. This suggests that the decrease in stability of *gas3* mRNA which follows growth induction may be regulated (either directly or indirectly) by de novo transcribed RNA(s) responsible for *gas3* mRNA degradation. If an RNA product is required for downregulation, it may not necessarily be translated into a protein product as cycloheximide did not alter the normal downregulation.

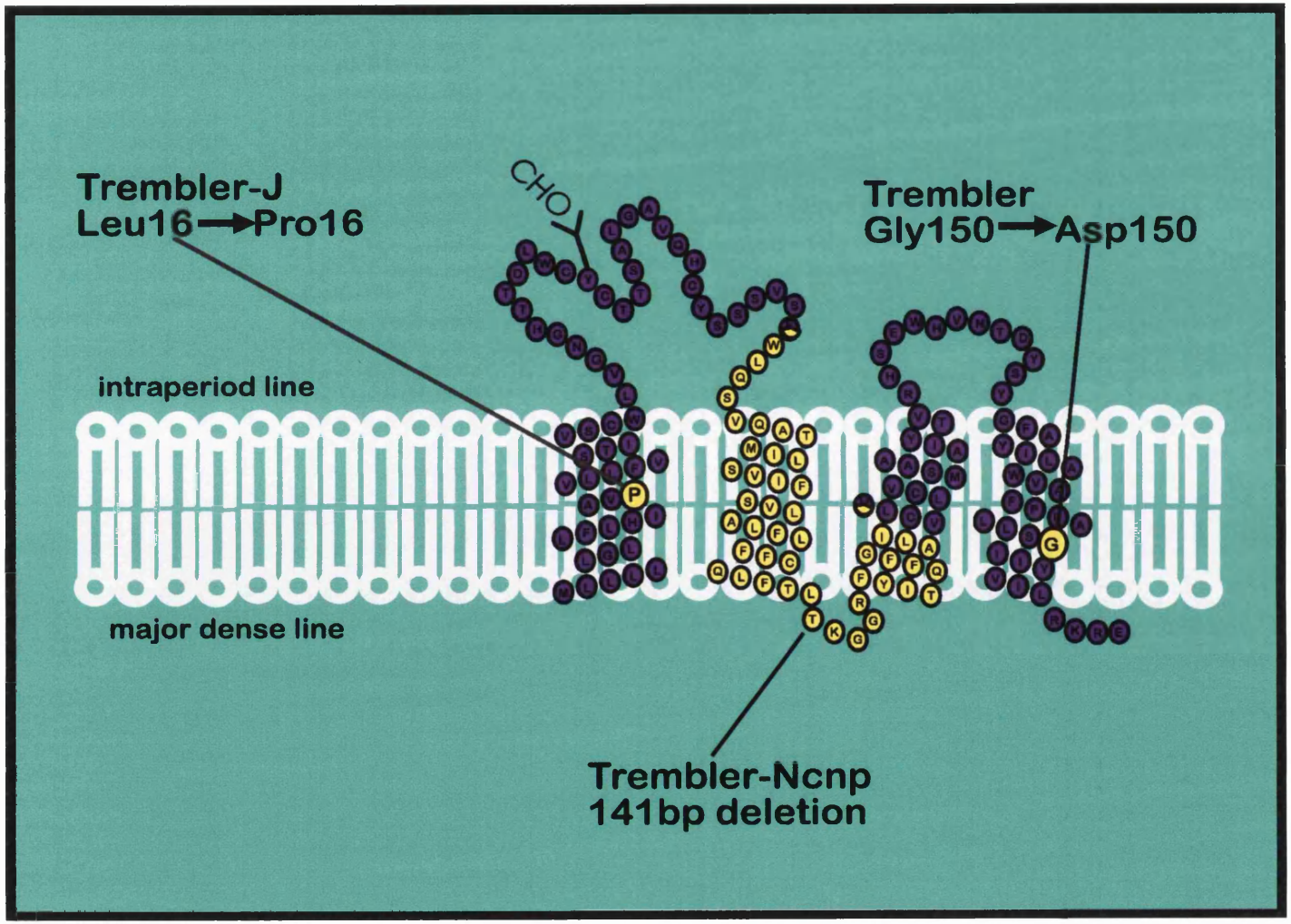

Figure 2.1 Diagrammatic representation of the PMP22 protein

2.4 REGULATION

Correlation with myelin formation during sciatic nerve development. The pattern of expression of PMP22 expression in the PNS during development is essentially identical to other proteins of PNS myelin such as P_0 and MBP (Wiggins et al. 1975; Lees & Brostoff 1984; Stahl et al. 1990). Northern blot analysis of total RNA isolated from sciatic nerves at different time points in development showed that a single 1.8-kb *Pmp22* mRNA species is initially expressed at low levels in the immediate postnatal period (10% of maximum) but is rapidly induced to adult levels over the first three postnatal weeks (Snipes et al. 1992). *Pmp22* mRNA expression reached half maximal levels between postnatal days two to seven and increased to near maximum by postnatal day 21. The production of PMP22 protein lags temporarily behind mRNA expression, overall protein and mRNA display parallel expression patterns (Snipes et al. 1992). Immunohistochemical analysis showed that PMP22 protein expression is restricted to myelin. It correlates temporally with the formation of myelin when compared to the expression of MBP, another component of compact myelin, and to myelin formation as analysed by examining stained plastic sections (Snipes et al. 1992).

Correlation with myelin degradation and remyelination during sciatic nerve regeneration. In the first 7 days following crush injury *Pmp22* mRNA levels rapidly declined to between 5-10% of normal levels (Welcher et al. 1991; Snipes et al. 1992). This was paralleled by a slower decline of PMP22 protein expression which was reduced to similar low levels 10-20 days after crush injury (Snipes et al. 1992).

Pmp22 mRNA levels had begun to approach normal by 40 days post crush as the regeneration process neared completion (Welcher et al. 1991; Snipes et al. 1992). When the nerve was permanently transected and regeneration prevented, *Pmp22* remained down regulated. Thus the *Pmp22* mRNA showed a similar time course to the patterns observed for the major myelin proteins P_0 and MBP (Welcher et al. 1991). The pattern of expression of PMP22 in the distal nerve stump after unilateral sciatic nerve crush was also comparable to the expression of other PNS myelin proteins (Trapp et al. 1988).

2.5 LOCALISATION

Tissues. Northern blot analysis showed *Pmp22* mRNA expression was high in normal adult rat sciatic nerves (Snipes et al. 1992). When introduced into a eukaryotic expression vector the PMP22 protein was immunoprecipitated with a polyclonal antiserum directed against purified myelin protein, demonstrating that the SR13 cDNA encodes a protein expressed in normal sciatic nerve. Synthetic peptides corresponding to the two predicted

major hydrophilic regions of the PMP22 molecule were used as immunogens. The antisera to both peptides were found to be specific for a 22-kDa protein by immunoblot analysis of total protein isolated from rat sciatic nerves (Snipes et al. 1992). Immunoperoxidase studies on plastic sections localised the PMP22 protein to the compact portion of the myelin sheaths of essentially all myelinated axons in the sciatic nerve. (Snipes et al. 1992). In situ hybridisation was performed on teased fibre preparations, the signal showing longitudinal periodicity of mRNA localised to the perinuclear cytoplasm of Schwann cells. This result was confirmed using double labelling combining in situ hybridisation for *Pmp22* mRNA and immunoperoxidase staining for the S100 protein, a specific marker for Schwann cells in peripheral nerves.

De León et al. (1994) observed immunoreactivity in the myelin sheath but unexpectedly also in the DRG both in satellite cells and neurons. RNA blot analysis revealed that *Pmp22* mRNA was present in DRG satellite cells but no accumulation was found in neuronal cells (De León et al. 1994). The neural immunostaining was in both the cell somata and nuclei. A heavy level of staining was also associated with the cell membrane. In the lumbar spinal cord PMP22-like immunoreactivity was seen predominantly within the superficial dorsal horn; both immunoreactive somata and processes were seen. Individual immunoreactive fibres and glial cells were seen within the spinal cord, and white matter. De Leon's results demonstrate that *Pmp22* expression may not be restricted to sciatic nerve Schwann cells. Alternatively the PMP22 protein may share an epitope with another protein. Pareek et al. (1993) used the same antibodies on cultured Schwann cells and found that they immunoprecipitated three proteins, 19, 22 and 45 kDa.

PMP22 has recently been found to be expressed in the skin and colon epithelium of mouse, rat, cattle and human. In the skin *statum papillare*, *stratum spinosum* (including *stratum basale*) and the inner layer of *stratum corneum* were positive but *stratum granulosum* showed no staining. In the colon PMP22 epithelial staining was not limited to secretory cells but also intense staining of the covering mucus layer was observed. This has been confirmed by mucus positive staining in human colon mucous (Liehr & Rautenstrauss 1997)

Ultrastructure. In normal nerves immunostaining for both PMP22 and P_0 detected identical populations of myelinated fibres. Immunoreactivity was located over regions of compact myelin but not over regions of the internode which contained Schmidt-Lanterman incisures (Haney et al. 1996). In addition to staining compact myelin, perinuclear cytoplasm of myelinating Schwann cells was consistently labelled by PMP22 antibodies. This labelling was less intense than that found over compact myelin and reflects the relatively low level of synthesis in adult nerve (Haney et al. 1996). Many of the gold particles were associated with vesicles located near Golgi membranes. This distribution is similar to that described for P_0

protein in perinuclear regions of myelinating Schwann cells (Trapp et al. 1981; Trapp et al. 1995). Significant labelling was associated with the Schwann cell membranes that surround unmyelinated axons in human peripheral nerve. Most of the immunoreactivity was located at or very near the Schwann cell plasma membrane.

2.6 EVIDENCE FOR A FUNCTION OF PMP22 OUTSIDE THE PERIPHERAL NERVOUS SYSTEM

2.6.1 *Pmp22* mRNA has been identified in a number of non-neural tissues.

Its high level of expression in myelinating Schwann cells has implicated PMP22 in the formation and maintenance of PNS myelin. However, *Pmp22* mRNA has also been found by Northern blot hybridisation techniques in several non-neural tissues, in particular the lung, the intestine, and the heart (Welcher et al. 1991; Manfioletti et al. 1990; Spreyer et al. 1991; Patel et al. 1992). Minor expression of *Pmp22* mRNA can also be found in the CNS, particularly in the motor nuclei of most of the cranial nerves and in the motor neurons in the ventral horn of the spinal cord (Parmantier et al. 1995). In contrast the sensory nuclei of cranial nerves and dorsal root ganglion neurons were PMP22 negative. High levels of *pmp*22 transcripts are also found in the villi of the adult gut (Baechner et al. 1995).

Baechner et al. (1995) detected *Pmp22* expression in various non-neural tissues during embryonic mouse development. In early embryogenesis (9.5 days post conception (dpc)), *pmp*22 RNA expression appeared to be restricted to the epithelial ectodermal layer. During early organogenesis (11.5 dpc), particularly high levels of expression were present in the capsule surrounding the liver and in the forming gut, while low levels of *Pmp22* mRNA were found in the precartilagous condensations forming the vertebrae and the ventricular layer of the myelencephalon. During midgestation development (14.6-16.5 dpc), the number of *Pmp22* positive tissues increased, and high expression was detected in several mesoderm-derived tissues, in particular connective tissues of the face region, bones including vertebrae, the lung mesenchyme, and in muscles. In addition, high expression was also found in fetal lens and in the early ectoderm (Baechner et al. 1995). In these tissues at this developmental stage, mitotically active cells and postmitotic cells which subsequently migrate out of the proliferation zone are intermixed with each other. In the two week old mouse, relatively high levels of *Pmp22* mRNA are observed specifically in the postmitotic epithelial cells of the gut. The pattern of *Pmp22* mRNA expression during the ongoing processes of differentiation and morphogenesis supports a function of PMP22 in cellular proliferation and/or differentiation.

2.6.2 PMP22 is a homologue of the growth arrest specific protein gas 3, implicating a role in cell cycle regulation.

The cell cycle concept introduced in 1953 (Howard & Pelc 1953) has helped to delineate many events governing the growth of mammalian cells.

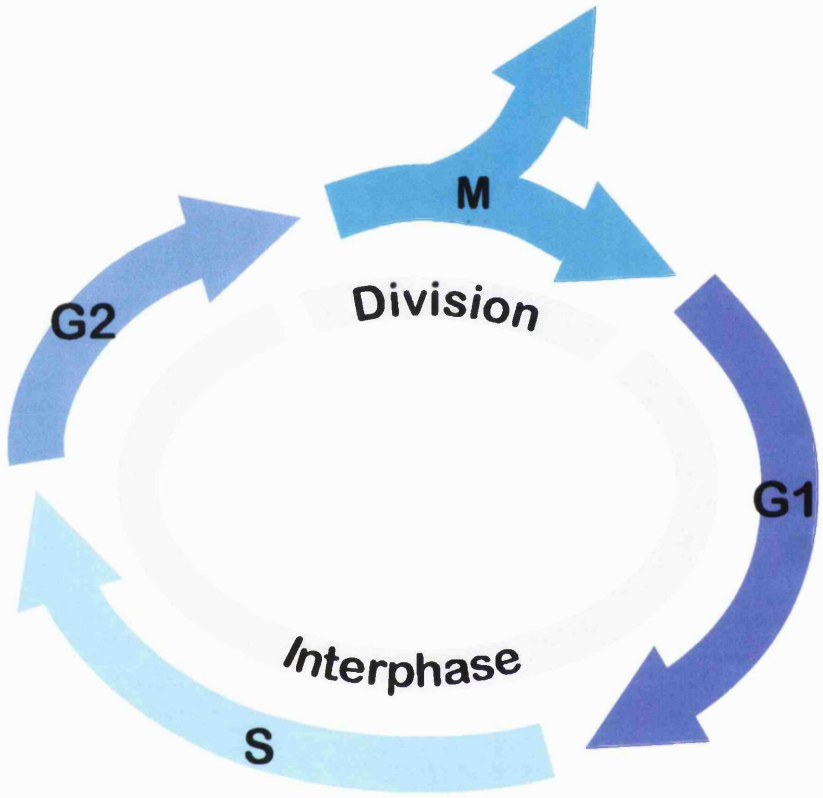

Fig 2.2. Cell replication. During interphase the cell grows continuously; during M phase it divides. DNA replication is confined to the part of interphase known as S phase. G1 phase is the gap between M phase and S phase. G2 is the gap between S phase and M phase

The control of cell proliferation occurs mainly in the G1 phase, and growth arrest of mammalian cell cultures can be accomplished early in this phase by the depletion of serum or growth factors. Six cDNA clones preferentially expressed in growth-arrested NIH 3T3 cells (mouse derived fibroblast cells) were identified (Schneider et al. 1988). The kinetics of regulation of one of these genes (*gas 3/Pmp22*) was investigated in the presence and absence of serum. *gas 3/Pmp22* was expressed in resting but not in proliferating mouse fibroblasts (Schneider et al. 1988).

Schwann cells and fibroblasts. *Pmp22* mRNA is translated into a myelin membrane glycoprotein in differentiated quiescent Schwann cells. After nerve injury the mRNA is down regulated at the time of Schwann cell proliferation (Welcher et al. 1991). Schwann cells cultured in a medium containing forskolin (an adenylate cyclase activator) produced *Pmp22* mRNA, the removal of forskolin from the medium resulted in downregulation (Pareek et al. 1993). PMP22 staining was found to be highest on Schwann cells flattened onto the substratum.

Zoidl et al (1995) demonstrated, in retrovirally transfected Schwann cells, that altered levels of *Pmp22* mRNA significantly modulated Schwann cell proliferation. Enhanced expression of *Pmp22* decreased DNA synthesis to 60% of control levels. Conversely, reduced levels of *Pmp22* mRNA led to enhanced DNA synthesis of ≈ 150%. Over expression of *Pmp22* delayed serum and forskolin stimulated entry of resting Schwann cells from G0/G1 into the S+G2/M phase by 8 h, whereas underexpression slightly increased the proportion of cells that entered the S+G2/M phase. These findings indicated a biological function of PMP22 as a negative modulator of cell growth at an early and critical stage. Based on these findings, Zoidl et al (1995) proposed that altered levels of *Pmp22* gene expression may impair peripheral myelination indirectly through abnormal growth of Schwann cells.

Pmp22 mRNA was also abundantly expressed in differentiated non-proliferating fibroblasts and is down regulated when the fibroblasts were induced to proliferate by the addition of serum (Manfioletti et al. 1990). *Pmp22* mRNA demonstrated density dependant inhibition when cells were cultured in high serum concentrations. PMP22 over expression in growing NIH-3T3 fibroblasts leads to an apoptotic-like phenotype which is characterised by typical membrane blebbing, rounding up and chromatin condensation, but with no evidence of DNA fragmentation (Fabbretti et al. 1995). On the other hand REF-52 fibroblasts seemed to be completely refractory to PMP22 overexpression suggesting that PMP22 does not induce apoptosis directly, but permits cellular entry to a state in which apoptosis becomes more readily accessible. When PMP22 point mutations (L16P, S79C, G150D) were over expressed in NIH-3T3 cells, the induced apoptotic phenotype was significantly reduced as compared to wild-type. Fabbretti et al (1995) suggested a role for altered Schwann cell apoptosis in the pathogenesis of CMT1A.

PC12 pheochromocytoma cells. The PC12 cell line has been used as an in vitro model to study sympathetic neuronal cell differentiation. The addition of NGF induces differentiating changes including cessation of proliferation and the extension of neurites. Untreated PC12 cells expressed low levels of SR13/*Pmp22* mRNA. When cultured under conditions that stimulated growth arrest (the addition of nerve growth factor to the medium) *Pmp22* mRNA levels increased (De León et al. 1994).

Differences between the response of Schwann cells in vivo and in culture. In cultured Schwann cells not elaborating myelin, PMP22 antibodies stained most heavily on cells flattened onto the culture substratum (Pareek et al. 1993). Staining was distributed throughout the cytoplasm and was not specifically localised on the cell membrane as might be expected for a myelin protein. Although this may reflect different cellular compartmentalisation of the PMP22 protein it could also be related to differences in PMP22 function between nonmyelinating Schwann cells in vitro and myelinating cells in vivo. Other differences between PMP22 in intact nerve and in cultured Schwann cells have also been detected. PMP22 expression is markedly lower in cultured Schwann cells than in intact nerves, even when production is stimulated by forskolin. The turnover rate of PMP22 is rapid in cultured Schwann cells having a half life of 30-60 min. Although it has not been directly measured, it seems likely that its turnover in peripheral nerves is much slower. Additionally *Pmp22* mRNA levels are markedly reduced relative to levels of protein in peripheral nerves of aged animals suggesting that once synthesised, PMP22 is not rapidly replaced. The cytoplasmic localisation of PMP22 in cultured Schwann cells may be related to the increased turnover rate in the absence of myelin formation. Increased quantities of PMP22 in the Schwann cell cytoplasm could be consistent with either a 'premyelin' localisation or an additional function (growth arrest).

In experiments comparing myelinating Schwann cells, explanted nerve segments and passaged nonmyelinating Schwann cells in vitro, De León et al (1994) found that antibodies to peptide 1 failed to recognise PMP22 protein produced by cultured Schwann cells but did recognise the protein synthesised by Schwann cells in segments of sciatic nerve. This suggests a difference in the nature of the carbohydrate moieties in PMP22 from the two sources. Antibody to peptide 1 recognised the 18kDa unglycosylated form of the molecule synthesised by cultured cells and nerve segments in the presence of tunicamycin, suggesting that the antibody recognises the epitopes against which it was raised but not when the consensus site is glycosylated by cultured Schwann cells.

In cultured Schwann cells PMP22 staining was found distributed throughout the cytoplasm (Pareek et al. 1993). In later studies additional PMP22 staining was seen when newly synthesised PMP22 localised in the ER and golgi apparatus on route to the plasma membrane (D'Urso et al. 1997). Examining the ultrastuctural localisation of PMP22 Haney et al. (1996) found no significant accumulation of PMP22 within intracellular compartments, including the endoplasmic reticulum (ER) and Golgi apparatus, of either myelinating or nonmyelinating Schwann cells or in endoneurial fibroblasts. These results demonstrate another difference between the localisation of PMP22 in Schwann cells in vitro and in vivo. In tissue culture, there is evidence that a critical signal, presumably originating from axonal contact, is required for efficient translocation of PMP22 protein to compact myelin (Pareek

et al. 1993). In the absence of this putative signal, PMP22 accumulates and is rapidly degraded within the ER and Golgi apparatus in cultured Schwann cells. When cultured cells were treated with forskolin (which has been proposed to partially mimic the effects of axonal contact on Schwann cell gene expression) the protein was still degraded within the ER and Golgi (Pareek et al. 1993).

2.6.3 STRUCTURE OF THE GENE: TWO PROMOTERS HAVE BEEN IDENTIFIED

Two different *Pmp22* cDNA clones, CD25 and SR13, have been identified in the rat by northern blot and polymerase chain reaction (Welcher et al. 1991; Spreyer et al. 1991). The CD25 and SR13 mRNA species encode the same protein but differ significantly in their 5'-untranslated region sequences. Detailed analysis of the 5'-flanking indicate that the *Pmp22* gene is regulated by two alternatively used promoters that are located immediately upstream of two alternative non-coding exons (exons 1A and 1B) (Suter et al. 1994b). While both transcripts are co-expressed in tissues and cell lines, the transcripts containing exon 1A (*CD25*) are preferentially expressed in myelinating Schwann cells, while the transcripts containing exon 1B (*SR13*) are preferentially expressed in tissues that do not form myelin (Suter et al. 1994b; Bosse et al. 1994).

The transcripts are differentially expressed during postnatal sciatic nerve development (Bosse et al. 1994; Suter et al. 1994b). The expression of exon 1A transcripts steadily increases from low levels in neonates to a maximum at P14. This 25 fold increase correlates closely with the formation of myelin. In contrast, exon 1B levels are elevated at birth but decrease throughout adulthood (Bosse et al. 1994). Both exon 1A and exon 1B are expressed in adult and developing brain at very low levels (Bosse et al. 1994).

In degenerating and regenerating segments of peripheral nerve changes in exon 1A mRNA levels clearly resemble the expression pattern of other myelin genes. This contrasts with the expression of exon 1B which is inversely correlated with the time course of Schwann cell proliferation (Bosse et al. 1994). Temporal changes in the relative abundance of the transcript in sciatic nerve by northern blot were analysed following two types of lesions (Bosse et al. 1994): i) crush injury which leads to Wallerian degeneration in the distal nerve segment prior to regeneration of axons from the proximal stump into the distal segment and ii) transection of nerve and permanent separation of both stumps in order to prevent axonal growth into the degenerating distal stump. In the proximal segments of both crush-lesioned and transected sciatic nerves only minor changes in mRNA abundance were observed for at least 6 and 4 weeks after injury, respectively. In the distal stump however the transcript levels rapidly declined within 2 days (crushed) or 7 days (transected). During the second

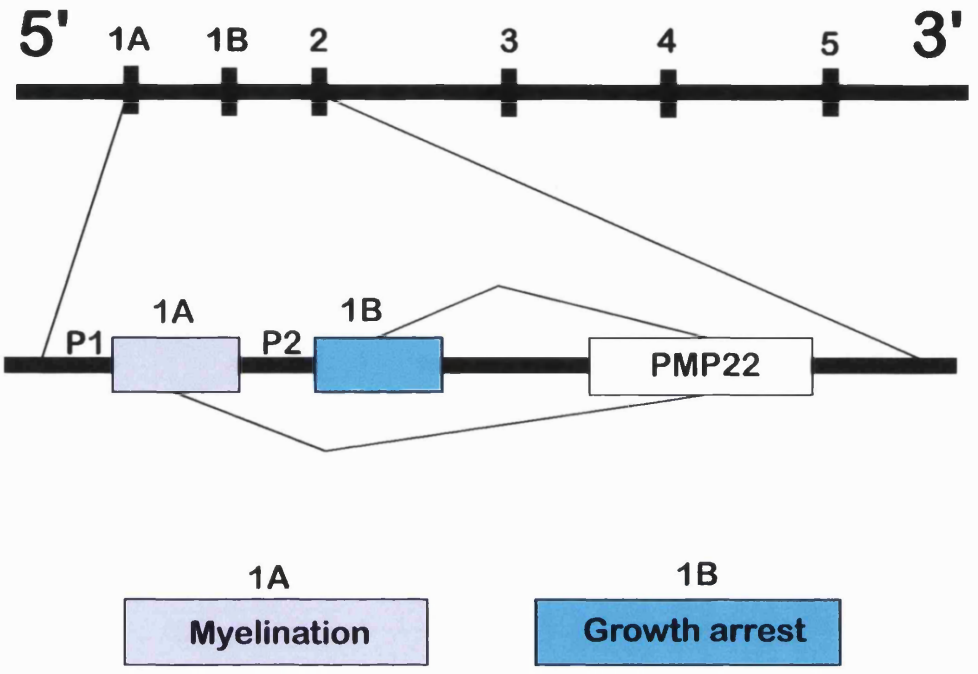

Fig 2.3 Diagram of the position of the two PMP22 transcripts and their promoters.

week, crush injury transcripts began to rise again, reaching near control levels at 6-12 weeks post lesion. In non-regenerating stumps of transected and ligated nerve no recovery of exon 1A or exon 1B could be seen, suggesting that the expression of both transcripts in Schwann cells is under the control of axonal signals (Bosse et al. 1994). Taken together these results substantiate the hypothesis, suggested by Doyle and Colman (1993), Lemke (1993) and Suter et al. (1993), that PMP22 serves two functions, one related to myelination (exon 1A) and another to cell growth (Exon1B).

The analysis of the primary sequence of the two alternative *PMP22* promoters provides some information as to their specific regulation (Suter et al. 1994b). The promoter-1 structure is similar to the tissue specific promoter with a non-canonical (T)ATA box at the optimal distance of 30bp upstream of the major transcription initiation site. An inverted CCAAT box is found upstream from the (T)ATA box. The sequence around the transcription initiation site, TCAG, is also found at the same or a similar position in several other myelin protein genes including Po, MBP and PLP. Co-ordinate myelin gene transcription may involve a

regulatory step using a common "initiation" site. Promoter 2 displays several features of a "housekeeping" gene promoter. No obvious TATA like sequence, and a generally high G/C content can be found in the first 352bp upstream from the transcription initiation site. There is also a consensus sequence for an Sp-1 binding site, a transcription factor often found involved in the regulation of housekeeping genes (Suter et al. 1994b).

Numerous studies have established that myelin gene expression is critically dependant on the presence of axons. In pure Schwann cell cultures, forskolin has been shown to upregulate the expression of the P_0 gene that encodes for the major myelin protein component of peripheral nerve myelin. This and other findings have led to the hypothesis that forskolin can replace the requirement of axonal contact for myelin gene expression in Schwann cells and indirectly implicated the cAMP pathway in the signal transduction cascade leading to myelin gene expression. In cultured rat meningeal fibroblasts exon 1B mRNA expression is strictly growth arrest specific and independent of forskolin. Regulation of exon1A mRNA levels in these cells is more complex with interfering affects of serum and forskolin. In cultured Schwann cells neither exon 1A or exon 1B expression is growth arrest specific. However both transcript levels are consistently enhanced by forskolin under all conditions of cell growth tested. Expression of exon 1A but not exon 1B depends on high Schwann cell density (Bosse et al. 1994).

2.6.4 THE PMP22 GENE FAMILY

Three proteins have been described that bear considerable sequence homologies to PMP22. CL20 (Marvin et al. 1995), epithelial membrane protein -1 (EMP-1) (Taylor et al. 1995),and lens specific membrane protein 20 (MP20) (Kumar et al. 1993). All four proteins share similar structural characteristics. Their genes code for similar sized proteins of 160,160,160 and 173 amino acids respectively and their hydrophobicity profiles suggest they all have four membrane spanning domains. The transmembrane regions of the proteins are the most highly conserved, in particular the second transmembrane domain and its N-linked glycosylation site. All the mutations in *PMP22* that are known to cause hereditary and motor sensory neuropathies (Suter & Patel 1994a) lie within the putative membrane spanning domains, and five of the six are conserved in rat EMP-1. This suggests functional significance for these regions. The N-linked glycosylation site has been associated with the carbohydrate epitope L2/HNK-1 in two of the proteins (PMP22 and CL20). These proteins are thought to function in relation both to the switch from proliferation to differentiation and the maintenance of critical functions in the differentiated state (Taylor et al. 1995).

CL20. The protein most closely related to PMP22 is CL20. The *CL20* gene is located on chromosome 12 and encodes a 17.8kDa protein which exhibits 43% identity to *PMP22* (Marvin et al. 1995). The positions of the four hydrophobic domains and the N-glycosylation site are conserved. In particular the second transmembrane domain is highly homologous between PMP22 and CL20, with 18 of the 26 amino acids being identical. CL20 contains two glycosylation sites at amino acid positions 35 and 43, the latter being conserved between the two proteins. Although the exact carbohydrate structure has not yet been established preliminary observations suggest that CL-20 resembles PMP22 in binding L2/HNK-1.

CL20 mRNA is most highly expressed in the squamous-differentiated epithelia of the tongue and the oesophagus. *CL20* is induced during squamous differentiation of rabbit tracheal cells in vitro. Squamous differentiation is a multi-stage process in which irreversible growth arrest occurs early and is followed by the expression of squamous cell specific genes. When treated with retinoids, which have been shown not to block growth arrest irreversibly but to suppress the expression of squamous-specific genes, *CL20* expression was repressed, suggesting that the function of CL20 protein relates to the differentiated phenotype rather than to growth arrest. *CL20* was found to be expressed in peripheral nerve but nerve injury and regeneration had little effect on mRNA expression levels.

EMP-1. EMP-1 is a protein of 160 amino acids with four transmembrane domains. It has a 40% amino acid identity to PMP22 (Taylor et al. 1995). The putative four membrane-spanning regions of EMP-1 and PMP22 are particularly well conserved. The first and second of the hydrophobic domains exhibit the highest degree of amino acid identity, 54% and 67% respectively. Translation of the *EMP-1* cDNA results in a 4-6 kDa increase in the molecular mass of the translation product consistent with the presence of a single N-linked glycosylation site. The deglycosylated protein migrates identically to the unglycosylated EMP-1 protein, suggesting that the putative N-terminal signal peptide is not removed during biosynthesis. A similar modification was seen with PMP22 (Kumar et al. 1993). All tissues expressing *EMP-1* mRNA contain the 2.8-kb EMP-1 transcript however in some regions and additional transcript of 1.7kb was found.

EMP-1 mRNA transcripts were found in all the organs examined with the exception of the liver. The most prominent expression was observed in tail derived skin and in the gastrointestinal tract, particularly in the stomach, with lower levels being detectable in the caecum and large intestine. The gastrointestinal tract is characterised by continual and rapid renewal of its epithelial surface that continues throughout the animal's life. Pluripotent stem cells in the isthmus/neck regions of the gastric glands give rise to progeny displaying increased proliferation and reduced potentiality, which progress to terminally differentiated

mature cells. During this process, the cells are highly migratory, with proliferation, migration and differentiation being tightly coupled. EMP-1 is found mainly in the proliferation and differentiation zones of the outer gastric glands as well as in the mature epithelial cells of the gastric pit region. In these regions EMP-1 appears to be associated with the plasma membrane, with no clear distinction between basal, apical and lateral aspects. The tissue distribution of *PMP22* mRNA and *EMP-1* mRNA is similar but they differ in their relative expression levels. *EMP-1* and *PMP22* mRNA are differently regulated after sciatic nerve injury and inversely regulated in both Schwann cells and NIH 3T3 cells during growth arrest. The conspicuous inverse regulation of *PMP22* and *EMP-1* during the cell cycle lends indirect support to a role of this protein family in the control of cell quiescence and proliferation.

MP20. Additional data base searches with the EMP-1 and PMP22 sequences revealed that both display a 30% amino acid homology to the lens fibre cell protein MP20 (Kumar et al. 1993). MP20 is a 173 amino acid protein with similar structural features to EMP-1 and PMP22. If MP20 is compared with PMP22 and EMP-1 simultaneously, the amino acid identity increased to 36% including strongly conserved motifs in the putative transmembrane domains. As in *PMP22* and *EMP-1*, the *CL20* gene does not have a signal cleavage consensus sequence and is unmodified at its N-terminus in vivo. MP20 is a lens-specific membrane protein that has been localised in fibre cell junctions. MP20 has been shown to be absent from proliferating epithelial cells of the lens, with expression becoming prominent in differentiating as well as in mature lens fibre cells.

2.7 L2/HNK-1 EPITOPE

Cell surface and extracellular matrix molecules are characterised by particular sets of carbohydrate structures, some of which are thought to modulate the functional capacities of the molecules bearing them (Schachner & Martini 1995a). The HNK-1 epitope, originally described as a cell surface component of human natural killer cells (Abo & Balch 1981), was found to be expressed in the central and peripheral nervous systems (Schuller-Petrovic et al. 1983; Wernecke et al. 1985). The epitope consists of a carbohydrate structure and when carried by a glycolipid has a 3'sulfated glucuronic acid at the non-reducing end of one or two lactosamine repeats (Chou et al. 1986; Ariga et al. 1987). L2/HNK-1 is expressed by many neural adhesion molecules (N-CAM, L1, MAG, P_0, J1/Tenascin (Cytotactin), j1/Janusin (j1-160/180), tag-1, some integrins and endymins (Kruse et al. 1984; Kruse et al. 1985; Schachner 1989; Jessell et al. 1990), and some glycolipids (Yoshihara et al. 1991; Chou et al. 1986; Kruse et al. 1984).

Monoclonal antibodies against the L2/HNK-1 carbohydate have been shown to disturb the migration of neural crest cells, and it has been suggested that the antibody interferes with the interaction of the L2/HNK-1 carbohydrate and a laminin-heparan sulphate proteoglycan complex (Bronner-Fraser 1987). Similarly, neurite outgrowth has been reported to depend on the interaction of the L2 carbohydrate with a complex of extracellular matrix molecules (Dow et al. 1988). L2/HNK-1 is capable of functionally blocking cell-cell and cell-substrate interactions. Adhesion of cerebellar cells to laminin could be strongly inhibited by the L2/HNK-1 carrying glycolipids (Hall et al. 1993), whereas neuron to astrocyte and astrocyte to astrocyte adhesion was inhibited to a lesser degree (Kunemund et al. 1988; Keilhauer et al. 1985). The cell (but not substrate) bound L2/HNK-1 epitope is a potent mediator of astrocytic and neuronal adhesion to laminin, which was strongly reduced in the prescence of the L2/HNK-1 carbohydrate-carrying glycolipids or Fab fragments of a monoclonal antibody against it (Hall et al. 1993). L2/HNK-1 interacts directly with the laminin molecule at binding site(s) which appear to be distinct from those for the glycosaminoglycan heparin and the glycolpid sulphatide (Hall et al. 1993).

Laminin is not only involved in interactions with other extracellular matrix components, but also in the interaction of cells leading to a variety of responses including cell proliferation, differentiation, cell migration and neurite outgrowth (Sanes et al. 1990; Reichardt & Tomaselli 1991).

In human PNS myelin the L2/HNK-1 epitope has been found on P_0, MAG and a group of glycoproteins with molecular masses ranging from 18 to 28 kDa (Inuzuka et al. 1984; Noronha et al. 1986; van den Berg et al. 1990). Snipes et al. (1993) demonstrated that at least one of these glycoproteins is PMP22. Quantitatively the L2/HNK-1 bearing proteins in the 18-28kDa molecular weight range, seemed to contain as much of the epitope per nerve as either P_0 or MAG. It is plausible that PMP22 is the major L2/HNK-1 epitope bearing protein in the lower molecular weight range and possibly in the PNS. Although P_0 has been shown to be a carrier of the L2 carbohydrate in human and in bovine nerve, it is not a prominent carrier of the L2 carbohydrate in mouse (Schachner et al. 1995b).

L2/HNK-1 has been identified as being involved in the homophilic binding of P_0, the major glycoprotein in the PNS, a neural recognition molecule. (Griffith et al. 1992). Thus not only protein-protein interactions mediate homophilic binding of P_0, but also interactions between the protein backbone and the L2 carbohydrate appear to be important. It has been suggested that the L2 carbohydrate may guide the loops of Schwann cell processes to spiral during myelin formation and to stabilise these loops in compact myelin in the adult (trans interaction) (Schachner et al. 1995b). It is conceivable that P_0 may interact with itself in the surface membrane (cis-interaction) to form clusters.

L2/HNK-1 in development. The L2/HNK-1 epitope was uniformly expressed in developing peripheral nerves where it showed a similar distribution to that observed for L1 and NCAM. It was detected on some, but not all, small axons, and intensely stained basement membranes and collagen fibrils (Martini & Schachner 1986). L2/HNK-1 was present on axons and adjacent Schwann cells before completion of 1.5-2 loops of Schwann cell membrane, but then disappeared. It is generally downregulated at the onset of myelination along with NCAM and L1 although it does remain expressed on a subpopulation of non-myelinating Schwann cells and small calibre axons (Nieke & Schachner 1985). L2/HNK-1 reappears during the third postnatal week in the compact myelin of motor axon-associated myelinating Schwann cells (Martini & Schachner 1986; Martini et al. 1992).

L2/HNK-1 expression in adult mouse nerve. L2/HNK-1 is expressed in the adult mouse by myelinating Schwann cells of ventral roots and muscle nerves, but rarely by those of dorsal roots or cutaneous nerves (Martini et al. 1988). Its characteristic pattern of expression and the fact that it is maintained in denervated nerves for 2-3 weeks led authors to suggest that it may be involved in pathfinding of motor axons after injury of mixed nerves where motor and sensory axons intermingle.

The possible functional involvement of L2/HNK-1 carbohydrate-positive Schwann cells in the regeneration of motor axons was tested on cryosections of L2/HNK-1 carbohydrate-positive and negative peripheral nerves (Martini et al. 1992). Motor neurons from chick embryos grew significantly longer on muscle nerves and ventral roots than on cutaneous nerve branches and dorsal roots. This preferential outgrowth of motor neurons on sections of ventral roots could be inhibited by L2/HNK-1 specific antibodies (Martini et al. 1992).

Myelinating Schwann cells previously associated with motor axons have been shown to express L2/HNK-1 following crush injury while previously sensory associated Schwann cells do not (Martini et al. 1994). Following femoral nerve lesions regenerating axons from cutaneous branches did not express L2/HNK-1 in muscle or cutaneous branches. Axons regenerating from muscle branches provoked a weak expression of L2/HNK-1 in a few Schwann cells in the cutaneous branch but a strong expression by many Schwann cells in the muscle branch. This upregulation of L2/HNK-1 during the early stages of reinnervation may provide motor axons regenerating into the appropriate pathway with an advantage over those regenerating in to an inappropriate sensory pathway (Martini et al. 1994).

Chapter 3 Genetically engineered PMP22 alterations

3.1 ANIMAL MODELS

3.1.1 PMP22 deficient mice

Two investigators have produced mouse models which are deficient in PMP22. Adlkofer et al. (1995) engineered a null mutant (PMP22 $^{0/0}$) and Maycox (1997) a transgenic strain expressing antisense PMP22 RNA. No PMP22 protein was detected in sciatic nerve homogenates of P24 or ten week old PMP22 $^{0/0}$ mice and the levels of P_0 and MBP were reduced (Adlkofer et al. 1995). The transgenic mice produced by Maycox expressed antisense RNA under the control of a P_0 gene promoter (Maycox et al. 1997). The strategy of using the P_0 promoter is known to restrict the expression of the transgene to myelinating Schwann cells (Lemke et al. 1988; Messing et al. 1992; Messing et al. 1994; Weinstein et al. 1995). Both homozygous and heterozygous antisense *Pmp22* mice exhibited moderately reduced levels of *Pmp22* mRNA (15% and 9% respectively) (Maycox et al. 1997).

Clinical features

Null mutants. PMP22 $^{0/0}$ mice could be behaviourally distinguished from their litter mates at P14. Affected animals had difficulties walking as a result of progressive paralysis of the hind limbs. Occasionally stress induced convulsions and tremor were observed. The tremor was reported as being less pronounced than the one seen in *Tr* mice (Adlkofer et al. 1995). Most of the mice heterozygous for the null mutation (PMP22$^{0/+}$) were indistinguishable from wild type mice but occasionally some animals showed signs of walking difficulties. In matings of heterozygous mice 28% of the offspring were homozygous indicating that embryonic development can proceed without PMP22 expression (Adlkofer et al. 1995).

Antisense mice. The behavioural phenotype observed in the antisense *Pmp22* transgenic line was characterised by an unusual gait disorder in young animals (Maycox et al. 1997). In the published frame by frame video montage a young

homozygous mouse shows an extremely high stepping action of the hindlimbs. Maycox also found that homozygous animals tended to avoid walking at all and explored the environment with both forelimbs, radially from a single point. The gait abnormality was first noted several weeks after birth and worsened with age.

Morphological abnormalities Both strains of PMP22 deficient mice have focal myelin thickenings (tomacula) as a prominent feature of their pathology.

Null mutants

PMP22 $^{0/0}$ mice. The absence of PMP22 resulted in abnormal myelin formation in development.

P4 In the pectineus nerve of P4 mice a population of large calibre axons had separated from the fetal bundles and were ensheathed singly by Schwann cells (Adlkofer et al. 1995). In wildtype animals 60% of these large calibre axons were surrounded by compact myelin whereas only 19% were myelinated in PMP22 $^{0/0}$ mice. In the population of axons that were myelinated, the myelin sheaths were already abnormally thickened with respect to axon diameter.

P24 In the femoral nerve of P24 mice many fibres had redundant myelin loops with normal myelin periodicity and a corresponding compression of the axon (Adlkofer et al. 1995). The myelin of some tomacula was disorganised and the axons were displaced, the authors considered this to reflect an early stage of degeneration. Many thinly myelinated axons, basal lamina-covered Schwann cells and onion bulbs were seen. Some large calibre axons were seen completely devoid of myelin and the Schwann cells ensheathing them were occasionally associated with degenerating myelin. Teased fibre analysis showed tomacula associated with every axon-Schwann cell unit. They were preferentially found at paranodal regions of myelinated fibres but internodal tomacula were also seen. Axonal loss was shown in the pectinous nerve at P24.

10 weeks Tomacula were rare and established signs of degeneration were observed in 10 wk mice. No abnormalities were noted outside the PNS. Axonal loss could not be quantified due to the presence of axonal sprouts

PMP22 $^{0/0}$ mice have abundant tomacula at a young age but show demyelination and reduced MNCVs (similar to CMT1) with progressing age. This suggests that tomacula are unstable transient structures that degenerate during maturation, their presence indicating a predisposition to demyelination. Aldkofer et al. concluded that focal hypermyelination followed by myelin degeneration is likely to be a common

Tomacula.

The term 'tomacula' was coined by Madrid and Bradley (1975) to describe elongated or sausage-shaped thickenings of the myelin sheath (*tomaculum*, Latin = sausage). The first description of globular thickenings of the myelin sheath is credited to Dayan et al. (1968). They also noted that the structures occurred in the presence of extensive segmental demyelination. Behse et al. (1972) also described sausage-like swellings of the myelin sheath and considered them to have arisen by the wrapping of redundant loops of myelin around the axon. Madrid and Bradley (1975) examined tomacula in patients with different clinical syndromes including hereditary neuropathy with liability to pressure palsies, recurrent familial brachial plexus neuropathy and chronic distal sensorimotor neuropathy. They described focal enlargements of the myelin sheath usually continuous with a myelin sheath of normal thickness. In thickened areas the myelin was frequently swollen, vacuolated and irregular in appearance. The tomacula appeared to be formed in different ways, with each of the different forms being found in each of the cases examined. *Hypermyelination.* The most simple tomaculum is an excessive thickening of the myelin sheath. It is thought to result from the Schwann cell failing to stop rotating at the appropriate stage of myelination resulting in the production of too many myelin lamellae for the diameter of the axon. The simple tomaculum was not found particularly frequently (Madrid & Bradley 1975). *Folding.* The most common form of tomaculum consisted of folding of the myelin sheath. This varied from simple outpouchings to various degrees of complex folding. Redundant myelin loops secondarily wrapped around the original myelinated axon either around the outside or turned inwards and wrapped internally around the axon. Occasionally redundant loops were derived internally within the myelin itself. *Degenerative changes.* Degenerate swollen myelin usually appeared to lie between a relatively preserved part of the myelin sheath and a structurally normal but compressed axon (Madrid & Bradley 1975). Focal myelin thickening was associated with constriction of the axon resulting in densely packed neurofilaments and neurotubules. Some internodes were diffusely thickened but more frequently the 'sausages' were paranodal and less frequently internodal. Occasionally there were several thickenings within one internode. All the cases examined by Madrid and Bradley (1975) showed extensive segmental demyelination and remyelination with the incidence of tomacula being highest when segmental demyelination was most prominent. Other features of the tomacula-associated demyelinating neuropathy included extensive variability of internodal length, abnormally thin myelin sheaths and occasionally onion bulb formation or acute segmental demyelination with the presence of myelin ovoids.

mechanism in neuropathies involving tomaculum-like structures (Adlkofer et al. 1995).

PMP22 $^{0/+}$ mice. Tomacula were less frequently seen in the femoral and pectineus nerves of P24 PMP22$^{0/+}$ mice when compared with age matched PMP22$^{0/0}$ mice. Their frequency increased with age so that by 10 wk almost every myelinating Schwann cell had formed internodal or paranodal tomacula. Onion bulbs were occasionally seen in the quadriceps nerves but there was no significant change in axon number.

In animals from 5 to 15 mo tomacula were prominent (Adlkofer et al. 1997). At 5 mo multiple tomacula were found within the same internodal segment. They were seen both internodally and paranodally but were more frequent in paranodal regions. By 10 mo the presence of many very thick tomacula became obvious. These expanded structures were interpreted as early onset degeneration in former tomacula (Adlkofer et al. 1997). In animals older than 10 mo the axon appeared compressed inside hypermyelinated structures. Splitting of the major dense line and intramyelin oedema was frequently seen as were Schwann cells with myelin debris present in the cytoplasm. At 15 mo tomacula were still seen frequently. Some myelin sheaths looked abnormally thin and were surrounded by cellular or basal lamina-type onion bulbs.

Antisense *Pmp22* mice.

The sciatic nerve of homozygous, heterozygous and wildtype animals were examined morphologically at 7 mo (Maycox et al. 1997). At the light microscopic level the differences between the groups was modest. However under EM examination the nerves of every homozygous animal examined exhibited tomacula, some of which appeared to be undergoing myelin breakdown. Onion bulb formations were prominent, indicating demyelination and subsequent remyelination and many axons were almost completely devoid of myelin. No morphological abnormalities were seen in either antisense *Pmp22* transgenic heterozygotes or normal animals.

Overall there was a good correlation between the relative reduction in *Pmp22* mRNA levels (*Pmp22* antisense homozygotes 15%, PMP22$^{0/+}$ 50% and PMP22$^{0/0}$ mice 100%) and the relative severity of the phenotype observed. The modest reductions in *Pmp22* levels in antisense transgenic mice eventually leads to the development of many features seen in null mutants but with a longer time course and with a reduced incidence of tomacula.

Nerve conduction studies Electrophysiologically $PMP22^{0/0}$ animals showed abnormalities typical of a severe myelin disorder. There was dramatic slowing of motor nerve conduction velocities (<20% of wildtype values), polyphasic compound muscle action potentials and increased motor latencies (Adlkofer et al. 1995). In $PMP22^{0/+}$ mice conduction velocities were near normal in the presence of tomacula.In 3-5 mo homozygous antisense animals compound distal latencies were no different from those found in wildtype nerves. In older homozygous antisense *Pmp22* mice (7-9mo) distal caudal nerve compound latencies were prolonged by 23% and distal sural nerve latencies by 24%. In contrast F wave latencies were significantly increased in the 3-5 mo group and by 7-9 mo no F waves were detected either in antisense *Pmp22* mice or controls.

3.1.2 PMP22 overexpressing mice

Pmp22 transgenic mice were identified by Southern blot analysis with 16 and 30 copies of the mouse PMP22 gene (Magyar et al. 1996). No *Pmp22* mRNA was detected in the kidney, stomach, thymus, spleen or liver. Low expression was found in the heart and the lung. A relative overexpression of approximately two fold was found in the heart but no defects were detected by histological analysis (Magyar et al. 1996). *Pmp22* mRNA expression in the sciatic nerve was reduced to 54% of control values. When standardised against P_0 expression there was a twofold increase in PMP22 expression. Both PMP22 and P_0 protein levels were dramatically reduced in transgenic mice. No significant differences were noted between the lines with different copy numbers either in phenotype or pathology.

Clinical features. The first behavioural abnormalities appeared 2 wk after birth and manifested as a slight shivering, most obvious in the head. At 4 wk an unsteady gait became apparent with signs of muscle atrophy present at 2-3 mo. Progresssion of the disease with age often culminated in pronounced paralysis of the hindlimbs. The lifespan of transgenic animals generally exceeded 8 mo.

Morphological abnormalities Morphological analysis at the light microscope level failed to demonstrate any detectable myelin in the nerves of P10, P21 or P70 *Pmp22* overexpressing animals. No other tissue showed any visible difference with the exception of neurogenic muscle atrophy and decreased body fat which was attributed to feeding difficulties.

In the sciatic nerve of P10 overexpressing mice most Schwann cells had formed a 1:1 relationship with their axons but no myelin sheaths were seen. There was no

evidence of either degenerating myelin or myelin debris, suggesting that the absence of myelin was a consequence of disrupted myelin formation rather than a result of myelin degeneration. By P21 the cytoplasm of Schwann cells associated with larger calibre axons had become more dense than in littermate controls or P10 mice and all the axon/Schwann cell units were now surrounded by redundant basal laminae. A few larger calibre axons were surrounded by thin compact myelin sheaths and occasionally degenerating myelin and myelin debris was noted. At P72 compact myelin was no longer found; this was thought to correlate with the occurrence of degeneration at P21. Redundant basal lamina was still frequently seen, but often disorganised or disrupted and it rarely contained Schwann cell processes. Remak fibres appeared normal.

Schwann cell proliferation. The number of nuclei in the nerves of P8 overexpressing mice was double that seen in wildtype littermates; the difference had increased to fourfold by 6wk. Continued proliferation was confirmed by observations of an increased number of cells incorporating BrdU at both P21 and P72. Electron microscope analysis of longitudinal sections showed that most of the Schwann cells were in contact with, and had lined up along, axons but had failed to elaborate myelin. There was no sign of significant numbers of invading macrophages, endoneurial fibroblasts or supernumerary Schwann cells.

Schwann cell antigen expression. The femoral quadriceps nerves of *Pmp22* overexpressing mice showed a strong upregulation of LNGFR in most Schwann cells. NCAM was also upregulated but to a lesser extent and L1 was weakly upregulated by some Schwann cells. This characteristic expression profile of Schwann cell development markers in combination with the positions of the Schwann cell along single axons indicates that the differentiation state of mutant Schwann cells closely resembles the characteristics of normal Schwann cells just before myelination (Jessen & Mirsky 1991).

We have recently described five lines of transgenic mice carrying increasing copy numbers of the human PMP22 gene and expressing increasing levels of the transgene (Huxley et al. 1998). From histological and electrophysiological observations there appears to be threshold below which expression of *Pmp22* has virtually no effect; below a ratio of human/mouse mRNA expression of 0.8, little effect is observed. Between a ratio of 0.8 and 1.5, abnormal histological and nerve conduction velocities are observed, but there are no behavioural signs of neuropathy. An expression ratio of >1.5 leads to a severe neuropathy. The level of expression

does not affect the type of demyelination, but influences the severity of involvement. The work in this thesis extends the morphological characterisation of a selection of these lines.

3.1.3 PMP22 overexpressing rats

The rat model generated by Sereda et al. (1996) had an estimated 3 copies of a microinjected mouse DNA fragment in the *Pmp22* transgene. There was considerable variation in the level of *Pmp22* mRNA among both transgenic and non-transgenic rats. Homozygote overexpressing animals showed up to a 6-fold elevation in mRNA levels at 4 wk. The degree of overexpression appeared to correlate with the severity of the phenotype.

Clinical features. All animals carrying the *Pmp22* gene displayed an unsteady gait which the authors considered reminiscent of the 'steppage' gait seen in CMT patients. Despite individual variations in phenotype, transgenic rats all failed in the bar test, a behavioural test of motor performance and grip strength. Homozygous animals displayed a more severe phenotype than heterozygous animals. They were never able to control their limb movements and occasionally spasticity and seizures were observed. The neuropathy was progressive many homozygous animals dying or having to be killed by 1 mo.

Morphological abnormalities.

Homozygous. Homozygous rats were completely lacking PNS myelin. Schwann cells, whose numbers were increased, had segregated with axons in a normal 1:1 ratio and had formed basal lamina, but failed to elaborate myelin. Overt myelin debris was not seen although fibroblasts frequently contained lipid droplets. Neither supernumerary Schwann cells nor onion bulbs were seen. No abnormalities were detected in CNS fibres or unmyelinated fibres of the PNS.

Heterozygous. The sciatic nerves of heterozygous transgenic rats contained many axons that had thin or absent myelin sheaths. The myelin sheaths that were present were well compacted with normal periodicity. The severity of abnormality was greater in the ventral nerve roots compared with the dorsal roots or the sciatic and tibial nerves. Consistent with this finding, predominantly motor (branch to the medial gastrocnemius) nerves were more severely affected than those that are predominantly sensory (distal tibial) (Sereda et al. 1996). Hypomyelination was generally more marked in larger diameter fibres, while many smaller fibres had

sheaths of normal or even increased thickness. Myelin thickness was found to be variable within a single internode. Myelin debris was only seen occasionally in Schwann cells, reactive macrophages were also only occasionally seen. At 6 wk early onion bulbs were very occasionally seen but by 6 mo they were commonly found. Axonal degeneration was rare, involving less than 1% of fibres. No abnormalities were noted in the cell bodies of the dorsal root ganglia and ventral horn or in CNS fibres.

Nerve conduction studies. At 6 wk *Pmp22* transgenic rats showed a decrease in conduction velocity and increased latency in both motor and sensory nerves. Recordings showed characteristic features which represent physiological signs of demyelination (Sereda et al. 1996).

3.2 CULTURED CELLS.

3.2.1 Myelinating cultures

By infecting rat Schwann cells with retroviruses carrying rat *Pmp22* D'Urso et al. (1997) produced Schwann cell lines which over or underexpressed *Pmp22*. *Pmp22* overexpressing (sense construct), underexpressing (antisense construct) and control Schwann cells were co-cultured with purified DRG neurons. *Pmp22* overexpression reduced the proliferation rate of Schwann cells by 60% under growth conditions in a medium which supported Schwann cell proliferation but did not allow basal lamina formation and myelination. When cultures were switched to medium which promoted myelination, *Pmp22* expression gradually increased in all cultures (D'Urso et al. 1997). *Pmp22* mRNA levels were increased in Schwann cells expressing the sense construct and slightly decreased in cells expressing the antisense construct when compared with control cultures. PMP22 immunoreactive fibres first appeared 7 d after the addition of ascorbate to the medium in all three culture types. Schwann cells in all cultures established contacts with axons, ensheathed them and formed myelin which looked normal when analysed by electron microscopy. No morphological differences were observed between control and recombinant cell-cultures in either proliferation or myelination medium. Overexpression of *Pmp22* did not affect either the onset of myelination or the expression of other myelin genes (D'Urso et al. 1997). Both P_0 and MBP immunoreactivity appeared synchronously with PMP22 and was correctly targeted to myelin membranes. PMP22 immunostaining was seen not only in the myelin sheath but also within the

cytoplasm of myelinating Schwann cells in overexpressing cultures (D'Urso et al. 1997). In contrast P_0 and MBP were localised only in compact myelin. On this basis the authors speculated that PMP22 may perform different functions in different cellular compartments during myelination. Only myelinating Schwann cells were able to target PMP22 to the plasma membrane, non-myelinating cells in overexpressing cocultures had detectable levels of PMP22 but the signal was only present in the perinuclear compartments. The authors concluded that PMP22 was not one of the key molecules involved in the early spiralling events that occur soon after a 1:1 relationship between Schwann cell and axon have been established but is more involved in controlling myelin thickness.

3.2.2. Cultured Schwann cells. Altered *Pmp22* levels significantly influenced DNA synthesis in cultured Schwann cells. In *Pmp22* overexpressing Schwann cells the level of DNA synthesis dropped to 60% of control values; conversely underexpression correlated with enhanced DNA levels (150% of control values) (Zoidl et al. 1995). Both the CD25 and the SR13 PMP22 mRNA transcripts increased as Schwann cells stopped proliferating and both were rapidly downregulated as they re-entered the cell cycle. Altered levels of *Pmp22* expression also altered the entry of quiescent cells into the cell cycle. Overexpression of *Pmp22* delayed serum and forskolin stimulated entry of resting cells from G0/G1 to the S+G2/M phase by 8 h. Cells expressing reduced *Pmp22* levels did not enter the cell cycle faster than controls, but the proportion of cells that re-entered the cell cycle was consistently higher. This suggests that low levels of *Pmp22* expression may facilitate the transition from G0/G1 to S phase for an increased number of resting cells.

The growth of Schwann cells purified from 3 d old *Pmp22* overexpressing rats (Sereda et al. 1996) showed growth characteristics very similar to control cultures. *Pmp22* transgenic Schwann cells showed no signs of premature growth arrest, and no evidence of increased apoptotic death.

3.2.3 Fibroblasts. Cultured fibroblasts overexpressing *PMP22/Pmp22* showed morphological hallmarks usually associated with programmed cell death (Fabbretti et al. 1995; Zoidl et al. 1997). These included a collapsed cellular body and condensed nuclei accompanied by cell rounding and membrane blebbing. Nuclear morphology was altered in 54% of *PMP22* overexpressing fibroblasts (Fabbretti et al. 1995). When transfected with cDNA constructs for *PMP22* point mutations (L16P, S79C, T118M) the point mutations showed a significantly decreased ability

to induce nuclear condensation and expressed normal nuclear morphology (Fabbretti et al. 1995). This decreased ability to induce morphological alterations was also found in fibroblasts overexpressing the Trembler alteration $PMP22^{Gly150A}$ (Zoidl et al. 1997). They found that the proportion of fragmented nuclei increased during the culture period in PMP22 (22% to 61%) and to a lesser extent $PMP22^{Gly150A}$ (12%-22%) overexpressing cells. This suggests that PMP22 acts in a physiological manner because intact PMP22 but not the mutant *Tr* protein promotes increased cell degeneration.

The lack of the apoptotic-like phenotype in REF-52 cells, which do not normally express PMP22, suggests a cell type specific response (Fabbretti et al. 1995). From this evidence Fabretti et al. concluded that PMP22 itself does not induce apoptosis but permits entry into a state in which apoptosis becomes more accessible (Fabbretti et al. 1995).

Elevated levels of PMP22 and $PMP22^{Gly150A}$ significantly reduced fibroblast proliferation with $PMP22^{Gly150A}$ having a less marked effect. An accumulation of cells in the G1 compartment of the cell cycle indicates that elevated expression levels prevent NIH3T3 fibroblasts from undergoing DNA replication (Zoidl et al. 1997).

3.2.4 Yeast cells. When human *PMP22* cDNAs were cloned into yeast cells northern blots showed a strong signal, while western blots did not. This was taken to mean that the PMP22 protein was degraded rapidly in yeast cells to protect the cells from its toxic effects. These toxic effects are implied by a decreased growth rate in PMP22 induced yeast cells. In contrast, following amplification of the *PMP22* gene in two human tumour cell lines, PMP22 was detected by western blot (Park et al. 1997).

Chapter 4 Mutations affecting the human *PMP22* gene

Numerically the largest class of hereditary peripheral neuropathies are those which involve both the sensory and motor components of the PNS, the hereditary motor sensory neuropathies (HMSN). These disorders have traditionally been termed Charcot-Marie-Tooth disease (CMT) following the descriptions of Charcot and Marie (1886) and Tooth (1886). Charcot-Marie-Tooth disease represents the most common inherited peripheral neuropathy. Its prevalence has been estimated to be 36 per 100,000 in Norway (Brust et al. 1978), 30 per 100,000 in Minnesota (Dyck et al. 1993) and 20 per 100,000 in the UK (Harding & Reilly 1995b)

4.1 HISTORICAL CLASSIFICATION OF INHERITED PERIPHERAL NEUROPATHIES

The CMT syndrome was originally believed to be specific for a single disorder. Symptoms listed by Charcot and Marie included progressive muscular weakness and atrophy initially involving the feet and legs and only after many years, affecting the hands and later still the forearms, together with foot deformity (usually pes cavus), vasomotor abnormalities and normal sensation (now known to be incorrect except in the 'spinal form' of CMT disease (Dyck & Lambert 1968a). The disorder described by Tooth was a peroneal type of progressive muscular atrophy whose features were similar to those listed by Charcot and Marie. It was Tooth who concluded that the disorder was due to disease of the peripheral nerves. It is now clear that the description of Charcot, Marie and Tooth was of a heterogeneous group of patients (Harding 1995a).

In 1893 Dejerine and Sottas (Dejerine & Sottas 1893) described a more severe form of peroneal muscular atrophy with progressive generalised loss of muscle function, severe sensory loss, and limb ataxia, Dejerine Sottas disease (DSD). Their patients like many CMT cases, showed marked hypertrophy of the peripheral nerves. Thus DSD and some examples of CMT disease have been referred to as hypertrophic neuropathies.

A seemingly unrelated hereditary neuropathy, hereditary neuropathy with liability to pressure palsies (HNPP) (also called tomaculous neuropathy) was recognised by Davies et al. (1954). They described an autosomal dominantly inherited, clinically homogeneous

syndrome characterised by a tendency towards repeated sensory and motor nerve palsies, brought about by minor pressure or trauma to individual peripheral nerves. The pathological hallmark of this disorder consists of multiple focal thickenings of myelin that form sausage-shaped, or tomaculous, enlargements along the nerve (Buchthal & Behse 1977).

Following the advent of nerve conduction studies in the late 1950s and 1960s it became apparent that there was heterogeneity in CMT disease for motor and sensory nerve conduction velocities. A widely used classification designates this group of disorders as hereditary motor and sensory neuropathies (HMSN). Several groups defined two main types of HMSN (Dyck & Lambert 1968a; Dyck & Lambert 1968b; Thomas & Calne 1974; Buchthal & Behse 1977). Type I HMSN (HMSNI) denotes individuals with a hypertrophic (onion bulb), demyelinating neuropathy and markedly reduced nerve conduction velocity, whereas type II (HMSNII) refers to patients with an axonal neuropathy and normal or near normal nerve conduction velocities. Dejerine-Sottas disease was designated as HMSNIII by Dyck and Lambert and defined as a severe demyelinating/hypomyelinating neuropathy with an onset in childhood and very slow nerve conduction velocities (<10 m/s) (Dyck & Lambert 1968a).

A small number of patients have a purely motor disorder, with evidence of denervated distal muscles but normal motor and sensory nerve conduction. This phenotype, the spinal form of CMT disease, runs true in families and is generally referred to as distal spinal muscular atrophy (SMA) or hereditary distal motor neuronopathy (Harding 1993). Most patients with the CMT syndrome, however, have sensory involvement.

CMT has now been adopted as the main gene symbol for the CMT syndrome (McKusick 1988). This has resulted in CMT and HMSN being used interchangeably, CMT1 is used to refer to HMSNI and CMT2 to HMSNII. This is not strictly correct, as CMT disease should include distal SMA but does not (Harding, 1995a). The underlying genetic defect has not been found for all of the HMSNs, so classifications using only "CMT" do not include all the clinical syndromes (Reilly, 1998).

4.2 CMT1 (HMSN1)

The first autosomal dominant HMSN I locus to be mapped was on chromosome I (Bird et al. 1982; Guiloff et al. 1982; Lebo et al. 1991) and suggested that CMT1 was linked to the Duffy (Fy) blood group. This type of HMSN has subsequently been found to be rare and has been termed CMT1B/HMSN1B. The human myelin protein gene (P_0) became an attractive candidate for CMT1B as it mapped to chromosome 1q22-q23 in the region of the CMT1B locus (Hayasaka et al. 1991). P_0 was known to be the major structural component of peripheral nervous system myelin (50% by weight) (Lemke et al. 1988). Analysis of P_0 as a

candidate gene for CMT1B detected point mutations in pedigrees with this disorder in four families (Hayasaka et al. 1993a; Hayasaka et al. 1993; Kulkens et al. 1993; Su et al. 1993) suggesting P_0 abnormalities are responsible for CMT1B.

At this point, families with CMT1 not linked to Duffy were designated CMT1A. The locus for the majority of cases was subsequently found to be on the short arm of chromosome 17 (Vance et al. 1989) and specifically to a duplication of the region 17p11.2-12 (Lupski et al. 1991; Raeymaekers et al. 1991). The majority of CMT1 families (>70%) have a duplication of the *PMP22* gene (type 1A, CMT1A/HMSN1A) (Raeymaekers et al. 1991; Lupski et al. 1991; Pentao et al. 1992; Wise et al. 1993; Nelis & VanBroeckhoven 1996). CMT1A is the gene symbol now used for CMT1 patients with abnormalities in the 17p11.2-12 locus, it includes both duplications and point mutations in the *PMP22* gene (Reilly 1998).

Families have since been described in which is there is no evidence for linkage to either chromosome 1 or 17 (Chance et al. 1990). These pedigrees with autosomal dominant CMT1 not mapping to chromosome 1q or 17p are designated as CMT1C.

The pattern of inheritance in other kindreds indicates x-linked inheritance (Rozear et al. 1987). The clinical features of CMTX include demyelinating neuropathy, absence of male to male transmission and a generally earlier and faster rate of progression of illness in males. In 27 CMTX families 27 different point mutations were found in the connexin32 (CX32) gene (Berghoffen et al. 1993). (Reilly, 1998). Connexin32 encodes a major component of gap junctions and is expressed in peripheral nerve (Berghoffen et al. 1993). Kindreds with CX32 mutations have been termed CMTX1 and those which are X linked but with unknown location CMTX2

Autosomal recessive inheritance, termed CMT4, has been described in HMSNI, II and III. CMT4A which features demyelination and basal laminal onion bulbs has been mapped to chromosome 8q in Tunisian families (Ben Othmane et al. 1993) and some families with a neuropathy displaying focally folded myelin (CMT4B) to chromosome 11 (Bolino et al. 1996). HMSN-Lom,, described in Gypsies, is an autosomal recessive demyelinating neuropathy associated with deafness has been mapped to chromosome 8q24 (Kalaydjieva et al. 1998). A further category is congenital hypomyelinating neuropathy (CHN). Affected individuals have a severe motor and sensory neuropathy with very reduced nerve conduction velocity or inexcitable nerves. Some cases are related to mutations in the early growth response gene (EGR2) (Warner et al. 1998).

4.3 PMP22 MUTATIONS IN CMT1A

The majority of CMT1 families (>70%) have a duplication of the *PMP22* gene (CMT1A/HMSN1A) (Lupski et al. 1991; Raeymaekers et al. 1991; Pentao et al. 1992; Wise et al. 1993; Nelis & VanBroeckhoven 1996). *PMP22* was proposed to be the candidate gene

for the CMT subtype 1A (also known as HMSN1A) on the basis of three main pieces of evidence (Suter et al. 1992).

1. The severe inherited hypomyelinating neuropathy found in the Tr and allelic Tr^J mice has been localised to mutations in the *pmp22* gene.
2. The *pmp22* gene has been localised on mouse chromosome 11 in a region of conserved synteny with the human chromosome 17 (Buchberg et al. 1991).
3. The CMT1A locus had been previously localised to a small portion of the short arm of chromosome 17 (Vance et al. 1989).

Cloning and subsequent analysis of this DNA fragment from affected individuals revealed that the major structural defect was a tandem intrachromosomal duplication of approximately 1.5Mb (Lupski et al. 1991; Raeymaekers et al. 1991). The human gene for *PMP22* has subsequently been analysed by several groups confirming that the entire *PMP22* gene is contained within the 1.5Mb duplicated region of chromosome 17 (17p11.2-17p12) (Matsunami et al. 1992) (Patel et al. 1992; Timmerman et al. 1992; Valentijn et al. 1992). The occurrence of cases with a duplication of *PMP22* predicted others in which it was deleted or mutated. Deletion of 17p11.2 was established by Chance et al. (1993) and is associated with hereditary neuropathy with liability to pressure palsies (HNPP). While some point mutations in *PMP22* give rise to a CMT1 phenotype (Valentijn et al. 1992; Roa et al. 1993b; Marrosu et al. 1997; Nelis et al. 1994; Valentijn 1995; Navon et al. 1996; Ionasescu et al. 1997b) others have been found in association with the severe congenital hereditary peripheral neuropathy DSD/HMSNIII (Roa et al. 1993a; Valentijn et al. 1995; Tyson et al. 1997).

Several lines of evidence support the hypothesis that *PMP22* is the main dosage sensitive gene within the CMT1A duplication and HNPP deletion. First, the finding of a CMT1A-like phenotype in several patients with partial trisomies that encompass the CMT1A-HNPP locus (Chance et al. 1992; Lupski et al. 1992; Ionasescu et al. 1993; Palau et al. 1993; Upadhyaya et al. 1993; Valentijn et al. 1993; Roa et al. 1996) One particular CMT1A family has been found to carry a small duplication of only 460 kilobases (Valentijn et al. 1993). As this particular duplication still includes the entire *PMP22* gene, it excludes most of the other genes present in the 1.5Mb CMT1A duplication from further consideration (Valentijn et al. 1993). Secondly a Dutch family with a severe inherited peripheral neuropathy, known to be linked to the *PMP22* gene but without the duplication, was found to have the same mutation as the Tr^J mouse (Valentijn et al. 1992). Thirdly, a 2bp frame-shifting deletion within the first translated exon of *PMP22* has been found to be associated with HNPP (Nicholson et al. 1994). This mutation would be expected to generate a null allele. The similarity of the

phenotypes generated by this mutation and the HNPP deletion directly implicates *PMP22* as the critical gene in HNPP.

Table 4.1 Duplications encompassing the *PMP22* gene associated with CMT1A

1.5 Mb duplication on the short arm of chomosome 17. (17p11.2p12)	(Raeymaekers et al. 1991) (Lupski et al. 1991)
Alternatively sized 17p duplications that encompass the *PMP22* gene	(Feldman et al. 1982) (Magenis et al. 1986) (Chance et al. 1992) (Lupski et al. 1992) (Upadhyaya et al. 1993) (Valentijn et al. 1993) (Ionasescu et al. 1993) (Palau et al. 1993) (Roa et al. 1996) 2 cases
Homzygous 17p duplication	(Lupski et al. 1991) (LeGuern et al. 1997) (Sturtz et al. 1997)

The size of the region which is duplicated or deleted in CMT1A and HNPP is quite consistent in multiple unrelated and ethnically diverse families (Chance et al. 1993; Lupski et al. 1991; Matsunami et al. 1992; Patel et al. 1992; Roa et al. 1995; Wise et al. 1993) and even *de novo* duplication or deletion patients (Wise et al. 1993; Chance et al. 1994; Lorenzetti et al. 1995). This implies a precise recombination event generating both the CMT1A duplication and the HNPP deletion. CMT1A and HNPP appear to be the result of a reciprocal unequal crossing over at meiosis mediated through the misalignment of homologous repeated sequences that are flanking the normal 1.4Mb monomeric region (Chance et al. 1994).

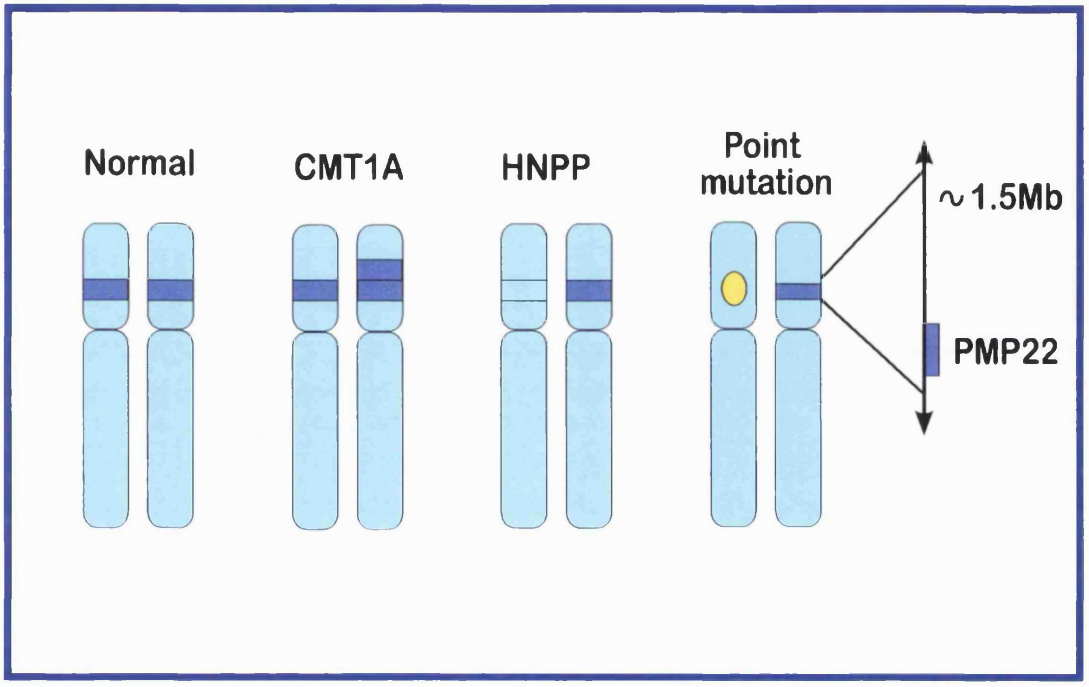

Fig 4.1 Diagram of the mutational mechanisms in the human *PMP22* gene

This mutational mechanism explains the high incidence of CMT1A (and probably HNPP) in the population and constitutes the first example of two human disorders with a Medelian pattern of inheritance that are the reciprocal results of an unequal crossing-over involving large internal chromosomal segments. Studies in *de novo* CMT1A duplication patients suggest that this unequal crossing over event is overwhelmingly of paternal origin (Palau et al. 1993). Reiter et al (1996) identified a hot spot for homologous recombination within the CMT1A repeat sequences (Reiter et al. 1996). Sequence analysis found that these regions had a significant homology to an insect transposon protein (African malaria protein mariner transposase gp/L10440). The region is thought to be transcribed into an RNA product but probably not transcribed into a functional transposase and the authors suggest several ways in which the transposon like element could mediate an increase in homologous recombination between the CMT1A repetitions. The putative transposon like element from the CMT1A repeat sequence was used as a probe; a low level of expression was found in the testis but no expression was found in the ovaries (Reiter et al. 1996). This may provide and explanation for the predominant paternal inheritance pattern common to CMT1A and HNPP.

4.4 CMT1A 17P11.2-12 DUPLICATION

Clinical presentation of patients with the 17p11.2-12 duplication. Only a modest percentage of patients (<10%) with HMSN I are thought to seek the help of a physician or neurologist, which suggests that many have few or no symptoms (Dyck et al. 1993).

Thomas et al. (1997) reported the clinical features of 61 patients with confirmed *PMP22* duplication. Thirty four of the cases were considered to have classical CMT syndrome. Evidence of HMSN was initially detected within the first decade of life in 75% of patients, 10% were noted during the second and only 7% in the third. The most consistent clinical abnormality was muscle wasting and weakness which was more prominent distally. Weakness in the limbs was usually associated with loss of tendon reflexes and foot deformity. If sensation was impaired it was distally accentuated and mild/moderately severe. Eight patients with confirmed 17p11.2-12 duplication displayed a prominent upper limb postural tremor associated with tendon areflexia, pes cavus and variable distal weakness and sensory loss, features typical of Roussy-Lévy syndrome. Additional features seen in association with classical CMT included CNS signs, associated focal peripheral nerve lesions, prominent muscle cramps, IgM paraproteinaemia, diabetes mellitus, parkinsonism. Some of these may be chance associations. Some patients with Roussy-Levy syndrome also had other symptoms including focal peripheral nerve lesions and hypertrophic cardiomyopathy. Other unusual presentations included neuropathy with prominent sensory loss, neuropathy with cramps, calf hypertrophy and atypical neuromyotonia. One patient was asymptomatic

LeGuern et al. (1997) studied a consanguinous CMT1 family with 4 affected siblings 3 of whom were homozygous for the 17p11.2-12 duplication and one who was heterozygous. The disease was variable among the homozygotes, one of whom was no more severely affected than the heterozygote. In another case an 8 year old homozygous child had a more severe clinical phenotype that his two heterozygote siblings but his MNCVs were in the same range as heterozygous CMT1A patients possibly due to his young age (Sturtz et al. 1997). Yet another patient carrying four copies of the *PMP22* gene had a severe disorder reported to resemble DSD (Lupski et al. 1991; Kaku et al. 1993). This suggests that the severity of the disease is not determined solely by the number of copies of the *PMP22* gene (LeGuern et al. 1997).

Pathological features of patients with the 17p11.2-12 duplication. Many authors have described pathological changes in HMSNI patients (Dyck et al. 1970; Dyck et al. 1968; Dyck & Lais 1970; Smith et al. 1980). As these are now known to be a

heterogeneous group of patients the summary of the pathology presented here will be limited to recent studies in which patient genotypes have been confirmed.

Thomas et al. (1997a) examined biopsies of 10 patients with confirmed 17p11.2-17p12 duplication. All showed a decrease in myelinated nerve fibre density (0.003% to 13% of control values). A study by Gabreëls-Festen et al. (1995) also found decreased myelinated fibre densities, but to a lesser degree (11-50% of control values). The difference in the degree of density decrease had been attributed largely to the different age spectra examined in the two studies. The majority of the patients (90%) studied by Thomas et al. (1997) were over 25 y, whereas in the study by Gabrëels-Festrn et al. (1995) the oldest patient examined was 26 y. From these two studies it appeared that the density of myelinated fibres decreased progressively with age. This theory is not supported by a recent study in which the density of myelinated fibres did not appear to differ between patients in three age groups (<15y, 16-44y and >45y) (Fabrizi et al. 1998).

Density decreases can in part be attributed to the hypertrophic changes in the nerves of patients, fasicular areas being increased by 100-400% (Gabreëls-Festen et al. 1995). As fascicular area does not appear to change with age Gabrëels-Festen considered that this implied a degree of fibre loss in older patients. The data from the Fabrizi study does not support this (Fabrizi et al. 1998).

Onion bulbs, typically consisting of concentrically proliferating Schwann cells surrounding a central myelinated axon or a cluster of regenerating axons, were reported by Thomas et al. (1997a) as being most evident in cases with higher myelinated fibre densities. This is in contrast to what was found in the younger patients where onion bulbs were found to increase in number with age, and decreasing myelinated fibre densities (Gabreëls-Festen et al. 1995). In the Fabrizi study neither the myelinated fibre or onion bulb densities altered with age (Fabrizi et al. 1998). It is likely that the incidence of onion bulbs increases progressively during childhood and adolescence and later regresses.

Changes in the thickness of the myelin sheath also appear to be age related. In the older patients examined by Thomas et al. (1997a) there was an increase in the proportion of thinly myelinated fibres when compared with controls (mean g ratio: patients =0.66, controls=0.58). However g ratios in younger patients suggested thickening of the myelin sheath (mean g ratio: patients =0.56, controls=0.66) (Gabreëls-Festen et al. 1995). An increase in myelin sheath thickness has previously been reported for HMSN patients (Nukada et al. 1983). The Fabrizi paper again differs from the other two, finding no difference in g ratios with age and a decrease in the percentage of demyelinated internodes with age (Fabrizi et al. 1998). Gabreëls-Festen et al. (1995) recorded active demyelination during childhood, whereas this is rare in adults.

Motor nerve conduction velocities in the lower limbs of CMT duplication patients were examined by Thomas et al. (1997). When they were obtainable, velocities in the lower limbs had a mean value of 17 m/s. In the upper limbs this value was 19.9 m/s. Sensory nerve action potentials were usually absent or severely depressed. Killian et al. (1996) examined 8 patients from a single pedigree with a proven CMT1A duplication and demonstrated that the MNCVs did not change appreciably over 22 years.

Ultrastructural localisation of PMP22 in CMT1A nerves. Although CMT1A nerves have significantly less myelin than normal nerves PMP22 was found to be present within compact myelin of the remaining myelin sheaths, even those with a reduced diameter (Haney et al. 1996). There was no evidence suggesting that myelin in CMT1A nerves was abnormal in periodicity or compaction, neither was there any evidence for abnormal intracellular accumulations of PMP22 protein (Haney et al. 1996). Based on these observations, it is apparent that the CMT1A phenotype does not prevent delivery of P_0 or PMP22 to compact myelin (Haney et al. 1996). In CMT1A nerves Schwann cell processes surrounding or associated with unmyelinated axon bundles or collagen pockets, were also PMP22 positive. In CMT1A patients PMP22 immunoreactivity was associated with both the axonal and adaxonal Schwann cell membranes. Schwann cell membranes comprising the layers of the classical onion bulbs in CMT1A nerves also contain PMP22 immunoreactivity, mostly located near the Schwann cell plasma membrane.

4.5 *PMP22* POINT MUTATIONS IN CMT1A

The finding of CMT1A patients with point mutations in the *PMP22* gene confirmed evidence that PMP22 has a primary role in the CMT1A phenotype (Valentijn et al. 1992; Roa et al. 1993b). A common feature of *PMP22* point mutations found so far in CMT1A, DSD, *Tr, Tr-ncnp* and Tr^J is their location in putative transmembrane domains. Because these domains are the most strongly conserved parts, evolutionarily, of the PMP22 protein it has been speculated that the membrane associated regions are significant to the proper function of PMP22 (Patel et al. 1992).

The 17p11.2-12 duplication and point mutations in the *PMP22* gene result in overlapping clinical and neurophysiological phenotypes, although generally the phenotype of the point mutations is more severe (Gabreëls-Festen et al. 1995). Gabreels-Festen et al. (1995) compared the morphological phenotype of 12 cases of CMT1A duplication with 4 cases of point mutations in the *PMP22* gene. Three patients from one family had the Leu 16 Pro substitution (as found in the Tr^J mouse) and the other patient a Leu105 Arg substitution (Valentijn et al. 1992; Valentijn 1995).

The reduction in myelinated fibre density showed a large degree of overlap between the two genotypes but on average was more severe in the cases with point mutations. In duplication patients the density of myelinated fibres was reduced to 31% of normal values whereas in patients with point mutations it was reduced to only 17% of control values. Small onion bulbs were present in approximately 30% of the myelinated fibres in younger duplication patients (3-5y); this proportion increased to 90% of fibres in older patients. In cases with point mutations onion bulbs were abundantly present from an early age surrounding nearly all fibres. This is thought to indicate an early, even prenatal, demyelinating process (Gabreëls-Festen et al. 1995). In *PMP22* duplicated cases the mean g-ratio was significantly lower than normal, implying that on average the myelin sheath exceeds normal thickness, despite the presence of demyelinated and incompletely remyelinated fibres. In contrast the average g-ratio in point mutations was 0.85, which means that nearly all fibres are demyelinated or severely hypomyelinated in relation to axonal diameter.

Table 4.2 ***Point mutations in the PMP22 gene associated with CMT1A***

Mutation	First identified by	Further details
L16P	(Valentijn et al. 1992)	Allelic heterogeneity was first noted by Hoogendijk 1993 (Hoogendijk et al. 1993) Transmembrane domain 1
S79C	(Roa et al. 1993b)	Transmembrane domain 2
L105R	(Valentijn 1995)	Transmembrane domain 3
Val107Gly	(Marrosu et al. 1997)	Transmembrane domain 3
T118M (recessive)	(Roa et al. 1993a)	It has recently been suggested that this mutation is a polymorphism (Nelis et al. 1997)
L147R	(Navon et al. 1996)	Transmembrane domain 4
G to A change at the first nucleotide of intron 3	(Nelis et al. 1994)	5' splice site mutation
Deletion of one nucleotide at position G330	(Ionasescu et al. 1997b)	Predicted to be associated with a frameshift mutation

4.6 PMP22 MUTATIONS IN DEJERINE-SOTTAS DISEASE

Dejerine-Sottas disease (DSD; alternatively known as HMSN III or hypertrophic neuropathy of infancy) is a severe infantile and childhood onset, hypertrophic demyelinating/ hypomyelinating neuropathy. Gabreels-Festen et al. (1994) stated that the disease was characterised by a chronic demyelinating motor and sensory neuropathy without CNS involvement, congenital or infantile onset, motor nerve conduction velocities of less than 6 m/s in all nerves and normal parents. The clinical features of DSD overlap with severe CMT1A. In the Dutch kindred described by Hoogendijk et al. (1993), later found to have the L16P mutation (Valentijn et al. 1992), the symptoms in most patients were severe and they would be given the diagnosis of HMSNIII (Tyson et al. 1997).

As in HMSNI the DSD phenotype has recently been shown to consist of more than one entity. Some cases are probably nongenetic phenocopies consisting of chronic imflammatory demyelinating polyneuropathy (Gabreëls-Festen & Gabreëls 1993). Others have been shown to be associated with de novo mutations of the *PMP22* (Roa et al. 1993a) or P_0 genes (Hayasaka et al. 1993b). They have been referred to as Dejerine-Sottas disease A and B respectively. Some authors consider it uncertain whether the DSD category should be retained or whether case may be better classified in terms of the specific mutation.

Many patients with DSD appear to represent sporadic cases and were traditionally presumed to result from an autosomal recessive gene. Yet all the mutations studied to date have been present in the heterozygous state suggesting that DSD may be caused by dominantly acting genetic defects which are often *de novo* mutations.

Molecular genetic data have made it clear that the pathogenesis of HMSN III is not distinct. Patients have severe peripheral neuropathy but this is not specific to any particular type of inherited or acquired demyelinating neuropathy (Chance & Fischbeck 1994).

Clinical features of DSD patients with *PMP22* mutations. DSD is characterised by generalised muscle weakness and atrophy especially in distal muscles, tendon areflexia and sensory loss. Typically motor development is much delayed in infancy; skeletal deformities including kyphoscoliosis are common.

Table 4.3 Point mutations in the *PMP22* gene associated with DSD

Mutation	First Identified by	Further details
H12Q	(Valentijn et al. 1995)	Transmembrane domain 1. Patient first described by (Ouvrier et al. 1987) case 13
M69K	(Roa et al. 1993a)	Transmembrane domain 2. Patient described (Dyck 1966) PATIENT III.2, kinship 5-13
S72L	(Roa et al. 1993a)	Transmembrane domain 2. Different families described by (Ionasescu et al. 1995) and (Marques et al. 1998)
Ser 72 Trp	(Tyson et al. 1997)	Transmembrane domain 2.
S76I	(Tyson et al. 1997)	Transmembrane domain 2.
S79C	(Roa et al. 1993b) CMT1A phenotype	Not thought to generate a change in secondary structure
S79P	(Bort et al. 1998)	Could act by destabilising the backbone torsional angles leading to a modification of structure in 2o domain. More aggressive phenotype than S79C
L80 2 bp deletion	(Ikegami et al. 1998)	Altered reading frame to produce a 49aa longer protein
Leu 80 Pro	(Tyson et al. 1997)	Transmembrane domain 2.
Deletion of Phe 84	(Silander et al. 1998)	
G100R	(Marques et al. 1998)	Transmembrane domain 3
G150D	(Ikegami et al. 1998)	Transmembrane domain 4
point mutation (intron 2)	(Muglia et al. 1998)	
Gln to Aspartic acid nucleotide 498 of the cDNA	(Ionasescu et al. 1997a)	Mother and son with the same point mutation

Table 4.4 Summary of the clincial features of DSD patients with *PMP22* mutations

	FIRST WALKED	AREFLEXIC	ATAXIC	MUSCLE WEAKNESS	SENSORY DEFICIT	ENLARGED NERVES
Met69Lys	15mo		Yes	Yes	Yes	Yes
Ser72Leu	7y	Yes		Yes	Yes	
	24mo			Yes	Yes	
	never walked unsupported	Yes		Yes	No	No
His12Gln	2y	Yes	Yes	Yes	No	Yes
Ser 76 Ile	5yr	Yes		Yes	Yes	Yes
Ser 72 Try	2y	Yes		Yes	Yes	No
	3y	Yes		Yes	Yes	No
Ser 79 Pro	not at 3y	Yes		Yes		
Leu 80 2bp deletion	7y	Yes		Yes	Yes	
Leu80 Pro	11y	Yes		Yes	Yes	Possible
Gln498Asp	6y	Yes		Yes	Yes	
Gly 150 Cys	Normal	Yes		Yes	Yes	

Pathology of DSD patients with known *PMP22* mutations. Morphological studies have been undertaken on a limited number of patients. The results are summarised below.

Table 4.5 Summary of the pathology of DSD patients with *PMP22* mutations

	Increased fascicle area	Decreased myelinated fibre density	Hypomyelination	Onion bulbs	Largest fibres
Met69Lys	Yes	Yes	g ratio = 0.85	Yes	4μm
	Some large axons with no myelin				
His12Gln	Yes	Yes	g ratio = 0.85	83%	8μm
	Normal density of unmyelinated fibres				
Ser76Ile		Yes		No	
	Excess collagen				
Ser 72 Try		Yes	Yes	Many	
	Nerve largely occupied by onion bulb formations occasionally with a demyelinated or thinly myelinated axon at their centre				
Ser 72 Leu			Yes	Yes	
Ser 79 Pro			Yes	Yes	
	Evidence of segmental demyelination and remyelination				

4.7 INHERITED LIABILITY TO PRESSURE PALSIES (HNPP)

Hereditary neuropathy with liability to pressure palsies (HNPP; also called tomaculous neuropathy or recurrent pressure-sensitive neuropathy) is an autosomal dominant disorder that produces an episodic, recurrent demyelinating neuropathy (Windebank 1993). The HNPP locus has been assigned to chromosome 17p11.2-12 (Chance et al. 1993) and is associated with a 1.5Mb deletion. HNPP and CMT1A are thought to be the reciprocal products of unequal crossing over during meiosis. The 17p11.2 duplication is the most common cause of HNPP. It has been detected in 13/13 Finnish, 3/3 Belgian, 7/7 French, 15/22 Dutch and 19 British patients from 12 of 13 families in which HNPP had been considered the most likely diagnosis (Silander et al. 1994; Verhalle et al. 1994; LeGuern et al. 1994; Mariman et al. 1994b; Tyson et al. 1996). Point mutations in the *PMP22* gene have

also been recorded. It is clear that defects in *PMP22* are not exclusively responsible for HNPP. Linkage to 17p11.2 has been excluded in one of the seven non deletion Dutch families (Mariman et al. 1994a). In one patient with typical clinical features of HNPP (Tyson et al. 1996) sequencing of the *PMP22* gene subsequently proved to be normal (Thomas et al. 1996).

Clinical presentation HNPP generally develops during adolescence and may cause attacks of numbness, muscular weakness and atrophy. Peroneal palsies, carpal tunnel syndrome and other entrapment neuropathies are frequent manifestations of this disorder. Motor and sensory nerve conduction studies usually show evidence of an underlying generalised neuropathy, with moderate slowing of conduction velocities and prolonged distal motor and sensory latencies. Nerve biopsy specimens show segmental demyelination and remyelination, focal myelin thickenings (tomacula) and a variable degree of axonal loss (Windebank 1993; Verhagen et al. 1993).

Pathological features of patients with HNPP. Peripheral nerve pathology has not been specifically reported in patients with confirmed 17p11.2 deletions. The following accounts of nerve pathology may be assumed to largely, but not exclusively, pertain to HNPP deletion patients.

The most distinctive feature of HNPP is the presence of sausage-shaped enlargements of the myelin sheath (tomacula: discussed in chapter 3.1.1) (Behse et al. 1972: Madrid & Bradley 1975). Windebank (1993) summarised histological findings of 25 nerve biopsies (largely sural nerve) from HNPP patients. In 17 of them focal thickening of the myelin sheath is reported and although not specifically commented on, suggested in photographs of two others. Six cases did not show these changes but showed non-specific findings with either extensive loss of fibres or excessive variability in thickness and length of myelin internodes, suggesting recurrent demyelination and remyelination. Generally the cases where tomaculous changes are not found are those which have a more advanced neuropathy and the major changes have included extensive fibre loss or demyelination and remyelination (CruzMartinez et al. 1997). A teased fibre study by Behse et al. (1972) demonstrated focal thickenings in 12.5 to 27.5% of fibres and serial photographs suggested that the axonal area was reduced in these regions. Tomacula are not specific to HNPP and may be found in other neuropathies (Thomas et al. 1996; Windebank 1993). Nerve biopsy specimens also show segmental demyelination and remyelination, focal myelin thickening and a variable degree of axonal loss (Windebank 1993; Verhagen et al. 1993).

In a study of six HNPP patients, both myelinated and unmyelinated fibre counts fell within the normal range (Behse et al. 1972). There appeared to be a relative shift to a population of

smaller diameter myelinated fibres in the affected cases compared with controls. The mean g ratios of ten patients with HNPP were examined by Gabreels-Festen et al. (1995) and found to average 0.63, which is slightly but not significantly below the normal values for age (0.66). The presence of only one PMP22 gene copy appears sufficient for normal myelination formation in view of the normal g ratios (Gabreëls-Festen et al. 1995).

Table 4.6 Point mutations in the *PMP22* gene associated with HNPP

Mutation	First identified by	Further details
Val 30 Met	(Chen et al. 1998)	
Insertion at codon 94	(Lenssen et al. 1998)	Predicted to result in an enlarged protein of 221 aa
Guanosine insertion at codon 94	(Young et al. 1997)	Predicted to result in a reading frameshift and a delayed termination signal
Nonsense mutation at codon 124	(Pareyson & Taroni 1996)	Predicted to result in a truncated protein
A 1 nucleotide deletion in the Leu 145 codon	(Taroni et al. 1995)	Predicted to result in a premature stop codon and to result in a truncated protein
2bp frameshifting deletion in first exon	(Nicholson et al. 1994) erratum appears in Nature Genetics (1994) 7:113	Predicted to result in a truncated protein
G to T mutation in the 5' donor splice site	(Bort et al. 1997)	

4.8 EXPRESSION OF THE *PMP22* GENE IN CMT1A AND HNPP

Expression of the *PMP22* gene in CMT1A nerves has been examined by two sets of authors. Consistent with the overexpression of the gene,Yoshikawa et al (1994) reported that *PMP22* mRNA was overexpressed in CMT1A nerves when normalised to P_0 mRNA levels. This is supported by an ultrstructural immunocytochemical study in which PMP22 levels were increased in CMT1A and decreased in HNPP patients when compared with controls (Vallat et al. 1996). In contrast, an immunochemical and reverse transcriptase polymerase chain reaction (RT-PCR) study of *PMP22* in CMT1A nerves, reported that total PMP22 protein

and mRNA expression was reduced in diseased compared to normal nerves (Hanemann et al. 1994). The apparent difference in the findings of the two studies may be related to the way the results were expressed. It is likely that both the P_0 and PMP22 levels are decreased in affected nerves reflecting the small amount of myelin formed, with the relative expression of PMP22 being higher than normal. Schenone et al. (1997) examined the sural nerves of HNPP deletion patients and found lowered PMP22mRNA levels. As there was no decrease in P_0 mRNA this demonstrates that decreased dosage of *PMP22* is the most likely pathogenic mechanism in HNPP and directly related to a decrease in *PMP22* gene product and not to the underlying demyelinating process (Schenone et al. 1997). PMP22 protein expression was examined relative to P_0 and MBP levels in CMT1A duplication and HNPP patients (Gabriel et al. 1997). When compared with controls PMP22 protein expression was increased in duplication and decreased in HNPP patients.

Chapter 5 Wallerian degeneration and regeneration

5.1 WALLERIAN DEGENERATION

The classical description of the sequence of events that occur when peripheral nerves are transected was made by Waller (1850). He examined and described the microscopic appearance of the hypoglossal and glossopharyngeal nerves of the frog following nerve section.

> *" At the end of the third or fourth day, we detect the first alteration by a slightly turbid or coagulated appearance of the medulla (*myelin sheath*). On the tenth day and upwards...the coagulated particles lose their amorphous structure and assume a granulated texture. About the twentieth day the medullary particles are completely reduced to a granular state....the presence of the nervous element merely indicated by numerous black granules, generally arranged in a row like the beads of a necklace"*
>
> *Waller 1850*

Many subsequent studies have documented different aspects of the breakdown of axons and the progressive degeneration of the myelin sheath (Ramón y Cajal 1928; Nageotte 1932; Holmes & Young 1942; Lubinska 1982) which results in either fibrosis or axonal and myelin regeneration.

5.2 AXONAL CHANGES

Following crush or transection injury the first visible change in the axon is the fragmentation of the endoplasmic reticulum into rows of vesicles. Between 24 and 48 h neurofilaments lose their longitudinal orientation, undergo dissolution and are replaced by a finely granular material which subsequently becomes clumped, lying within a clear matrix (Vial 1958; Honjin et al. 1959). The triggering event for axonal degeneration appears to be an intracellular increase in calcium concentration. Axonal disintegration is mediated by calcium sensitive proteases that are intrinsic to the axon (Schlaepfer 1974; Schlaepfer 1977). After nerve transection, axons continue to conduct for a variable period of time depending upon

the length of the distal stump and the species of animals examined. (Griffin & Hoffman 1993). In the mouse C57BL6/Ola substrain axons survive for long periods of time (over 28 days) after nerve transection (Lunn et al. 1989). This trait is under the control of a single dominant gene and the responsible defect appears to lie in the in Ola axon itself. The breakdown of axonal integrity varies with species but corresponds with the loss of its capacity to generate and conduct a nerve action potential (Griffin & Hoffman 1993).

5.3 SCHWANN CELL RESPONSES

Changes in the myelin sheath. During the first 24 h following axotomy there are few visible alterations in the distal stump. There is a rapid decrease in the synthesis of myelin lipids (White et al. 1989) and a down regulation in the levels of myelin protein mRNAs (Trapp et al. 1988). The first visible sign of the onset of myelin degeneration is the retraction of the myelin sheath from the nodes of Ranvier and the development of a wrinkled outline in the myelin sheath (Webster 1965). At the Schmidt-Lanterman incisures there is a widening of the incisural intraperiod line gap together with a splitting of the intraperiod line in the myelin adjacent to the incisure. The myelin sheath then collapses into these spaces and is progressively broken down into smaller 'digestive chambers' or 'ellipsoids' which are degraded along with the remnants of the axoplasm and axolemma. This process begins in the Schwann cell perikaryon and in the Schmidt -Lanterman incisures; the myelin ellipsoids are then increasingly divided into smaller fragments and finally spherical droplets (Webster 1965). Some of these droplets are situated within Schwann cell cytoplasm; others lie within the basal laminal tube (Thomas 1964). During the course of the progressive breakdown of myelin debris, Schwann cell processes become interlaced within the original basement membrane. Within two weeks of sustaining injury these processes develop cytoskeletal structure characterised by an increase in the number and density of intermediate filaments. Three weeks following injury most of the myelin in rodent nerve has been cleared. Following the removal of the myelin and axon debris the Schwann cell basal laminal tubes persist (Thomas 1964). The distal stump contains columns of Schwann cells enclosed within the tube of the old Schwann cell basement membrane, collectively named the bands of Büngner.

Schwann cell proliferation. In normal and intact myelinated and unmyelinated fibres Schwann cell division is rare (Asbury 1967). Following nerve transection, while myelin breakdown is taking place, Schwann cells throughout the distal stump undergo a series of mitosies within basal laminal tubes (Abercrombie & Johnson 1946; Abercrombie et al. 1959; Archer & Griffin 1993; Thomas 1948). The prelude to mitosis is a phase of "hypertrophy" of the Schwann cell perikaryon. The perikaryon occupies the whole cross sectional area of the

nerve fibre, during this process the myelin sheath is divided into two halves (Stoll et al. 1989). Division occurs longitudinally and as a result the two daughter nuclei are adjacent to each other encircled by their own Golgi apparatus and granular endoplasmic reticulum. With each subsequent division the Schwann cell nuclei become increasingly scattered throughout the old internode. In contrast to Schwann cell behaviour during segmental demyelination, Schwann cells do not leave the basal laminal tube during Wallerian degeneration in vivo (Griffin & Hoffman 1993).

During Wallerian degeneration in the sciatic nerve of the rabbit, the number of intratubal nuclei (Schwann cell and macrophage) increases to a maximum at around 25 d after section (Abercrombie & Johnson 1946). At this stage nuclei are 13.4 times more numerous than in uninjured nerve. This initial increase is followed by a rapid decline in numbers and by 225 days after section the number of nuclei appears to be stable at 7.3 times basal levels. Thomas (1948) examined the nuclear population in the nerve to the medial head of the gastrocnemius muscle (ngm) which consists mainly of large fibres and compared it with the sural nerve which consists mostly of small fibres. The nuclear populations showed the same general trend with an increase in nuclei number up to 25 d and then a decline. At its maximum the number of intratubal nuclei in the ngm had increased to 17 times that of control values whereas in the sural nerve the increase was only five times. The peroneal nerve, with an intermediate fibre size spectrum, showed an intermediate level of nuclei increase. Thomas (1948) considered that there was a relation between nuclear multiplication and the amount of degenerating myelin in the nerve. Abercrombie et al. (1959) and colleagues examined the proliferation of Schwann cells in unmyelinated fibres in the abdominal vagus nerve of the rabbit. They found a 60% increase in nuclei number during the first 5 days after transection and then a decline beginning 10 days after injury. Twenty five days after nerve injury the numbers of Schwann cell nuclei had decreased to near normal levels.

The stimuli for Schwann cell division in Wallerian degeneration remain to be defined. The onset of mitogenesis is synchronous in the Schwann cells of myelinated and unmyelinated fibre populations (Clemence et al. 1989; Archer & Griffin 1993) and also in several other cell types including fibroblasts, endothelial cells and mast cells. That the mitogenic stimulus affects Schwann cells of unmyelinated fibres even though their axons are intact was demonstrated by Archer & Griffin (1993). Transection of the L5 ventral root, which contains only myelinated fibres, results in wallerian degeneration of these fibres throughout the sciatic nerve with an associated proliferation of Schwann cells. No unmyelinated fibres are injured in the transection yet the Schwann cells of many of the unmyelinated fibres in the sciatic nerve proliferate. This observation strongly suggests that at least some of the stimuli from Schwann cell proliferation are diffusible.

Wood & Bunge (1975) first reported that when a mitotically quiescent population of Schwann cells was presented to neurites in vitro, the Schwann cells proliferated vigorously. This was corroborated with an in vivo model which demonstrated that Schwann cells in the reinnervated distal stump undergo mitosis coincident with the arrival of regenerating axons (Pellegrino & Spencer 1985). Many trophic factors that signal and/or trigger Schwann cell mitosis have been identified in cell culture studies.

In mature nerve and in established co-cultures Schwann cells eventually cease to proliferate even in the continued presence of neurons (Salzer & Bunge 1980; Muir et al. 1990). Even though cultured Schwann cells can produce a number of potential autocrine mitogens (laminin, glial maturation factor, transforming growth factor -β) they remain virtually quiescent even in high cell density, long term cultures. Muir et al (1990) demonstrated that Schwann cells negatively regulated their own proliferation by showing that conditioned media from Schwann cell cultures inhibited the proliferation of mitogen-stimulated test cultures.

Siironen et al. (1994) compared Schwann cell proliferation following nerve transection under three different conditions. The continuous presence of axons (proximal stump), loss of axonal contact and subsequent reinnvervation (distal stump) and after permanent loss of axonal contact (denervated distal stump). The extent of Schwann cell proliferation was found to be similar with and without axonal innervation. Siironen et al (1994) concluded that during the first 56 d after rat sciatic nerve section proliferation is regulated by degenerative or nerve trauma associated factors rather than 'regenerative mitotic factors'.

Table 5.1 Factors that are known to either signal or trigger Schwann cell mitosis

Trophic factors	
• Leukocyte derived factor	(Lisak et al. 1985)
• Growth factors	(Davis & Stroobant 1990)
• Platelet derived growth factor	(Yong et al. 1988)
• Glial maturation factor	(Bosh et al. 1984)
• Transforming growth factors $ß_1$ and $ß_2$	(Ridley et al. 1989)
• Fibroblast growth factor	(Davis & Stroobant 1990)
Factors which raise intracellular cAMP levels	
• Cholera toxin	(Muir et al. 1989)
• Forskolin	(Sobue et al. 1986)
	(Stewart et al. 1991)
Extracellular matrix components	
• Laminin	(Muir et al. 1989)
• Fibronectin	
Myelin fractions/degradation products	(Komiyama & Suzuki 1992)
• Myelin fractions	(Perry et al. 1987).
• Myelin degradation products	(Baichwal & DeVries 1989)
• MBP processed by macrophages	
Axolemmal fragments	
• Tissue culture studies	(Dent et al. 1992; Ratner et al. 1985; Ratner et al. 1988; Sobue et al. 1984; Wood & Bunge 1975)
• in vivo	(Pellegrino & Spencer 1985)

5.4 MACROPHAGE RESPONSE. Normal peripheral nerves contain a population of resident macrophages which are usually found closely associated with blood vessels. Two-three days after nerve injury the number of macrophages increases dramatically although the resident population only responds to a limited extent (Stoll et al. 1989; Hann Bonnekoh et al. 1989). Evidence suggests that the majority are recruited from the circulation. These macrophages migrate specifically to degenerating fibres and are so closely associated with them that they are isolated with the degenerating fibre during teasing (Stoll et al. 1989). Williams and Hall (1971a) identified three main cell populations within the endoneruial space distal to a crush site at 7 d after injury: these were the original Schwann cells containing myelin ellipsoids, small electron dense gobules and axonal remnants. Cells identified as newly differentiating Schwann cells containing 'active' cytoplasm and a few small dense globules and globule containing macrophages. Macrophages were not implicated in the initial lysis of myelin but arrived when myelin breakdown was already microscopically evident. Degenerating myelin has been shown to be important in macrophage recruitment. In the Ola mouse axonal degeneration is markedly delayed, as a result myelin breakdown and macrophage recruitment are also delayed (Lunn et al. 1989). During lysophosphatidyl choline induced demyelination in the Ola mouse macrophages are recruited into the nerve in the absence of axonal breakdown (Hall 1993).

The relative roles of the Schwann cell and the macrophage in the early and late catabolism of degenerating myelin in the PNS are still controversial (Goodrum et al. 1994). Studies of nerve segments degenerating in situations that exclude macrophages suggest that the macrophage has an essential and exclusive role in myelin degradation (Beuche & Friede 1984; Crang & Blakemore 1986). Beuche and Friede (1984;1986) demonstrated that macrophages participate in phagocytosis of large degenerating nerve fibres. When nerves were allowed to degenerate within millipore filters within the abdominal cavity, myelin debris remained for weeks as the pore sizes were to small too admit macrophages; larger pore sizes resulted in prompt myelin clearance. Information from morphological studies of cell types containing myelin debris and lipid droplets following nerve crush suggest that the Schwann cell is solely responsible for the absorption and degradation of degenerating myelin (Boyles et al. 1990). Immunochemical determination of cell types combined with morphology concluded that the Schwann cell participates in the early degradation of myelin, but the macrophage is responsible for most of the myelin degradation in peripheral nerve (Stoll et al. 1989).

Fatty acids are released during the breakdown of phospholipids which occurs in the early stages following nerve crush. At least a portion of the myelin cholesterol in peripheral nerve is also retained within the nerve following a nerve crush, and is subsequently reutilized for the synthesis of new myelin during regeneration of the nerve (Rawlins et al. 1970; Rawlins

et al. 1972). Following the distribution of radiolabelled myelin lipids using electron microscopy, Goodrum et al. (1994) confirmed the reutilization of myelin cholesterol by Schwann cells to form new myelin. However most of the myelin debris was phagocytosed by macrophages within 1-2 weeks following nerve injury. These debris laden macrophages persist within the nerve for many weeks, indicating that much of the salvaged cholesterol is not reutilized for myelin regeneration.

5.5 REGENERATION.

The growth cone, the extending terminal of the axonal sprout, represents the site at which the regenerating neuron meets the local environment. It expresses receptors for laminin, and extracellular matrix and basal lamina components (Griffin & Hoffman 1993). Following degeneration the original basement membrane is slowly broken down so that for a period of time this provides a source of laminin and other materials that are the preferred substrate for axonal growth (Griffin & Hoffman 1993). Schwann cells in the Büngner bands express surface adhesion molecules such as L1 and NG-CAM and both NGF and NGF receptors (Burgoon et al. 1991; Heumann et al. 1987; Martini & Schachner 1986). This results in an attractive environment for invasion by regenerating sprouts and a highly favourable one for effective axonal elongation

The growth cone extends highly motile spike-like processes (filopodia) as well as motile expansions of the membrane (lamellipodia) (Bunge et al. 1972; Yamada et al. 1971). In responsive neurites NGF has the direct effect of increasing the rate of outgrowth of the growing tip. In the absence of nerve growth factor, extension is halted and filopodia make exploratory movements (Griffin & Hoffman 1993). The growth cone contains specialisations of the axonal cytoskeleton and the smooth membrane system with the filopodia and lamellpodia extending on a meshwork of actin microfilaments (Bray & Chapman 1985).

The success of nerve regeneration after enrve transection depends largely on the axonal sprouts passing between the proximal and distal stumps and then reaching the appropriate connections to the periphery. Like any surgical wound, the interstump zone is characterised by exudation, cell proliferation and collagen synthesis. Schwann cells emerge into the gap from the proximal and distal stumps forming cords or columns in the gap approaching each other. Both matrix formation and non-neuronal cellular bridges are necessary to ensure axonal regeneration. Sprouts reaching a band of Büngner initially lie on the surface of the Schwann cells, but later become embedded in the Schwann cell cytoplasm (Allt 1976)

Early regenerating units are structurally very similar to normal unmyelinated nerve fibres. The presence of reduplicated basal lamina and very small axons suggests that they are regenerating fibres (Griffin & Hoffman 1993). Schwann cell mitoses are frequently associated with regenerating units of this type.

Maturation of the axonal sprouts. Limited maturation of the axon occurs before the growing tip reaches an appropriate target. Schwann cells ensheath bundles of regenerating axons and then develop a one-to-one relationship with those destined to become myelinated (Griffin & Hoffman 1993). This process recapitulates the process of segregation seen in development and is a necessary prelude to myelination. Nerve transplant studies demonstrate that the axon contains the signal for maturation into segregated and myelinated axon-Schwann cell units; the regenerating sprouts of unmyelinated nerve fibres remain as typical unmyelinated nerve fibres (Aguayo et al. 1976a; Weinberg & Spencer 1976). The onset of myelination of regenerating sprouts results in an increase in axonal calibre with associated changes in the cytoskeleton (Windebank et al. 1985). The thickness of the myelin sheath of regenerating sprouts rarely reaches that of the parent axons, even though axonal calibre may approach that of the parent. This is related to the reduced internodal length of regenerated fibres (see section 5.6).

5.6 MYELIN SHEATH REMODELLING IN REGENERATED NERVE.

In normal nerves, the internodal length increases regularly with fibre diameter (Hildebrand et al. 1994). This pattern is the combined result of the initial Schwann cell length, the elongation of the nerve related to body growth following the initiation of myelination and, in some nerves, myelin sheath remodelling. The largest fibres are the first to myelinate and thus are subject to the greatest elongation during growth (Jacobs & Cavanagh 1969; Harel et al. 1989). In regeneration following crush injury in an adult animal, myelination occurs without the internodal elongation since no growth in length is occurring in that part of the body. Regenerated mammalian myelinated fibres do not recover the normal linear relationship between length and diameter (Hiscoe 1947; Vizoso & Young 1948; Cragg & Thomas 1964; Ghabriel & Allt 1977). Since post-crush regenerated nerves in adult animals do not grow in length, it has been assumed that the nodal spacing in regenerated mammalian nerve (approx 300μm) reflects the basic Schwann cell length at the onset of myelination (Hiscoe 1947). The large surplus of Schwann cells in regenerated nerve together with the lack of length growth explains why the internodes which first form along regenerated axons are so short. Friede and coworkers (Friede & Bischhausen 1980; Friede et al. 1981; Friede & Bischhausen 1982) have suggested that in some fashion the Schwann cell responds to internodal distance as well as to axonal calibre in determining number of myelin lamellae and total myelin volume. They postulate that the failure of myelin sheaths to obtain their original L/D ratio reflects the shorter internodal distances present in regenerating fibres.

Fewer very short internodes are noted after long periods of regeneration. The greater internodal length variation at early stages was thought to suggest the disappearance of some

short sheaths through their fusion into longer ones (Vizoso & Young 1948). In regenerating rat nerve the total number of Schwann cells associated with myelinated axons decreases dramatically 2-12 months after surgery, long after the cessation of active regeneration. There is no corresponding drop in the number of myelinated axons. Lugnegård et al. 1984) calculated that one third of the myelin-related Schwann cells present at two months have disappeared by one year. Schwann cell competition for longitudinal axonal space results in elimination of some internodes in regenerated rat sciatic nerve (Hildebrand et al. 1994). The process of elimination includes internodal shortening and nodal migration, myelin sheath breakdown and demyelination, elimination of redundant Schwann cells and nodal fusion (Hildebrand et al. 1985; Hildebrand et al. 1986). The eventual fate of the eliminated Schwann cells in regenerated nerves is unknown. They might join the pool of endoneurial Schwann cells without axonal contact (Hildebrand et al. 1994). The occasional presence of necrotic cells suggests that some of the eliminated Schwann cells die (Spencer & Weinberg 1978; Hildebrand et al. 1986).

5.7 EXPERIMENTAL DEMYELINATION AND REMYELINATION.

In the peripheral nervous system, experimental demyelination is usually followed by a period of remyelination. It has been suggested that there are two mechanisms by which repair of damaged paranodal regions occurs (Cavanagh & Jacobs 1964; Jacobs 1967). If the damaged region exceeds 15 μm in length, a new Schwann cell is inserted into the gap and forms a short intercalated segment. These segments vary in length but are never shorter than 15 μm. This is thought to be associated with the formation of new myelin internodes where nodes and paranodal regions have been extensively damaged. If the widening of the nodal gap was less than 15μm, the original damaged Schwann cell is thought to reconstruct the damaged myelin and the node of Ranvier.

Most internodes in remyelinating regions exhibit morphological characteristics similar to those described in newly myelinating fibres (Allt 1969b). The cytoplasm in the nuclear region of the regenerating Schwann cell 22 d, after the injection of diptheria toxin, contains abundant ER, ribosomes, mitochondria and Golgi apparatus, similar to that seen in the immature rat (Allt 1969b; Allt & Cavanagh 1969). The initial stage of remyelination is represented by loose lamellae with Schwann cell cytoplasm between them (Allt 1969a). As more lamellae are laid down compaction begins to occur in the outer lamellae. When the sheath is compact it has the same spacing and appearance as normal adult myelin (Allt 1969a).

The regenerating node of Ranvier has the same shape as the developing node in the immature rat (Allt 1969a). Paranodal bulbs of the axon and nodal constriction of the axon are slight or absent. The nodal axoplasm generally does not show an increased electron density

compared with the internode as it does in a mature node. Myelin lamellae terminate in the same was as they do in the developing node, lamellae separate from each other and open out into a loop containing Schwann cell cytoplasm. All loops reach the axolemma presenting a longitudinal series, unlike the situation seen in the adult node where many loops fail to meet the axolemma and instead form a "herringbone" configuration. Adjacent Schwann cells may simply abut or overlap at the node (Allt 1969a) each of these parallels the situation in normal development (Allt 1969b). This can be interpreted in terms of the establishment of a whole new internodal segment by a Schwann cell laying down myelin de novo onto a denuded axon. The second type of nodal regeneration occurs when a nodal gap has not been grossly widened. It seems to be that the original internodal length and contact with the adjacent cell has been re-established by the superimposition of new myelin lamellae on the withdrawn sheath.

5.8 ABNORMAL REMYELINATION

In a proportion of fibres remyelination does not proceed as in development but shows abnormal features (Geren 1954; Allt 1972; Ballin & Thomas 1969).

Attenuation of the normal paranodal myelin sheath. In some cases the whole thickness of the sheath does not round off into a typical paranodal bulb. Small groups of 5-6 lamellae peel off from the main sheath, indistinguishable from those associated with a normal paranode. The rest of the sheath continues, much thinned, along the fibre for a further 20- 30μm finally forming a new paranodal bulb (Hall 1973; King et al. 1975).

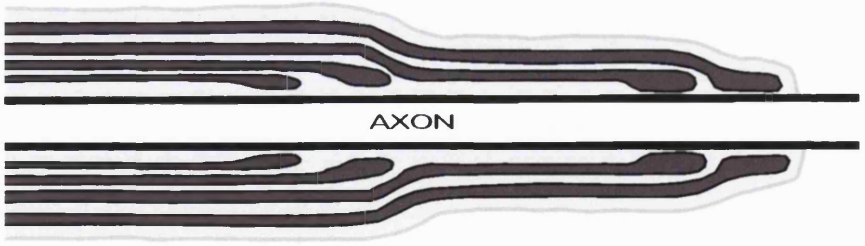

Fig 5.1 Diagramatic representation of attenuation of the normal paranodal myelin sheath

Pseudonodes Pseudonodes closely resemble nodes of Ranvier in some aspects of their basic organisation. They have two groups of apposing Schwann cell cytoplasm filled loops, separated by Schwann cell cytoplasm continuous with that in the loops (King et al. 1975; Hall 1973). Pseudonodes are often asymmetrical with differences in the thickness of the internodal myelin sheaths on either side of the pseudonode. When myelin lamellae terminate

at an insisure, the axolemma in contact with the terminal loops of the lamellae may be specialised in the same manner as the nodes of Ranvier (Hall 1973). As the remyelinating sheath increases in thickness continuity is established between the two sides of the pseudonode. At this stage it is not unusual to find Schmidt-Lanterman insisures in which the innermost lamellae terminate at the axolemma in node-like loops. These features disappear as remyelination progresses suggesting that the cytoplasmic processes are withdrawn as remyelination proceeds and/or incorporated into a remodelled sheath (Hall 1973).

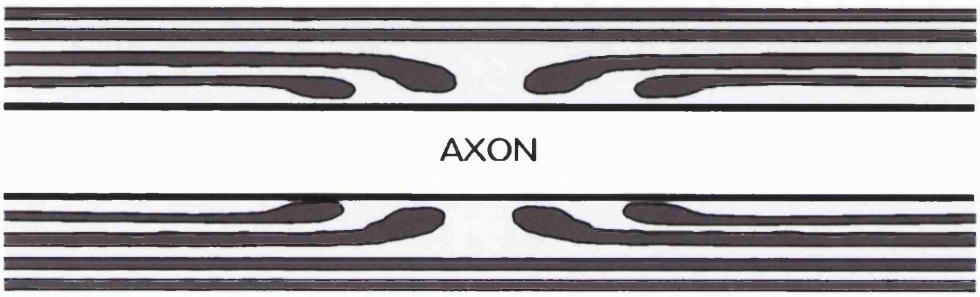

Fig 5.2 Diagramatic representation of a pseudonode

Overriding The overriding by a Schwann cell in contact with an axon may occur over an adjacent Schwann cell in contact with the same axon. The outer Schwann cell could produce myelin around the inner cell which itself may have already myelinated the axon (Ballin & Thomas 1969; Hall 1973)

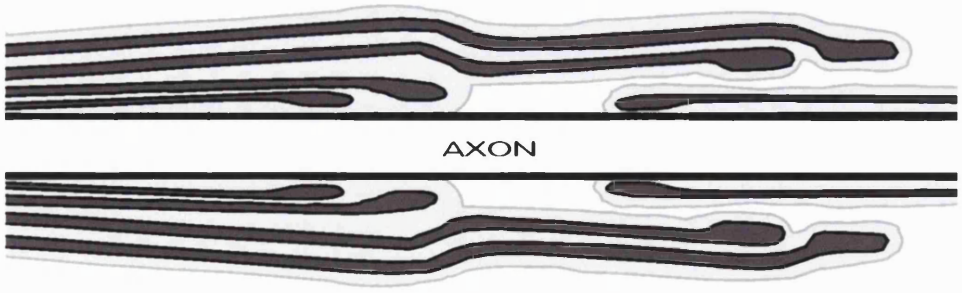

Fig 5.3 Diagramatic representation of overriding

Tunication Raine et al. (1969) described a mechanism of early remyelination in which an axon is enveloped by several Schwann cell processes which appose to form new myelin. The number of lamellae vary in number around the axon circumference. At a later stage of remyelination only one Schwann cell process surrounds the axon and the myelin sheath is

uniform in thickness. In remyelinated internodes following EAN 29% of axons were surrounded by more than one Schwann cell process (Allt 1972). The processes were closely apposed to each other giving the appearance of multiple mesaxons which were not seen when the myelin sheath consisted of more than 5-6 lamellae. It is thought to be most likely that the overlapping processes are all derived from the same Schwann cell (Hall 1973). These 'supernumerary' processes were frequently seen within the confines of the original basement membrane. Occasionally they assumed the concentric array characteristic of 'onion bulbs' (Ballin & Thomas 1969; Allt 1972).

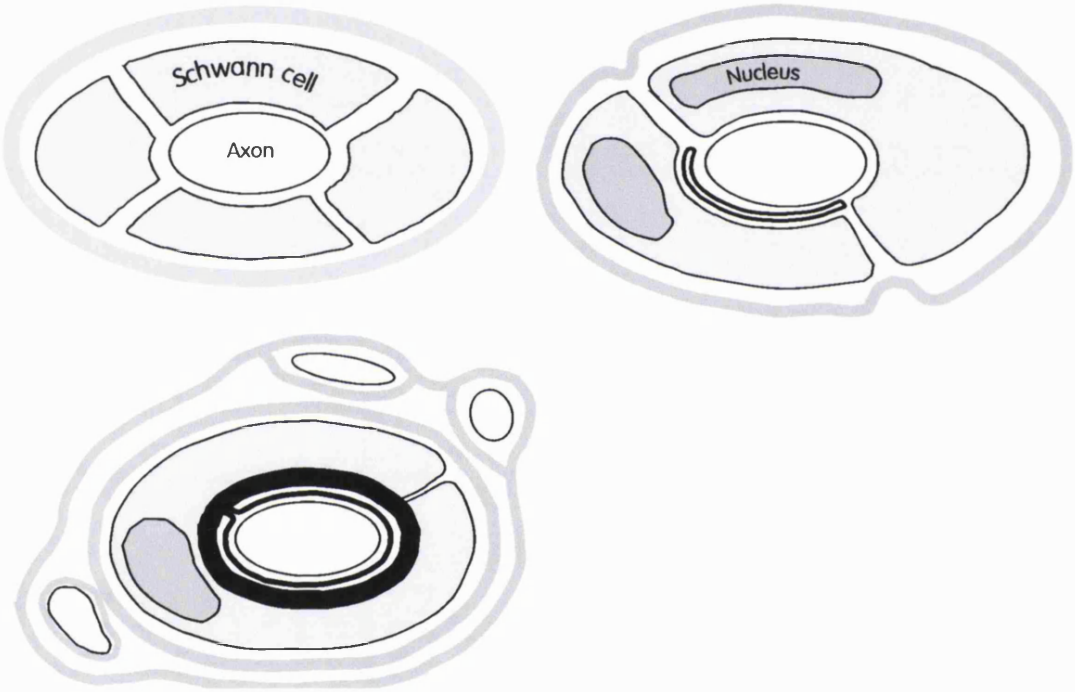

Fig 5.4 Diagrammatic representation of myelination by tunication

Other abnormal features include short apparently normally myelinated internodes in continuity with remyelinating internodes proximally and distally. The paranodal bulbs of the internode with normal myelin thickness show considerable infolding and occasional osmiophillic globules within the Schwann cell cytoplasm (Hall 1973). Irregularities of the myelin sheath thickness along the remyelinating internode particularly near the Schwann cell nucleus are seen (Hall 1973). Node-like discontinuities in the remyelinating sheath are frequently observed in perinuclear regions (Hall 1973).

5.9 MULTIPLE EPISODES OF DEMYELINATION

The most prominent finding in nerves that have undergone episodes of multiple injury is an increased number of Schwann cells (Hall 1984; Ohara & Ikuta 1988; Thomas 1970). Ohara and Ikuta (1988) studied the effects of multiple crush injuries on the phrenic nerve of young adult mice. The number of Schwann cell nuclei (SCN) increased with each successive crush reaching 10-15x their normal value after 4 successive crushes on the same site. In all crushes 70-80% of the Schwann cell nuclei were supernumerary and most of these were found as part of onion-bulb formations. Basal laminal onion bulbs were also seen.

Thomas (1970) examined multiple crush injury (up to 9X) in the peroneal nerve of rabbits and also found a progressive increase in the numbers of SCN with successive crushes. In contrast to Ohara and Ikuta's study, Thomas found that 'clusters' of Schwann cells formed longitudinal columns in the nerve and did not form 'onion bulbs'.

Hall (1984) looked at the effect of multiple intraneural injections of lysophosphatidylcholine (LPC) in adult mouse tibial nerve. Following intraneural injections of LPC the myelin sheath undergoes a characteristic progressive vesicular breakdown, while the axon and the Schwann cell apparently remain undamaged (Hall & Gregson 1971). In singly injected nerves a moderate proliferation of Schwann cells is seen (60% of which are supernumerary Schwann cells (SSC)). These SSC progressively disappeared and by 240 days many remyelinated axons were found surrounded by empty basal laminal tubes, or by double or single fragments of basal lamina (Hall 1973). Following multiple LPC injections the pattern of myelin breakdown was essentially similar to that seen in single injected nerves but the time course differed. The early phases of repair, from the initiation of myelinolysis to the appearance of promyelinated fibres, were achieved more rapidly in multiple injected nerves. During days 5-10 post injection this early lead was reversed. The majority of axons in 8X injected nerves were still either promyelinated or associated with debris laden cells, presumably Schwann cells, within the basal lamina. During the first three days post injection most SSC within the lesion had disappeared, although their basal laminae remained in close association with the demyelinating axons. This is interesting in view of the assumption that repeated episodes of demyelination and remyelination will produce layers of Schwann cell cytoplasm around the axon in the form of onion bulbs, and may explain why onion bulbs were not seen in this study.

The effects of the initial demyelination produced by LPC were exacerbated in multiple injected nerves by a local, self limiting, immune mediated demyelination. The presence of macrophages in these lesions suggests that either the cells or some factors released by them may play a role in initiating myelin damage. Compartmentalisation of the endoneurium by fine cytoplasmic processes of perineurial cells was a feature of multiple injected nerve (Hall 1984; Hall 1983). It occurred in some nerves injected 4 times and in most injected 8 times.

The cytoplasmic processes frequently enclosed axons, either singly or in small groups of two or three.

Chapter 6 Materials and Methods

6.1 THE BREEDING COLONY

Proven breeding pairs of Trembler-J mice were imported from Jackson laboratories (USA). The semidominant Tr^J gene was maintained in animals of the C57BL/6 strain and was linked to a rex (*Re*) coat marker. Both heterozygous and homozygous *Re* animals should have curly whiskers and a wavy coat (Carter 1951; Crew & Auerbach 1939). The waviness of the coat disappears in adults, but the vibrissae and guard hairs remain curly (Carter 1951; Crew & Auerbach 1939). The *Re* gene is a dominant and is located on chromosome 11. It is known to be 23 recombination units away from the Tr gene on linkage group five (Falconer & Sobey 1953). Falconer (1953) estimated that 15% of animals with the *Re* phenotype would not be affected. This was confirmed by Low (1976b) who found that 15% of animals that were phenotypically *Re* at birth were subsequently found not to be carrying the *Tr* mutation. Specific linkage data for the Tr^J is not available but as the mutation is located on the same gene as *Tr* we have assumed that these figures also apply to Tr^J. The *Re* gene should allow recognition of animals carrying the Tr^J gene; this was intended to be used before the clinical syndrome become apparent.

Six heterozygote $Tr^J/+$ breeding pairs were imported. One affected female died before leaving quarantine. The five remaining pairs were transferred to the RFHSM animal facility. Two of the pairs failed to produce any progeny. The remaining three pairs produced ten, five and two offspring each. The colony was maintained for 4-6 generations on the basis of the *Re* coat marker. We were unable to identify curly whiskers in any of the *Re* animals.

DNA analysis using PCR was established to determine the genotype of animals in the early postnatal stages of development. Initially P7-P10 animals from *Re/Re* matings were processed for microscopy and tissue taken for DNA analysis. Of the 27 animals examined none were found to be carrying the Tr^J gene. We then performed DNA analysis on a further 41 *Re* progeny from 16 breeding pairs, only 4 animals were carrying the Tr^J gene. At this stage the use of the *Re* marker was abandoned and the breeding colony maintained using animals unequivocally showing clinical symptoms at 8 wk of age.

Breeding statistics were compared for Tr^J and C57BL/6 colonies maintained in the same facility. In breeding pairs where one of the parents was Tr^J/+, significantly fewer litters were produced per pair than in the control colony. Neither the mean litter size (n) or the proportion of progeny weaned differed between Tr^J and control colonies.

Table 6.1 Comparison of the breeding success of Tr^J compared with C57BL/6 colonies

	Litter number	Mean litter size	Progeny per pair	Weaning success
C57BL/6				
11 pairs	6.0 ± 0.45	7.8 ± 0.38	47.0 ± 4.6	81.9% ± 4.7%
TrJ				
39 pairs	3.3 ± 0.31	6.8 ± 0.26	22.7 ± 2.3	73.5% ± 3.2%
p value	p<0.001	NS	p<0.001	NS

(Mean ± SEM) Mann-Whitney U test

Breeding pairs containing affected Tr^J males were compared with those containing affected females. There was no difference in litter number, size of litter or weaning success indicating that either of the two breeding strategies was equally viable. This differs from that found in the *Tr* mouse (Henry & Sidman 1988). Henry (1988) found that *Tr* /+ and *Tr/Tr* females mated and bore progeny easily, but males of both genotypes mated poorly.

Table 6.2 Comparison of the breeding success with sex of the affected parent

	Litter number	Progeny per pair	Weaning success
TrJ affected female			
19 pairs	3.8 ± 0.42	26.2 ± 3.2	72.9% ± 3.8%
TrJ affected male			
20 pairs	2.9 ± 0.40	19.4 ± 3.3	66.4% ± 7.2%
p value	NS	NS	NS

Mean ± STD Mann-Whitney U test

To ensure the continuance of the Tr^J line 20 breeding pairs were maintained. Animals clearly affected at 8 wk of age usually became severely affected by 3 mo . The overall clinical severity of the Tr^J disorder in the colony then increased to a point where many 8 wk old animals were to severely affected to be used for breeding. This combined with the small

number of litters from *Tr*^{J} pairs has resulted in a larger number of breeding pairs than usual being kept to ensure the continuation of the gene in the colony.

6.2 MICROSCOPY

Perfusion fixation. Animals were perfused with fixative while under deep anaesthesia (Sagatal 18 mg/animal). The thorax was opened and a butterfly needle attached to a cannula inserted into the left ventricle of the heart. The right atrium was incised and blood washed out with 1N saline at 37^{0}C. This was followed by perfusion with 1% paraformaldehyde (BDH) and 1% glutaraldehyde in 0. 1M PIPES (piperazine-N,N'-bis-[2-ethanesulfonic acid]) buffer (pH 7.4), initially at 37^{0}C and then at room temperature. The sciatic nerves were removed and laid on pieces of card which were then placed in fresh fixative for 1 h. The vertebral column was removed and immersion fixed for 1 h, it was then opened to expose the spinal cord, nerve roots and ganglion and fixed for a further 1h. The dorsal and ventral roots were excised together with the dorsal root ganglia. The lumbosacral spinal cord was also removed.

In situ fixation. Early postnatal animals (<P15) and transgenic animals were not perfused. The sciatic nerve and spinal cord were fixed in situ for at least 15 min and then were removed and immersion fixed for a minimum of 1 h before dissection. The vertebral column was opened to expose the spinal roots and ganglia to the fixative.

Processing

All tissue was then fixed for a further 2 h, washed in PIPES buffer plus 2% sucrose and then postfixed in 1% osmium tetroxide in PIPES buffer with 2% sucrose, 3% sodium iodate and 1.5% potassium ferricyanide. The specimens were dehydrated in increasing concentrations of ethanol (15% 2 X 5min, 30% 2 X 10min, 50% 2 X 15min, 70% 2 X 30 min, 100% 3 X 20 min followed by 2 X 60 min) and transferred to epoxy resin via 1,2 epoxypropane as an intermediary (2 X 15 min propylene oxide, 60 min 1:1 resin/ propylene oxide mixture, overnight 3:1 resin/ propylene oxide mixture). The following day samples were transferred to 100% resin for 24 h and then embedded or stored at -20°C and embedded at a later date.

Tissue staining

Semithin sections were cut and stained with thionin and counterstained with acridine orange. Thin sections (yellow to gold inference pattern) were stained with 0.25% lead citrate (BDH Chemicals Ltd, Poole, UK) and counterstained with a saturated solution of uranyl acetate (Agar Scientific Ltd, Stanstead, UK) dissolved in 50% methyl alcohol (BDH Laboratory Supplies, Poole, UK).

6.3 MORPHOMETRY

Measurements of axon diameter, total fibre diameter and g ratio (axon diameter/ total fibre diameter) were confined to fibres with a one-to-one axon/Schwann cell relationship; these included amyelinate or demyelinated fibres. The numbers of Schwann cell nuclei in each section was counted and supernumerary Schwann cells recorded separately. All measurements were taken from whole fascicles viewed with a X100 objective and a X1.2 optivar on a Zeiss Axioplan microscope (Zeiss UK Ltd, Welwyn Garden City, Herts, UK) connected on-line through a television camera to a Kontron IBAS AT image analyser (Imaging Associates,Thame, UK). Many fibres in Tr^{J} and C22 animals had myelin that was too thin to be identified (less than 5 myelin lamellae) at the light microscope level. In these cases the axon was measured and the fibres assigned a g ratio of 1. The proportion of fibres incompletely surrounded by Schwann cell cytoplasm was counted in non overlapping electron micrographs. At least 200 fibres from each dorsal and ventral root were counted. Sections were taken from pairs of dorsal and ventral roots immediately proximal to the dorsal root ganglia.

6.4 CRUSH INJURY

Animals were anaesthetised with 0.2 ml of Sagatal (6mg/ml) and maintained under Halothane vapour. While this was satisfactory for control animals it proved to be fatal to many affected Tr^{J} animals and was discontinued in favour of Halothane alone. The sciatic nerve was exposed at the upper thigh and traced upwards to the sciatic notch and crushed using No 7 curved forceps. Pressure was applied until the contents of the perineurium could be seen to be separated with care being taken not to transect the perineurium itself. The wound was then closed with Mitchell clips, sprayed with Op site and the animal taken to the recovery room.

6.5 DNA ANALYSIS

Extraction. DNA was extracted from heart muscle and purified using a phenol/chloroform extraction method modified from Blin and Safford (1976). Tissue was taken, placed in liquid nitrogen and stored at -70 °C until use. The sample was placed on a cleaned glass slide and cut with a scalpel blade until it was a pulpy consistency. It was then transferred to a glass/teflon homogeniser and 2 ml of extraction buffer was added (75mM NaCl, 50mM

EDTA (K+)) and homogenised until no pieces of tissue were visible (at least 20X). The homogenate was transferred to a sterile test tube where filter sterilised SDS (final concentration 0.5%) and proteinase K (final concentration 2mg/ml) were added. The mixture was incubated at 56 °C while shaking (150 rpm) for 3 h. A further 2 mg/ml of proteinase K was added, the temperature lowered to 37.5°C and the digestion continued overnight. The following day an equal volume of TE saturated phenol was added to the sample which was mixed for 20 min on a whirly wheel. The suspension was then spun at 4000 rpm in a Beckmann GPR centrifuge. The aqueous phase was withdrawn with a sterile plastic pipette, with care taken not to disturb the interface layer, and transferred to new sterile tube. This process was repeated three times. To the final aqueous phase and equal volume of a 25:1 Chloroform/isopropanol mixture was added and mixed on the whirly wheel for 5 min then spun for 20 min at 4000 rpm and the upper phase removed to a sterile tube. To each ml of the upper phase 100 µl of 3M sodium acetate and 2 ml of ice cold 100 % ethanol was added and the mix placed at -70°C for at least 2h. The tubes were spun at 10000 rpm for 20 min, the ethanol tipped off and the pellet rinsed with cold 70% ethanol and left to dry. Once all the ethanol had evaporated the pellet was resuspended in 200 µl of TE buffer and left for a least 3h to dissolve. An aliquot was then used for spectrophotometry and the concentration and purity of the DNA determined (Harris 1987).

Polymerase Chain Reaction (PCR) Specific segments of DNA were amplified using the polymerase chain reaction (PCR) (Mullis et al. 1986; Mullis & Faloona 1987). The PCR reaction was performed in a 50 µl reaction volume under the following conditions. 1µl of DNA 100ng/µl was added to a PCR mixture containing 50 mM KCl, 10 mM Tris HCl (pH 9.0), 0.1% Triton-X 100, 0.32 mM of each A,T,C and G dNTP, 1.5 mM $MgCl_2$, 0.2µM of upstream primer TrJU5 and 0.2 µM of the downstream primer TrJU3.The reaction mixture was overlayed with 80µl of sterile liquid paraffin oil and placed in a Hybaid ™ TR2 thermal reactor (Hybaid Ltd, Teddington, UK) for the following reaction cycle. 94°C for 4 min, 72°C for 30 sec at this stage the reaction was paused and 1.25 Units of Taq DNA polymerase (Promega, UK Ltd, Southampton, UK) added then restarted. 94°C 30 s, 55°C for 1 min, 72°C for 40 s for thirty cycles followed by an extension period of 10 min at 72°C .

Table 6. 3 Primer sequences used for DNA analysis

TrJU5	5'-GAT CCC GAG CCC AAC TC-3'
TrJU3	5'-CTG ACG GTG GAG AC-3'

Analysis. 15µl of the reaction product was restricted with 4 units of Ban I (Stratagene Ltd, Cambridge, UK) in the reaction buffer supplied at 37.5 °C overnight and then run on a 2% agarose gel. The total PCR product was 103 bp in length; the mutated allele is visualised by the appearance of 70bp and 33 bp fragments.

Ban I	Recognition sequences 5'G/GPyPuCC3' and 3'CCPuPyG/G5'

The primers were tested using mouse PMP22 cDNA (a gift from Prof. Dr. U. Suter) to confirm that they were amplifying the correct sequence.

6.6 mRNA ANALYSIS

Animals were killed by exposure to an increasing concentration of CO_2, death was confirmed by cervical dislocation. The sciatic nerve was exposed from the bifurcation of the tibial and peroneal branches to above the sciatic notch, quickly excised and placed into a liquid nitrogen filled petri dish which was placed in a tray of ice. The nerves were then cut into at least two pieces each and placed in a liquid nitrogen filled cryotube and stored in liquid nitrogen until use.

mRNA extraction. mRNA was extracted using the Micro-FastTrack ™ mRNA isolation kit (Invitrogen BV, De Schelp, Netherlands). Samples were tipped from the cryotubes into a glass homogenising tube quickly covered with 1ml of lysis buffer (1ml of Stock buffer and 20 µl of Protein/RNase degrader) and homogenised until no pieces of tissue were visible (approx 20 X). This mixture was transferred to a 1.5ml eppendorf tube and the process continued according to the manufacturers instructions. In brief, the kit utilises a detergent based lysis step followed by binding of mRNA to oligo dT cellulose, a low salt wash to reduce the amount of rRNA , and the elution of mRNA. The mRNA pellet was resuspended in 5 µl of elution buffer and immediately following determination of mRNA concentration (DNA Dipsticks), used for first strand cDNA synthesis.

First strand cDNA synthesis. First strand cDNA was synthesised using, cDNA cycle kit (Invitrogen BV, De Schelp, Netherlands). mRNA was reverse transcribed using oligo dT primer and AMV reverse transcriptase and then purified with a phenol extraction and ethanol precipitation prior to freezing at -70°C until use.

PCR and analysis. Control and *Tr*^{J} samples were paired and the cDNA concentrations adjusted until they were identical (3-5 μg/reaction). Aliquots of the PCR mixture containing the downstream primer, cDNA and ^{32}P were split between two tubes containing alternative upstream primers. PCR was performed in a reaction volume of 20μl, with final concentrations of 10 mM Tris-HCl pH 8.3, 50 mM KCl,1.5 mM $MgCl_2$, 0.001% gelatin, 0.1 mM each of dNTPs, 0.2 μCi of [$\alpha^{32}P$] dCTP (1000 Ci/mM), 1.2 units of AmpliTaq Gold ™ (Perkin Elmer), 0.32 μM of the downstream primer and 0.32 μM of either the myelin associated (CD25) or the growth arrest related (SR13) upstream primers. The sequence for the different 5' regions was taken from the published mouse SR13 sequence. Primers specific for the SR13 (growth arrest specific) (Manfioletti et al. 1990) transcript produce a 486 bp reaction product whereas those for the myelin related CD25 transcript produce a 524 bp fragment. The CD25 5' region is not specifically published for the mouse gene so the published sequence of the rat transcript was used (Bosse et al. 1994). Primers sequences for the house keeping gene hypoxanthine-guanine phosphoribosyl transferase (HPRT) were used in addition to amplifying both PMP22 trancripts. HPRT is a salvage enzyme in the nucleotide metabolic pathway. cDNA would be expected to amplify in any peripheral nerve sample providing a marker of mRNA/cDNA viability.

Table 6. 4 Primer sequences used for mRNA analysis

Downstream primer	5' GTG TCT CAC TGT GTA GGC CGC TGC ACT 3'
Myelin associated (CD25)	5' AGC AGC AGA GCT CCG AGT CTG GTC TGC TGT 3'
Growth arrest related (SR13)	5' GGG GGA AGC CAG CAA CCT AGA GGA CGC 3'
HPRT	5' CAT GAA TTC TTA TGC TGA GGA TTT GGA AAG GGT G 3' 5' CAT AAG CTT AAG TCT GCA TTG TTT TGC CAG TGT G 3'

PCR was performed for 1 cycle of 12 min at 95°C followed by 27 cycles of 20 s at 96°C, 1 min at 57 °C, 2 min at 72 °C, and a final 10 min extension at 72°C. A 10 μl aliquot of the reaction product was run on an 1.6% agarose gel which was dried and the amount of incorporated radioactivity quantified on a phosphoimager.

Chapter 7 Results

7.1 ADULT TREMBLER-J

7.1.1. CLINICAL FEATURES. Affected *Tr*^{J} animals developed a neuropathy that could be detected in the most severely affected animals at between 4 and 6 wk of age. The disorder primarily affected the hind limbs, resulting in an abnormal gait with splaying of the hind limbs, muscle wasting and weakness. Severity varied within a litter but breeding pairs which produced severely affected offspring did so consistently. Clinical phenotype was not seen in some mildly affected animals until several months of age and often worsened in females after giving birth. 'Convulsions', which were described as a feature in the *Tr* mouse (Braverman 1953), were not observed.

7.1.2 MORPHOLOGY The sciatic nerve, dorsal and ventral roots and dorsal root ganglia were examined by light and electron microscopy in adult animals. The most obvious features of *Tr*^{J} nerves were a lack of myelin and an increased number of Schwann cell nuclei, as previously reported for both the *Tr*^{J} and *Tr* (Ayers & Anderson 1973; Henry et al. 1983; Low & McLeod 1975; Aguayo et al. 1977; Perkins et al. 1981a). Myelination was most severely affected in the ventral roots and both posterior and anterior roots were more severely affected than the sciatic nerve **(Fig 7.1.a-e.)**. Only minor structural changes were seen in the dorsal root ganglion cells. There was no evidence of active demyelination at any of the sites sampled and Schwann cell mitoses were not encountered.

In the spinal roots examined, myelin was very thin and in many fibres consisted of only 1 or 2 turns. Myelin was frequently uncompacted, especially near the nodes of Ranvier. The nodes of Ranvier were often widened similar to those seen during development. Sections of severely affected roots showed axons incompletely surrounded by Schwann cell cytoplasm **(Fig7.2a.)**. The proportion of such fibres was not significantly different between the dorsal and ventral roots **(Table 7.1)**.

Figure 7.1.

Electronmicrographs from the spinal roots and sciatic nerves of 3 mo *Tr*^{J} and control mice

(a,c,e) Electron micrographs from the same 3 mo *Tr*^{J} mouse. (a) Ventral root. Axons of a size that would normally be myelinated are completely devoid of myelin (open arrows). Others are surrounded by myelin which is inappropriately thin for the size of the axon. Where myelin is present it is commonly uncompacted (filled arrows). (c) Dorsal root. Fibres are surrounded by more myelin than those in the ventral root. Myelin is uncompacted (filled arrows). (e) Sciatic nerve. Many thinly myelinated fibres, occasionally with uncompacted myelin (filled arrow)

(b,d,f) Electron micrographs from the same 3 mo control mouse. (b) Ventral root. (d) Dorsal root. (f) Sciatic nerve.

Scale Bar, 10 μm (applies to all panels)

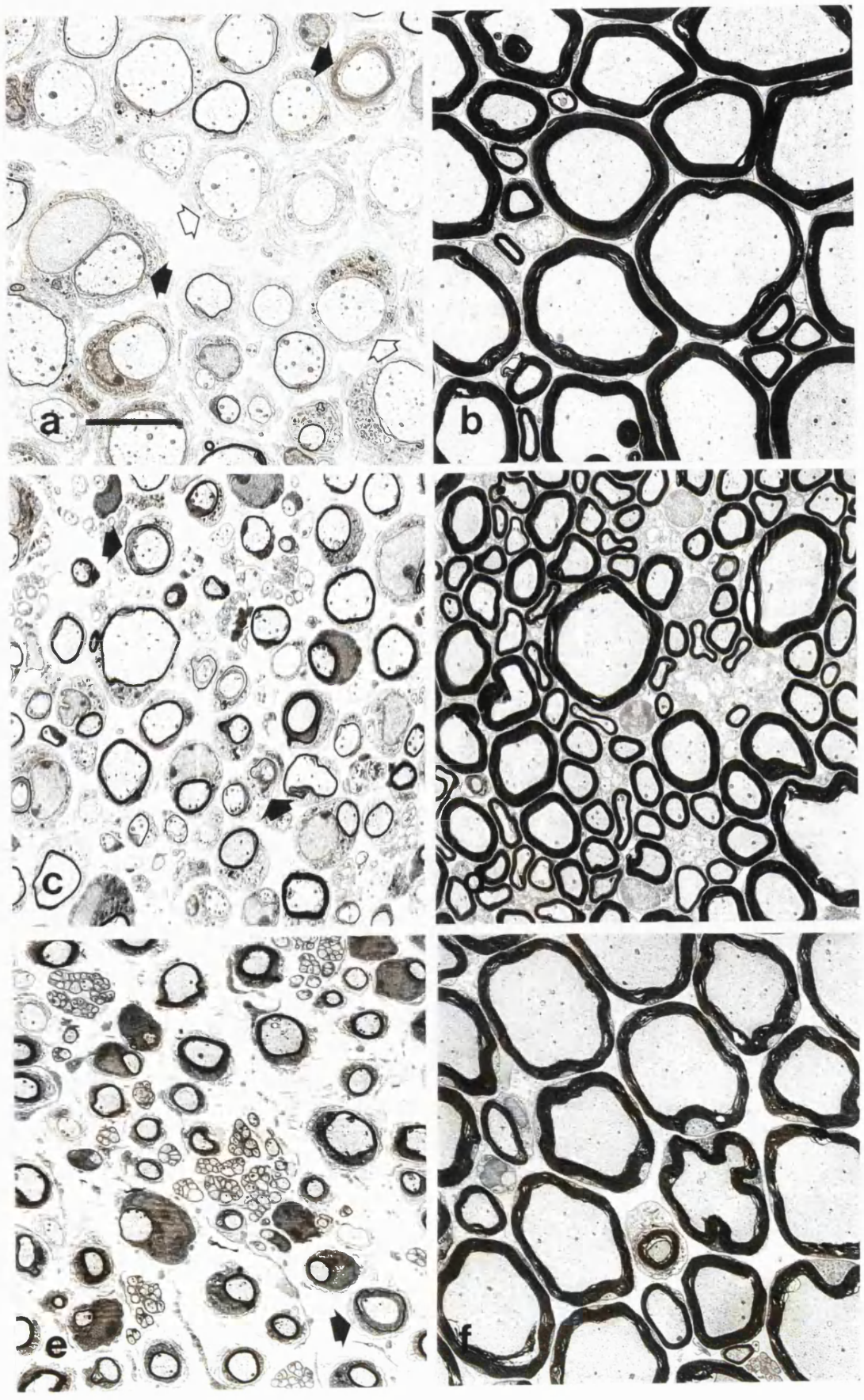
a
b
c
e
f

Figure 7.2.

Abnormal features found in the sciatic nerve of a 12mo *Tr*^{J} animal

(a) Dorsal root of a 3 mo *Tr*^{J} animal. Many fibres are incompletely surrounded by Schwann cell cytoplasm, (arrows). Scale bar, 1 μm. (b) Dorsal root of a 3 mo *Tr*^{J} animal. Schwann cell processes project into the endoneurium (open arrow). Paired redundant basement membrane (filled arrows), one with a small amount of remaining cytoplasm, are considered to be indicative of the Schwann cell extending processes and then withdrawing them. Scale bar, 1 μm

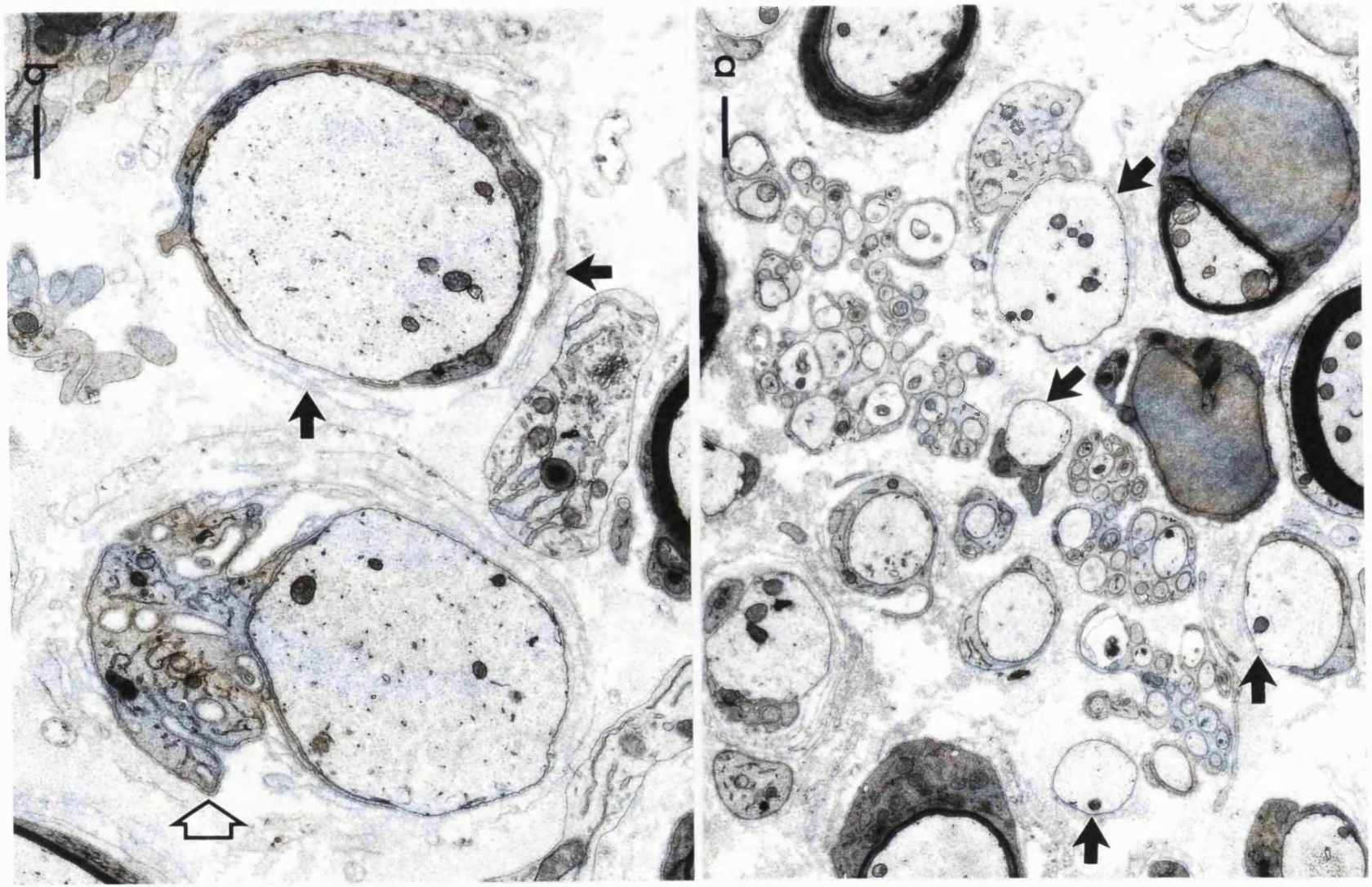
a
a

TABLE 7.1. Proportion of fibres incompletely surrounded by Schwann cell cytoplasm in the spinal roots of adult *Tr*^{J} mice

		Proportion of incompletely surrounded fibres
Dorsal root	(n=4)	29.0 % ± 1.7%
Ventral root	(n=4)	24.5% ± 3.4%
p value Mann-Whitney U		0.49

Mean ± SEM

Supernumerary Schwann cells unassociated with axons were not seen and concentric Schwann cell proliferation producing 'classical' onion bulbs was not evident. Instead many 'basal laminal onion bulbs' consisting of concentric or sectorial arrays of cell processes were frequently seen **(Fig 7.2b, 7.3a).** These were much more prominent in the sciatic nerve than in either of the nerve roots and consisted of many more layers.

Several previously unreported abnormalities for the *Tr*^{J} mouse were observed. Schwann cell nuclei were often not located at the centre of the internode as is usually the case but were found very close to one end of the internode, often over the terminal loops **(Fig. 7.3c,d).** The incidence of this increased with the severity of the neuropathy. Their nuclei had abnormally rounded profiles. Exuberant protrusions of Schwann cell cytoplasm into the endoneurium was also a feature of the *Tr*^{J} animals **(Fig 7.2b).** The cytoplasm of Schwann cells in *Tr*^{J} animals tended to be concentrated in the perinuclear region with an attenuated layer extending on either side towards the nodes of Ranvier. Terminal loops of the myelin sheaths were occasionally found turning outwards into the extracellular space instead of terminating on the axon **(Fig. 7.3b).**

Figure 7.3.

Electron micrographs from the sciatic nerve of a 12 mo *Tr*^{J} animal. (a) Fibres encircled by layers of redundant basal lamina Scale bar, 1 μm. (b) Terminal myelin loops turning outwards from the axon (arrow). Scale bar 2 μm. (c) Schwann cell nuclei placed at the ends of the internode, close to the nodes of Ranvier (arrows). Scale bar 5 μm. (d) Nucleus located over a node of Ranvier (arrow). Scale bar 1 μm.

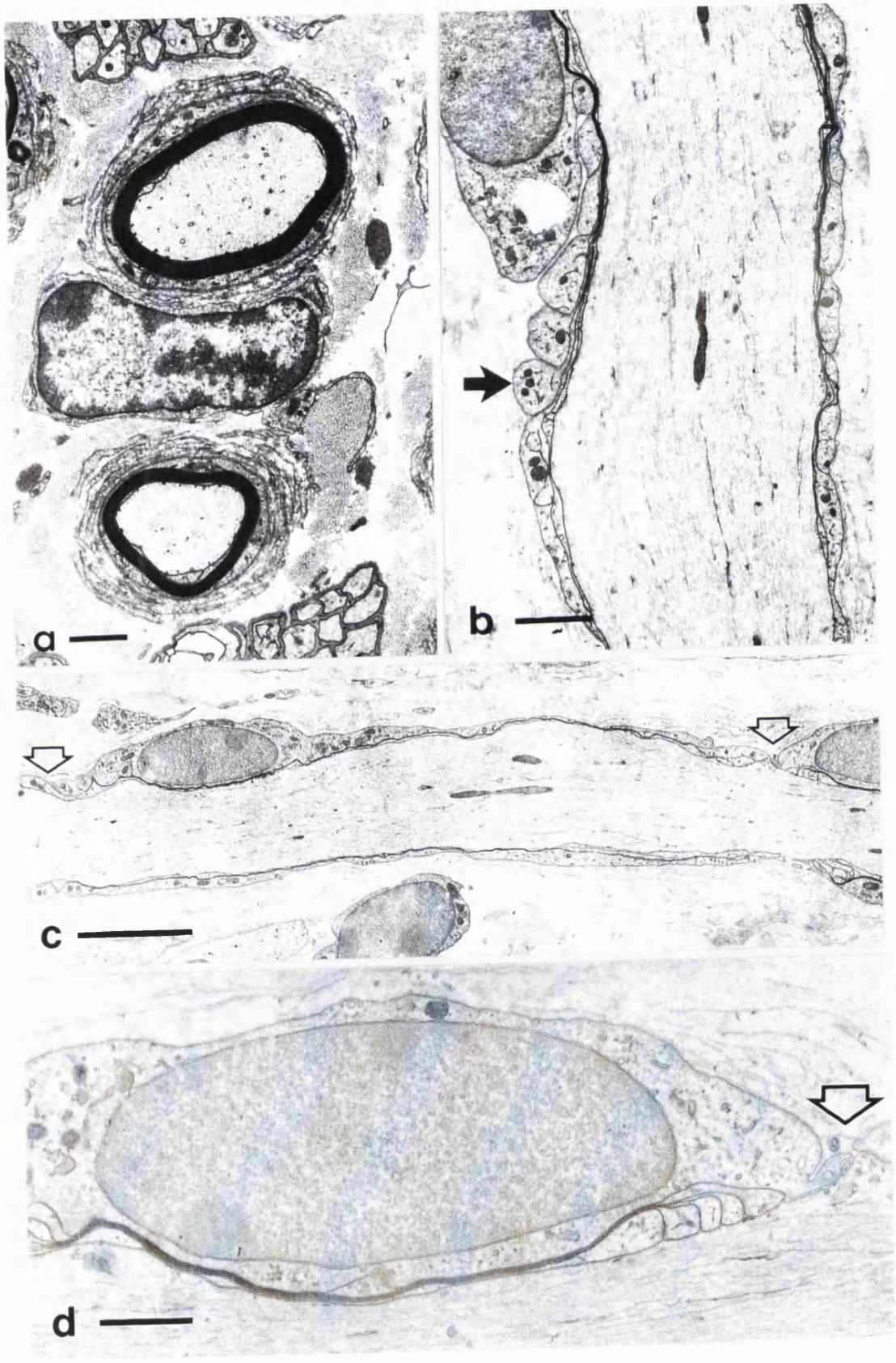
a
b
c
d

7.1.3. MORPHOMETRY

Myelin thickness. Many axons in *Tr*^{J} animals were either devoid of myelin or surrounded by myelin too thin to be measured at the light microscopic level (20% in the sciatic nerve increasing to 60% in the ventral root) **(Fig7.4)**. In 12 m old animals myelination was most affected in the ventral root where 60-65% of fibres had myelin that was considered too thin to quantify accurately (less than 5 turns of myelin). The dorsal roots were significantly less affected than the ventral with only 40-50% of fibres falling into this category ($P<0.01$). The sciatic nerve was less affected than either of the spinal roots, only 20% of fibres were severely dysmyelinated. The dorsal/ventral root difference was not significant in the 3 mo animals.

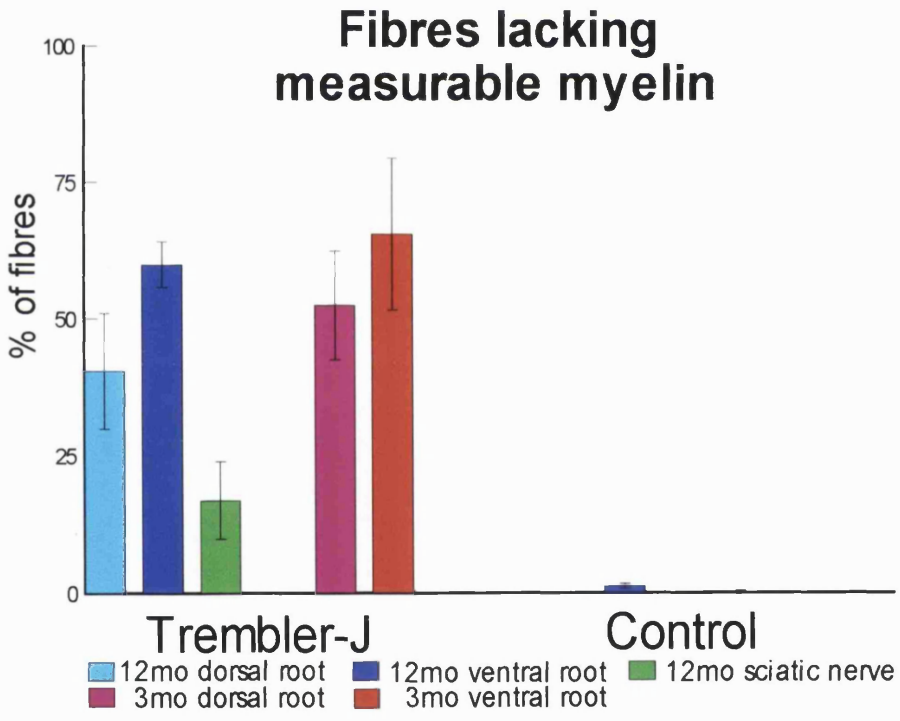

Figure 7.4. The proportion of fibres lacking measurable myelin in the spinal roots and sciatic nerves of *Tr*^{J} and control mice (less than 5 turns).

When the myelin thickness was measured in the remainder of fibres, Tr^{J} animals had a higher proportion of fibres with inappropriately thin myelin (g ratio >0.8) than controls **(Fig 7.5)**. The ventral roots were more severely affected (20-26%) than the dorsal root (4-6%) both in 3 and 12 mo animals (P=0.004 and P=0.04) with the sciatic nerve showing a level of affectedness between the two.

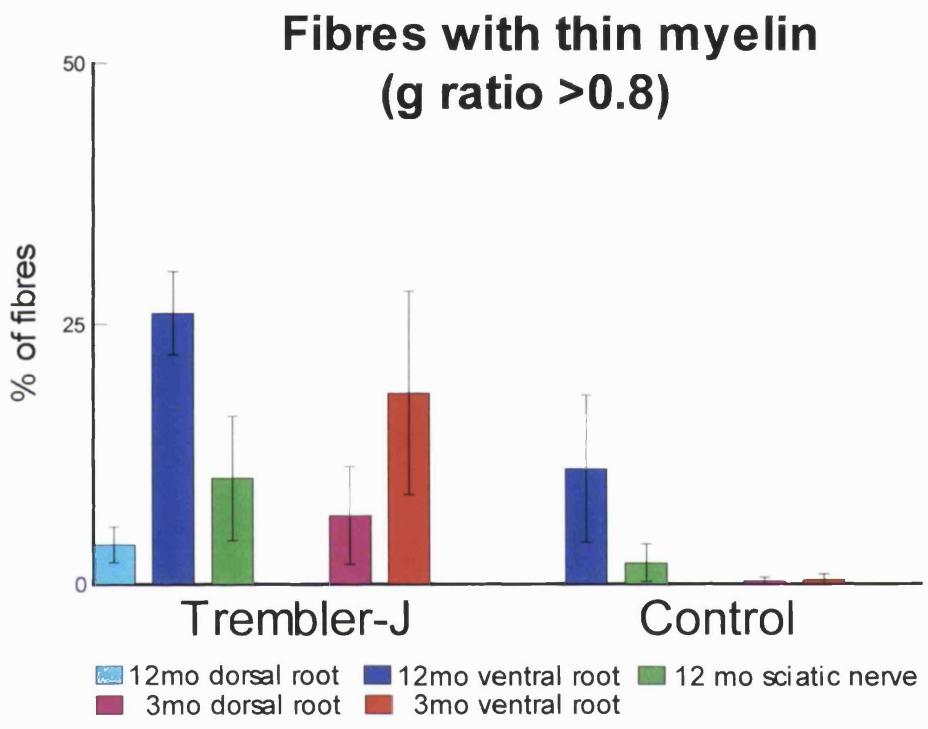

Fig 7.5. The proportion of fibres with thin myelin in the spinal roots and sciatic nerves of Tr^{J} and control mice (excluding fibres lacking measurable myelin).

Schwann cell numbers. The number of Schwann cell nuclei / 100 axons in cross sections of dorsal and ventral roots was 4-5 times higher in the spinal roots both in 3 and 12-mo-old *Tr*^{J} animals when compared with age matched controls. There was no alteration with age in the number of nuclei/100 axons either in control or *Tr*^{J} animals **(Fig 7.6).** The number of Schwann cell nuclei/100 axons did not alter in the different levels of the nerves examined despite a large variation in severity of demyelination.

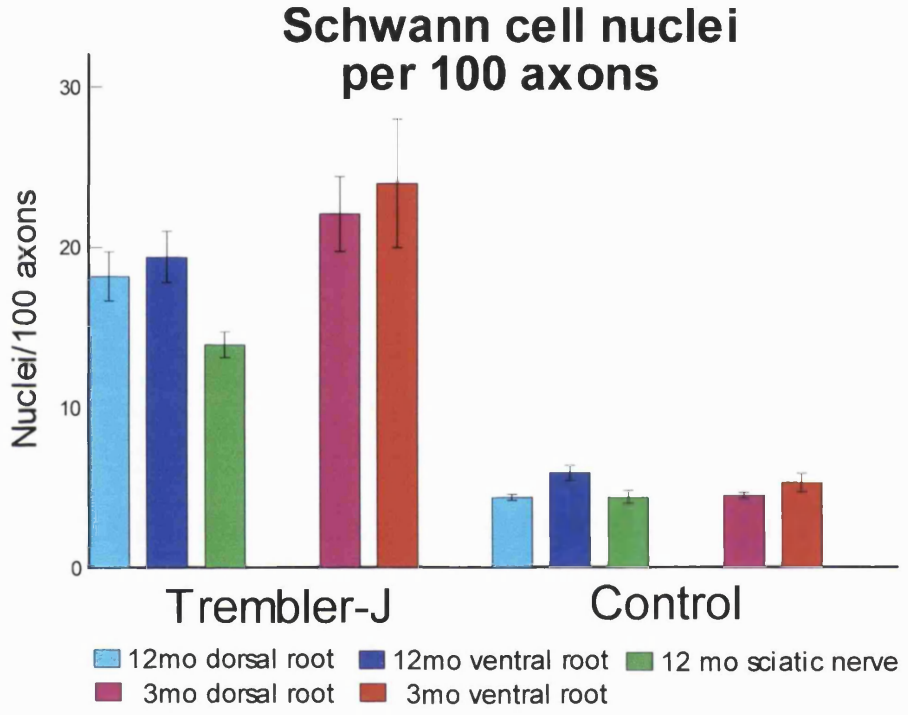

Fig 7.6 The number of Schwann cell nuclei counted in the spinal roots and sciatic nerves of *Tr*^{J} and control mice (expressed as counts per 100 axons).

Fascicle area and fibre density. Total fascicular area was not significantly affected either by strain or age **(Table 7.2).** In the ventral root there was no difference in fibre density between *Tr*^{J} and controls, although both strains demonstrated a significant age related decrease in density **(Fig 7.7).** In the dorsal roots, however, there was a significant decrease in fibre density in *Tr*^{J} animals when compared with age matched controls **(Fig 7.7).** As there were no significant alterations in fascicle area this probably represents axonal loss in the dorsal roots of *Tr*^{J} animals.

TABLE 7.2. Fascicle areas (μm^2) in the spinal roots and sciatic nerves of *Tr*^{J} and control mice

	12 months			3 months	
	Dorsal root	Ventral root	Sciatic nerve	Dorsal root	Ventral root
***Tr*^{J}**	15151±1072	50539 ± 9052	141283 ± 16158	41931± 4432	3551 ± 3288
Control	34173± 4333	74526±14361	129178 ± 15154	34244± 5179	4316 ± 7060
	NS	NS	NS	NS	NS

p value Mann-Whitney U . Mean ± SEM

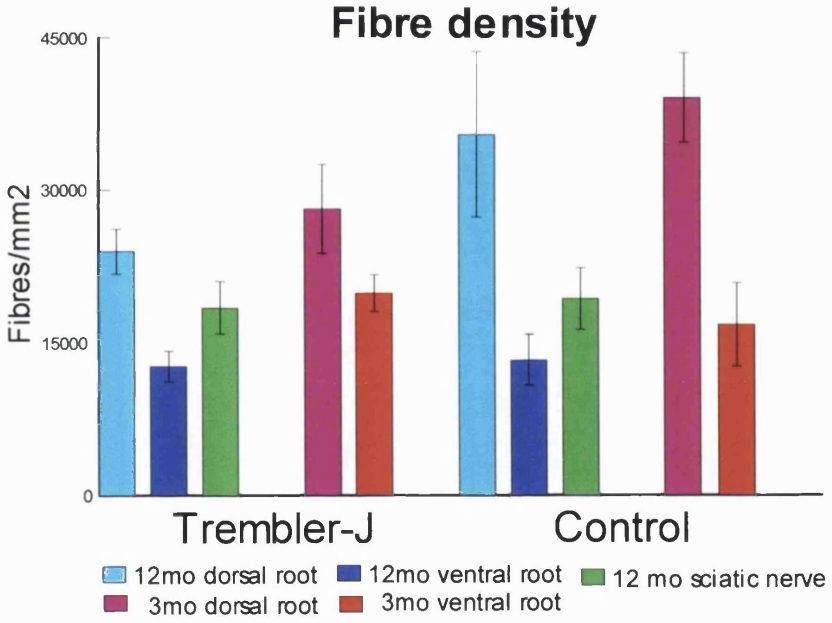

Fig 7.7. The density of fibres /mm^2 in the spinal roots and sciatic nerves of *Tr*^{J} and control mice

Fibre sizes. In all the *Tr*^{J} nerves examined there was a significant increase in the proportion of small fibres and a concomitant decrease in the proportion of large fibres (**Fig 7.8 a-e**). Axon diameters followed the same pattern as fibre diameters with an increased proportion of small and a decreased proportion of large fibres (data not shown). In the ventral roots of *Tr*^{J} animals both fibre and axon diameters increased with age.

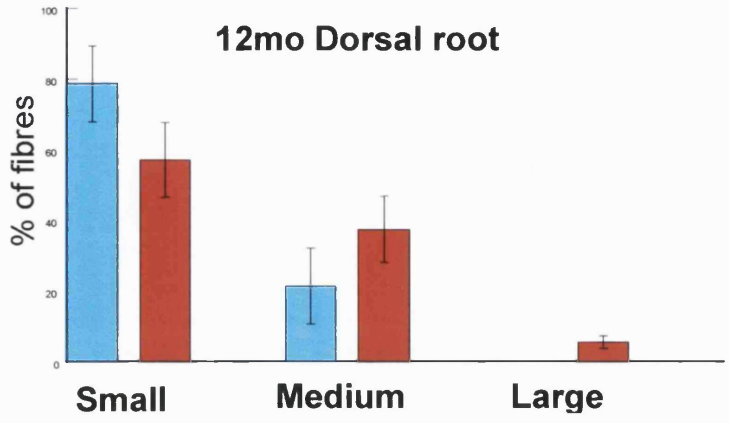

Fig 7.8 (a)

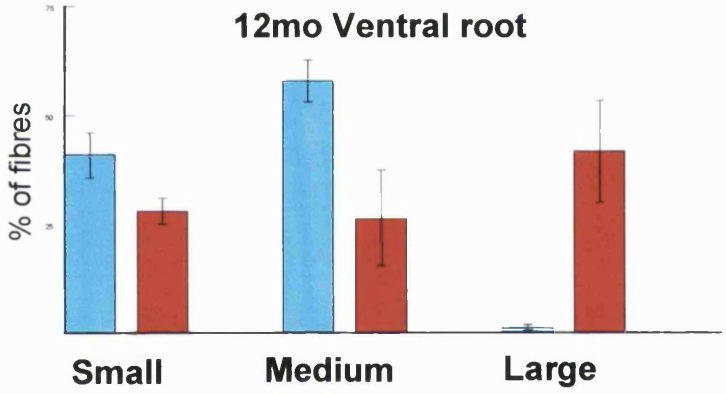

Fig 7.8 (b)

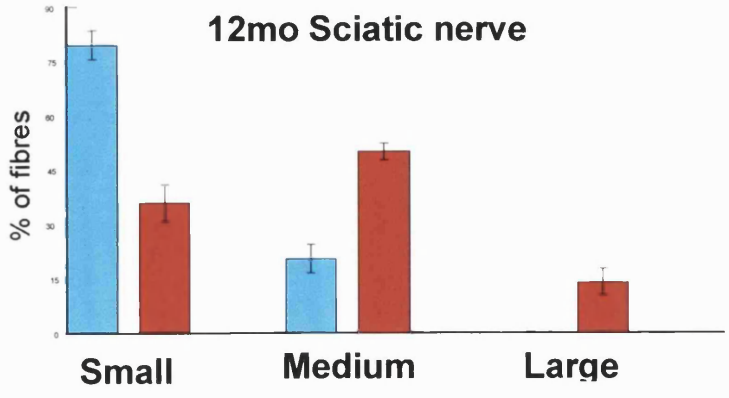

Fig7.8 .(c)

Small	0<5 μm,
Medium	5<10μm,
Large	10-15μm

Trembler-J
Control

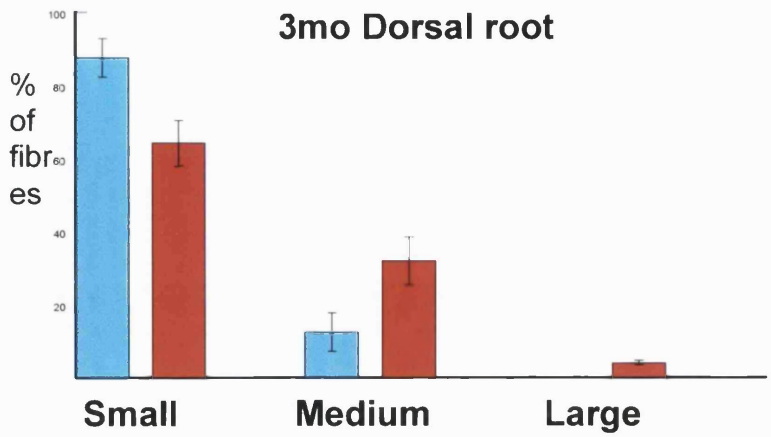

Fig 7.8 (d)

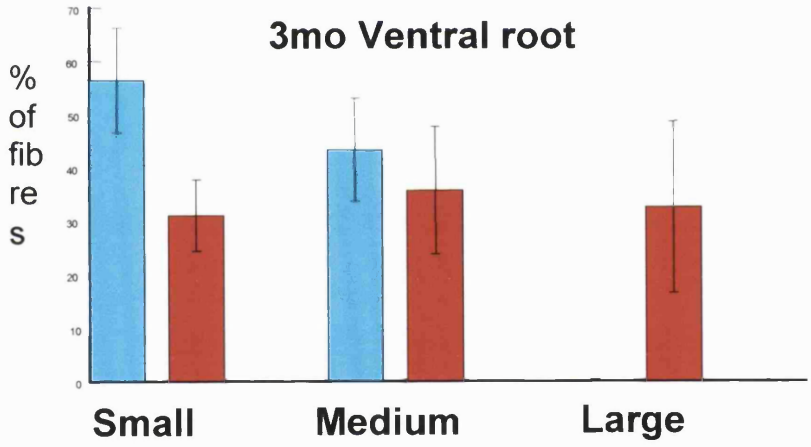

Fig 7.8 (e)

Small	**0<5 μm,**
Medium	**5<10μm,**
Large	**10-15μm**

Trembler-J
Control

Fig 7.8 (a-e) Histograms of the fibre size distribution in adult *Tr*^{J} and control mice

7.2 PATIENTS WITH THE P16L (TR^J) MUTATION

Three patients with the P16L mutation have been reported and their morphological phenotype published (Gabreëls-Festen et al. 1995). Schwann cell nuclear counts were not done on these patients. To allow me to make of better comparison of the human and mouse phenotypes Anneke Gabreëls-Festen kindly sent me a block from each of these patients. In addition to the published data she also sent me some further information about the clinical features of the patients and some data relating to their myelinated fibre distributions.

CLINICAL INFORMATION

Patient 1. Female. The patient first walked at 12 mo. She showed progressive deterioration from the age of three and by 27 y she was using a wheelchair. The child's first neurological examination at 8 y of age showed weakness and atrophy of distal lower limbs, dysfunction of vibration/position sense in lower limbs, slight sensory ataxia, areflexia and slight kyphoscoliosis. Daughter of patient 3.
Electrophysiological tests: Peroneal nerve MNCV, no response. Ulnar nerve, no motor or sensory responses.

Patient 2. Male. The patient's first neurological examination at 17 y was undertaken at the request of the school medical officer. The examination showed distal weakness of the lower legs, slight sensory ataxia, areflexia, pes cavus, slight scoliosis, no palpable nerves.
Electrophysiological tests: Median nerve MNCV 7m/s, distal motor latency 7.1m/s, distal sensory conduction latency 17.0 m/s, amplitude 2 μV. Peroneal nerve MNCV, no response.

Patient 3. Male. There was no reliable information about the patient's first years of life. He had poliomyelitis at the age of 6 y. The patient had several orthopaedic corrections of the right foot for pes equinovarus. His first neurological examination (27 y) showed weakness and severe atrophy of the hand muscles, lower legs and feet, R>L, distal sensory loss in the legs, areflexia, left foot pes cavus, mild clawing of hands, slight scoliosis. Peripheral nerves were thickened. His mother (deceased) and four brothers showed distal paresis and atrophy.
Electrophysiological tests: Ulnar MNCV unrecordable.

Table 7.3. Previously published morphometric data from patients with the P16L mutation

	Total fascicular area (% of normal)	Myelinated fibre density (% of normal)	Onion bulbs (% of myelinated fibres)	g ratio
Patient 1	458	15	90	0.88
Patient 2	448	20	97	0.72
Patient 3	-----	15	99	0.81

Fibre size distributions

In the mouse I have divided the fibre size distribution into three classes, small (0<5 μm), medium (5<10μm) and large (10<15μm). As the fibre size distribution in humans is bimodal I have used only two size classes, small (0<4μm) and large (>4μm).

Table 7.4. Myelinated fibre distribution; data from patients with the P16L mutation (percent of total fibre number)

	Small (0<4μm)	Large (>4μm).
Human Tr^{J} mutation		
Patient 1	79%	21%
Patient 2	90%	10%
Patient 3	70%	30%

Schwann cell numbers

Additional counts of Schwann cell nuclei and axons were performed at the Royal Free Hospital School of Medicine on the material from the three patients provided by Anneke Gabreëls-Festen.

Table 7.5. Schwann cell nuclei /100 axons in patients with the P16L mutation

	Axon associated	Supernumerary
Human Tr^J mutation		
Patient 1 9 y (mean of 3 fascicles)	20.6	35.2
Patient 2 17 y (mean of 3 fascicles)	17.0	19.7
Patient 3 30 y (mean of 2 fascicles)	15.0	50.0
TrJ mice (n=5)	13.9 ±0.8	rarely seen

The number of axon associated Schwann cell nuclei was similar in mice and humans but the patients had a large number of supernumerary Schwann cell nuclei. These were very rarely seen in the mice.

Figure 7.9.

Light microscope photos of mice and humans with the P16L mutation.

(a) Light micrograph from a Trembler-J mouse. Scale bar 100 μm.

(b) Light micrograph from a patient with the same mutation. Scale bar 100μm.

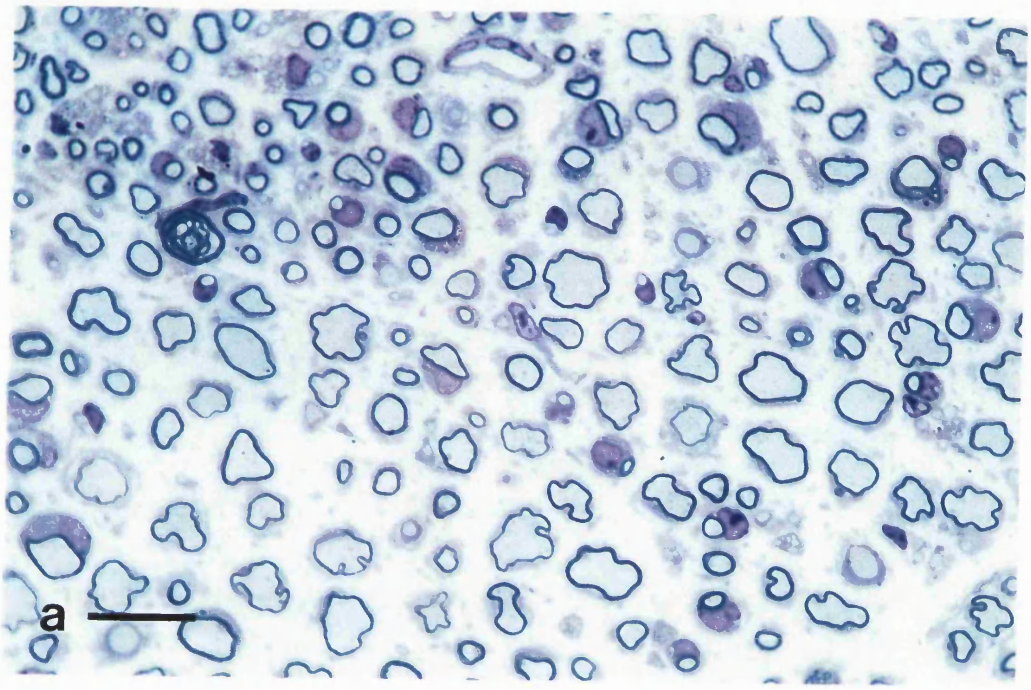
a

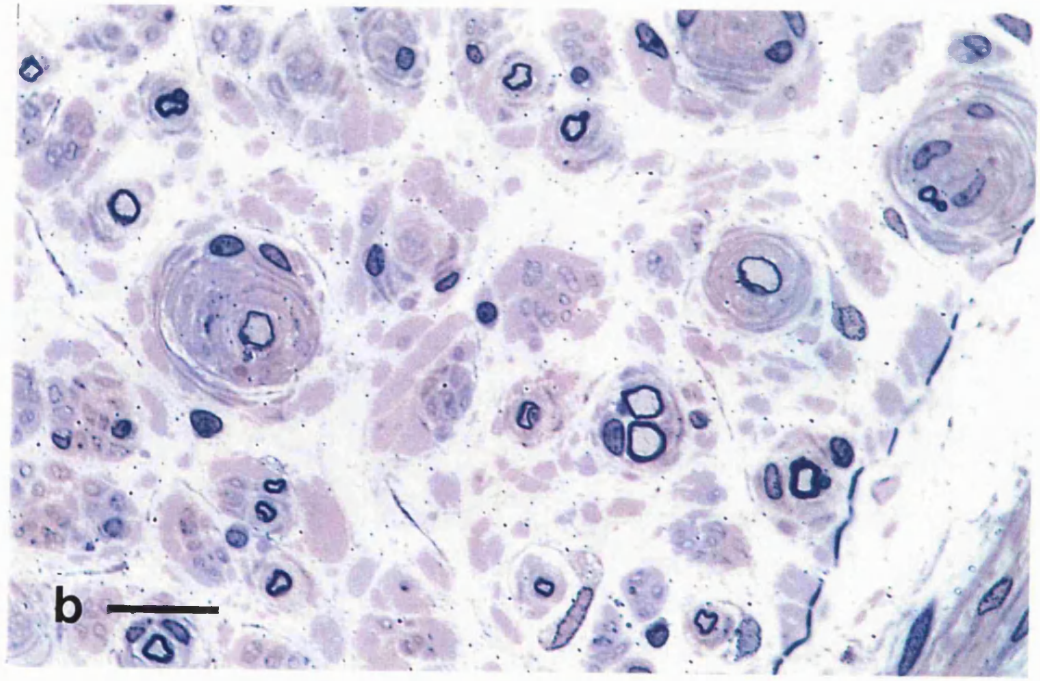
b

7.3 Adult Transgenic

A summary of the results of a preliminary study has been published (Huxley et al 1998). The summary table and histological results are included here.

Table 7.6 Previously published features of Transgenic mice

Mouse genotype	Copy number	Ratio human/mouse mRNA	Mean MNCV m/s	Histology	Visible phenotype
Wildtype	0	-	38	normal	none
C2 het	1	0.4	not done	normal	none
C2 hom	2	0.8	41	normal	none
C1 het	2	0.5	46	normal	none
C58 het	2	0.6	49	normal	none
C1 hom	4	1.3	26	mild demyelination	do not mate well
C58 hom	4	not done	21	mild demyelination	do not mate well
C61 het	4	1.0	25	mild demyelination	none
C22 het	7	1.6	4	demyelination	peripheral neuropathy
C61 hom	8	not done	4	demyelination	peripheral neuropathy
C22 hom	14	-	-	-	never produced

7.3.1. MORPHOLOGY. Comparison of sections of sciatic nerves from the same mice as used for the nerve conduction studies showed different degrees of severity of demyelination depending on the genotype. C22 heterozygous and C61 homozygous mice showed severe demyelination affecting most of the large axons. C1 homozygotes, C58 homozygotes and C61 heterozygotes all had intermediate degrees of demyelination, while C2 homozygotes, C1 heterozygotes and C58 heterozygotes showed only occasional demyelination. Electron microscopic examination of the nerves of mice of different genotypes showed that they had a

similar pattern of demyelination although different numbers of fibres were affected. Features included uncompacted myelin characteristically on the outsides of the myelin sheaths of medium sized axons **(Fig. 7.10 a),** demyelination of large axons with reduplicated basal lamina (basal laminal onion bulbs) **(Fig. 7.10 b),** completely demyelinated large axons **(Fig. 7.10 c),** and macrophages indicating the occurrence of active demyelination **(Fig. 7.10d).** Three lines of adult (7mo) transgenic mice with a range of PMP22 mRNA expression and copy numbers were chosen for further study. C22 het (7 copy), C61 het (4 copy) and C2 (2 copy) **(Fig. 7.11 a,b,c,d.).**

7.3.2. MORPHOMETRY

Myelin thickness. The degree of myelin deficit was quantified using categories of g ratio (axon diameter/fibre diameter). Demyelinated fibres and those with extremely thin myelin (less than 5 turns) were given a g ratio of 1.1. Those with values between 0.8 and 1 were considered to have myelin that was too thin for the size of the axon. Fibres with a g ratio below 0.4 are considered to have unusually thick myelin.

Both seven and four copy animals had an increased percentage of fibres with extremely thin myelin (g ratio =1.1). In C22 animals a large proportion of axons (40%) were either devoid of myelin or surrounded by myelin too thin to be measured at the light microscopic level. In the C61 strain only 3% of fibres fell into this severe hypomyelination category. Animals with 2 additional copies of PMP22 did not differ from controls. All the transgenic animals had significantly more fibres with thin myelin (g ratio 0.8-1.0). The percentage of thinly myelinated fibres increased with increasing copy number. An increase in the proportion of thinly myelinated fibres was the only discernible abnormality in C2 animals. There were only a few fibres with thick myelin (<0.4) in any of the genotypes.

Table 7.7 g ratios in transgenic mice

	Control	7 copy (C22)	4 copy (C61)	2 copy (C2)
Extremely thin or no myelin (1.1)	0.89 ± 0.3	42.4 ± 4.6	3.1 ± 2.1	1.0 ± 0.3
Thin myelin (0.8-1.0)	0.69 ± 0.4	8.82 ± 0.2	4.36 ± 2.1	1.46 ± 0.6
Thick myelin (<0.4)	0.07 ± .14	0.32 ± 0.33	0.57 ± 0.71	0.0 ±0.0

Figure 7.10.

Electron micrographs from the sciatic nerve of a severely affected C61 homozygote mouse (8 copies of the human *PMP22* gene). (a) Uncompacted myelin characteristically on the outside of the myelin sheath of medium sized axons. Scale bar 1 μm. (b) Hypomyelination of large axons with reduplicated basal lamina (centre). Scale bar 2 μm. (c) Thin myelin or complete lack of myelin around large axons which are often incompletely surrounded be Schwann cell cytoplasm (arrows). Scale bar 2 μm. (d) Macrophage indicating active demyelination or fibre degeneration. Scale bar 2 μm.

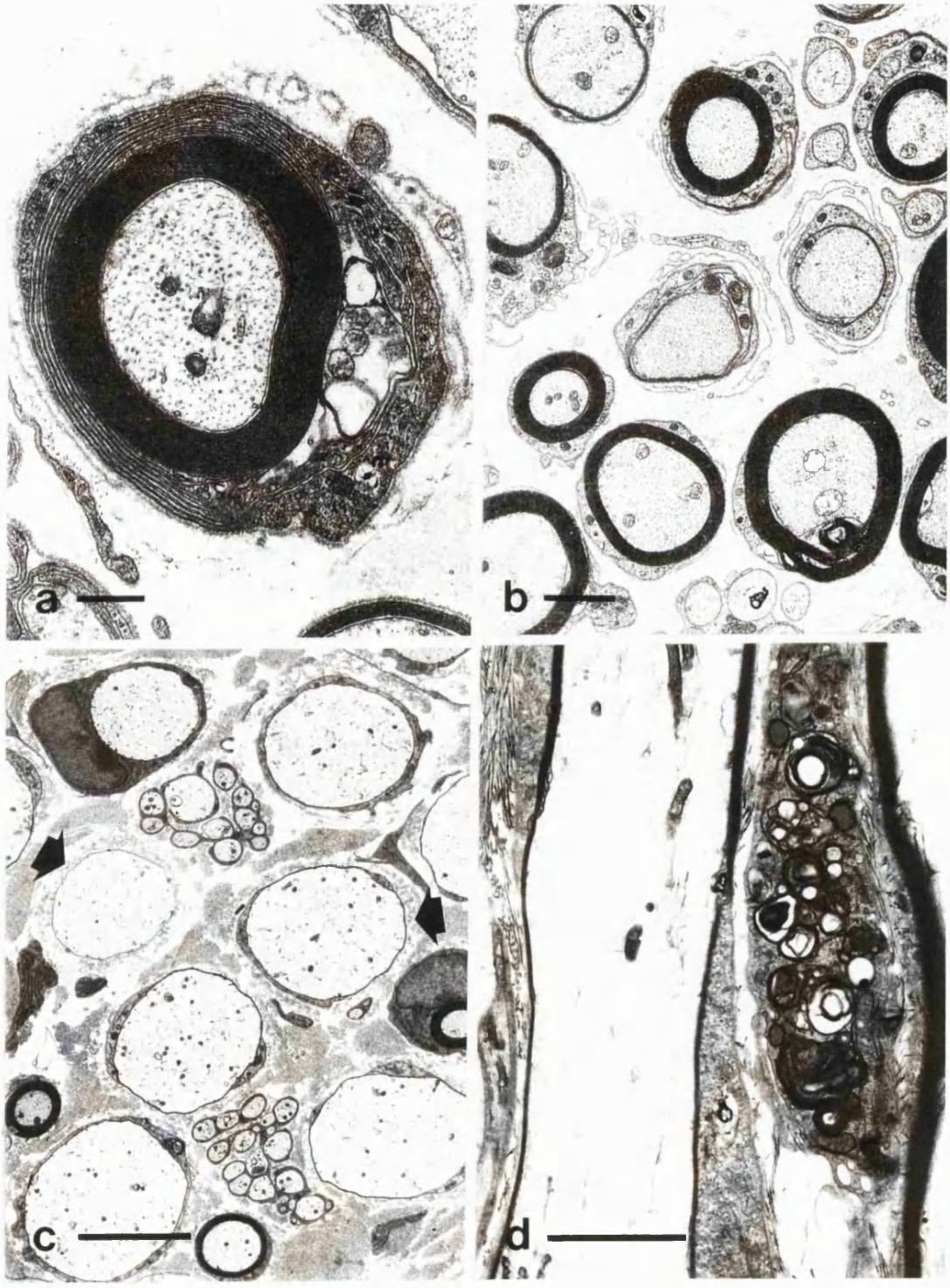
a
b
c
d

Figure 7.11.

Transverse sections of the sciatic nerves of mice with different copy numbers of the human transgene. (a) C22 heterozygote (seven copies). Nerves showed severe demyelination with most of the large axons being surrounded either by very few turns of myelin or none at all. (b) C61 heterozygote (four copies). Some thinly myelinated fibres are present. (c) C2 homozygote (two copies). Degenerating or demyelinated fibres were rare, (d) Control sciatic nerve.

Scale bar 10 μm, applies for all panels.

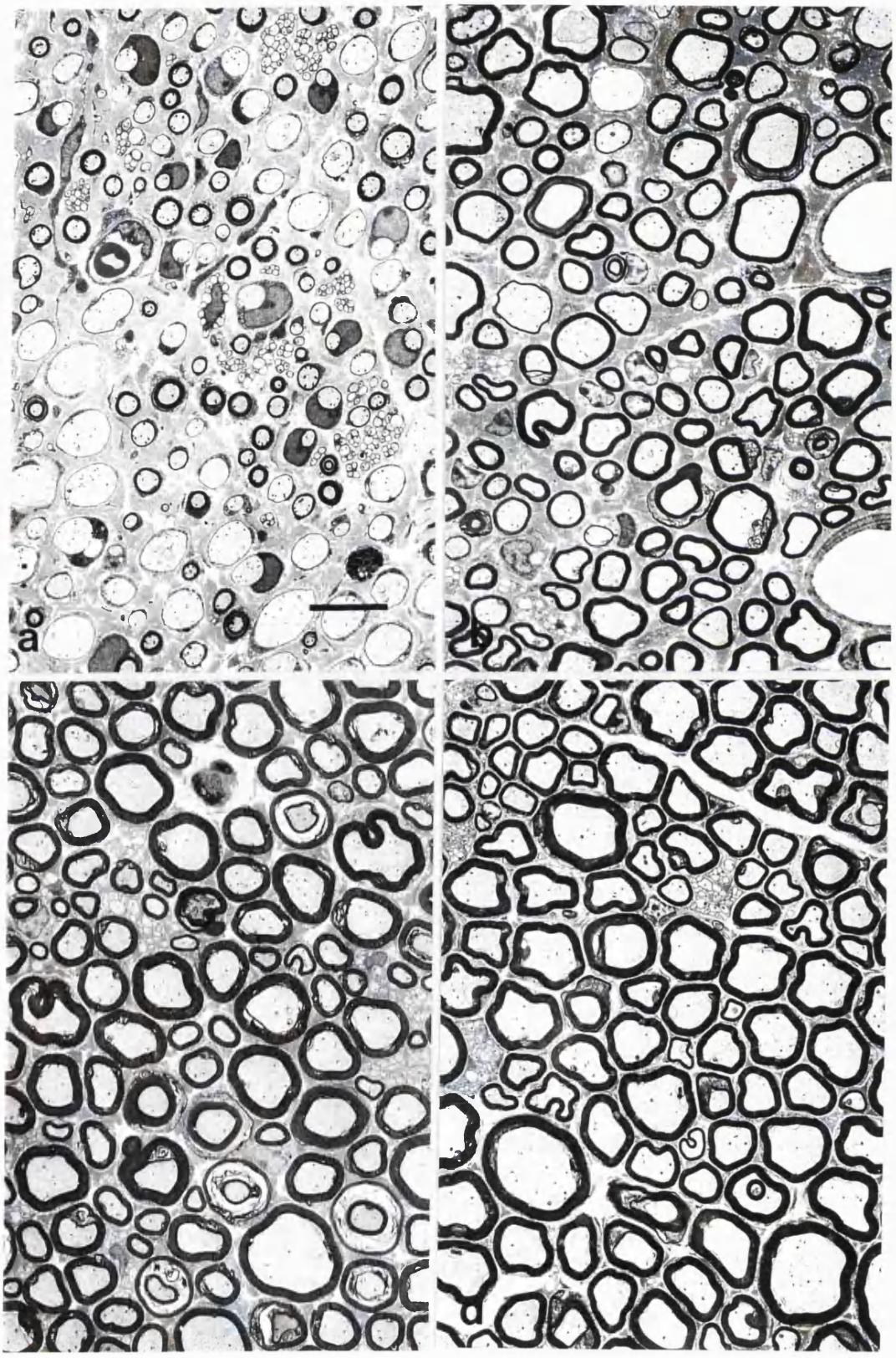
a

Schwann cell numbers.

Only the C22 strain had an increased number of Schwann cell nuclei.

Table 7.8 Schwann cell nuclei/ 100 axons in transgenic mice

	Control	7 copy (C22)	4 copy (C61)	2 copy (C2)
Number of Schwann cell nuclei per fascicle	4.6± 0.3	12.8 ± 1.0	5.4 ± 0.5	4.9 ± 0.4

Fascicle area and fibre density. Fibre density was not decreased in any of the transgenic mutants when compared with controls. The opposite was true of the most severely affected C22 strain which had an increased fibre density due to a decreased fascicle size, presumably related to the lack of myelin in the nerves. There was no evidence of hypertrophy in any of the nerves examined.

Table 7.9 Fibre density in sciatic nerves of adult transgenic mice (includes axons with very thin or no myelin)

	Control	7 copy (C22)	4 copy (C61)	2 copy (C2)
Fibres/ mm^2	20598 ± 1505	33777± 3268	20947 ± 4757	20167 ± 2087

Mean ± S.E.M.

Table 7.10 Fascicle area in transgenic mice

	Control	7 copy (C22)	4 copy (C61)	2 copy (C2)
Fascicle area (μm^2)	103616 ± 6714	64197 ± 8255	107803 ± 6492	106269 ± 6269

Fibre sizes The C22 strain had an altered fibre diameter spectrum with an increased proportion of small diameter fibres (<0.5 μm) and a concomitant decrease in both medium (5-10 μm) and large (10-15 μm) fibres. The more mildly affected C61 animals had a decreased proportion of large fibres. The axon size distribution paralleled that of the fibre sizes (data not shown).

Tabie 7.11 The spectrum of fibre diameters in transgenic mice

	Control	7 Copy (C22)	4 copy (C61)	2 copy (C2)
0<5 μm	33.7 ± 5.1	85.2 ± 2.4	42.9 ± 12.9	35.6 ± 4.11
5<10 μm	55.9 ± 3.0	14.6 ± 2.3	54.6 ± 11.8	56.1 ± 1.8
10<15 μm	10.3 ± 3.2	0.2 ± 0.1	2.5 ± 1.8	8.3 ±2.4

Mean ± S.E.M.

7.4 CRUSH INJURY

At 14 d post injury regeneration in the sciatic nerve was well established and myelination beginning in a large proportion of fibres. There was still a large amount of myelin debris present in the nerves of control animals but virtually none in the nerves of *Tr*^{J} animals.

7.4.1 MORPHOLOGY. Previous work on the *Tr*^{J} model has shown ultrastructural abnormalities of the Schwann cell which suggest cytoskeletal abnormalites affecting Schwann cells and their relationship with the axon and extracellular matrix. These include terminal myelin loops at the node of Ranvier that are directed outwards instead of being attached to the paranodal axolemma **(Fig. 7.12),** abnormally positioned Schwann cell nuclei **(Fig. 7.13a)**, and 'spiky' external protrusions of cytoplasm particularly in fibres lacking myelin but with axonal diameters in the myelinated fibre range **(Fig. 7.13b)** (associated with basement membrane). All these abnormal ultrastructural features found in *Tr*^{J} mice were reproduced in the early stage of regeneration following crush injury with a greater frequency than found in uninjured nerve. The 'spiky' projections seen in *Tr*^{J} animals appeared to be associated with the original basement membrane of the fibres **(Fig. 7.14a).** In addition regenerating fibres from *Tr*^{J} animals had a tendency to have a prolonged association with the original basal lamina. They were more commonly found in promyelinated fibres from *Tr*^{J} animals than in control animals but were found in both. **(Fig. 7.14a.b)** In *Tr*^{J} animals myelinated fibres were occasionally seen still associated with the original basement membrane; this association was never seen in control animals **(Fig. 7.14c,d)**.

Fibre counts. Axonal regeneration appeared to proceed normally in *Tr*^{J} mice. Both the total number of regenerating axons and the proportion of those axons that were unmyelinated were the same in regenerating nerve from *Tr*^{J} and control animals **(Table 7.12)**. The proportion of promyelinated fibres was increased and myelinated fibres decreased in *Tr*^{J} animals when compared with controls **(Fig. 7.15)** indicating a delay in the initiation of the myelination process.

Table 7.12. Axon numbers in *Tr*^{J} and control sciatic nerves 14 days after crush injury

	Total number of axons	Unmyelinated axons (% of total axons)
Control (n=6)	1892 ± 148	83.5 ± 0.8
Tr^{J} (n=5)	1632 ± 99	78.9 ± 3.3
Mann Whitney U test	NS	NS

Mean ± S.E.M

Figure 7.12.

Electron micrograph from the sciatic nerve of a *Tr*^{J} animal 14 days post crush injury.

The terminal myelin loops at the node of Ranvier are directed outwards instead of being attached to the paranodal axolemma. Scale bar 1 μm.

Figure 7.13.

Electron micrographs from the sciatic nerve of *Tr*^{J} animals 14 days post crush injury. (a) Schwann cell nuclei positioned abnormally close to the node of Ranvier (arrow).Scale bar 10 μm (b) 'Spikey' cytoplasmic projections associated with regions of the axons that are not covered with myelin. Processes appear to be adhering to original basement membrane (arrow). Scale bar 4 μm.

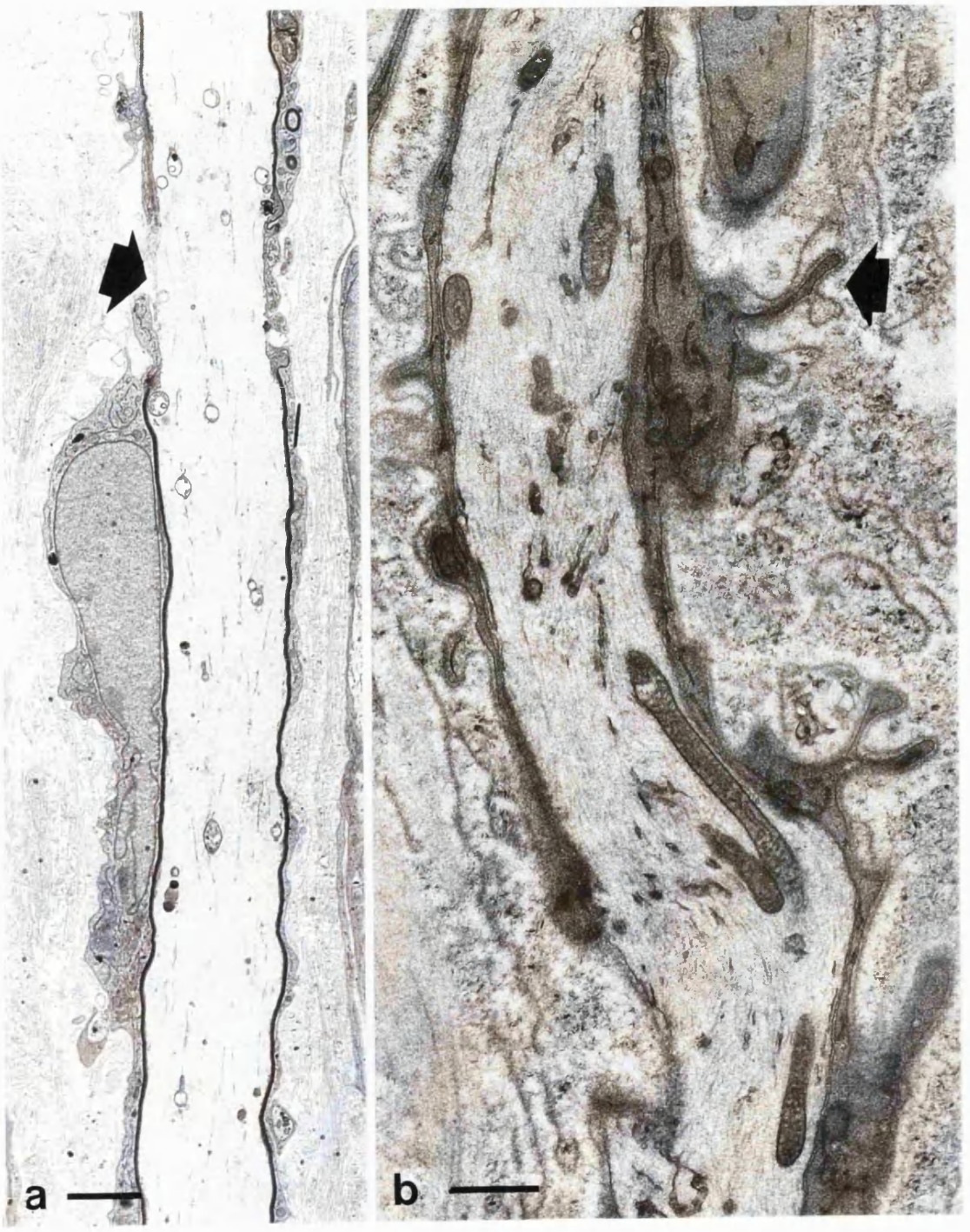
a
b

Figure 7.14.

Electron micrographs from the sciatic nerve of *Tr*^{J} and control animals 14 days post crush injury.

(a) A promyelin fibre from a regenerating *Tr*^{J} nerve. Cytoplasmic processes appear to be associated with the original basement membrane (arrow). Scale bar 1 μm. (b) A typical promyelinated fibre from a regenerating control nerve. Scale bar 1 μm. (c) A recently regenerated fibre from a *Tr*^{J} animal. The fibre has cytoplasmic processes that appear to be associated with remnants of the original basement membrane (arrow). Scale bar 1 μm. (d) A recently regenerated fibre from a control animal. The new fibre is within the original basement membrane but is not adhering to it. Scale bar 1 μm.

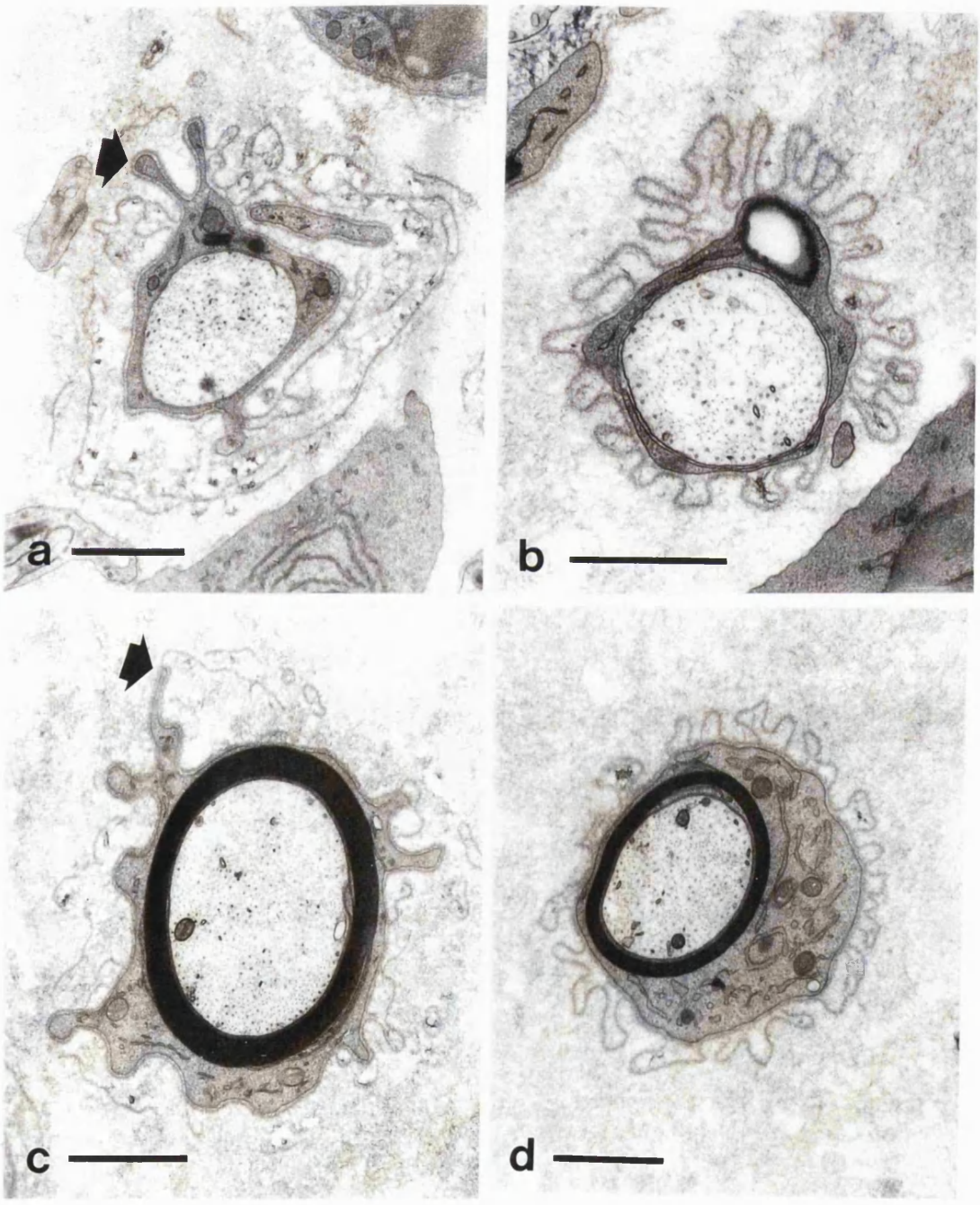
a
b
c
d

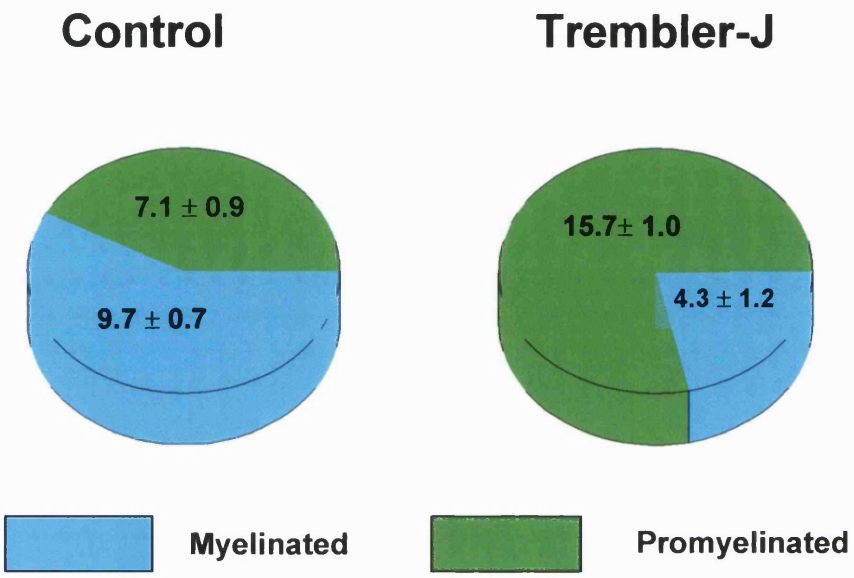

Figure 7.15 The proportion of myelinated and promyelin axons in Tr^{J} and control mice 14 days after crush injury.

Schwann cell numbers. Surprisingly we found an increase in the number of Schwann cells associated with unmyelinated axons. In crushed control nerve there were 13.4 Remak bundles/ 100 unmyelinated axons; in Tr^{J} animals the number had increased to 20.8 **(Fig 7.16).** The increase in the number of Schwann cells associated with unmyelinated axons was not confined to regenerating Tr^{J} nerve but was also found in uninjured Tr^{J} sciatic nerve (control 8.1/100, Tr^{J} 12.7/100) **(Fig. 7.16).** The proportional increase in crushed (55%) and uninjured (56%) nerve was remarkably similar and therefore unlikely to be related to the injury but a feature of the Tr^{J} phenotype. (See discussion).

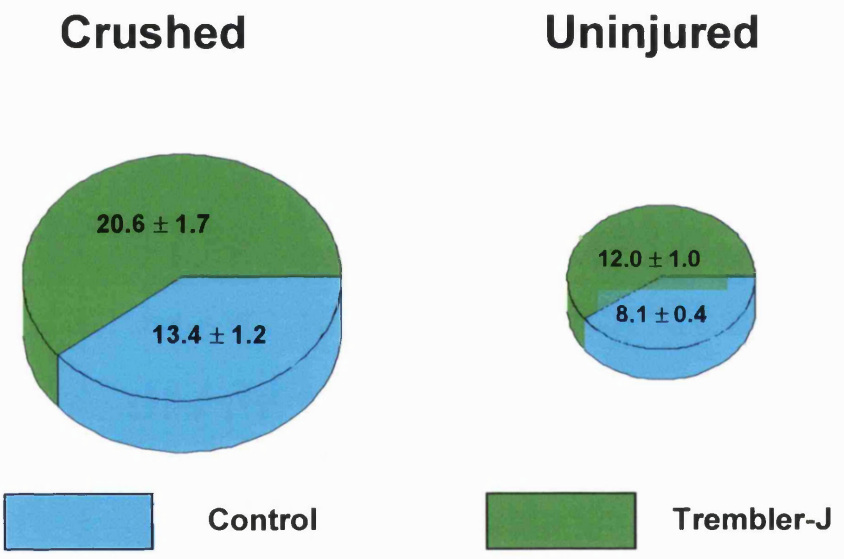

Fig 7.16 Number of Schwann cell nuceli /100 axons in injured and uninjured sciatic nerve of Tr^{J} and control mice

7.4.2 mRNA

Levels of the two PMP22 transcripts. The level of the myelination associated transcript (CD25) was decreased in *Tr*^{J} animals compared with controls (82% ± 26%) but there was no alteration in the growth arrest (SR13) transcript, which showed a much greater variation (168% ± 166%).

Table 7.13. The expression of alternative PMP22 transcripts in Tr^{J} nerve as a percentage of control values.

	CD25	SR13
Mean percentage of control value.	82%	168%
S.D.	26%	166%
Mann-Whitney U test	P<0.01	NS

Table 7.14. The ratio of mRNA transcripts in injured and uninjured mutant and control nerve

	Tr^{J}	Control
Uninjured	1.34 ± 0.5 (n=8)	0.77 ± 0.2 (n=6)
Crushed	1.22 ± 0.3 (n=6)	Not detected (n=6)
Mann-Whitney U test		p=0.75

Mean ± SD.

Neither of the two PMP22 transcripts were detected in the regenerating nerve of control animals two weeks after crush injury. To confirm that this was not due to degradation of the mRNA these experiments were repeated in a further 6 control and 5 *Tr*^{J} animals. Primer sequences for the house keeping gene hypoxanthine-guanine phosphoribosyl transferase (HPRT) were used in addition to amplifying both PMP22 trancripts. HPRT is a salvage enzyme in the nucleotide metabolic pathway. cDNA would be expected to amplify in any peripheral nerve sample providing a marker of mRNA/cDNA viability. The previous results were confirmed, cDNA from all samples amplified with the HPRT primers but only the cDNA from *Tr*^{J} resulted in PMP22 transcript amplification.

7.5. DEVELOPMENTAL STUDIES

On examination of semithin sections at postnatal day 4, affected C22 and homozygous *Tr*^{J} animals were easily recognised as they had markedly decreased numbers of myelinated fibres **(Fig. 7.17 a,c,e)** In heterozygous *Tr*^{J} animals, the decrease in myelinated fibres was difficult to judge by eye but they also could be distinguished from controls by the presence of many fibres with irregular contours **(Fig. 7.17f).** The C61 strain could not be distinguished morphologically from controls **(Fig. 7.17b).**

Fibre counts In all mutant strains the process of axon separation from fetal bundles into a 1:1 relationship with individual Schwann cells appeared to proceed normally. At P4 there was no difference in the total number of singly ensheathed fibres in the different strains **(Table 7.15).**

Table 7.15. Total number of singly ensheathed fibres in transgenic animals at postnatal day 4.

	Control	4 copies (C61)	7 copies (C22)	*Tr*^{J} het	*Tr*^{J} hom
P4	643 ± 20	630 ± 62	657 ± 25	538 ± 98	761 ± 68

Mean ± S.E. (n=6)

A myelination deficit was already present at P4 in C22 (7 copy) and both heterozygous and homozygous *Tr*^{J} animals. Homozygous *Tr*^{J} animals were the most severely affected with less than 2% of the singly ensheathed axons being myelinated. The proportion of myelinated fibres increased with age in control, C61(4 copies) and heterozygous *Tr*^{J} animals but C22 (7 copies) remained very poorly myelinated and homozygous *Tr*^{J} animals developed very little myelin before their death around weaning **(Figure7.18).**

Figure 7.17.

Electron micrographs of the sciatic nerve of P10-12 transgenic and *Tr*^{J} animals. (*a*) Control. (*b*) 4 copies of *PMP22* (C61). (*c*) 7 copies of *PMP22* (C22). (*d*) *Tr*^{J} heterozygote; Incompletely surrounded axons (filled arrow), Naked axons (open arrows). (*e*) *Tr*^{J} homozygote. (*f*) *Tr*^{J} heterozygote, Schwann cell cytoplasm with an irregular outline. Such irregular outlines as were commonly seen in heterozygotes and permitted them to be distinguished from C61 and control animals as early as P4. Uncompacted myelin (open arrow). Scale bar, 1 μm.

Scale bar 2.5 μm applies for panels *a-e*

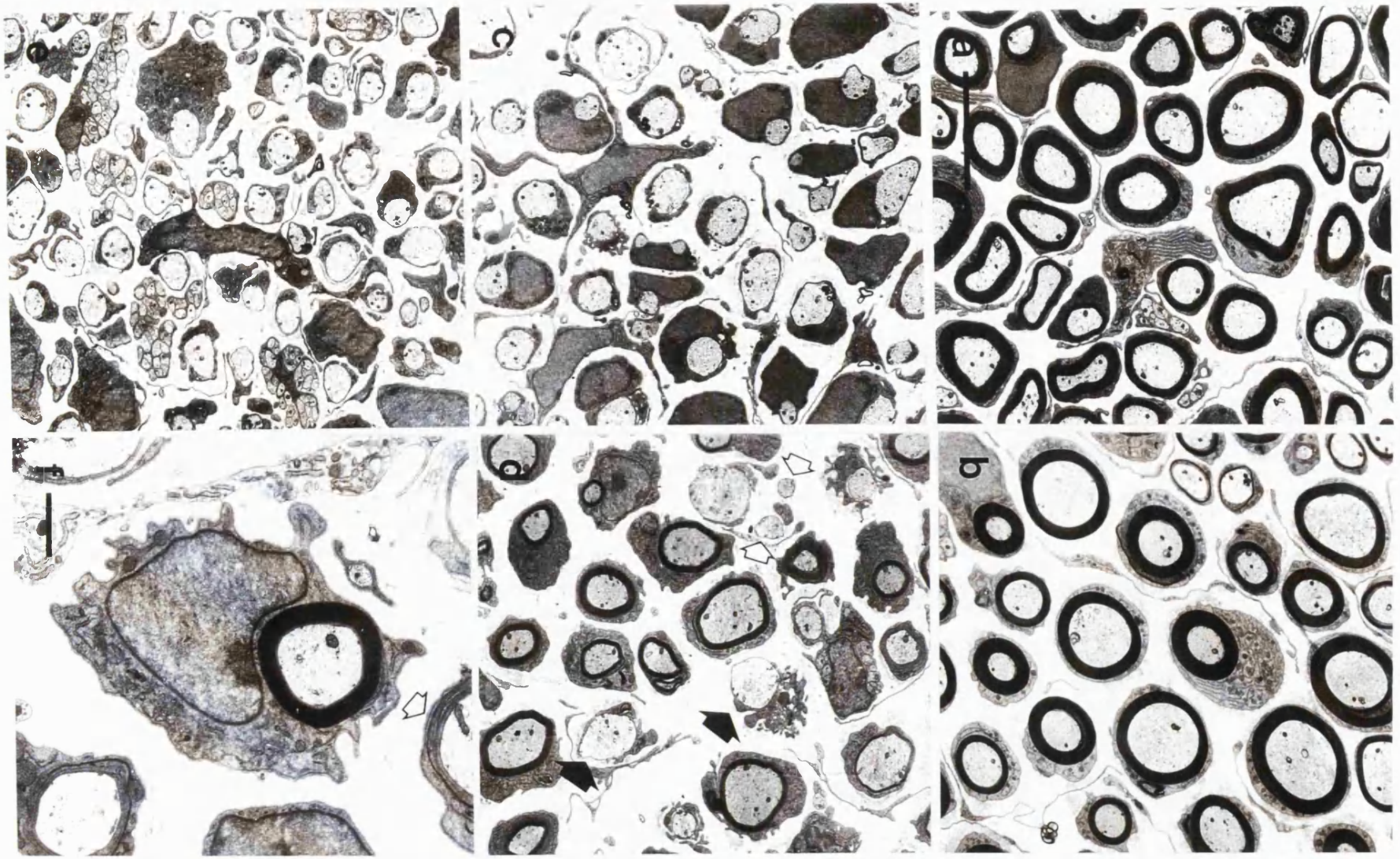
a
c
e
d
f
b

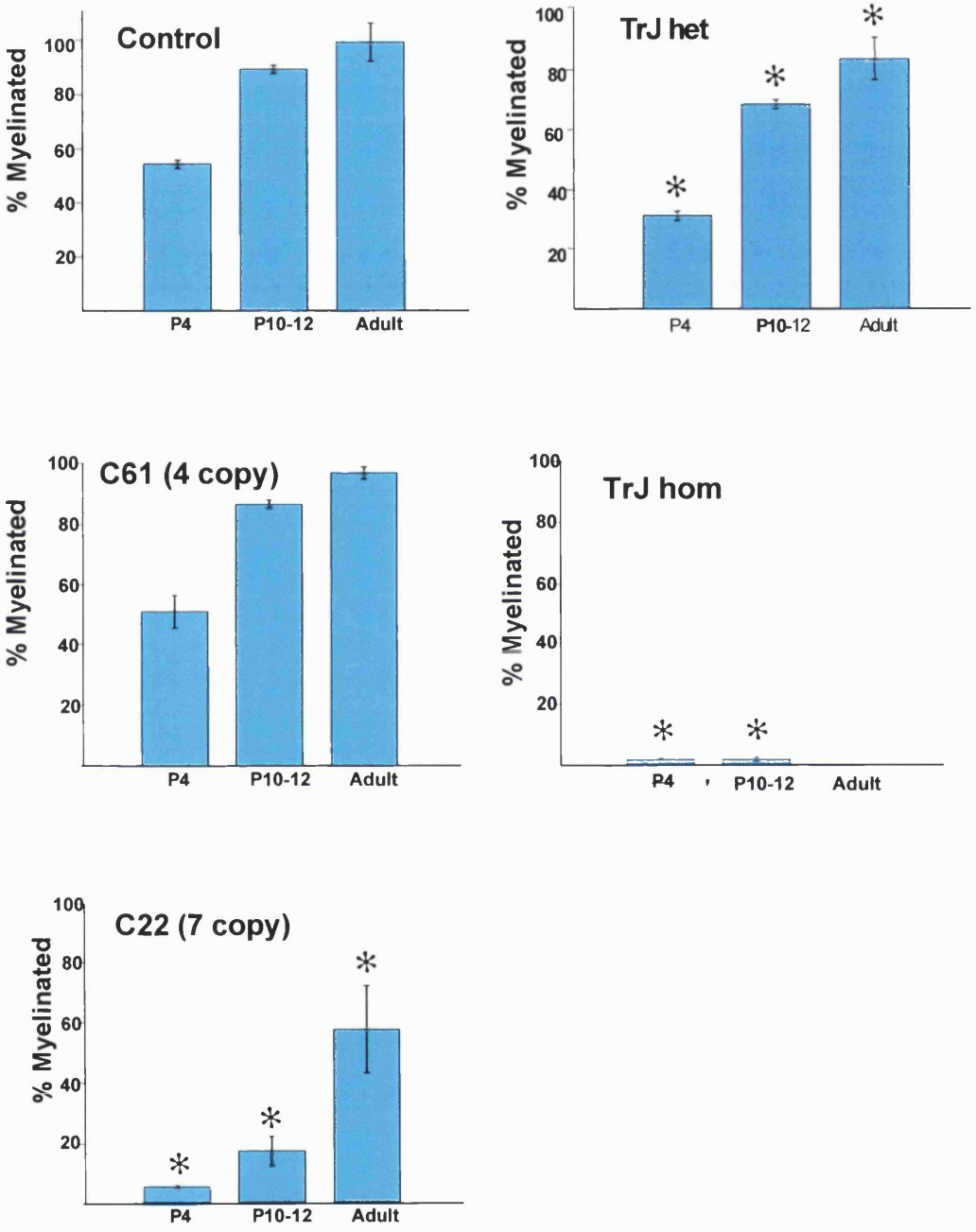

Figure 7.18. Percentage of singly ensheathed fibres that were myelinated in transgenic and *Tr*^{J} animals at the different ages examined.

* Indicates significantly different from controls at the same age.

An increased number of Schwann cells is a feature of most PMP22 disorders. At P4 the C22 mutants already had a significantly higher number of Schwann cells compared with controls. By P12 *Tr*^{J} heterozygotes and *Tr*^{J} homozygotes also had significantly increased numbers of Schwann cells. Between P4 and P12 the number of Schwann cells per 100 axons decreased both in controls and in the mildly affected C61 strains as myelination progressed. In the other mutants the number of Schwann cells increased **(Fig 7.19).** When comparing early postnatal and adult values the percentage of Schwann cells decreases in control and C61 animals. In almost all the singly ensheathed fibres are myelinated. In C22 and *Tr*^{J} heterozygote nerves the percentage of Schwann cells does not alter from early postnatal values.

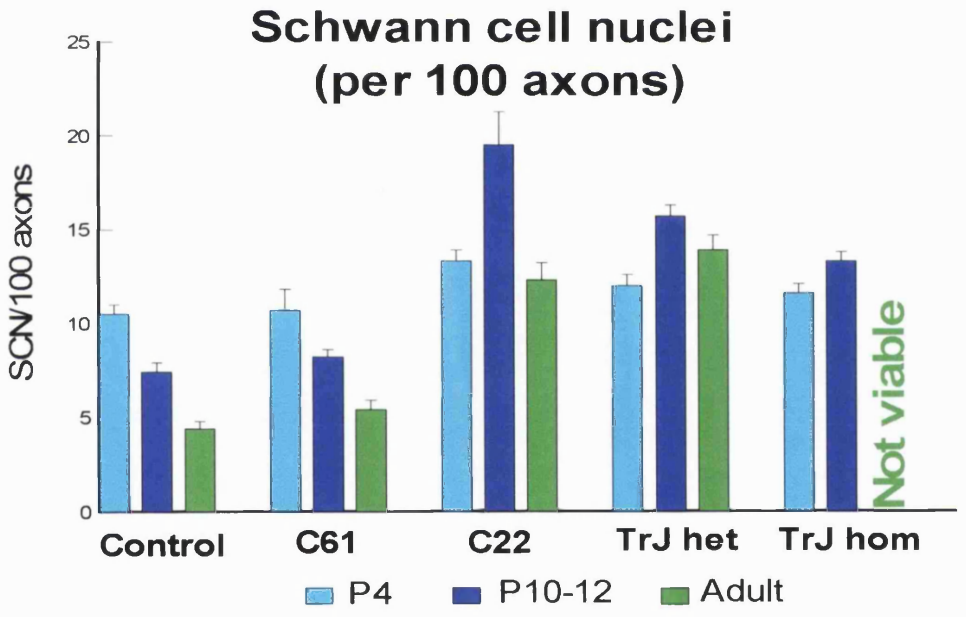

Fig 7.19 Schwann cell nuclei/100 axons in the sciatic nerve of P10-P12 transgenic and Tr^{J} animals

Incompletely surrounded fibres. At both P4 and P12 all the mutants had an increased number of fibres that were incompletely surrounded by Schwann cell cytoplasm. In C22 animals this number did not alter during development but in all the other strains the number decreased with age **(Fig 7.20).** It is interesting to note that the only feature in which C61 mice differ from control animals is the inability of the Schwann cell to surround a fibre completely.

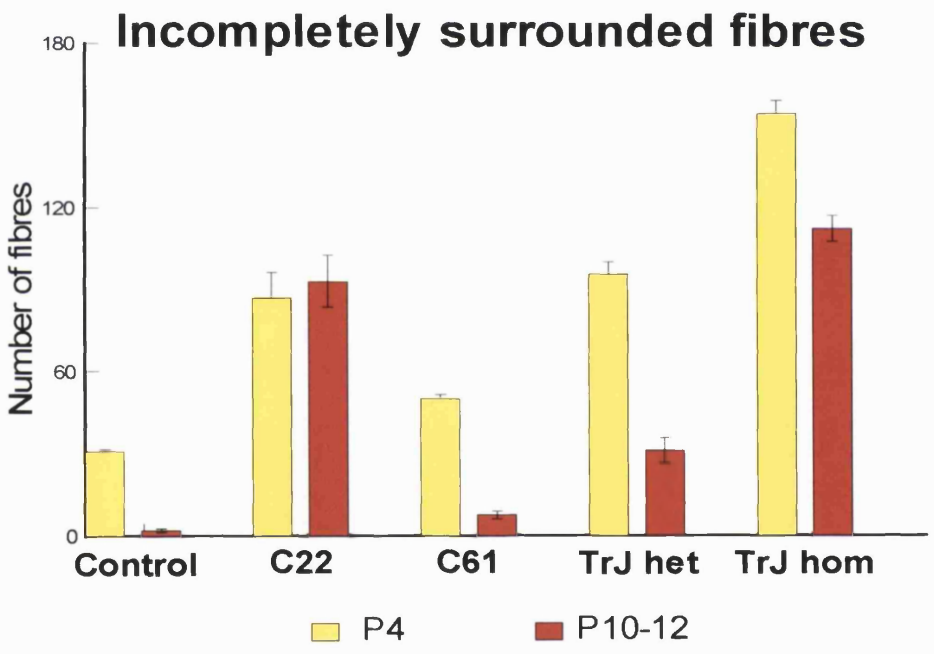

Fig 7.20 The number of fibres incompletely surrounded by Schwann cell cytoplasm in the sciatic nerve of P10-P12 transgenic and Tr^{J} animals

The two most affected strains (Tr^J/Tr^J and C22) could be morphologically distinguished from each other by P10-12. Schwann cell cytoplasm in the promyelin fibres of Tr^J/Tr^J animals failed to complete a full turn around the axon **(Fig 7.21 a),** in C22 animals many had progressed so that a mesaxon had been formed **(Fig 7.21 b).**

Beyond P10-12. Sciatic nerve sections of transgenic animals were examined at P28-29, 3 mo and 6 mo in addition to those used for morphometric analysis at 7 mo. C2 animals, with 2 extra copies of PMP22 were not noticeably affected at any of the ages we examined. C61 animals appeared to myelinate more or less normally in the first 10-12 d. The first indication of a myelin deficit was seen at P28 when occasional thinly myelinated large fibres could be seen in some animals. At 3 mo a few more fibres were becoming affected and by 6 mo a population of thinly myelinated fibres and axons with no myelin were clearly seen. Demyelination specifically affected the large fibre population. In C22 animals the degree of myelination improves steadily from P10-12 through to adulthood but never approaches normal levels. Even in adult animals less than 60% of fibres fall within the normal g ratio spectrum of normal fibres.

Figure 7.21. Features of the stage at which delay in myelination occurs in fibres from Tr^J homozygous and C22 animals at P10-12

(*a*) Fibres from a 7 copy (C22) animal in which the Schwann cell cytoplasm has completed a full turn around the axon. Scale bar, 1 μm. (*b*) Fibres from a *Tr*^{J} homozygous animal in which the Schwann cell cytoplasm fails to complete a full turn around the axon. Scale bar, 1 μm.

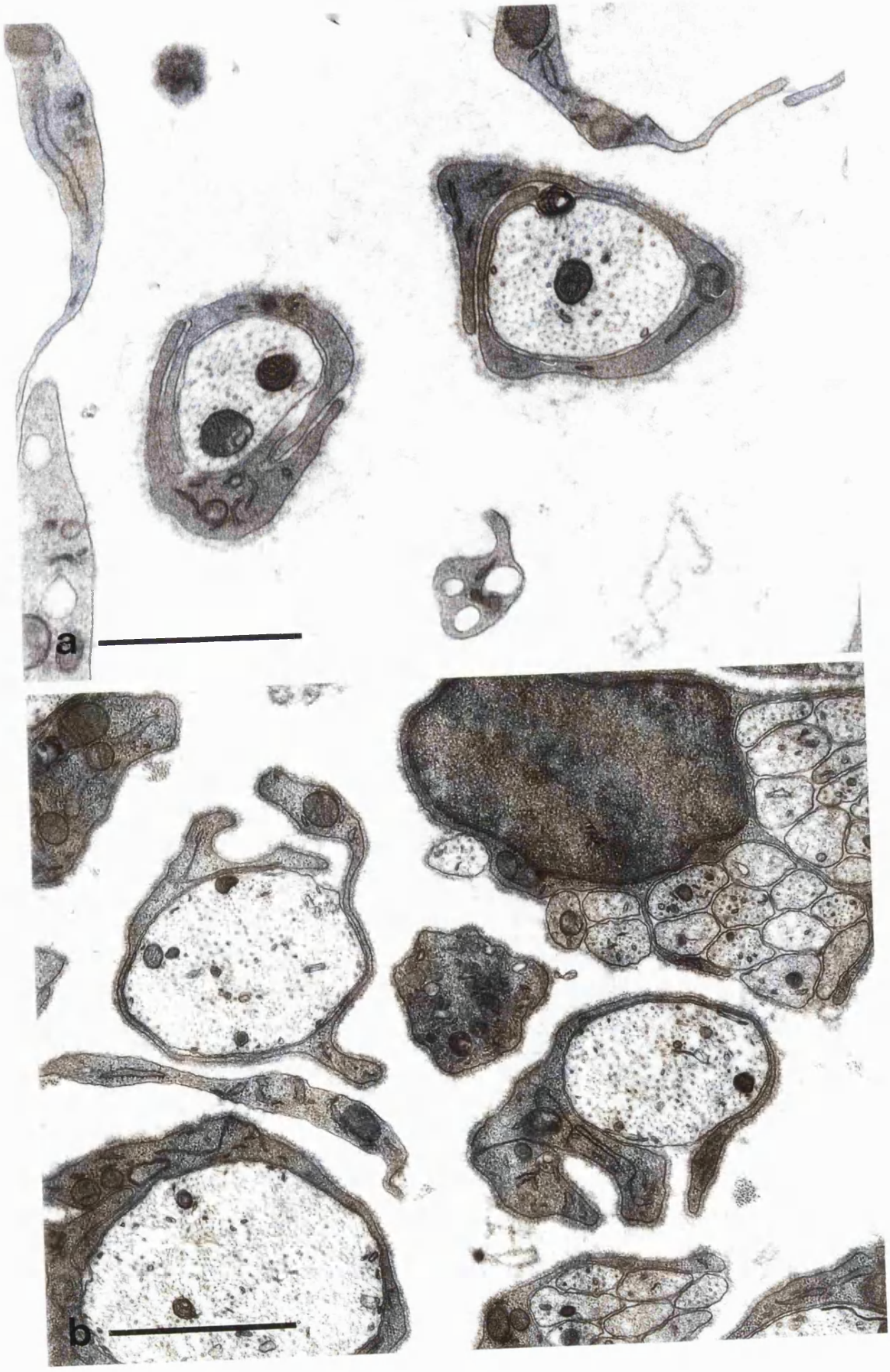
a
b

Chapter 8 Discussion

8.1 THE RESULTS OF THESE STUDIES

Adult *Tr*^{J} morphology. The dominant features of the *Tr*^{J} neuropathy are a myelination deficit, an increased number of Schwann cells and a failure of the Schwann cells to ensheath the axons fully. Myelination was most severely affected in the ventral roots both in the 3 and 12 mo animals. The dorsal roots were significantly less affected and the sciatic nerve less so. Fibre density was significantly reduced in the dorsal roots both in the 3 and 12 mo *Tr*^{J} animals when compared with controls. As there was no alteration in fascicular area this indicates a degree of axonal loss. Axonal loss was limited to the dorsal roots and was not related to the degree of myelination or to the lack of ensheathment of axons by Schwann cells. There are no comparable data currently available on axonal loss in the other murine models with point mutations in PMP22 (*Tr* and *Tr-Ncnp*). There is no loss in the L4 ventral root or in the ulnar nerve (Perkins et al. 1981b) of *Tr* mice.

As the distribution of PMP22 is not known to differ significantly between the dorsal and ventral roots, it is difficult to suggest a mechanism whereby the dorsal roots should be more susceptible to axonal loss than the ventral, or why myelination should be more affected in the ventral roots.

There are two possible contributing factors; firstly, the different expression of the L2/HNK-1 epitope in motor and sensory nerves (Martini et al. 1994) and secondly, a minor disease contributing effect of motorneuron-expressed PMP22 (Parmantier et al. 1995).

The number of Schwann cell nuclei was 3-5 times higher in *Tr*^{J} than in age matched control animals and did not alter with age. The number of nuclei was higher in the dorsal roots when compared with the ventral roots this difference was significant in 12 mo *Tr*^{J} animals but not in 3 mo *Tr*^{J} animals or controls. The increase in Schwann cell number does not reflect the severity of dysmyelination.

No classical onion bulbs were seen in any *Tr*^{J} nerves. In contrast basal laminal onion bulbs were more common. These layers of collapsed basement membrane have been suggested as indicating that the Schwann cells become reactive, extend cytoplasmic processes and then withdraw them (Ayers & Anderson 1975). Schwann cell protrusions were evident in the present material (see Fig 7.2).The occasional sectorial distribution of the empty basal laminal layers (Fig 7.2) would favour this explanation. An alternative explanation for the presence of basal laminal rather than classical onion bulbs would be ongoing Schwann cell proliferation

with loss of the redundant supernumerary Schwann cells . Against this explanation is the lack of morphological evidence of cell death.

Additional abnormal morphological features were seen in the nerves of 1y Tr^J nerves which we suggest provides ultrastructural evidence of altered axon-Schwann cell interactions. Schwann cell nuclei have been found adjacent to the nodes of Ranvier whereas in normal animals they are located near the centre of the internodes. This altered positioning may reflect either a mistaken sense of position or altered interaction with the Schwann cell cytoskeleton. In some fibres the terminal myelin loops faced outwards into the extracellular space instead of turning inwards and terminating on the axon. The frequency of these abnormalities increased with increasing severity of the disorder.

Crush morphology. We have found that the nerves of elderly Tr^J mice show a number of morphological abnormalities (Robertson et al. 1997); however, because of the advanced age of the animals used in this study, it was possible that the alterations seen were secondary to repeated cycles of de/remyelination. In the crush injury study we found that all the abnormal features seen in elderly Tr^J mice were reproduced during nerve regeneration following crush injury. This indicates that these alterations are due to an intrinsic abnormality of Tr^J Schwann cells and their interactions with axons and the ECM and not a result of repeated cycles of demyelination/remyelination. Ultrastructural alterations in Tr^J nerves, apart from the hypomyelination, appeared to be based around abnormal interactions of the Schwann cells with the cytoskeleton and also, particularly with the original basal lamina. The previously noted 'spikey' projections (Robertson et al. 1997) and the new observation of prolonged association of the Schwann cells of regenerating fibres with the original basal lamina suggest this as the main site of abnormal interaction.

Schwann cell proliferation is a well documented feature of the pathology in disorders associated with PMP22 defects, but has been thought only to affect fibres that are challenged to form myelin (Aguayo et al. 1977; Perkins et al. 1981a). Unmyelinated fibres in the nerves of Trembler animals are reported as appearing morphologically normal and are not associated either with increased Schwann cell numbers or the altered proliferation rates that affect myelinated nerves (Perkins et al. 1981b). The results presented here provide the first evidence of a significant increase in Schwann cells associated with unmyelinated axon bundles. The proportion of Schwann cell increase (50%) is much less than that seen in myelinated fibres in the sciatic nerve (340 %). As PMP22 is found localised in the Schwann cell plasmalemma of unmyelinated fibres, this result suggests that the increase in Schwann cell numbers is a feature of all PMP22 producing Schwann cells. This also suggests that the abnormality in Tr^J does not lie solely in its role as a myelin protein. Given the putative function of PMP22 as a growth arrest associated protein, it seemed possible that the

increased number of Schwann cells was related to a dysfunction in the PMP22 transcript which has been associated with growth arrest (SR13).

Crush mRNA Peripheral nerve expresses both the myelin associated (transcript 1) and growth arrest associated (transcript 2) transcripts. A dysfunction of transcript 1 is likely to affect myelination directly but it is also possible that a dysfunction in transcript 2 may result in the *Tr*^{J} phenotype. If PMP22 in peripheral nerve acts as a growth arrest protein whose effect is impaired by the mutation, persistent Schwann cell division could lead to dedifferentiation of the cell and consequent demyelination.

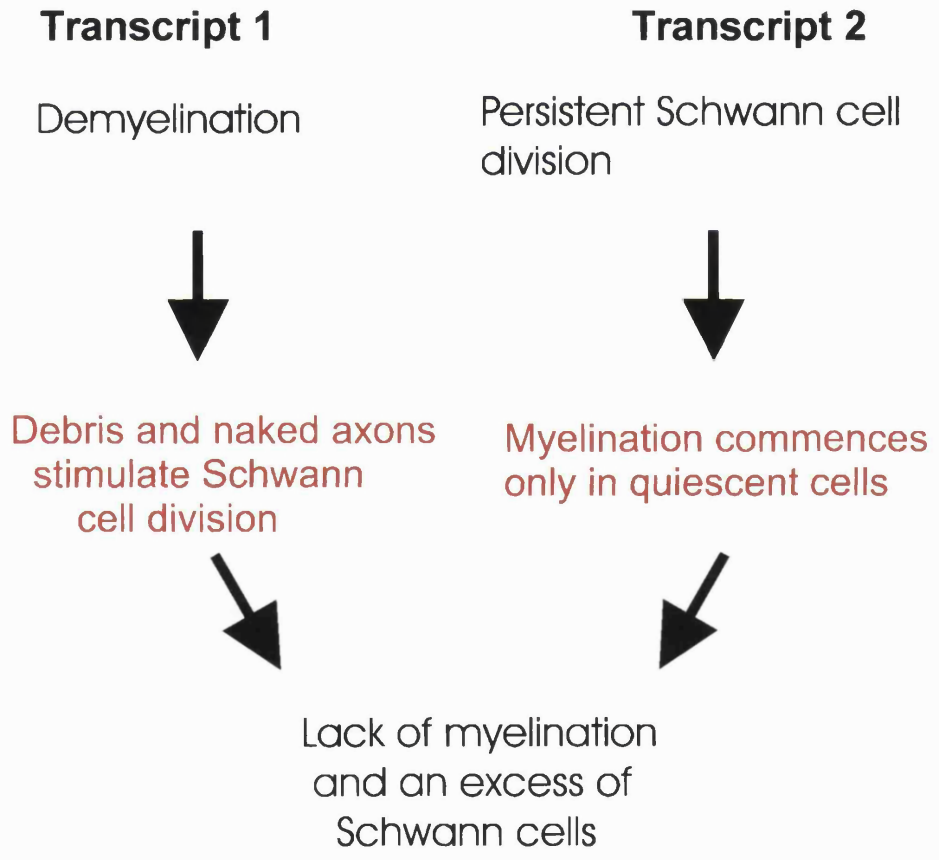

Figure 8.1 Alternative mechanisms which may result in excess Schwann cell production

We examined the expression of both transcripts in the nerves of injured and uninjured *Tr*^{J} and control nerves. In both crushed and uninjured *Tr*^{J} nerve there was an increase in the ratio of SR13/CD25 when compared with control animals. This was found to be due to a decrease

in the amount of the myelin related transcript (CD25) rather than an increase in the growth arrest associated transcript (SR13). In crushed control nerve neither transcript was detected in any of the animals suggesting that there may be a degree of myelin protein reutilization in regenerating nerve.

Following the identification of two different PMP22 mRNA transcripts, Garbay et al. (1995) examined their respective levels of expression in the peripheral nervous system of the Trembler mouse during the myelination period. Steady state levels of the exon 1A-containing transcript were greatly reduced in both heterozygous and homozygous Trembler mice when compared with controls. No such difference was noted for the exon 1B-containing transcript. It is well documented that Schwann cells continue to proliferate throughout the lifespan of *Tr* animals but the results of both these studies indicate that Schwann cell proliferation is not directly linked to a down regulation of the 1B transcript.

Adult transgenic morphology In this study we found that increasing the number of copies of PMP22 resulted in an increasing severity of phenotype. Rather than the phenotype becoming increasingly more severe with each increase in dose of PMP22, it became more severe in a stepped manner. Animals with 2 extra copies of PMP22 were scarcely affected. The only difference between the C2 strain and control animals was a 0.8% increase in the number of thinly myelinated fibres (g ratio >0.8<1.0). This is unlikely to represent any degree of functional deficit. C61 animals with 4 additional copies of the human PMP22 gene have a mild peripheral neuropathy with a small percentage of both thinly myelinated and extremely thinly myelinated fibres. Myelination appears to develop normally in C61 animals until P28 when occasional thinly myelinated large fibres could be seen in some animals. At 3mo a few fibres were affected in most animals. At 6mo a distinct population of thinly myelinated or demyelinated axons was seen in affected animals. Myelin loss only affected the large fibre population. This indicates that the myelin initially forms normally but is in some way unstable and breaks down in larger fibres. In C22 animals the myelin deficit is of a completely different nature, myelin formation is delayed or non-existent in many fibres. In the population of fibres which do myelinate, the myelin formed is disproportionately thin for the axon size.

Developmental transgenic morphology. Delayed myelination is found with underexpression (null mutants) (Adlkofer et al. 1995); overexpression (Magyar et al. 1996) and mutations of the PMP22 gene. This suggests that PMP22 has a role in the initiation of myelination. The myelination process was arrested at the promyelin stage in all the PMP22 mutants that we examined. This study showed that the axons separate normally into a 1:1

relationship with individual Schwann cells. The high proportion of fibres that are incompletely surrounded by Schwann cell cytoplasm indicate that the first abnormality and, by implication, the first function of PMP22 predates myelin formation and involves the attachment and movement of the Schwann cell around the axon. This is related specifically to axons that are destined to myelinate and is not a generic feature of mutant Schwann cells. There was no evidence of ensheathment abnormalities in the unmyelinated fibre population. Additional evidence for an early function of PMP22 in myelin initiation comes from the two most severely affected strains, C22 and *Tr*^{J} homozygotes. These two strains could be distinguished from each other by differences in the initial ensheathment of axons. In homozygous *Tr*^{J} animals the two apposing edges of Schwann cell cytoplasm failed to overlap but in the C22 strain there was usually a small overlap of Schwann cell membranes and initial mesaxon formation. This suggests that PMP22 is involved in either mesaxon formation or the guidance/recognition processes involved in the spiralling of Schwann cell cytoplasm to form the myelin sheath.

Two features of this early developmental morphology can be produced by interrupting Schwann cell differentiation with the thymidine analogue, 5-bromodeoxyuridine (BrdU). Following treatment of demyelinated nerve with BrdU, Hall and Gregson (1977) reported an increased number of promyelin fibres with cytoplasm that was irregular in outline. These are morphologically very similar to the irregular fibres characteristic of *Tr*^{J} heterozygote animals. Additionally many cells possessed pseudopodial processes a feature also commonly found in both heterozygous and homozygous *Tr*^{J} nerves.

These results raise 2 possible interpretations, firstly that the mutant phenotype results from a failure of the differentiation process or, secondly, that it results from disrupted cell/cell interactions.

If the Schwann cells fail to differentiate fully in their myelinating phenotype, they are unlikely to be capable of responding appropriately to axonal signals to myelinate. During the differentiation process, Schwann cells cease to proliferate and grow both longitudinally (internode length) and radially (myelin sheath thickness). An inability of mutant Schwann cells to surround axons and subsequently to rotate around them to form myelin may be seen as an extension of failed differentiation.

Alternatively, if PMP22 functions in mediating the interaction between cell types, it is possible that differentiation failure itself is secondary to defective cell interactions. In a previous study we proposed that adult *Tr*^{J} animals exhibited abnormalities that were consistent either with defective Schwann cell/axon or Schwann cell/extracellular matrix interactions (Robertson et al. 1997). Axonal contact is known to be a prerequisite for the initiation of myelination. If the Schwann cell only partially surrounds the axon, the signal

may be insufficient to produce differentiation and myelination. Similarly Schwann cells in culture only cease to divide and commence myelin formation when they are in contact with the extracellular matrix (De Vries 1993). In this study, the only feature that distinguished the C61 (4 copy) strain from controls was the increased number of fibres that were not surrounded by Schwann cell cytoplasm. This leads us to conclude that the axon/Schwann cell interaction is more likely to be the site of abnormality than Schwann cell/extracellular matrix interaction.

In either of these 2 scenarios, the lack of myelination in these PMP22 disorders can be seen as a secondary feature. This is largely overcome with time in most of the models, the degree of myelination improving from P10-12 to adult. *Tr*^{J} homozygous animals all die at around P21 but it is difficult to suggest a reason for their death based on a lack of myelin: both *Tr* homozygotes and C22 progeny are equally severely dysmyelinated and yet C22 have a normal lifespan. Comparative observations on the severity of associated axonal loss will be of interest in the C61 strain, which is relatively unaffected during the early stages of development. In these a relatively small proportion of larger fibres (7%) become hypomyelinated in adult mice suggesting that a moderate overexpression of PMP22 leads to myelin instability later in life (data not shown).

From the present results the increased Schwann cell numbers found in adult *Tr*^{J} heterozygote and C22 animals appear not to result from persistent Schwann cell proliferation but mainly from a failure in the normal maturational decrease in density per unit length of nerve (or cross sectional area) related to the cessation of mitosis after myelination and the progressive increase in Schwann cell length during development. If demyelination subsequently occurs, this will result in Schwann cell proliferation. Schwann cell proliferation occurs at the onset of myelination, protracted length of the myelination period may result in the increase in Schwann cell number seen in *Tr*^{J} heterozygote and C22 transgenic animals between P4 and P12.

Schwann cell proliferation. Schwann cell proliferation is a well documented feature of murine neuropathies involving altered PMP22. In these studies we have found that the number of Schwann cells in adult animals is increased in C22 and both heterozygous and homozygous *Tr*^{J} animals when compared with age matched controls.
Several theories have been postulated to explain this increase, although they relate largely to the *Tr* mouse in which Schwann cells continue to divide throughout the animals' lifetime. In the animal models we have examined there is no evidence of continuing Schwann cell proliferation, the number of Schwann cell nuclei being relatively constant or even decreasing, from early postnatal to adult stages.

Myelin debris. The presence of myelin debris is a well documented stimulus for Schwann cell division (Komiyama & Suzuki 1992; Baichwal & DeVries 1989; Perry et al. 1987). In cell culture studies, proliferating Schwann cells were found to be the ones which were participating in the digestion of myelin debris (Salzer & Bunge 1980). This led Ayers and Anderson (1976) to postulate that the increase in Schwann cells in the *Tr* mouse was a reactive response to the presence of myelin debris (Ayers & Anderson 1976). This seems unlikely as the increase in Schwann cell nuclei in the *Tr* mouse is seen very early in development (P3) (Koenig et al. 1991). Three days following nerve injury Schwann cells begin to increase in number, this would leave barely enough time for the Schwann cells to react to myelin debris. In Tr^{J} and C22 animals there was very little active demyelination seen in animals older than one month. This may contribute to the fact that Schwann cells do not continue to divide in Tr^{J} as they do *Tr* which do show increased amounts of myelin debris.

Some authors (Aguayo et al. 1977; Aguayo et al. 1979) suggest that the abnormalities in the *Tr* mouse are related to the Schwann cells being challenged to myelinate. While this is clearly a dominating factor it does not explain the increased number of SCN associated with unmyelinated fibres in Tr^{J} mice. The degree of SCN increase is clearly much less in unmyelinated fibres but this suggests that Schwann cell increases are not entirely related to the myelination process. They are also contributed to, either by another process occurring at a similar time in development, or to proliferation associated with a diffusable mitogenic stimulus that affects both the myelinated and unmyelinated populations (Archer & Griffin 1993).

Axonal stimulus. Low (1976) did not agree with Ayers and Anderson's (1976) theory that myelin debris was likely to be the stimulus for Schwann cell division as in *Tr* animals the number of Schwann cells was already increased before myelin breakdown occurred (Low 1976a; Low 1976b). He considered that the presence of a developing or markedly hypomyelinated axon would provide adequate stimulus for Schwann cell division. Like myelin debris, naked axolemma and axolemmal fragments are also known to provide stimulus for Schwann cell division (Pellegrino & Spencer 1985; Wood & Bunge 1975). The present results suggest that a response to naked axolemma alone is unlikely to explain the increased numbers of Schwann cells, although it may contribute. If naked axolemma were the primary stimulus to Schwann cell division, we should also expect the number of SCN to reflect the difference in severity of demyelination between Tr^{J} and C22 sciatic nerves. The proportion of axons with no detectable myelin was 30% in the C22 strain and only 15 % in Tr^{J}. Similarly, in the ventral roots of 12 mo Tr^{J} animals, 60-65% of axons had no detectable myelin but in the dorsal root this was only 40-50%, yet the number of SCN did not differ.

Developmental failure of Schwann cell growth. Aguayo et al. (1977) commented that, although the hypercellularity seen in the *Tr*^{J} mouse could be due to a chronic demyelinating process, it could also be secondary to a developmental failure of myelination. Sheath thickness has been found to relate not only to axon calibre but also to internode length. Foreshortened internodes have slightly thinner myelin than long internodes of the same fibre calibre (Friede 1985). If the myelin sheaths are relatively thin for the axon calibre, this is generally taken as a sign of insufficient myelin formation. Beuche and Friede (1985) noted that the reverse interpretation is also valid; proliferation of Schwann cells may cause excessively short, rudimentary internodes which develop only abortive sheaths. They also raised the possibility of the existence of dissociated and independent disturbances of myelin formation and of Schwann cell proliferation.

Failure of Schwann cell growth is the most satisfactory explanation for the increased Schwann cell numbers in PMP22 mutants. Protracted SC multiplication in young animals is likely to function as a compensatory mechanism to ensure ensheathment of individual axons. It is also plausible that the different levels of Schwann cell proliferation in the ventral and dorsal roots are related to this growth failure. There is a different growth pattern found in motor and sensory fibres with the largest (presumably motor) fibres being the first to myelinate (Williams & Wendell-Smith 1971b). Assuming that fibres in the dorsal root begin to myelinate slightly later than those in the ventral root and that, once they have begun to myelinate, they are capable of longitudinal growth (Koenig et al. 1991), this is likely to correspond to the time period in which maximum body growth occurs. The degree of proliferation required to ensure axon coverage is likely to be greater.

In conclusion Schwann cell proliferation in *pmp22* mutant mice can been seen as a secondary manifestation of a myelination disorder rather than a primary Schwann cell defect. Schwann cell proliferation is manifest in almost any peripheral neuropathy as a consequence of demyelination or axonal degeneration. The only exception to this is radiation neuropathy. When mouse nerves are irradiated soon after crush injury (3 days), Schwann cell proliferation is severely and persistantly reduced. Many fibres show segmental failure of myelination and internodes adjacent to nonmyelinated regions were abnormally long (Love 1983).

PART 2 COMPARISONS

Comparisons between PMP22 overexpressing humans and mice

The morphology of overexpressing mice was distinctly different from human duplication patients. The murine duplication models showed none of the hypertrophic changes or classical onion bulbs that characterise HMSN1a. Instead many, fibres were surrounded by

basal laminal onion bulbs. The significance of the two types of onion bulb is unclear. Classic onion bulbs are composed of paired basement membranes that usually contain Schwann cell cytoplasm. The Schwann cells that compose classic onion bulbs are considered to be supernumerary cells related to recurrent demyelination/remyelination. In contrast, basal laminal onion bulbs are thought to be formed as a result of Schwann cell movement, the Schwann cell extending processes and then withdrawing them leaving behind a single layer of basal lamina. Basal laminal onion bulbs are not necessarily associated with Schwann cell division. Although both the human and mouse duplications result in an excess of Schwann cells, they are likely to have developed from different types of responses. The excess number of Schwann cells in the murine mutants probably result from a response to the lack of myelination seen early in development, presumably because the Schwann cells divide to cover the length of the axon adequately. In contrast, the Schwann cells in human classic onion bulbs divide and do not remain axon associated; they appear to be additional to what is necessary for axon coverage.

Human duplication patients have a greatly reduced myelinated fibre density from an early age (10 y) (Gabreëls-Festen et al. 1995; Thomas et al. 1997; Fabrizi et al. 1998). Although our results show no difference in fibre density in the transgenic animals, our fibre counts have included those fibres with no detectable myelin. The proportion of these fibres is significant in all of the transgenic animals. This means that the myelinated fibre density is also likely to be decreased in all the transgenic strains. The present results show that the axons that are not surrounded by myelin do not degenerate. This differs from what is thought to happen in the human situation. In humans it is likely that axons are actually lost. In biopsy material there is evidence of axonal sprouting which must result from previous axonal degeneration (Dr R. King, personal communication). In affected humans determination of axonal loss is difficult as the variable degrees of nerve hypertrophy make fibre densities an unsuitable measure to quantify axonal loss. The alternative is counting all the myelinated fibres in a whole nerve at a specific level. As whole nerve biopsies are not commonly performed this is not a feasible option. Lack of axonal loss in the mouse is presumably due to a combination of factors. Mice have a considerably shorter life span in which to develop abnormalities. In addition, the smaller distance from the cell body to the nerve endings in the mouse could reduce the degree of strain imposed on the cell body in terms of maintaining the axon.

In both human and mouse, axons are markedly decreased in size. In the C22 strain this is probably due to the fact that axons are never fully myelinated and never attain a normal size distribution. In the C61 strain it is more likely to represent atrophy as a result of demyelination. The lack of developmental data on the human duplication makes it difficult to determine whether decreased axon size is due to atrophy or retarded growth.

In models where we have murine/human comparisons, L16P and overexpression, the resulting phenotype differs significantly. In the overexpression studies it is likely that this is partly due to incompatibility between the human and mouse PMP22 genes. However, there are features which the two comparisons have in common. In both cases the mouse model does not produce 'classic' but 'basal laminal' onion bulbs. The mouse is capable of forming classic onion bulbs as they are commonly seen in antisense PMP22 mice (Adlkofer et al. 1995), although the number of Schwann cell layers is relatively small. There is also no evidence of nerve hypertrophy in either of the murine disorders.

The composition of PNS myelin differs between species (Lees & Brostoff 1984) as does the carbohydrate compositions of a given protein (Schachner et al. 1995b). In human and bovine PNS, P_0 is the dominant carrier of the L2/HNK-1 epitope, whereas in mouse, L2/HNK-1 is predominantly carried by a 18-28 kDa protein, presumably PMP22. If the functional epitopes carried by PMP22 differ between species, this is likely to contribute to the different pathologies.

In our previous study we noted that there appeared to be a threshold effect with respect to PMP22 dosage (Huxley et al. 1998). With two or fewer additional copies of the PMP22 gene, there was little electrophysiological or histological effect. This threshold effect may also apply in humans, although in general the effects of increased gene dosage are more severe. Homozygous and heterozygous duplication patients, with 2 and 1 extra copy of the PMP22 gene respectively, have overlapping phenotypes. Within families homozygous children have variously been reported as being both more and less severely affected than heterozygous siblings (LeGuern et al. 1997; Lupski et al. 1991; Sturtz et al. 1997). This is consistent with what has been found in our studies, that below a certain threshold level of expression there appears to be an overlap of phenotypes.

Comparisons between Trembler and Trembler-J mice.

Although *Tr* and *Tr^J* are essentially similar, demonstrating largely the same features, they are not identical. *Tr^J* animals tend to be less severely affected than *Tr*. In the sciatic nerves of *Tr^J* almost all axons in a one-to-one relationship with a Schwann cell are surrounded by at least a few turns of myelin. In contrast, in the *Tr* mouse many axons do not progress beyond the stage of single ensheathment (promyelin fibres) but remain completely devoid of myelin and often incompletely surrounded by Schwann cell cytoplasm. This lack of ensheathment is rare in the sciatic nerves of *Tr^J* animals but is commonly seen in the more severely affected spinal roots.

In the early reports of pathology in the *Tr* mouse frequent onion bulbs were seen (Perkins et al. 1981b). A review of the literature shows that these are a mixture of classic and basal laminal onion bulbs (Ayers & Anderson 1973; Ayers & Anderson 1975; Low 1977). There was very

little evidence in *Tr*^{J} either of active demyelination or of cycles of demyelination/remyelination leading to concentric proliferation of Schwann cells around nerve fibres with the formation of hypertrophic or 'classic' onion bulbs. However most fibres were surrounded by well developed basal laminal onion bulbs.

Perkins et al. (1981b) showed that Schwann cell proliferation continues throughout the life of the *Tr* animals, whereas in *Tr*^{J} the number of Schwann cells does not appear to change beyond the initial stages of myelination. This may provide an explanation for the difference in the type of onion bulbs seen in the two strains. The ongoing demyelination and constant presence of myelin debris found in *Tr*, but not in *Tr*^{J}, may lead to continuing Schwann cell division followed by proliferation and remyelination with an excess of proliferated cells that accumulated circumferentially around the axons thus producing the classic onion bulb, as originally suggested for human hypertrophic neuropathy (Thomas & Lascelles 1967). Whereas in *Tr*^{J} there is no appreciable amount of active demyelination to begin this cycle; they have instead almost exclusively basal laminal onion bulbs, reflecting Schwann cell movement (Ayers & Anderson 1975).

The literature reports that *Tr* mice initially have frequent 'convulsions'. Convulsions were never seen in *Tr*^{J} animals although under deep anaesthesia they occasionally exhibited rigidity. A letter from Toyka et al (1997) describes neuromyotonia in aged mice either homozygously deficient for, or carrying an increased gene dosage of, PMP22 (Toyka et al. 1997b). This probably represents the supposed convulsions seen in *Tr* mice. Neuromyotonia is a feature of a number of human neuropathies.

Viability of homozygous mutants differs between the two point mutations. Homozygous *Tr*^{J} animals can be distinguished from littermates by P8-10, they are noticeably smaller in size, not necessarily in body length but due to a lack of musculature. They exhibit a noticeable tremor, are extremely weak and move with difficulty. Most animals died at around P18-20, but a few survive beyond weaning (a further 4-5 d). In contrast, homozygous *Tr* mutants were indistinguishable from heterozygous litter mates at 4 mo and appeared quite healthy at 1 y despite a maximum number of 6 myelinated fibres(Henry & Sidman 1988). Adlkofer et al. (1995) cross bred Tr/+ aniamls with PMP22 null mutants (PMP22 0/0). The resulting *Tr*/0 animals died at P18-24. It is difficult to suggest a reason for the death of Trembler -J homozygotes based on a lack of myelin or why one copy of a mutant protein (*Tr/0*) should have a more severe effect than two (*Tr/Tr*), given that null mutants (PMP22 *0/0*) survive until adulthood (Adlkofer et al. 1995).

Defective transport of PMP22 to the plasma membrane has been proposed as a disease mechanism in both *Tr*^{J} and *Tr*. PMP22 immunoreactivity in *Tr* animals has not only been seen in compact myelin but also in the cytoplasm of myelinating Schwann cells (Naef et al. 1997). Immunohistochemical studies of cells transfected with wildtype and/or *Tr* PMP22 showed that, while wildtype PMP22 was transported to the plasma membrane, *Tr* protein was localised mainly in the endoplasmic reticulum. The *Tr* protein did not reach the plasma membrane, endocytic pathway or lysosomes. Further evidence that *Tr* PMP22 is not transported to myelin comes from Tr/0 mice in which the myelin debris stained strongly for P_0 but not at all for PMP22 (Naef et al. 1997). As in *Tr* animals, *Tr*^{J} PMP22 immunoreactivity also accumulates not only in compact myelin but also in the Schwann cell cytoplasm. Studies on PMP22 transport in *Tr*^{J} animals showed that in these animals PMP22 is transported beyond the ER and transverses the Golgi apparatus, followed by accumulation in lysosomes (Notterpek et al. 1997). Abnormally high levels of both structural components of lysosomes (LAMP1) and lysosomal enzyme activity (CatD) are found in *Tr*^{J} nerves demonstrating activation of the endosomal /lysosomal pathways. PMP22, P_0 and MBP were all shown to be degraded at an increased rate in *Tr*^{J} nerve demonstrating increased myelin turnover or decreased myelin stability (Notterpek et al. 1997).

This idea of disrupted protein trafficking in PMP22 mutants has been corroborated by D'Urso et al. (1998) who demonstrated a similar effect in cultured Schwann cells expressing *Tr* and *Tr*^{J} mutant PMP22. Both forms were abundantly present in the ER and Golgi apparatus, but were not targeted to the plasma membrane. This study did not show any difference in localisation between *Tr* and *Tr*^{J} mutations. Trafficking abnormalities have also been seen in humans with PMP22 mutations. The nerve of a patient with the L16P mutation showed an accumulation of PMP22 staining in the cell body of myelinating Schwann cells that was not seen in control patients or patients with an acquired inflammatory demyelinating polyneuropathy. (D'Urso et al. 1998). Naef and Suter (1998) have inserted the human H12Q mutation into COS cells and found that the protein was retained intracellularly. This provides support for disrupted trafficking as a common factor to the disease mechanism in peripheral neuropathies due to alterations in the PMP22 protein.

In the normal situation almost all PMP22 is retained in the ER and rapidly degraded. A recent paper by Naef and Suter (1998) postulates that misfolding may be the reason for the intracellular degradation and that pathology in PMP22 mutants may result from increasing the amount of misfolded protein above a critical threshold level. This provides a possible explanation for point mutations and altered gene dosage resulting in similar pathology.

Different phenotypes produced by the L16P mutation in humans and mice.

The most obvious difference between humans and mice with the L16P mutation is the degree of severity of the resulting neuropathy. The dominant pathological feature in the human is the almost complete absence of myelin. This contrasts with the *Tr*^{J} mouse in which most of the fibres are surrounded by a thin layer of myelin.

In the adult human mutant, most fibres (90%) are surrounded by onion bulbs. In the mouse. classic onion bulbs were not found at all. Although the majority of fibres were surrounded by redundant basal lamina there were seldom more than one or two layers. The increase in Schwann cell numbers was also much greater in humans and of a different nature. In the human L16P mutants, axon associated Schwann cell nuclei represented 12, 17.6 and 20.6 nuclei/100 axons (patients14-16 in (Gabreëls-Festen et al. 1995)). These values are similar those found in mice (13.9 ±0.8.). In the human, a further 20-40 Schwann cell nuclei/100 axons were found supernumerary to axons. In the *Tr*^{J} mouse, supernumerary Schwann cells were seldom seen. These two differences illustrate a fundamental difference in the murine and human response to the same mutation.

PART 3 THE FUNCTION OF PMP22

Proper PMP22 expression is crucial for the formation and maintenance of PNS myelin. Functionally, abnormalities caused by alterations in the PMP22 gene all relate to the process of myelination and myelin stability. The results of this study provide evidence that in addition to its role in maintaining the stability of compact myelin, PMP22 functions in the initiation of myelination. Disruptions of this initial stage of myelin development also result in myelin deficiency. This may reflect the two different roles of PMP22 in the PNS (one early and one late) it is unlikely that they are part of a single function.

MYELIN FORMATION AND STABILITY

The initiation of myelination. The initial stages of myelin formation appear to be extremely sensitive to any perturbations in PMP22 expression. It is interesting to note that myelination is delayed at the promyelin stage in all the murine models with perturbations of the PMP22 gene. The spontaneously occurring *Tr* (Ayers & Anderson 1975; Ayers & Anderson 1976; Low 1976a), *Tr*^{J} (Henry et al. 1983), and the newly discovered Tr-Ncnp (Suh et al. 1997) mutants, all exhibit a delay in the progression of myelinogenesis, as do mice overexpressing (Magyar et al. 1996) and underexpressing (null mutants) (Adlkofer et al. 1995) PMP22. The delay of fibres at the promyelin stage in various spontaneous and transgenic rodent strains led to the suggestion that PMP22 was involved in the initiation of myelination (Adlkofer et al. 1995; Sereda et al. 1996). This is supported by the data obtained in this study. The first abnormality noted in early postnatal mice with perturbations in the

PMP22 gene was the delay of myelination. We have extended this observation to show that the myelination delay is probably secondary to a failure of Schwann cells to completely surround axons. The data from C22 and *Tr*^{J} homozygotes indicate that mesaxon formation and the initial spiralling of Schwann cell membranes around the axon is dependant upon correct PMP22 function.

Thickness of the myelin sheath. Although PMP22 perturbations all ultimately result in a degree of hypomyelination, its evolution differs between strains of mice. In the C22, and Trembler-J strains thin myelin is largely a result of a developmental failure of myelination (dysmyelination). This study also demonstrates that PMP22 functions in the maintenance of myelin sheath thickness later in development. In the C61, strain myelin appears to form normally; the first incidence of thin myelin sheaths was not noted until the animals were 4 wk old. The number of affected fibres then increased with age. In the C2 strain there was no obvious myelin deficit even in 8mo animals. The small proportion of thinly myelinated fibres noted in morphometric studies are unlikely to represent any degree of functional loss.

ADDITIONAL ROLES SUGGESTED FOR PMP22

While many of the roles postulated for PMP22 relate to the myelination process several additional roles have been proposed. Naef and Suter (1998) have speculated that promoter 1 has been acquired specifically during evolution to allow high level expression in myelinating Schwann cells and that this additional function differs from the original role of PMP22. This type of scenario has been suggested for some members of the crystallin family which are expressed as stress related proteins in a variety tissues but also function as a structural component of the lens. Aspects of the regulation of PMP22 suggest that the second function of PMP22 is not restricted to the non-neural tissues it is expressed in but is also functional in Schwann cells.

1. Growth arrest

The majority of the evidence for PMP22 acting as a growth arrest protein comes from cell culture studies. The PMP22 protein was first isolated from growth arrested fibroblasts and was expressed in resting but not proliferating cells. Altered levels of PMP22 expression were found to alter Schwann cell proliferation and DNA synthesis significantly. This led Zoidl et al. (1995) to propose that altered levels of PMP22 gene expression may impair myelination directly through the abnormal growth of Schwann cells.

Studies have been performed on both the *Tr* and *Tr*^{J} mice. In both cases, although the CD25 myelinating transcript was decreased, there was no evidence of any alteration in the growth arrest transcript. This is now not a plausible explanation for the increased number of Schwann cells seen in these two strains.

2. Gene family suggestive either of differentiation or cell/cell interactions

Differentiation. The morphological features of regenerating *Tr*^{J} nerve in many ways resemble those seen in demyelinated nerve treated with 5-bromodeoxyuridine (BrdU), a thymidine analogue which has been widely used to inhibit differentiation in mammalian cells. In BrdU treated nerve Hall and Gregson (1978) described the Schwann cell cytoplasm surrounding many fibres as having an irregular outline and possessing pseudopodial processes. The myelin that was formed was abnormally thin and sometimes uncompacted, both of these being features commonly found in *Tr*^{J} mice. In the present study axonal regeneration in *Tr*^{J} animals appeared to proceed normally and there was no difference either in the total number of regenerating axons or in the proportion of axons that were in unmyelinated bundles. Regenerating nerves of *Tr*^{J} animals displayed a significant delay in the progression of axons from the promyelin to the myelinated state;this was also a prominent feature of BrdU treated nerve.

In overexpressing transgenic mice, adult Schwann cells expressed the markers low-affinity NGF receptor (LNGFR), NCAM and L1 in a pattern similar to those normally seen in developing Schwann cells (Magyar et al. 1996). These authors suggested that impaired Schwann cell differentiation may be the mechanism which results in myelination deficits in mice overexpressing PMP22. The similarity in morphology in *Tr*^{J} and BrdU treated nerve suggests that a failure of differentiation may be the mechanism by which the *Tr*^{J} mutation delays the process of myelination.

Given the proposed role of the other members of the PMP22 family in differentiation and maintenance of the differentiated state is seems plausible that PMP22 has an early function in the initial stages of myelinogenesis related to a switch enabling or permitting the differentiation of Schwann cells beyond the promyelin stage. As early as 1981, Perkins et al. postulated that the *Tr* mutation could be reguarded as a failure of Schwann cell differentiation beyond the stage of early myelinogenesis. They regarded Schwann cell multiplication as a compensatory mechanism for a lack of radial (myelin thickness) and longitudinal (internodal length) cell growth.

If PMP22 does function in the switch between proliferating and differentiating phenotypes this may explain the difference in Schwann cell proliferation between *Tr* and *Tr*^{J}. In *Tr* PMP22 is thought not to exit the Golgi apparatus, therefore there would be almost no signal to differentiate. Hence the continued Schwann cell multiplication and secondarily the low levels of myelination (28%). In *Tr*^{J} however the protein does exit the Golgi apparatus and is incorporated into the myelin sheath, but is thought to be degraded quickly. This may push the Schwann cell a little further along the differentiation path enabling better myelination.

Cell/cell interaction with the axon or cytoskeleton. EMP-3 (HNMP-1), which has the highest amino acid homology to PMP22 (44%), is transiently expressed by Schwann cells during sciatic nerve myelination. The EMP-3 protein itself is axon associated and is thought to play a role in axon-Schwann cell interactions (Bolin et al. 1997). If PMP22 functions in mediating the interaction between cell types it is possible that differentiation failure itself is secondary to defective cell interactions. In a previous study we proposed that adult *Tr*^{J} animals exhibited abnormalities that were consistent either with defective Schwann cell/axon or Schwann cell/extracellular matrix interactions (Robertson et al. 1997). Axonal contact is known to be a prerequisite for the initiation of myelination. If the Schwann cell only partially surrounds the axon, the signal may be insufficient to produce differentiation and myelination. Similarly Schwann cells in culture only cease to divide and commence myelin formation when they are in contact with the extracellular matrix (De Vries 1993). In this study the only feature that distinguished the C61 (4 copy) strain from controls was the increased number of fibres that were not surrounded by Schwann cell cytoplasm. This leads us to the conclusion that the axon/Schwann cell interaction is more likely to be the site of abnormality than Schwann cell/extracellular matrix interaction.

3. Adhesion function

It is tempting to speculate on the possible role of the L2/HNK-1 epitope in this disorder. In at least 2 members (PMP22 and CL20) in the family of proteins the L2/HNK epitope is associated with the glycosylation site on the highly conserved 1st transmembrane domain (Marvin et al. 1995; Snipes et al. 1993). The HNK-1 epitope forms the basis of a large family of recognition molecules and is thought to serve as a ligand for adhesion. (Kunemund et al. 1988; Griffith et al. 1992). L2/HNK-1 is known to be expressed in developing peripheral nerve where it is thought to be involved in Schwann cell-axon interactions (Martini & Schachner 1986; Martini et al. 1994). L2/HNK-1 is involved in cell/cell and cell/laminin interactions and antibodies directed against it are capable of functionally blocking neural adhesion to laminin in the presence of heparin (Kunemund et al. 1988; Keilhauer et al. 1985; Hall et al. 1993). It is likely that PMP22 is the major L2/HNK-1 expressing glycoprotein in peripheral nerve (Snipes et al. 1993) and in the light of the ultrastructural abnormalities found in the *Tr*^{J} mouse it seems plausible that altered interaction of a mutated protein and the carbohydrate moiety may be involved.

Reference List

ABERCROMBIE M, EVANS DHL, MURRAY JG. (1959) Nuclear multiplication and cell migration in degenerating unmyelinated nerves. *Journal of Anatomy* **93**, 9-14.

ABERCROMBIE M, JOHNSON ML. (1946) Quantitative histology of Wallerian degeneration.I. Nuclear population in rabbit sciatic nerve. *Journal of Anatomy* **80**, 37-50.

ABO T, BALCH CM. (1981) A differentiation antigen of human NK and K cells identified by a monoclonal antibody (HNK-1). *Journal of Immunology* **127**, 1024-1029.

ADLKOFER K, FREI R, NEUBERG DH-H, ZIELASEK J, TOYKA KV, SUTER U. (1997) Heterozygous peripheral myelin protein deficient mice are affected by a progressive demyelinating tomaculous neuropathy. *Journal of Neuroscience* **17**, 4662-4671.

ADLKOFER K, MARTINI R, AGUZZI A, ZIELASEK J, TOYKA KV, SUTER U. (1995) Hypermyelination and demyelinating peripheral neuropathy in *Pmp22*-deficient mice. *Nature Genetics* **11**, 274-280.

AGUAYO AJ, ATTIWELL M, TRECARTEN J, PERKINS S, BRAY GM. (1977) Abnormal myelination in transplanted Trembler mouse Schwann cells. *Nature* **265**, 73-75.

AGUAYO AJ, BRAY GM, PERKINS SC. (1979) Axon-Schwann cell relationships in neuropathies of mutant mice. *Annals of the New York Academy of Sciences* **317**,512-531.

AGUAYO AJ, CHARRON L, BRAY GM. (1976a) Potential of Schwann cells from unmyelinated nerves to produce myelin: a quantiative ultrastructural and radiographic study. *Journal of Neurocytology* **5**, 565-573.

AGUAYO AJ, EPPS J, CHARRON L, BRAY GM. (1976b) Multipotentiality of Schwann cells in cross-anastomosed and grafted myelinated and unmyelinated nerves: quantitative microscopy and radioautography. *Brain Research* **104**, 1-20.

AGUAYO AJ, PEYRONNARD JM, TERRY LC, ROMINE JS, BRAY GM. (1976c) Neonatal axonal loss in rat superior cervical ganglia: retrograde effects on developing preganglionic axons and Schwann cells. *Journal of Neurocytology* **5**, 137-155.

ALLT G. (1969a) Repair of segmental demyelination in peripheral nerves: An electron microscope study. *Brain* **92**, 639-646.

ALLT G. (1969b) Ultrastructural features of the immature peripheral nerve. *Journal of Anatomy* **105**, 283-293.

ALLT G. (1972) An ultrastructural analysis of remyelination following segmental demyelination. *Acta Neuropathologica* **22**, 333-344.

ALLT G. Pathology of the peripheral nerve. (1976) In D.N. Landon (Ed.) *The peripheral nerve*, Chapman and Hall, London.

ALLT G, CAVANAGH JB. (1969) Ultrastructural changes in the region of the node of Ranvier in the rat caused by diphtheria toxin. *Brain* **92**, 459-468.

ARCHER DR, GRIFFIN JW. (1993) "Bystander" proliferation of cells in the sciatic nerve is induced by lumbar radiculopathy.Quoted in GRIFFIN JW. AND HOFFMAN PN. (1993) Degeneration and regeneration in the peripheral nervous system. In P.J. Dyck, P.K. Thomas, J.W. Griffin, P.A. Low and J.F. Poduslo (Eds.) *Peripheral Neuropathy*, W.B.Saunders Company, Philadelphia, pp. 361-376.

ARIGA T, KOHRIYAMA T, FREDDO L, LATOV N, SAITO M, KON K, ANDO S, SUZUKI M, HEMLING ME, RINEHART KL, KUSUNOKI S, YU RK. (1987) Characterization of sulfated glucuronic acid containing glycolipids reacting with IgM M-proteins in patients with neuropathy. *The Journal of Biological Chemistry* **262**, 848-853.

ASBURY AK. (1967) Schwann cell proliferation in developing mouse sciatic nerve. A radioautographic study. *The Journal of Cell Biology* **34**, 735-743.

AYERS MM, ANDERSON RM. (1973) Onion bulb neuropathy in the Trembler mouse: A model of hypertrophic interstitial neuropathy (Dejerine-Sottas) in man. *Acta Neuropathologica* **25**, 54-70.

AYERS MM, ANDERSON RM. (1975) Development of onion bulb neuropathy in the Trembler mouse. Comparison with normal nerve maturation. *Acta Neuropathologica* **32**, 43-59.

AYERS MM, ANDERSON RM. (1976) Development of onion bulb neuropathy in the Trembler mouse. Morphometric study. *Acta Neuropathologica* **36**, 137-152.

BAECHNER D, LIEHR T, HAMEISTER H, ALTENBERGER H, GREHL H, SUTER U, RAUTENSTRAUSS B. (1995) Widespread expression of the peripheral myelin protein-22 gene (pmp22) in neural and non-neural tissues during murine development. *Journal of Neuroscience Research* **42** , 733-741.

BAICHWAL RR, DEVRIES GH. (1989) A mitogen for Schwann cells derived from myelin basic protein. *Biochemical and Biophysical Research Communications* **164**, 883-888.

BALLIN RHM, THOMAS PK. (1969) Electron microscope observations on demyelination and remyelination in experimental allergic neuritis. Part 2.Remyelination. *Journal of the Neurological Sciences* **8**, 225-237.

BASCLES L, BONNET J, GARBAY B. (1992) Expression of the PMP-22 gene in Trembler mutant mice: Comparison with the other myelin protein genes. *Developmental Neuroscience* **14**, 336-341.

BASCLES L, BONNET J, GARBAY B. (1994) Over-expression of MBP and PLP messenger RNA in 8-day-old trembler brain. *Neuroreport* **5**, 1221-1223.

BEHSE F, BUCHTHAL F, CARLSEN F, KNAPPEIS GG. (1972) Hereditary neuropathy with liability to pressure palsies-Electrophysiological and histopathological aspects. *Brain* **95**, 777-794.

BEN OTHMANE K, MIDDLETON LT, LOPREST LJ, WILKINSON KM, LENNON F, ROZEAR MP, STAJICH J, GASKELL PC, ROSES AD, PERICAK-VANCE MA, VANCE JM. (1993) Localization of a gene (CMT2A) for autosomal dominant Charcot-Marie-Tooth disease type 2 to chromosome 1p and evidence of genetic heterogeneity. *Genomics* **17**, 370-375.

BERGHOFFEN J, SCHERER SS, WANG S, SCOTT MO, BONE LJ, PAUL DL, CHEN K, LENSCH MW, CHANCE PF, FISCHBECK KH. (1993) Connexin mutations in X-linked Charcot-Marie-Tooth disease. *Science* **262**, 2039-2042.

BEUCHE W, FRIEDE RL. (1984) The role of non-resident cells in Wallerian degeneration. *Journal of Neurocytology* **13**, 767-796.

BEUCHE W, FRIEDE RL. (1985) A quantitative assessment of myelin sheaths in the peripheral nerves of Dystrophic, Quaking and Trembler mutants. *Acta Neuropathologica* **66**, 29-36.

BEUCHE W, FRIEDE RL. (1986) Myelin phagocytosis in Wallerian degeneration depends on silica-sensitive, bg/bg-negative and Fc-positive monocytes. *Brain Research* **378**, 97-106.

BIRD TD, OTT J, GIBLETT ER. (1982) Evidence for linkage of Charcot-Marie-Tooth neuropathy to the Duffy locus on chromosome 1. *American Journal of Human Genetics* **34**, 388-394.

BLIN N, STAFFORD DW. (1976) A general method for isolation of high molecular weight DNA from eukaryotes. *Nucleic Acids Research* **3**, 2303-2308.

BOEGMAN R, AGUAYO AJ, BRAY GM. (1977) Axoplasmic transport in (Trembler mouse) nerves with a widespread disorder of myelination. *Journal of Neuropathology and Experimental Neurology* **36**, 590

BOLIN LM, MCNEIL T, LUCIAN LA, DEVAUX B, FRANZ-BACON K, GORMAN DM, ZURAWSKI S, MURRAY R, MCCLANAHAN TK. (1997) HNMP-1: A novel hematopoietic and neural membrane protein differentially regulated in neural development and injury. *The Journal of Neuroscience* **17**, 5493-5502.

BOLINO A, BRANCOLIN, V, BONO F, BRUNI A, GAMBARDELLA A, ROMEO G, QUATTRONE A, DEVOTO M. (1996) Localization of a gene responsible for autosomal recessive demyelinating neuropathy with focally folded myelin sheaths to chromosome 11q23 by homozygosity mapping and haplotype sharing. *Human Molecular Genetics* **5**, 1051-1054.

BORT S, NELIS E, TIMMERMAN V, SEVILLA T, CRUZMARTINEZ A, MARTINEZ F, MILLAN JM, ARPA J, VILCHEZ JJ, PRIETO F, VANBROECKHOVEN C, PALAU F. (1997) Mutational analysis of the MPZ, PMP22 and Cx32 genes in patients of Spanish ancestry with Charcot-Marie-Tooth disease and hereditary neuropathy with liability to pressure palsies. *Human Genetics* **99**, 746-754.

BORT S, SEVILLA T, GARCIAPLANELLS J, BLESA D, PARICIO N, VILCHEZ JJ, PRIETO F, PALAU F. (1998) Dejerine-Sottas neuropathy associated with De Novo S79P mutation of the peripheral myelin protein 22 (PMP22) gene. *Human Mutation* **S1**, S95-S98

BOSH EP, ASSOULINE JG, MILLER JF, LIM R. (1984) Glial maturation factor promotes proliferation and morphologic expression of rat Schwann cells. *Brain Research* **304**, 311-319.

BOSSE F, ZOIDL G, WILMS S, GILLEN CP, KUHN HG, MÜLLER HW. (1994) Differential expression of two mRNA species indicates a dual function of peripheral myelin protein *PMP22* in cell growth and myelination. *Journal of Neuroscience Research* **37**, 529-537.

BOYLES JK, NOTTERPEK LM, ANDERSON LJ. (1990) Accumulation of apolipoproteins in the regenerating and remyelinating mammalian peripheral nerve. *The Journal of Biological Chemistry* **265**, 17805-17815.

BRAVERMAN IM. (1953) Neurological actions caused by the mutant gene "Trembler" in the house mouse (Mus Musculus, L.): an investigation. *Journal of Neuropathology and Experimental Neurology* **12**, 64-72.

BRAY D, CHAPMAN K. (1985) Analysis of microspike movements on the neuronal growth cone. *The Journal of Neuroscience* **5**, 3204-3213.

BRONNER-FRASER M. (1987) Perturbation of cranial neural crest migration by the HNK-1 antibody. *Developmental Biology* **123**, 321-331.

BUCHBERG AM, MOSKOW JJ, BUCKWALTER MS, CAMPER SA. (1991) Mouse chromosome 11. *Mammalian Genome* **1**, S158-S191

BUCHTHAL F, BEHSE F. (1977) Peroneal muscular atrophy (PMA) and related disorders. I. Clinical manifestations as related to biopsy findings, nerve conduction and electromyography. *Brain* **100**, 41-66.

BUNGE MB, WILLIAMS AK, WOOD PM. (1972) Further evidence that neurons are required for the formation of basal lamina around Schwann cells. *The Journal of Cell Biology* **83**, 130

BURGOON MP, GRUMET M, MAURO V, EDELMAN GM, CUNNINGHAM BA. (1991) Structure of the chicken neuron-glia cell adhesion molecule, Ng-CAM: Origin of the polypeptides and relation to the Ig superfamily. *The Journal of Cell Biology* **112**, 1017-1029.

CARLSTEDT T. (1980) Internodal length of nerve fibres in dorsal roots of cat spinal cord. *Neuroscience Letters* **19**, 251-256.

CARTER TC. (1951) Wavy-coated mice: phenotypic interactions and linkage tests between rex and (*a*) waved-1, (*b*) waved-2. *Journal of Genetics* **50**, 268-276.

CAVANAGH JB, JACOBS JM. (1964) Some quantitative aspects of diphtheritic neuropathy. *British Journal of Experimental Pathology* **45**, 309-322.

CHANCE PF, ABBAS N, LENSCH MW, PENTAO L, ROA BB, PATEL PI, LUPSKI JR. (1994) Two autosomal dominant neuropathies result from reciprocal DNA duplication/deletion of a region on chromosome 17. *Human Molecular Genetics* **3**, 223-228.

CHANCE PF, ALDERSON MK, LEPPIG KA, LENSCH MW, MATSUNAMI N, SMITH B, SWANSON PD, ODELBERG SJ, DISTECHE CM, BIRD TD. (1993) DNA deletion associated with hereditary neuropathy with liability to pressure palsies. *Cell* **72**, 143-151.

CHANCE PF, BIRD TD, MATSUNAMI N, LENSCH MW, BROTHMAN AR, FELDMAN GM.(1992) Trisomy 17p associated with Charcot-Marie-Tooth neuropathy type 1A phenotype: Evidence for gene dosage as a mechanism in CMT1A. *Neurology* **42**, 2295-2299.

CHANCE PF, BIRD TD, O'CONNELL P, LIPE H, LALOUEL J-M, LEPPERT M.(1990) Genetic linkage and heterogeneity in type I Charcot-Marie-Tooth disease (hereditary motor and sensory neuropathy type I). *American Journal of Human Genetics* **47**, 915-925.

CHANCE PF, FISCHBECK KH. (1994) Molecular genetics of Charcot-Marie-Tooth disease and related neuropathies. *Human Molecular Genetics* **3**, 1503-1507.

CHARCOT J-M, MARIE P. (1886) Sur une forme particluiere d'atrophie musculaire progressive souvent familiale debutant par les pieds et les jambes et atteignant plus tard les mains. *Révue Medicale* **6**, 97-138.

CHEN L, FREIMER F, SAHENK Z. (1998) A novel Val30Met PMP22 mutation causes HNPP. *Neurology* **50 S4**, S08.001

CHOU DKH, ILYAS AA, EVANS JE, COSTELLO C, QUARLES RH, JUNGALWALA FB. (1986) Structure of sulfated glucuronyl glycolipids in the nervous system reacting with HNK-1 antibody and some IgM paraproteins in neuropathy. *The Journal of Biological Chemistry* **261**, 11717-11725.

CLEMENCE A, MIRSKY R, JESSEN KR. (1989) Non-myelin-forming Schwann cells proliferate rapidly during Wallerian degeneration in the rat sciatic nerve. *Journal of Neurocytology* **18**, 185-192.

CRAGG BG, THOMAS PK. (1964) The conduction velocity of regenerated peripheral nerve fibres. *Journal of Physiology* **171**, 164-175.

CRANG AJ, BLAKEMORE WF. (1986) Observations on Wallerian degeneration in explant cultures of cat sciatic nerve. *Journal of Neurocytology* **15**, 471-482.

CREW FAE, AUERBACH C. (1939) Rex: a dominant autosomal monogenic coat texture character in the mouse. *Journal of Genetics* **38**, 341-344.

CRUZMARTINEZ A, BORT S, ARPA J, DUARTE J, PALAU F. (1997) Clinical, genetic and electrophysiologic correlation in hereditary neuropathy with liability to pressure palsies with involvement of PMP22 gene in chromosome 17p11.2. *European Journal of Neurology* **4**, 274-286.

D'URSO D, PRIOR R, GREINER-PETTER R, GABREËLS-FESTEN AAWM, MULLER HW. (1998) Overloaded endoplasmic reticulum-golgi compartments, a possible pathomechanism of peripheral neuropathies caused by mutations of the peripheral myelin protein PMP22. *The Journal of Neuroscience* **18**, 731-740.

D'URSO D, SCHMALENBACH C, ZOIDL G, PRIOR R, MÜLLER HW. (1997) Studies on the effects of altered PMP22 expression during myelination in vitro. *Journal of Neuroscience Research* **48**, 31-42.

DAVIES DM. (1954) Recurrent peripheral nerve palsies in a family. *Lancet* **2**, 266-268.

DAVIS JB, STROOBANT P. (1990) Platelet-derived growth factors and fibroblast growth factors are mitogens for rat Schwann cells. *The Journal of Cell Biology* **110**, 1353-1360.

DAVISSON MT, RODERICK TH. (1978) Status of the linkage map of the mouse. *Cytogenetics and Cell Genetics* **22**, 552-557.

DAYAN AD, GRAVESON GS, ROBINSON PK, WOODHOUSE MA. (1968) Globular neuropathy-A disorder of axons and Schwann cells. *Journal of Neurology, Neurosurgery and Psychiatry* **31**, 552-560.

DE LEÓN M, NAHIN RL, MENDOZA ME, RUDA MA. (1994) SR13/PMP-22 expression in rat nervous system, in PC12 cells, and C6 glial cell lines. *Journal of Neuroscience Research* **38**, 167-181.

DE VRIES GH. (1993) Schwann cell proliferation. In P.J. Dyck, P.K. Thomas, J.W. Griffin, P.A. Low and J.F. Poduslo (Eds.) *Peripheral Neuropathy*, W.B.Saunders company, Philadelphia, pp. 290-298.

DEJERINE J, SOTTAS J. (1893) Sur la névrite interstitielle, hypertophique et progressive de l'enfance. *Comptes Rendue de la Société de Biologie* **45**, 63-96.

DENT EW, IDA J.A.JR, YOSHINO JE. (1992) Isolated growth cones stimulate proliferation of cultured Schwann cells. *Glia* **5**, 105-111.

DO THI NA, KOENIG HL, VIGNY M, FOURNIER M, RESSOUCHES A. (1993) In vivo proliferative pattern of Trembler hypomyelinating Schwann cells is modified in culture: An experimental analysis. *Developmental Neuroscience* **15**, 10-21.

DOW KE, MIRSKI SEL, RODER JC, RIOPELLE RJ. (1988) Neuronal proteoglycans: Biosynthesis and functional interaction with neurons in vitro. *The Journal of Neuroscience* **8**, 3278-3289.

DOYLE JP, COLMAN DR. (1993) Glial-neuron interactions and the regulation of myelin formation. *Current Opinion in Cell Biology* **5**, 779-785.

DUNCAN D. (1934) A relation between axon diameter and myelination determined by measurement of myelinated spinal root fibres. *Journal of Comparative Neurology* **60**, 437

DYCK PJ. (1966) Histologic measurements and fine structure of biopsied sural nerve: normal, and in peroneal muscular atrophy, hypertrophic neuropathy, and congenital sensory neuropathy. *Mayo Clinic Proceedings* **41**, 742-774.

DYCK PJ. (1975) Pathological alterations of the peripheral nervous system in man. In P.J. Dyck, P.K. Thomas and E.H. Lambert (Eds.) *Peripheral Neuropathy*, Saunders, Philadelphia, pp. 296-336.

DYCK PJ, CHANCE P, LEBO R, CARNEY JA (1993) Hereditary motor and sensory neuropathies. In P.J. Dyck, P.K. Thomas, J.W. Griffin, P.A. Low and J.F. Poduslo (Eds.) *Peripheral Neuropathy*, W.B.Saunders Company, Philadelphia, pp. 1094-1136.

DYCK PJ, ELLEFSON RD, LAIS AC, SMITH RC, TAYLOR WF, VAN DYKE RA. (1970) Histologic and lipid studies of sural nerves in inherited hypertrophic neuropathy: preliminary report of lipid abnormality in nerve and liver in Dejerine-Sottas disease. *Mayo Clinic Proceedings* **45** , 286-327.

DYCK PJ, GUTRECHT JA, BASTRON JA, KARNES WE, DALE AJD. (1968) Histologic and teased-fiber measurements of sural nerve in disorders of lower motor and primary sensory neurons. *Mayo Clinic Proceeding* **43**, 81-123.

DYCK PJ, LAIS AC. (1970) Electron microscopy of teased nerve fibers: method permitting examination of repeating structures of the same fiber. *Brain Research* **23**, 418

DYCK PJ, LAMBERT EH. (1968a) Lower motor and primary sensory neuron diseases with peroneal muscular atrophy. I. Neurogenic, genetic, and electrophysiologic findings in hereditary polyneuropathies. *Archives of Neurology* **18**, 603-618.

DYCK PJ, LAMBERT EH.(1968b) Lower motor and primary sensory neuron diseases with peroneal muscular atrophy. II. Neurologic, genetic, and electrophysiologic findings in various neuronal degenerations. *Archives of Neurology* **18**, 619-625.

FABBRETTI E, EDOMI P, BRANCOLINI C, SCHNEIDER C. (1995) Apoptotic phenotype induced by overexpression of wild-type *gas3/PMP22*: its relation to the demyelinating peripheral neuropathy CMT1A. *Genes and Development* **9**, 1846-1856.

FABRIZI GM, SIMONATI A, MORBIN M, CAVALLARO T, TAIOLI F, BENEDETTI MD, EDOMI P, RIZZUTO N. (1998) Clinical and pathological correlations in Charcot-Marie-Tooth neuropathy type 1A with the 17p11.2-12 duplication: A cross-sectional morphometric and immunohistochemical study in twenty cases. *Muscle and Nerve* **21**, 869-877.

FALCONER DS. (1951) Two new mutants,'Trembler' and 'Reeler' with neurological actions in the house mouse (*Mus musculus* L.). *Journal of Genetics* **50**, 192-201.

FALCONER DS, SOBEY WR. (1953) The location of "Trembler" in linkage group VII of the house mouse. *Journal of Heredity* **44**, 159-160.

FELDMAN GM, BUAMER JG, SPARKES RS. (1982) Brief clinical report; the dup (17p) syndrome. *American Journal of Medical Genetics* **11**, 299-304.

FRAHER JP. (1972) A quantitative study of anterior root fibres during early myelination. *Journal of Anatomy* **112**, 99-124.

FRAHER JP. (1978a) Quantitative studies on the maturation of central and peripheral parts of individual ventral motorneuron axons I. Myelin sheath and axon calibre. *Journal of Anatomy* **126**, 509-533.

FRAHER JP. (1978b) Quantitative studies on the maturation of central and peripheral parts of individual ventral motorneuron axons. II. Internodal length. *Journal of Anatomy* **127**, 1-15.

FRAHER JP, KAAR GF, BRISTOL DC, ROSSITER JP. (1988) Development of ventral spinal motorneurone fibres: A correlative study of the growth and maturation of central and peripheral segments of large and small fibre classes. *Progress in Neurobiology* **31**, 199-239.

FRIEDE RL, BISCHHAUSEN R. (1980) The precise geometry of large internodes. *Journal of the Neurological Sciences* **48**, 367-381.

FRIEDE RL, BISCHHAUSEN R. (1982) How are sheath dimensions affected by axonal caliber and internode length? *Brain Research* **235**, 335-350.

FRIEDE RL, MEIER T, DIEM M. (1981) How is the exact length of an internode determined? *Journal of the Neurological Sciences* **50**, 217-228.

FRIEDE RL, SAMORAJSKI T. (1967) Relation between the number of lamellae and axon circumference in fibres of vagus and sciatic nerves of mice. *Journal of Comparative Neurology* **130**, 223-231.

FRIEDE RL, SAMORAJSKI T. (1968) Myelin formation in the sciatic nerve of the rat. *Journal of Neuropathology and Experimental Neurology* **27**, 546-570.

GABREËLS-FESTEN A, GABREËLS F. (1993) Hereditary demyelinating motor and sensory neuropathy. *Brain Pathology* **3**, 135-146.

GABREËLS-FESTEN AAWM, BOLHUIS PA, HOOGENDIJK JE, VALENTIJN LJ, ESHUIS EJHM, GABREËLS FJM. (1995) Charcot-Marie-Tooth disease type 1A: morphological phenotype of the 17p duplication versus PMP22 point mutations. *Acta Neuropathologica* **90**, 645-649.

GABREËLS-FESTEN AAWM, GABREËLS FJM, JENNEKENS FGI, JANSSEN-VAN KEMPEN TW. (1994) The status of HMSN type III. *Neuromuscular Disorders.* **4**, 63-69.

GABRIEL JM, ERNE B, PAREYSON D, SGHIRLANZONI A, TARONI F, STECK AJ. (1997) Gene dosage effects in hereditary peripheral neuropathy-Expression of peripheral myelin protein 22 in Charcot-Marie-Tooth disease type 1A and hereditary neuropathy with liability to pressure palsies nerve biopsies. *Neurology* **49**, 1635-1640.

GARBAY B, BOIRON-SARGUEIL F, CASSAGNE C. (1995) Expression of the exon 1A-containing PMP22 transcript is altered in the trembler mouse. *Neuroscience Letters* **198**, 157-160.

GEREN BB. (1954) The formation from the Schwann cell surface of myelin in the peripheral nerves of chick embryos. *Experimental Cell Research* **7**, 558-562.

GHABRIEL MN, ALLT G. (1977) Regeneration of the node of Ranvier: a light and electron microscope study. *Acta Neuropathologica* **37**, 153-163.

GOODRUM JF, EARNHARDT T, GOINES N, BOULDIN TW. (1994) Fate of myelin lipids during degeneration and regeneration of peripheral nerve: an autoradiographic study. *The Journal of Neuroscience* **14**, 357-367.

GRIFFIN JW. AND HOFFMAN PN. (1993) Degeneration and regeneration in the peripheral nervous system. In P.J. Dyck, P.K. Thomas, J.W. Griffin, P.A. Low and J.F. Poduslo (Eds.) *Peripheral Neuropathy*, W.B.Saunders Company, Philadelphia, pp. 361-376.

GRIFFITH LS, SCHMITZ B, SCHACHNER M. (1992) L2/HNK-1 carbohydrate and protein-protein interactions mediate the homophilic binding of the neural adhesion molecule PO. *Journal of Neuroscience Research* **33**, 639-648.

GUILOFF RJ, THOMAS PK, CONTRERAS M, ARMITAGE S, SCHWARTZ G, SEDWICK EM. (1982) Linkage of type-1 hereditary motor and sensory neuropathy (HMSN) to the Duffy (FY) locus on chromosome-1. *Journal of Medical Genetics* **19**, 372.

HAHN AF, CHANG Y, WEBSTER HdeF. (1987) Development of myelinated nerve fibres in the 6th cranial nerve of the rat: a quantitative electron microscope study. *Journal of Comparative Neurology* **260**, 491-500.

HALL H, LIU L, SCHACHNER M, SCHMITZ B. (1993) The L2/HNK-1 carbohydrate mediates the adhesion of neural cells to laminin. *European Journal of Neuroscience* **5**, 34-42.

HALL SM. (1973) Some aspects of remyelination after demyelination produced by the intraneural injection of lysophosphatidyl choline. *Journal of Cell Science* **13**, 461-477.

HALL SM. (1983) The response of the (myelinating) Schwann cell to multiple episodes of demyelination. *Journal of Neurocytology* **12**, 1-12.

HALL SM. (1984) The effects of multiple sequential episodes of demyelination in the sciatic nerve of the mouse. *Neuropathology and Applied Neurobiology* **10**, 461-478.

HALL SM. (1993) Observations on the progress of Wallerian degeneration in transected peripheral nerve of C57BL/Wld mice in the presence of recruited macrophages. *Journal of Neurocytology* **22**, 480-490.

HALL SM, GREGSON NA. (1971) The *in vivo* and ultrastructural effects of the intraneural injection of lysophosphatidylcholine into myelinated peripheral nerve fibres of the adult mouse. *Journal of Cell Science* **9**, 769-789.

HALL SM, GREGSON NA. (1978) The effect of 5-bromodeoxyuridine on remyelination in the peripheral nervous system of the mouse. *Neuropathology and Applied Neurobiology* **4**, 117-127.

HANEMANN CO, STOLL G, D'URSO D, FRICKE W, MARTIN JJ, VAN BROECKHOVEN C, MANCARDI GL, BARTKE I, MULLER HW. (1994) Peripheral myelin protein-22 expression in Charcot-Marie-Tooth disease type 1a sural nerve biopsies. *Journal of Neuroscience Research* **37**, 654-659.

HANEY C, SNIPES GJ, SHOOTER EM, SUTER U, GARCIA CA, GRIFFIN JW, TRAPP BD. (1996) Ultrastructural distribution of PMP22 in Charcot-Marie-Tooth disease type 1A. *Journal of Neuropathology and Experimental Neurology* **55**, 290-299.

HANN BONNEKOH PG, SCHEIDT P, FRIEDE RL. (1989) Myelin phagocytosis by peritoneal macrophages in organ cultures of mouse peripheral nerve. A new model for studying myelin phagocytosis *in vitro*. *Journal of Neuropathology and Experimental Neurology* **48**, 140-153.

HANTAZ-AMBROISE D, VIGNY M, ALLIOT F. (1988) Effects of Trembler mouse serum and laminin on oligodendrocyte proliferation and differentiation in culture. *International Journal of Developmental Neuroscience* **6** , 289-299.

HARDING AE, Inherited neuronal atrophy and degeneration predominantly of lower motor neurons. In P.J. Dyck, P.K. Thomas, J.W. Griffin, P.A. Low and J.F. Poduslo (Eds.) *Peripheral Neuropathy*, W.B. Saunders, Philadelphia, 1993, pp. 1051-1064.

HARDING AE. (1995a) From the syndrome of Charcot, Marie and Tooth to disorders of peripheral myelin proteins. *Brain* **118**, 809-818.

HARDING AE AND REILLY M. (1995b) Molecular genetics of inherited peripheral neuropathies. In A.K. Asbury and P.K. Thomas (Eds.) *Peripheral Nerve Disorders 2.*, Butterworth-Heinmann, London, pp. 118-139.

HAREL A, FAINARU M, SHAFER Z, HERNANDEZ M, COHEN A, SCHWARTZ M. (1989) Optic nerve regeneration in adult fish and apoliprotein A-I. *Journal of Neurochemistry* **52**, 1218-1228.

HARRIS DA. (1987) Spectrophotomeric assays. In D.A. Harris and C.L. Bashford (Eds.) *Spectrophotometry and spectrofluorimetry. A practical approach*, IRL Press Ltd, Oxford,p. 64.

HAYASAKA K, HIMORO M, SATO W, TAKADA G, UYEMURA K, SHIMIZU N, BIRD TD, CONNEALLY PM, CHANCE PF. (1993a) Charcot-Marie-Tooth neuropathy type 1B is associated with mutations of the myelin Po gene. *Nature Genetics* **5**, 31-34.

HAYASAKA K, HIMORO M, SAWAISHI Y, NANAO K, TAKAHASHI T, TAKADA G, NICHOLSON GA, OUVRIER RA, TACHI N. (1993b) De novo mutation of the Po gene in Dejerine-Sottas disease (hereditary motor and sensory neuropathy type III). *Nature Genetics* **5**, 266-268.

HAYASAKA K, NANAO K, TAHARA M, SATO W, TAKADA G, MIYURA M, UYEMURA K. (1991) Isolation and sequence determination of cDNA encoding the major structural protein of human peripheral myelin. *Biochemical and Biophysical Research Communications* **180**, 515-518.

HAYASAKA K, TAKADA G, IONASESCU VV. (1993) Mutation of the myelin Po gene in Charcot-Marie-Tooth neuropathy type 1B. *Human Molecular Genetics* **22**, 1369-1372.

HENRY EW, COWEN JS, SIDMAN RL. (1983) Comparison of Trembler and Trembler-J mouse phenotypes: Varying severity of peripheral hypomyelination. *Journal of Neuropathology and Experimental Neurology* **42**, 688-706.

HENRY EW, SIDMAN RL. (1988) Long lives for homozygous Trembler mutant mice despite virtual absence of peripheral nerve myelin. *Science* **241**, 344-346.

HEUMANN R, LINDHOLM D, BANDTLOW C, MEYER M, RADEKE MJ, MISKO TP, SHOOTER E, THOENEN H. (1987) Differential regulation of mRNA encoding nerve growth factor and its receptor in rat sciatic nerve during development, degeneration, and regeneration: Role of macrophages. *Proceedings of the National Academy of Sciences of the United States of America* **84**, 8735-8739.

HILDEBRAND C, BOWE CM, REMAHL IN. (1994) Myelination and myelin sheath remodelling in normal and pathological PNS nerve fibres. *Progress in Neurobiology* **43**, 85-141.

HILDEBRAND C, KOCSIS JD, BERGLUND S, WAXMAN SG. (1985) Myelin sheath remodelling in regenerated rat sciatic nerve. *Brain Research* **358**, 163-170.

HILDEBRAND C, MUSTAFA GY, WAXMAN SG. (1986) Remodelling of internodes in regenerated rat sciatic nerve: Electron microscopic observations. *Journal of Neurocytology* **15**, 681-692.

HISCOE HB. (1947) Distribution of nodes and incisures in normal and regenerated nerve fibres. *Anatatomical Record* **99**, 447-475.

HOLMES W, YOUNG JZ. (1942) Nerve regeneration after immediate and delayed suture. *Journal of Anatomy* **77**, 63-96.

HONJIN R, NAKAMURA T, IMURA M. (1959) Electron microscopy of peripheral nerve fibres. III On the axoplasmic changes during Wallerian degeneration. *Okajimas Folia Anatomica Japonica*, 131-156.

HOOGENDIJK JE, JANSSEN EAM, GABREËLS-FESTEN AAWM, HENSELS GW, JOOSTEN EMG, GABREËLS FJM, ZORN I, VALENTIJN LJ, BAAS F, ONGERBOER DER VISSER

BW, DE VISSER M, BOLHUIS PA. (1993) Allelic heterogeneity in hereditary motor and sensory neuropathy type Ia (Charcot-Marie-Tooth disease type 1a). *Neurology* **43**, 1010-1015.

HOWARD A, PELC SR. (1953) Synthesis of deoxyribonucleic acid in normal and irradiated cells and its relation to chromosome breakage. *Heredity* **6**, 261-273.

HUXLEY C, PASSAGE E, ROBERTSON AM, YOUL B, HUSTON S, MANSON A, SABERRAN-DJONIEDI S, FIGARELLA-BRANGER D, PELLISSIER JF, THOMAS PK, FONTES M. (1998) Correlation between varying levels of PMP22 expression and the degree of demyelination and reduction in nerve conduction velocity in transgenic mice. *Human Molecular Genetics* 7, 449-458.

IKEGAMI T, IKEDA H, AOYAMA M, MATSUKI T, IMOTA T, FUKUUCHI Y, AMANO T, TOYOSHIMA I, ISHIHARA Y, ENDOH H, HAYASAKA K. (1998) Novel mutations of the peripheral myelin protein 22 gene in two pedigrees with Dejerine-Sottas disease. *Human Genetics* **102**, 294-298.

INUZUKA T, QUARLES RH, HEATH J, TRAPP B. (1985) Myelin-associated glycoprotein and other proteins in Trembler mice. *Journal of Neurochemistry* **44**, 793-797.

INUZUKA T, QUARLES RH, NORONHA AB, DOBERSON MJ, BRADY RO. (1984) A human lymphocyte antigen is shared with a group of glycoprotiens in peripheral nerve. *Neuroscience Letters* **51**, 105-111.

IONASESCU VV, IONASESCU R, SEARBY C, BARKER DF. (1993) Charcot-Marie-Tooth neuropathy type 1A with both duplication and non-duplication. *Human Molecular Genetics.* **2**, 405-410.

IONASESCU VV, IONASESCU R, SEARBY C, NEAHRING R. (1995) Dejerine-Sottas disease with de novo dominant point mutation of the PMP22 gene. *Neurology* **45**, 1766-1767.

IONASESCU VV, SEARBY CC, IONASESCU R, CHATKUPT S, PATEL N, KOENIGSBERGER R. (1997a) Dejerine-Sottas neuropathy in mother and son with same point mutation of PMP22 gene. *Muscle and nerve* **20**, 97-99.

IONASESCU VV, SEARBY CC, IONASESCU R, REISIN R, RUGGIERI V, ARBERAS C. (1997b) Severe Charcot-Marie-Tooth neuropathy type 1A with 1-base pair deletion and frameshift mutation in the peripheral myelin protein 22 gene. *Muscle and Nerve* **20**, 1308-1310.

JACOBS JM. (1967) Experimental diphtheritic neuropathy in the rat. *British Journal of Experimental Pathology* **48**, 204-216.

JACOBS JM, CAVANAGH JB. (1969) Species differences in internode formation following two types of peripheral nerve injury. *Journal of Anatomy* **105**, 295-306.

JESSELL TM, HYNES MA, DODD J.(1990) Carbohydrates and carbohydrate-binding proteins in the nervous system. *Annual Review of Neuroscience* **13**, 227-255.

JESSEN KR, MIRSKY R. (1991) Schwann cell precursors and their development. *Glia* **4**, 185-194.

KAKU DA, PARRY GJ, MALAMUT R, LUPSKI JR, GARCIA CA. (1993) Nerve conduction studies in Charcot-Marie-Tooth polyneuropathy associated with a segmental duplication of chromosome 17. *Neurology* **43**, 1806-1808.

KALAYDJIEVA L, NIKOLOVA A, TURNEV I, PETROVA J, HRISTOVA A, ISHPEKOVA B, PETKOVA I, SHMAROV A, STANCHEVA S, MIDDLETON L, MERLINI L, TROGU A, MUDDLE JR, KING RHM, THOMAS PK. (1998) Hereditary motor and sensory

neuropathy-Lom, a novel demyelinating neuropathy associated with deafness in gypsies. Clinical, electrophysiological and nerve biopsy findings. *Brain* **121**, 399-408.

KEILHAUER G, FAISSNER A, SCHACHNER M. (1985) Differential inhibition of neurone-neurone, neurone-astrocyte and astrocyte-astrocyte adhesion by L1, L2, and N-CAM antibodies. *Nature* **316**, 728-730.

KILLIAN JM, TIWARI PS, JACOBSON S, JACKSON RD, LUPSKI JR. (1996) Longitudinal studies of the duplication form of Charcot-Marie-Tooth polyneuropathy. *Muscle and Nerve* **19**, 74-78.

KING RHM, POLLARD JD, THOMAS PK. (1975) Aberrant remyelination in chronic relapsing experimental allergic neuritis. *Neuropathology and Applied Neurobiology* **1**, 367-378.

KITAMURA K, SUZUKI M, UYEMURA K. (1976) Purification and partial characterisation of two glycoproteins in bovine peripheral nerve myelin membrane. *Biochimica et Biophysica Acta* **455**, 806-816.

KOENIG H, DO THI A, FERZAZ B, RESSOUCHES A. (1991) Schwann cell proliferation during postnatal development, wallerian degeneration and axon regeneration in Trembler dysmyelinating mutant. *Advances in Experimental Medicine and Biology* **296**, 227-238.

KOMIYAMA A, SUZUKI K. (1992) Age-related differences in proliferative responses of Schwann cells during Wallerian degeneration. *Brain Research* **573**, 267-275.

KRUSE J, KEILHAUER G, FAISSNER A, TIMPL R, SCHACHNER M. (1985) The J1 glycoprotein-a novel nervous system cell adhesion molecule of the L2/HNK-1 family. *Nature* **316**, 146-148.

KRUSE J, MAILHAMMER R, WERNECKE H, FAISSNER A, SOMMER I, GORIDIS C, SCHACHNER M. (1984) Neural cell adhesion molecules and myelin-associated glycoprotein share a common carbohydrate moiety recognized by monoclonal antibody L2 and HNK-1. *Nature* **311**, 153-155.

KULKENS T, BOLHUIS PA, WOLTERMAN RA, KEMP S, TE NIJENHUIS S, VALENTIJN LJ, HENSELS GW, JENNEKENS FGI, DE VISSER M, HOOGENDIJK JM, BASS F. (1993) Deletion of the serine 34 codon from the major peripheral myelin protein Po gene in Charcot-Marie-Tooth disease type 1B. *Nature Genetics* **5**, 35-39.

KUMAR NM, JARVIS LJ, TENBROEK E, LOUIS CF. (1993) Cloning and expression of a major rat lens membrane protein, MP20. *Experimental Eye Research* **56**, 35-43.

KUNEMUND V, JUNGALWALA F, FISCHER G, CHOU DKH, KEILHAUER G, SCHACHNER M. (1988) The L2/HNK-1 carbohydrate of neural cell adhesion molecules is involved in cell interactions. *The Journal of Cell Biology* **106**, 213-223.

LEBO RV, CHANCE PF, DYCK PJ, REDILA-FLORES MT, LYNCH ED, GOLBUS MS, BIRD TD, KING MC, ANDERSON LA, HALL J, WIEGANT J, JIANG Z, DAZIN PF, PUNNETT HH, SCHONBERG SA, MOORE K, SHULL MM, GENDLER S, HURKO O, LOVELACE RE, LATOV N, TROFATTER J. (1991) Chromosome 1 Charcot-Marie-Tooth disease (CMT1B) locus in the Fc gamma receptor gene region [published erratum appears in Hum Genet 1993 Apr; 91(3):301]. *Human Genetics* **88**, 1-12.

LEES MB AND BROSTOFF SW. (1984) Proteins of myelin. In P. Morell (Ed.) *Myelin*, Plenum Publishing Corp, New York, pp. 197-224.

LEGUERN E, GOUIDER R, MABIN D, TARDIEU S, BIROUK N, PARENT P, BOUCHE P, BRICE A. (1997) Patients homozygous for the 17p11.2 duplication in Charcot-Marie-Tooth type 1A disease. *Annals of Neurology* **41**, 104-108.

LEGUERN E, STURTZ F, GUGENHEIM M, GOUIDER R, BONNEBOUCHE C, RAVISE N, GONNAUD PM, TARDIEU S, BOUCHE P, CHAZOT G, AGID Y, VANDENBERGHE A, BRICE A. (1994) Detection of deletion within 17p11.2 in 7 French families with hereditary neuropathy with liability to pressure palsies (HNPP). *Cytogenetics and Cell Genetics* **65**, 261-264.

LEMKE G. (1993) The molecular genetics of myelination: An update. *Glia* **7**, 263-271.

LEMKE G, LAMAR E, PATTERSON J. (1988) Isolation and analysis of the gene encoding peripheral myelin protein zero. *Neuron* **1**, 73-83.

LENSSEN PP, GABREËLS-FESTEN AAWM, VALENTIJN LJ, JONGEN PJH, VAN BEERSUM SEC, VAN ENGELEN BGM, VAN WENSEN PJM, BOLHUIS PA, GABREËLS EJM, MARIMAN ECM. (1998) Hereditary neuropathy with liability to pressure palsies-phenotypic differences between patients with the common deletion and a PMP22 frame shift mutation. *Brain* **121**, 1451-1458.

LIEHR T, RAUTENSTRAUSS B. (1997) The peripheral myelin protein 22kDa (*PMP22*) gene is expressed in non-neural epithelial tissues of mouse, rat, cattle and human. *American Journal of Human Genetics* **61SS Abstract**, 1015

LISAK RP, SOBUE G, KUCHMY D, BURNS JB, PLEASURE DE. (1985) Products of activated lymphocytes stimulate Schwann cell mitosis in vitro. *Neuroscience Letters* **57**, 105-111.

LORENZETTI D, PAREYSON D, SGHIRLANZONI A, ROA BB, ABBAS NE, PANDOLFO M, DIDONATO S, LUPSKI JR.(1995) A 1.5 Mb deletion in 17.2p11.2-p12 is frequently observed in Italian families with hereditary neuropathy with liability to pressure palsies. *American Journal of Human Genetics* **56**, 91-98.

LOVE S. (1983) An experimental study of peripheral nerve regeneration after x-iradiation. *Brain* **106**, 39-54.

LOW PA. (1976a) Hereditary hypertrophic neuropathy in the Trembler mouse. Part 2. Histopathological studies: Electron microscopy. *Journal of the Neurological Sciences* **30**, 343-368.

LOW PA. (1976b) Hereditary hypertrophic neuropathy in the Trembler mouse. Part 1. Histopathological studies: Light microscopy. *Journal of the Neurological Sciences* **30**, 327-341.

LOW PA. (1977) The evolution of 'onion bulbs' in the hereditary hypertrophic neuropathy of the Trembler mouse. *Neuropathology and Applied Neurobiology* **3**, 81-92.

LOW PA, MCLEOD JG. (1975) Hereditary demyelinating neuropathy in the Trembler mouse. *Journal of the Neurological Sciences* **26**, 565-574.

LUBINSKA L. (1982) Patterns of Wallerian degeneration of myelinated fibres in short and long peripheral stumps and in isolated segments of rat phrenic nerve. Interpretation of the role of axoplasmic flow of the trophic factor. *Brain Research* **223**, 227-240.

LUGNEGÅRD H, BERTHOLD C-H, RYDMARK M. (1984) Ultrastructural morphometric studies on regeneration of the lateral sural cutaneous nerve in the white rat after transection of the sciatic nerve. II. Regeneration after nerve suture and nerve grafting. *Scandinavian Journal of Plastic and Reconstructive Surgery (suppl)* **20**, 47-64.

LUNN ER, PERRY VH, BROWN MC, ROSEN H, GORDON S. (1989) Absence of Wallerian degeneration does not hinder regeneration in peripheral nerve. *European Journal of Neuroscience* **1**, 27-33.

LUPSKI JR, DE OCA-LUNA LM, SLAUGENHAUPT S, PENTAO L, GUZZETTA V, TRASK BJ, SAUCENDO-CARDENAS O, BARKER DF, KILLIAN JM, GARCIA CA, CHAKRAVARTI A, PATEL PI. (1991) DNA duplication associated with Charcot-Marie-Tooth disease type 1A. *Cell* **66**, 219-232.

LUPSKI JR, WISE CA, KUWANO A, PENTAO L, PARKE JT, GLAZE DG, LEDBETTER GH, GREENBERG F, PATEL PI. (1992) Gene dosage is a mechanism for Charcot-Marie-Tooth disease type 1A. *Nature Genetics* , 29-33.

MADRID R, BRADLEY WG. (1975) The pathology of neuropathies with focal thickening of the myelin sheath (Tomaculous neuropathy). Studies on the formation of the abnormal myelin sheath. *Journal of the Neurological Sciences* **25**, 415-448.

MAGENIS RE, BROWN MG, ALLEN L, REISS J. (1986) De novo partial duplication of 17p [dup(17)(p12 p11.2)]: clinical report. *American Journal of Medical Genetics* **24**, 415-420.

MAGYAR JP, MARTINI R, RUELICKE T, AGUZZI A, ADLKOFER K, DEMBIC Z, ZIELASEK J, TOYKA KV, SUTER U. (1996) Impaired differentiation of Schwann cells in transgenic mice with increased *PMP22* gene dosage. *The Journal of Neuroscience* **16**, 5351-5360.

MANFIOLETTI G, RUARO ME, DEL SAL G, PHILIPSON L, SCHNEIDER C. (1990) A growth arrest-specific (*gas*) gene codes for a membrane protein. *Molecular and Cellular Biology* **10**, 2924-2930.

MARIMAN ECM, GABREËLS-FESTEN AAWM, VAN BEERSUM SEC, JONGEN PJ, VAN DE LOOIJ E, BAAS F, BOLHIUS PA, ROPERS HH, GABREELS FJ. (1994a) Evidence for genetic heterogeneity underlying hereditary neuropathy with liability to pressure palsies. *Human Genetics* **93**, 151-156.

MARIMAN ECM, GABREËLS-FESTEN AAWM, VAN BEERSUM SEC, VALENTIJN LJ, BAAS F, BOLHUIS PA, JONGEN PJ, ROPERS HH, GABREELS FJ. (1994b) Prevalence of the 1.5Mb 17p deletion in families with hereditary neuropathy with liability to pressure palsies. *Annals of Neurology* **36**, 650-655.

MARQUES W, THOMAS PK, SWEENEY MG, CARR L, WOOD NW. (1998) Dejerine-Sottas neuropathy and PMP22 point mutations: A new base pair substitution and a possible "hot spot" on Ser 72. *Annals of Neurology* **43**, 680-683.

MARROSU MG, VACCARGIU S, MARROSU G, VANNELLI A, CIANCHETTI C, MUNTONI F (1997) A novel point mutation in the peripheral myelin protein 22 (*PMP22*) gene associated with Charcot-Marie-Tooth disease type 1A. *Neurology* **48**, 489-493.

MARTINI R, BOLLENSEN E, SCHACHNER M. (1988) Immunocytological localization of the major peripheral nervous system glycoprotein Po and the L2/HNK-1 and L3 carbohydrate structures in developing and adult mouse sciatic nerve. *Developmental Biology* **129**, 330-338.

MARTINI R, SCHACHNER M. (1986) Immunoelectron microscopic localization of neural cell adhesion molecules (L1, N-CAM, and MAG) and their shared carbohydrate epitope and myelin basic protein in developing sciatic nerve. *The Journal of Cell Biology* **103**, 2439-2448.

MARTINI R, SCHACHNER M, BRUSHART TM. (1994) The L2/HNK-1 carbohydrate is preferentially expressed by previously motor axon-associated Schwann cells in reinnervated peripheral nerves. *The Journal of Neuroscience* **14**, 7180-7191.

MARTINI R, XIN Y, SCHMITZ B, SCHACHNER M. (1992) The L2/HNK-1 carbohydrate epitope is involved in the preferential outgrowth of motor neurons on ventral roots and motor nerves. *European Journal of Neuroscience* **4**, 628-639.

MARVIN KW, FUJIMOTO W, JETTEN AM. (1995) Identification and characterization of a novel squamous cell-associated gene related to *PMP22*. *The Journal of Biological Chemistry* **270**, 28910-28916.

MATSUNAMI N, SMITH B, BALLARD L, LENSCH MW, ROBERTSON M, ALBERTSEN H, HANEMANN CO, MULLER HW, BIRD TD, WHITE R. (1992) Peripheral myelin protein-22 gene maps in the duplication in chromosome 17p11.2 associated with Charcot-Marie-Tooth 1A. *Nature Genetics* **1**, 176-179.

MATTHEWS MA. (1968) An electron microscopic study of the relationship between axon diameter and the initiation of myelin production in the peripheral nervous system. *Anatomical Record* **161**, 337-351.

MAYCOX PR, ORTUNO D, BURROLA P, KUHN R, BIERI PL, ARREZO JC, LEMKE G .(1997) A transgenic mouse model for human hereditary neuropathy with liability to pressure palsies. *Molecular and Cellular Neuroscience* **8**, 405-416.

MCKUSICK VA (1988) *Mendelian inheritance in man*, Johns Hopkins University Press, Baltimore.

MESSING A, BEHRINGER RR, HAMMANG JP, LEMKE G. (1992) Po promoter directs expression of reporter and toxin genes to Schwann cells of transgenic mice. *Neuron* **8**, 507-520.

MESSING A, BEHRINGER RR, WRABETZ L, HAMMANG JP, LEMKE G, PALMITER RD, BRINSTER RL. (1994) Hypomyelinating peripheral neuropathies and schwannomas in transgenic mice expressing SV40 T-antigen. *The Journal of Neuroscience* **14**, 3533-3539.

MITHEN FA, COCHRAN M, CORNBROOKS CJ, BUNGE RP. (1982) Expression of the Trembler mouse mutation in organotypic cultures of dorsal root ganglia. *Developmental Brain Research* **1982**, 407-415.

MUGLIA M, GABRIELE AL, LEONE O, LEONARDIS D, MAGARIELLO A, CARACCIOLO M, QUATTRONE A. (1998) A novel point mutation within intron2 of PMP22 gene in a patient with Dejerine-Sottas disease. *European Journal of Human Genetics* **6 S1 (Abstract)**, 4244

MUIR D, GENNRICH C, VARON S, MANTHORPE M. (1989) Rat sciatic nerve Schwann cell microcultures: responses to mitogens and production of trophic and neurite-promoting factors. *Neurochemical Research* **14**, 1003-1012.

MUIR D, VARON S, MANTHORPE M. (1990) Schwann cell proliferation in vitro is under negative autocrine control. *The Journal of Cell Biology* **111**, 2663-2671.

MULLIS K, FALOONA F, SCHARF S, SAIKI R, HORN G, ERLICH H. (1986) Specific enzymatic amplification of DNA in vitro:The polymerase chain reaction. *Cold Spring Harbor Symposia on Quantitative Biology* **51**, 263-273.

MULLIS KB, FALOONA F. (1987) Specific synthesis of DNA in vitro via a polymerase-catalyzed chain reaction. *Methods in Enzymology* **155**, 335-350.

NAEF R, ADLKOFER K, LESCHER B, SUTER U. (1997) Aberrant protein trafficking in Trembler suggests a disease mechanism for hereditary human peripheral neuropathies. *Journal of Neurocytology* **20**, 439-449.

NAEF R, SUTER U. (1998) Many facets of the peripheral myelin protein PMP22 in myelination and disease. *Microscopy Research and Technique* **41**, 359-371.

NAGEOTTE J. (1932) Sheaths of the peripheral nerves, nerve degeneration and regeneration. In W. Penfield (Ed.) *Cytology and cellular pathology of the nervous system*, Hoeber, New York, pp. 189-239.

NAVON R, SEIFRIED B, SHOHAM GAL-ON N, SADEH M. (1996) A new point mutation affecting the fourth transmembrane domain of PMP22 results in severe de novo Charcot-Marie-Tooth disease. *Human Genetics* **97**, 685-687.

NELIS E, HOLMBERG B, ADOLFSSON R, HOLMGREN G, VANBROECKHOVEN C. (1997) *PMP22* Thr (118) Met: recessive CMT1 mutation or polymorphism?. *Nature Genetics* **15**, 13-14.

NELIS E, TIMMERMAN V, DE JONGHE P, VAN BROECKHOVEN C. (1994) Identification of a 5' splice site mutation in the PMP-22 gene in autosomal dominant Charcot-Marie-Tooth disease type 1. *Human Molecluar Genetics.* **3**, 515-516.

NELIS E, VANBROECKHOVEN C. (1996) Estimation of the mutation frequencies in Charcot-Marie-Tooth disease type-1 and hereditary neuropathy with liability to pressure palsies- A European collaborative study. *European Journal of Human Genetics* **4**, 25-33.

NICHOLSON GA, VALENTIJN LJ, CHERRYSON AK, KENNERSON ML, BRAGGS TL, DE KROON RM, ROSS DA, POLLARD JD, MCLEOD J.G., BOLHUIS PA, BAAS F (1994) A frame shift mutation in the PMP22 gene in hereditary neuropathy with liability to pressure palsies. *Nature Genetics* **6**, 263-266.

NIEKE J, SCHACHNER M. (1985) Expression of neural adhesion molecules L1 and N-CAM and their common carbohydrate epitope L2/HNK-1 during development and after transection of the mouse sciatic nerve. *Differentiation* **30**, 141-151.

NORONHA AB, ILYAS A, ANTONICEK H, SCHACHNER M, QUARLES RH. (1986) Molecular specificity of L2 monoclonal antibodies that bind to carbohydrate determinants of neural cell adhesion molecules and their resemblance to other monoclonal antibodies recognizing the myelin-associated glycoprotein. *Brain Research* **385**, 237-244.

NOTTERPEK L, SHOOTER EM, SNIPES GJ. (1997) Upregulation of the endosomal-lysosomal pathway in the Trembler-J neuropathy. *The Journal of Neuroscience* **17**, 4190-4200.

NUKADA H, DYCK PJ, KARNES JL. (1983) Thin axons relative to myelin spiral length in hereditary motor and sensory neuropathy type I. *Annals of Neurology* **14**, 648-655.

OHARA S, IKUTA F. (1988) Schwann cell responses during regeneration after one or more crush injuries to myelinated nerve fibres. *Neuropathology and Applied Neurobiology* **14**, 229-245.

OUVRIER RA, MCLEOD JG, CONCHIN TE. (1987) The hypertrophic forms of hereditary motor and sensory neuropathy: a study of hypertrophic Charcot-Marie-Tooth disease (HMSN type I) and Dejerine-Sottas disease (HMSN type III) in childhood. *Brain* **110**, 121-148.

PALAU F, LOFGREN A, DE JONGHE P, BORT S, NELIS E, SEVILLA T, MARTIN JJ, VILCHEZ J, PRIETO F, VAN BROECKHOVEN C. (1993) Origin of the de novo duplication in Charcot-Marie-Tooth disease type 1A: unequal nonsister chromatid exchange during spermatogenesis. *Human Molecular Genetics* **2**, 2031-2035.

PAREEK S, SUTER U, SNIPES GJ, WELCHER AA, SHOOTER EM, MURPHY RA. (1993) Detection and processing of peripheral myelin protein PMP22 in cultured schwann cells. *The Journal of Biological Chemistry* **268**, 10372-10379.

PAREYSON, D. and TARONI, F. (1996) Deletion of the PMP22 gene and hereditary neuropathy with liability to pressure palsies. *Current Opinion in Neurology* **9**, 348-354.

PARK O, LIEHR T, RAUTENSTRAUSS B. (1997) Which role plays the PMP22 gene in cell growth regulation? *American Journal of Human Genetics* **61SS Abstract**, 1033

PARMANTIER E, CABON F, BRAUN C, D'URSO D, MÜLLER HW, ZALC B. (1995) Peripheral myelin protien-22 is expressed in rat and mouse brain and spinal cord motorneurons. *European Journal of Neuroscience* **7**, 1080-1088.

PATEL PI, WELCHER AA, SCHOENER-SCOTT R, TRASK BJ, PENTAO L, SNIPES GJ, GARCIA CA, FRANCKE U, SHOOTER EM, LUPSKI JR, SUTER U. (1992) The gene for the peripheral myelin protien PMP22- is a candidate for Charcot-Marie-Tooth disease type IA. *Nature Genetics* **1**, 159-165.

PELLEGRINO RG, SPENCER P. (1985) Schwann cell mitosis in response to regenerating peripheral axons in vivo. *Brain Research* **241**, 16-25.

PENTAO L, WISE CA, CHINAULT AC, PATEL PI, LUPSKI JR. (1992) Charcot-Marie-Tooth type 1A duplication appears to arise from recombination at repeat sequences flanking the 1.5Mb monomer unit. *Nature Genetics* **2**, 292-300.

PERKINS CS, AGUAYO AJ, BRAY GM. (1981a) Behaviour of Schwann cells from the Trembler mouse unmyelinated fibres transplanted into myelinated nerves. *Experimental Neurology* **71**, 515-526.

PERKINS CS, AGUAYO AJ, BRAY GM .(1981b) Schwann cell multiplication in Trembler mice. *Neuropathology and Applied Neurobiology* **7**, 115-126.

PERRY VH, BROWN MC, GORDON S. (1987) The macrophage response to central and peripheral nerve injury. A possible role for macrophages in regeneration. *Journal of Experimetnal Medicine* **165**, 1218-1223.

PETERS A, MUIR AR. (1959) The relationship between axons and Schwann cells during development of peripheral nerves in the rat. *Quarterly Journal of Experimental Physiology* **44**, 117-130.

POLLARD JD, MCLEOD JG. (1980) Nerve grafts in the Trembler mouse. An electrophysiological and histological study. *The Journal of Neuroscience* **46**, 373-383.

PRINEAS JW. (1971) Demyelination and remyelination in recurrent idiopathic polyneuropathy. *Acta Neuropathologica* **18**, 34-57.

RAEYMAEKERS P, TIMMERMAN V, NELIS E, DE JONGHE P, HOOGENDIJK JE, BAAS F, BARKER DF, MARTIN JJ, DE VISSER M, BOLHUIS PA. (1991) Duplication in chromosome 17p11.2 in Charcot-Marie-Tooth neuropathy type 1a (CMT1a).The HMSN Collaborative research group. *Neuromuscular Disorders.* **1**, 93-97.

RAINE CS, WISNIEWSKI H, PRINEAS J. (1969) An ultrastructural study of experimental allergic encephalomyelitis in the peripheral nervous system. *Laboratory Investigations* **21**, 316-327.

RAMÓN Y CAJAL S. (1928) *Degeneration and regeneration of the nervous system*, Oxford University Press, London.

RATNER N, BUNGE RP, GLASER L. (1985) A neuronal cell surface heparan sulfate proteoglycan is required for dorsal root ganglion neuron stimulation of Schwann cell proliferation. *The Journal of Cell Biology* **101**, 744-754.

RATNER N, HONG D, LIEBERMAN MA, BUNGE RB, GLASER L. (1988) The neuronal cell-surface molecule mitogenic for Schwann cells is a heparin-binding protein. *Proceedings of the National Academy of Sciences of the United States of America* **85**, 6992-6996.

RAWLINS FA, HEDLEY-WHITE ET, VILLEGAS G, UZMAN BG. (1970) Reutilization of cholesterol-1,2-^{3}H in the regeneration of peripheral nerve. An autoradiographic study. *Laboratory Investigation* **22**, 237-240.

RAWLINS FA, VILLEGAS G, HEDLEY-WHITE ET, UZMAN BG. (1972) Fine structural localisation of cholesterol-1-2-^{3}H in degenerating and regenerating mouse sciatic nerve. *The Journal of Cell Biology* **52**, 615-625.

REICHARDT LF, TOMASELLI KJ. (1991) Extracellular matrix molecules and their receptors: Functions in neural development. *Annual Review of Neuroscience* **141**, 531-570.

REILLY M. (1998) Genetically determined neuropathies. *Journal of Neurology* **245**, 6-13.

REITER LT, MURAKAMI T, KOEUTH T, PENTAO L, MUZNY DM, GIBBS RA, LUPSKI JR. (1996) A recombination hotspot responsible for two inherited peripheral neuropathies is located near a *mariner* transposon-like element. *Nature Genetics* **12**, 288-296.

RIDLEY AJ, DAVIS JB, STROOBANT P, LAND H. (1989) Transforming growth factors-beta 1 and beta 2 are mitogens for rat Schwann cells. *The Journal of Cell Biology* **109**, 3419-3424.

ROA B, ANANTH U, GARCIA CA, LUPSKI JR. (1995) Molecular diagnosis of CMT1A and HNPP. *Laboratory Medical International* **12** , 22-24.

ROA BB, DYCK PJ, MARKS HG, CHANCE PF, LUPSKI JR. (1993a) Dejerine-Sottas syndrome associated with point mutation in the peripheral myelin protein 22 (*PMP22*) gene. *Nature Genetics* **5**, 269-272.

ROA BB, GARCIA CA, SUTER U, KULPA DA, WISE CA, MUELLER J, WELCHER AA, SNIPES GJ, SHOOTER EM, PATEL PI, LUPSKI JR. (1993b) Charcot-Marie-Tooth disease type 1A :association with a spontaneous point mutation in the *PMP22* gene. *New England Journal of Medicine.* **329**, 96-101.

ROA BB, GREENBERG F, GUNARATNE P, SAUER CM, LUBINSKY MS, KOZMA C, MECK JM, MAGENIS RE, SHAFFER LG, LUPSKI JR. (1996) Duplication of the *PMP22* gene in 17p partial trisomy patients with Charcot-Marie-Tooth type-1A neuropathy. *Human Genetics* **97**, 642-649.

ROBERTSON AM, KING RHM, MUDDLE JR, THOMAS PK. (1997) Abnormal Schwann cell/axon interactions in the Trembler-J mouse. *Journal of Anatomy* **190**, 423-432.

ROZEAR MP, PERICAK-VANCE MA, FISCHBECK KH, STAJICHJ.M., GASKELL JR PC, KRENDEL DA, GRAHAM DG, DAWSON DV, ROSES AD.(1987) Hereditary motor and sensory neuropathy, X-linked: a half century follow up. *Neurology* **37**, 1460

SALZER JL, BUNGE RP. (1980) Studies of Schwann cell proliferation. I. An analysis in tissue culture of proliferation during development, Wallerian degeneration, and direct injury. *The Journal of Cell Biology* **84**, 739-752.

SANES JR, HUNTER DD, GREEN TL, MERLIE JP. (1990) S-laminin. *Cold Spring Harbor Symposium on Quantitative Biology* **55**, 419-430.

SCHACHNER M. (1989) Families of neural adhesion molecules. In G. Bock and S. Harnett (Eds.) *Carbohydrate recognition in cellular function*, John Wiley, Chichester, pp. 156-172.

SCHACHNER M, MARTINI R. (1995a) Glycans and the modulation of neural-recognition molecule function. *Trends In Neurosciences* **18**, 183-191.

SCHACHNER M, MARTINI R, HALL H, ORBERGER G. (1995b) Functions of theL2/HNK-1 carbohydrate in the nervous system. *Progress in Brain Research* **105**, 183-188.

SCHENONE A, NOBBIO L, MANDICH P, BELLONE E, ABBRUZZESE M, AYMAR F, MANCARDI GL, WINDEBANK AJ. (1997) Underexpression of messenger RNA for peripheral myelin protein 22 in hereditary neuropathy with liability to pressure palsies. *Neurology* **48**, 445-449.

SCHLAEPFER WW. (1974) Calcium-induced degeneration of axoplasm in isolated segments of rat phrenic nerve. *Brain Research* **69**, 203-215.

SCHLAEPFER WW. (1977) Structural alterations of peripheral nerve induced by the calcium ionophore A23187. *Brain Research* **136**, 1-9.

SCHLAEPFER WW, MYERS FK. (1973) Relationship of myelin internode elongation and growth in the rat sural nerve. *Journal of Comparativ Neurology* **147**, 255-266.

SCHNEIDER C, KING RM, PHILIPSON L. (1988) Genes specifically expressed at growth arrest of mammalian cells. *Cell* **54**, 787-793.

SCHULLER-PETROVIC S, GEBHART W, LASSMANN H, RUMPOLD H, KRAFT D. (1983) A shared antigenic determinant between natural killer cells and nervous tissue. *Nature* **306**, 179-181.

SEREDA M, GRIFFITHS I, PUHLHOFER A, STEWART H, ROSSNER MJ, ZIMMERMANN F, MAGYAR JP, SCHNEIDER A, HUND E, MEINCK H-M, SUTER U, NAVE KA. (1996) A transgenic rat model of Charcot-Marie-Tooth disease. *Neuron* **16**, 1049-1060.

SIDMAN RL, COWEN JS, EICHER EM. (1979) Inherited muscle and nerve diseases in mice: A tabulation with commetary. *Annals New York Academy of Sciences* **317**, 497-505.

SIIRONEN J, COLLAN Y, RÖYTTÄ M. (1994) Axonal reinnervation does not influence Schwann cell proliferation after rat sciatic nerve transection. *Brain Research* **654**, 303-311.

SILANDER K, HALONEN P, SARA R, KALIMO H, FALCK B, SAVONTAUS M-L. (1994) DNA analysis in Finnish patients with hereditary neuropathy with liability to pressure palsies (HNPP). *Journal of Neurology and Neurosurgery* **57**, 1260-1262.

SILANDER K, MERETOJA P, JUVONEN V, IGNATIUS J, PIHKO H, SAARINEN A, WALLDEN T, HERRGARD E, AULA P, SAVONTAUS M-L .(1998) Spectrum of mutations in Finnish patients with Charcot-Marie-Tooth disease and related neuropathies. *Human Mutation.* **12**, 59-68.

SKRE H. (1974) Genetic and clinical aspects of Charcot-Marie-Tooth's disease. *Clinical Genetics* **6**, 98-118.

SMITH TW, BHAWAN J, KELLER RB, DE GIROLAMI U. (1980) Charcot-Marie-Tooth disease with hypertrophic neuropathy: a neuropathologic study of two cases. *Journal of Neuropathology and Experimental Neurology* **39**, 420-440.

SNIPES GJ, SUTER U, SHOOTER EM. (1993) Human peripheral myelin protein-22 carries the L2/HNK-1 carbohydrate adhesion epitope. *Journal of Neurochemistry* **61**, 1961-1964.

SNIPES GJ, SUTER U, WELCHER AA, SHOOTER EM. (1992) Characterization of a novel peripheral nervous system myelin protein (PMP-22/SR13). *The Journal of Cell Biology* **117**, 225-238.

SOBUE G, BROWN MJ, KIM SU, PLEASURE D. (1984) Axolemma is a mitogen for human Schwann cells. *Annals of Neurology* **15**, 449-452.

SOBUE G, SHUMAN S, PLEASURE D.(1986) Schwann cell responses to cyclic AMP: proliferation, change in shape, and appearance of surface galactocerebroside. *Brain Research* **362**, 23-32.

SPEIDEL CC. (1964) In vivo studies of myelinated nerve fibres. *International Review of Cytology* **16**, 173

SPENCER PS AND WEINBERG. (1978). Axonal specification of Schwann cell expression and myelination. In S.G. Waxman (Ed.) *Physiology and Pathobiology of Axons*, Raven Press, New York, pp. 389-405.

SPREYER P, KUHN G, HANEMANN CO, GILLEN C, SCHAAL H, KUHN R, LEMKE G, MULLER HW. (1991) Axon-regulated expression of a Schwann cell transcript that is homologous to a 'growth arrest-specific' gene. *EMBO Journal* **10**, 3661-3668.

STAHL N, HARRY J, POPKO B. (1990) Quantitative analysis of myelin protein gene expression during development in the rat sciatic nerve. *Molecular Brain Research* **8**, 209-212.

STEWART HJ, ECCLESTON PA, JESSEN KR, MIRSKY R. (1991) Interaction between cAMP elevation, identified growth factors, and serum components in regulating Schwann cell growth. *Journal of Neuroscience Research* **30**, 346-352.

STOLL G, GRIFFIN JW, LI CY, TRAPP BD. (1989) Wallerian degeneration in the peripheral nervous system: Participation of both Schwann cells and macrophages in myelin degradation. *Journal of Neurocytology* **18**, 671-683.

STURTZ FG, LATOUR P, MOCQUARD Y, CRUZ S, FENOLL B, LEFUR JM, MABIN D, CHAZOT G, VANDENBERGHE A. (1997) Clinical and electrophysiological phenotype of a homozygously duplicated Charcot-Marie-Tooth (Type 1A) disease. *European Neurology* **38**, 26-30.

SU Y, BROOKS DG, LI L, TROFATTER JA, RAVETCH JV, LEBO RV. (1993) Myelin protein zero gene mutated in Charcot-Marie-Tooth type 1B patients. *Proceedings of the National Academy of Sciences of the USA* **90**, 10856-10860.

SUH J-G, ICHIHARA N, SAIGOH K, NAKABAYASHI O, YAMANISHI T, TANAKA K, WADA K, KIKUCHI T. (1997) An in-frame deletion in peripheral myelin protein-22 gene causes hypomyelination and cell death of the Schwann cells in the new *TREMBLER* mutant mice. *Neuroscience* **79**, 735-744.

SUTER U, MOSKOW J, WELCHER A, SNIPES J, KOSARAS B, SIDMAN R, BUCHBERG A, SHOOTER M. (1992) A leucine to proline mutation in the putative first transmembrane domain of the 22-kDa peripheral myelin protein in the Trembler-J mouse. *Proceedings of the National Academy of Sciences of the USA* **89**, 4382-4386.

SUTER U, PATEL PI. (1994a) Genetic basis of inherited peripheral neuropathies. *Human Mutation* **3**, 95-102.

SUTER U, SNIPES GJ, SCHOENER-SCOTT R, WELCHER AA, PAREEK S, LUPSKI JR, MURPHY RA, SHOOTER EM, PATEL PI. (1994b) Regulation of tissue-specific expression of alternative peripheral myelin protein-22 (*PMP22*) gene transcripts by two promotors. *The Journal of Biological Chemistry* **269**, 25795-25808.

SUTER U, WELCHER AA, ÖZCELIK T, SNIPES GJ, KOSARAS B, FRANCKE U, BILLINGS-GAGLIARDI S, SIDMAN RL, SHOOTER EM. (1992) *Trembler* mouse carries a point mutation in a myelin gene. *Nature* **356**, 241-244.

SUTER U, WELCHER AA, SNIPES GJ. (1993) Progress in the molecular understanding of hereditary peripheral neuropathies reveals new insights into the biology of the peripheral nervous system. *Trends in Neurosciences* **16**, 50-56.

TARONI F, BOTTI S, SGHIRLANZONI A, BOTTEON G, DIDONATO S, PAREYSON D. (1995) A nonsense mutation in the PMP22 gene in hereditary neuropathy with liability to pressure palsies (HNPP) not associated with the 17p11.2 deletion. Meeting abstract. *American Journal of Human Genetics* **57**, ss 1327

TAYLOR V, WELCHER AA, AMGEN EST PROGRAM, SUTER U. (1995) Epithelial Membrane protein-1, peripheral myelin protein 22 , and lens membrane protein 20 define a novel gene family. *The Journal of Biological Chemistry* **270**, 28824-28833.

TERRY LC, BRAY GM, AGUAYO AJ. (1974) Schwann cell multiplication in developing rat unmyelinated nerves. A radioautographic study. *Brain Research* **69**, 144-148.

THOMAS GA. (1948) Quantitative histology of Wallerian degeneration. II.Nuclear population in two nerves of different fibre spectrum. *Journal of Anatomy* **97**, 135-145.

THOMAS PK, CALNE DB. (1974) Motor nerve conduction velocity in peroneal muscular atrophy: evidence for genetic heterogeneity. *Journal of Neurology, Neurosurgery, and Psychiatry* **37**, 68-75.

THOMAS PK. (1955) Growth changes in the myelin sheath of peripheral nerve fibres in fishes. *Proceedings of the Royal Societyof London [Biol]* **143**, 380

THOMAS PK. (1964) Changes in the endoneurial sheaths of peripheral myelinated nerve fibres during Wallerian degeneration. *Journal of Anatomy* **98**, 175-182.

THOMAS PK. (1970) The cellular response to nerve injury. 3. The effect of repeated crush injuries. *Journal of Anatomy* **106**, 463-470.

THOMAS PK, KING RHM, SMALL JR, ROBERTSON AM. (1996) The pathology of Charcot-Marie-Tooth disease and related disorders. *Neuropathology and Applied Neurobiology* **22**, 269-284.

THOMAS PK, LANDON DN, KING RHM. (1997) Diseases of the peripheral nerves. In D.I. Graham and P.L. Lantos (Eds.) *Greenfield's Neuropathology*, Arnold, London, pp. 367-487.

THOMAS PK, LASCELLES RG. (1967) Hypertrophic neuropathy. *Quarterly Journal of Medicine* **36**, 223-238.

THOMAS PK, MARQUES JR W, DAVIS MB, SWEENEY MG, KING RHM, BRADLEY JL, MUDDLE JR, TYSON J, MALCOM S, HARDING AE. (1997a) The phenotypic manifestations of chromosome 17p11.2 duplication. *Brain* **120**, 465-478.

TIMMERMAN V, NELIS E, VAN HUL W, NIEUWENHUIJSEN BW, CHEN KL, WANG S, OTHMAN K, CULLEN B, LEACH RJ, HANEMANN CO, DE JONGHE P, RAEYMAEKERS P, VANOMMEN GJB, MARTIN JJ, MULLER HW, VANCE JM, FISCHBECK KH, VANBROECKHOVEN C. (1992) The peripheral myelin protein gene PMP-22 is contained within the Charcot-Marie-Tooth disease type 1A duplication [published erratum appears in Nat Genet 1992 Sept;2(1):84]. *Nature Genetics* **1**, 171-175.

TOOTH HH. (1886) *The peroneal type of progressive muslular atrophy*, Lewis, London,

TOYKA K, ZIELASEK J, RICKER K, ADLKOFER K, SUTER U.(1997a) Hereditary neuromyotonia: a mouse model associated with deficiency or increased gene dosage of the PMP22 gene. *Journal of Neurology Neurosurgury & Psychiatry* **63**, 812-813.

TOYKA K, ZIELASEK J, RICKER K, ADLKOFER K, SUTER U. (1997b) Hereditary neuromyotonia: a mouse model associated with deficiency or increased gene dosage of the PMP22 gene. *Journal of Neurology Neurosurgury & Psychiatry* **63**, 812-813.

TRAPP BD, HAUER P, LEMKE G .(1988) Axonal regulation of myelin protein mRNA levels in actively myelinating Schwann cells. *The Journal of Neuroscience* **8**, 3515-3521.

TRAPP BD, ITOYAMA Y, STERNBERGER NH, QUARLES RH, WEBSTER HD. (1981) Immunocytochemical localization of Po protein in Golgi complex membranes and myelin of developing rat Schwann cells. *The Journal of Cell Biology* **90**, 1-6.

TRAPP BD, KIDD GJ, HAUER PE, MULRENIN E, HANEY CA, ANDREWS SB. (1995) Polarization of myelinating Schwann cell surface membranes: Role of microtubules and the trans-Golgi network. *The Journal of Neuroscience* **15**, 1797-1807.

TYSON J, ELLIS D, FAIRBROTHER U, KING RHM, MUNTONI F, JACOBS J, MALCOM S, HARDING AE, THOMAS PK. (1997) Hereditary demyelinating neuropathy of infancy. A genetically complex syndrome. *Brain* **120**, 47-63.

TYSON J, MALCOLM S, THOMAS PK, HARDING AE. (1996) Deletions of chromosome 17p11.2 in multifocal neuropathies. *Annals of Neurology* **39**, 180-186.

UPADHYAYA M, ROBERTS SH, FARNHAM J, MACMILLAN JC, CLARKE A, HEATH JP, HODGES ICG, HARPER PS. (1993) Charcot-Marie-Tooth disease 1A (CMT1A) associated with a maternal duplication of chromosome 17p11.2-12. *Human Genetics.* **91**, 392-394.

VALENTIJN LJ. (1995) The molecular basis of Charcot-Marie-Tooth disease type 1A. Thesis, Universtiy of Amsterdam, Netherlands.

VALENTIJN LJ, BAAS F, WOLTERMAN RA, HOOGENDIJK JE, BOSCH NHA, ZORN I, GABREËLS-FESTEN AAWM, DE VISSER M, BOLHIUS PA. (1992a) Identical point mutations of PMP-22 in Trembler-J mouse and Charcot-Marie-Tooth disease type 1A. *Nature Genetics* **2**, 288-291.

VALENTIJN LJ, BOLHUIS PA, ZORN I, HOOGENDIJK JE, VAN DEN BOSCH N, HENSELS GW, STANTON,UP,HOUSEMAN DE,FISCHBECK KH,ROSS DA. (1992) The peripheral myelin gene PMP-22/GAS-3 is duplicated in Charcot-Marie-Tooth disease type 1A. *Nature Genetics* **1**, 166-170.

VALENTIJN LJ, BAAS F, ZORN I, HENSELS GW, DE VISSER M, BOLHIUS PA. (1993) Alternatively sized duplication in Charcot-Marie-Tooth disease type 1A. *Human Molecular Genetics.* **2**, 2143-2146.

VALENTIJN LJ, OUVRIER RA, BOSCH NHA, BOLHIUS PA, BAAS F, NICHOLSON GA. (1995) Dejerine-Sottas neuropathy is associated with a de novo PMP22 mutation. *Human Mutation.* **5**, 76-80.

VALLAT JM, SINDOU P, PREUX PM, TABARAUD F, MILOR AM, COURATIER P, LEGUERN E, BRICE A. (1996) Ultrastructural PMP22 expression in inherited demyelinating neuropathies. *Annals of Neurology* **39**, 813-817.

VAN DEN BERG LH, SADIQ SA, THOMAS FP, LATOV N. (1990) Characterization of HNK-1 bearing glycoproteins in human peripheral nerve myelin. *Journal of Neuroscience Research* **25**, 295-299.

VANCE JM, NICHOLSON GA, YAMAOKA LH, STAJICH J, STEWART CS, SPEER MC, HUNG WY, ROSES AD, BARKER D, PERICAK-VANCE MA .(1989) Linkage of Charcot-Marie-Tooth neuropathy type 1a to chromosome 17. *Experimental Neurology* **104**, 186-189.

VERHAGEN WIM, GABREËLS-FESTEN AAWM, VAN WENSEN PJM, JOOSTEN EMG, VINGERHOETS HM, GABREËLS FJM, DE GRAAF R .(1993) Hereditary neuropathy with liability to pressure palsies; a clinical, electrophysiological and morphological study. *Journal of the Neurological Sciences* **116**, 176-184.

VERHALLE D, LOFGREN A, NELIS E, DEHAENE I, THEYS P, LAMMENS M, DOM R, VAN BROECKHOVEN C, ROBBERECHT W. (1994) Deletion in the CMT1A locus on chromosome 17p11.2 in hereditary neuropathy with liability to pressure palsies. *Annals of Neurology* **35**, 704-708.

VIAL JD. (1958) The early changes in the axoplasm during Wallerian degeneration. *Journal of Biophysical and Biochemical Cytology*, 551-556.

VIZOSO AD, YOUNG JZ. (1948) Internode length and fibre diameter in developing and regenerating nerve. *Journal of Anatomy* **82**, 110-134.

WALLER A. (1850) Experiments on the section of the glossopharangeal and hypoglossal nerves of the frog, and observations of the alterations produced thereby in the structure of their primitive fibres. *Philosophical Transactions of the Royal Society* **140**, 423-429.

WARNER LE, MANCIAS P, BUTLER IJ, MCDONALD CM, KEPPEN L, KOOB KG, LUPSKI JR. (1998) Mutations in the early growth response 2 (EGR2) gene are associated with hereditary myelinopathies. *Nature Genetics* **18**, 382-384.

WEBSTER HdeF. (1965) The relationship between Schmidt-Lantermann incisures and myelin segmentation during Wallerian degeneration. *Annals of the New York Academy of Sciences* **122**, 29-38.

WEBSTER HdeF. (1971) The geometry of peripheral myelin sheaths during their formation and growth in rat sciatic nerves. *The Journal of Cell Biology* **48**, 348-367.

WEBSTER HdeF. (1993) Development of peripheral nerve fibers. In P.J. Dyck, P.K. Thomas, J.W. Griffin, P.A. Low and J.F. Poduslo (Eds.) *Peripheral Neuropathy*, W.B.Saunders Company, Phiadelphia, pp. 243-266.

WEBSTER HdeF, MARTIN JR, O'CONNELL MF. (1973) The relationships between interphase Schwann cells and axons before myelination:A quantitative electron microscopic study. *Developmental Biology* **32**, 401-416.

WEINBERG HJ, SPENCER PS. (1976) Studies on the control of myelinogenesis. II. Evidence for neuronal regulation of myelin production. *Brain Research* **113**, 363-378.

WEINSTEIN DE, BURROLA P, LEMKE G. (1995) Premature Schwann cell differentiation and hypermyelination in mice expressing a targeted antagonist of the POU transcription factor SCIP. *Molecular and Cell Neuroscience* **6**, 212-229.

WELCHER AA, SUTER U, DE LEON M, SNIPES GJ, SHOOTER EM. (1991) A myelin protein is encoded by the homologue of a growth arrest- specific gene. *Proceedings of the National Academy of Sciences of the United States of America* **88**, 7195-7199.

WERNECKE H, LINDNER J, SCHACHNER M. (1985) Cell type specificity and developmental expression of the L2/HNK-1 epitope in mouse cerebellum. *Journal of Neuroimmunology* **9**, 115-130.

WHITE FV, TOEWS AD, GOODRUM JF, NOVICKI DL, BOULDIN TW, MORELL P .(1989) Lipid metabolism during early stages of Wallerian degeneration in the rat sciatic nerve. *Journal of Neurochemistry* **52**, 1085-1092.

WIGGINS RC, BENJAMINS JA, MORELL P. (1975) Appearance of myelin proteins in rat sciatic nerve during development. *Brain Research* **89**, 99-106.

WILLIAMS PL, HALL SM. (1971a) Chronic Wallerian degeneration - an *in vivo* and ultrastructural study. *Journal of Anatomy* **109**, 487-503.

WILLIAMS PL, WENDELL-SMITH CP. (1971b) Some additional parametric variations between peripheral nerve fibre populations. *Journal of Anatomy* **109**, 505-526.

WINDEBANK AJ. (1993) Inherited recurrent focal neuropathies. In P.J. Dyck, P.K. Thomas, J.W. Griffin et al. (Eds.) *Peripheral Neuropathy*, W.B. Saunders, Philadelphia, pp. 1137-1148.

WINDEBANK AJ, WOOD P, BUNGE RP, DYCK PJ. (1985) Myelination determines the caliber of dorsal root ganglion neurons in culture. *The Journal of Neuroscience* **6**, 1563-1569.

WISE CA, GARCIA CA, DAVIS SN, HEJU A, PENTAO L, PATEL PI, LUPSKI JR. (1993) Molecular analyses of unrelated Charcot-Marie-Tooth (CMT) disease patients suggest a high frequency of the CMT1A duplication. *American Journal of Human Genetics* **53**, 853-863.

WOOD PM, BUNGE RP. (1975) Evidence that sensory axons are mitogenic for Schwann cells. *Nature* **256**, 662-664.

YAMADA KM, SPOONER BS, WESSELLS NK. (1971) Ultrastructure and function of growth cones and axons of cultured nerve cells. *The Journal of Cell Biology* **49**, 614-635.

YONG VW, KIM SU, KIM MW, SHIN DH. (1988) Growth factors for human glial cells in culture. *Glia* **1**, 113-123.

YOSHIHARA Y, OKA S, WATANABE Y, MORI K. (1991) Developmentally and spatially regulated expression of HNK-1 carbohydrate antigen on a novel phosphatidylinositol-anchored glycoprotein in rat brain. *The Journal of Cell Biology* **115**, 731-744.

YOSHKAWA K, NISHIMURA T, NAKATSUJI Y, FUJIMURA H, HIMORO M, HAYASAKA K, SAKODA S, YAZAKI T, YANGAGIHARA T. (1994) Elevated expression of messenger RNA for peripheral myelin protein 22 in biopsied peripheral nerves of patients with Charcot-Marie-Tooth disease type 1A. *Annals of Neurology* **35**, 445-450.

YOUNG P, WIEBUSCH H, STOGBAUER F, RINGELSTEIN B, ASSMAN G, FUNKE H. (1997) A novel frameshift mutation in *PMP22* accounts for hereditary neuropathy with liability to pressure palsies. *Neurology* **48**, 450-452.

ZOIDL G, BLASS-KAMPMANN S, D'URSO D, SCHMALENBACH C, MÜLLER HW. (1995) Retroviral-mediated gene transfer of the peripheral myelin protein PMP22 in Schwann cells :modulation of cell growth. *The EMBO Journal* **14**, 1122-1128.

ZOIDL G, BLASS-KAMPMANN S, SCHMALENBACH C, KUHN R, MÜLLER HW. (1997) Influence of elevated expression of rat wild-type PMP22 and its mutant PMP22 ^{Trembler} on cell growth of NIH3T3 fibroblasts. *Cell and Tissue Research* **287**, 459-470.

Publications

J. Anat. (1997) 190, pp. 423–432, with 4 figures. Printed in Great Britain

Abnormal Schwann cell/axon interactions in the Trembler-J mouse

A. M. ROBERTSON, R. H. M. KING, J. R. MUDDLE AND P. K. THOMAS

Department of Clinical Neurosciences, Royal Free Hospital School of Medicine, London, UK

(*Accepted 25 November 1996*)

ABSTRACT

The Trembler-J (Tr^J) mouse has a point mutation in the gene coding for peripheral myelin protein 22 (PMP22). Disturbances in PMP22 are associated with abnormal myelination in a range of inherited peripheral neuropathies both in mice and humans. PMP22 is produced mainly by Schwann cells in the peripheral nervous system where it is localised to compact myelin. The function of PMP22 is unclear but its low abundance (~ 5% of total myelin protein) means that it is unlikely to play a structural role. Its inclusion in a recently discovered family of proteins suggests a function in cell proliferation/differentiation and possibly in adhesion. Nerves from Tr^J and the allelic Trembler (Tr) mouse are characterised by abnormally thin myelin for the size of the axon and an increased number of Schwann cells. We report ultrastructural evidence of abnormal Schwann cell–axon interactions. Schwann cell nuclei have been found adjacent to the nodes of Ranvier whereas in normal animals they are located near the centre of the internodes. In some fibres the terminal myelin loops faced outwards into the extracellular space instead of turning inwards and terminating on the axon. In severely affected nerves many axons were only partially surrounded by Schwann cell cytoplasm. All these features suggest a failure of Schwann cell–axon recognition or interaction. In addition to abnormalities related to abnormal myelination there was significant axonal loss in the dorsal roots.

Key words: Peripheral nerve; myelination; hypomyelination; Schwann cells; peripheral myelin protein 22; Trembler-J mouse.

INTRODUCTION

The Trembler-J mouse (Tr^J) was discovered by Sidman et al. (1979) within a colony of C57BL/6J mice. At approximately 3 wk of age, affected animals could be distinguished from their nonaffected littermates by an action tremor and gait abnormality. The latter involved primarily the hindlimbs and consisted of extension of the knees and ankles and splaying of the hindlimbs (Henry et al. 1983). On the basis of genetic and morphological studies Tr^J was judged to be a mutation at the same locus as Trembler (Tr) (Sidman et al. 1979), a neurological mouse mutant discovered by Falconer (1951). Pathology in both strains of mice is confined to the peripheral nervous system and is characterised by a myelin deficit and an increased number of Schwann cells (Ayers & Anderson, 1973; Low & McLeod, 1975; Aguayo et al. 1977; Perkins et al. 1981). Myelin in these animals is inappropriately thin for the size of the axon (Low, 1976*a*, *b*, 1977) and has a tendency to be uncompacted, especially near the nodes of Ranvier (Ayers & Anderson, 1973, 1975; Low, 1977). Both Tr^J and Tr have been found to be associated with point mutations in the gene coding for peripheral myelin protein 22 (PMP22) (Suter et al. 1992*a*, *b*). The PMP22 gene encodes an 18 kDa protein with 4 putative transmembrane domains and 1 N-linked glycosylation site (Manfioletti et al. 1990; Welcher et al. 1991; Suter et al. 1992*a*). The resulting 22 kDa glycoprotein is produced in the peripheral nervous system mainly by Schwann cells where it is localised in the compact myelin of essentially all myelinated fibres (Snipes et al. 1992). Tr^J has a point mutation which replaces a leucine with a proline residue at amino acid position 16 (Suter et al. 1992*a*). The Tr^J mutation is in the 1st transmembrane domain of PMP22 whereas the abnormality in Tr is the replacement of a glycine by an

Correspondence to Andrea Robertson, Department of Clinical Neurosciences, Royal Free Hospital School of Medicine, Rowland Hill Street, London NW3 2PF, UK.

aspartic acid residue at amino acid position 150 in the 4th transmembrane region (Suter et al. 1992*b*). Although most strongly expressed in peripheral nerve, PMP22 mRNA is found in other adult tissues including lung, colon and brain (Spreyer et al. 1991; Welcher et al. 1991; Bosse et al. 1994; Suter et al. 1994). PMP22 mRNA is also expressed in early organogenesis in the gut and surrounding the liver capsule, and later in several mesoderm derived connective tissues and ectoderm derived cells of the lens and in the skin (Baechner et al. 1995). Its widespread expression in other tissues suggests a role for PMP22 outside the nervous system. The gene for PMP22 was found to be identical to the growth arrest specific gene, *gas 3* (Spreyer et al. 1991; Welcher et al. 1991) which belongs to a group of genes whose expression is specifically associated with the quiescent cell state and which may be involved in the regulation of general cell growth (Manfioletti et al. 1990; Zoidl et al. 1995). Pathological changes in mice with alterations in PMP22 are confined specifically to the peripheral nervous system. In PMP22 deficient mice the onset of myelination is delayed, followed by hypermyelination and subsequent demyelination (Adlkofner et al. 1995). This suggests that PMP22 functions in the initial stages of myelin formation and later in controlling myelin thickness and stability. Ultrastructurally, PMP22 immunoreactivity has been localised to regions of compact myelin and was not detected over the regions of the internodes which contain the uncompacted Schmidt–Lanterman incisures (Snipes et al. 1992). PMP22 has also been localised on the plasma membrane of Schwann cells of Remak fibres, the membranes of Schwann cell processes that surround collagen pockets and Schwann cell plasma membranes in the cell laminae of onion bulbs in the nerves of type 1A Charcot-Marie-Tooth disease (CMT1A) (Haney et al. 1996). This suggests that all Schwann cells, not only those involved in the myelination process, constitutively express PMP22.

The recent discovery of a novel gene family of structurally related proteins of which PMP22 is a member provides the strongest indications of the generalised physiological role of PMP22 (Taylor et al. 1995). The 4 proteins so far discovered, EMP-1 (Taylor et al. 1995), MP30 (Kumar et al. 1993), CL20 (Marvin et al. 1995) and PMP22 (Snipes et al. 1992) each have 4 putative transmembrane domains with a conserved N-linked glycosylation site on the 2nd transmembrane domain. The high degree of identity, particularly of the first 2 transmembrane domains, suggests they may serve a similar and important function. The other members of this protein family apart from PMP22 are found in differentiating and mature cells rather than being associated with growth arrest. The function of this family may be related both to the switch from proliferation and to the maintenance of critical functions in the differentiated state (Taylor et al. 1995). In the present study, the morphological changes in the peripheral nerves have been examined in the Tr^{J} mouse to seek indications as to the mechanisms operative in the development of the neuropathy.

METHODS

Male and female affected ($Tr^{J}/+$) and unaffected ($+/+$) littermates were used at 3 and 12 mo of age. Animals were killed by perfusion while under deep anaesthesia (Sagatal 18 mg/animal). The thorax was opened and a butterfly needle attached to a cannula inserted into the left ventricle of the heart. The right atrium was incised and blood washed out with 1 N saline at 37 °C. This was followed by perfusion with 1% paraformaldehyde and 1% glutaraldehyde in 0.1 M PIPES (piperazine-N,N′-bis-[2-ethanesulfonic acid]) buffer (pH 7.4), initially at 37 °C and then at room temperature. The sciatic nerve was removed and laid on pieces of card which were then placed in fresh fixative. The dorsal and ventral roots were excised together with the dorsal root ganglia. The lumbosacral spinal cord was also removed. All tissue was then fixed for a further 2 h, washed in PIPES buffer plus 2% sucrose and then postfixed in 1% osmium tetroxide in PIPES buffer plus 2% sucrose, 3% sodium iodate and 1.5% potassium ferricyanide. The specimens were dehydrated in increasing concentrations of ethanol and transferred to epoxy resin via 1,2-epoxypropane as an intermediary. Semithin sections were cut and stained with thionin.

Measurements of axon diameter, fibre diameter and g ratio (axon diameter/total fibre diameter) were confined to fibres with a one-to-one axon/Schwann cell relationship; these included amyelinate or demyelinated fibres. The numbers of Schwann cell nuclei in each section were obtained from transverse sections through the dorsal and ventral spinal roots. All measurements were taken from whole fascicles viewed with a × 100 objective and a × 1.2 optivar on a Zeiss Axioplan microscope (Zeiss UK, Welwyn Garden City, Herts, UK) connected on-line through a television camera to a Kontron IBAS AT image analyser (Imaging Associates, Thame, UK). Many fibres in the Tr^{J} animals had myelin that was too thin to be identified (less than 5 myelin lamellae) at the

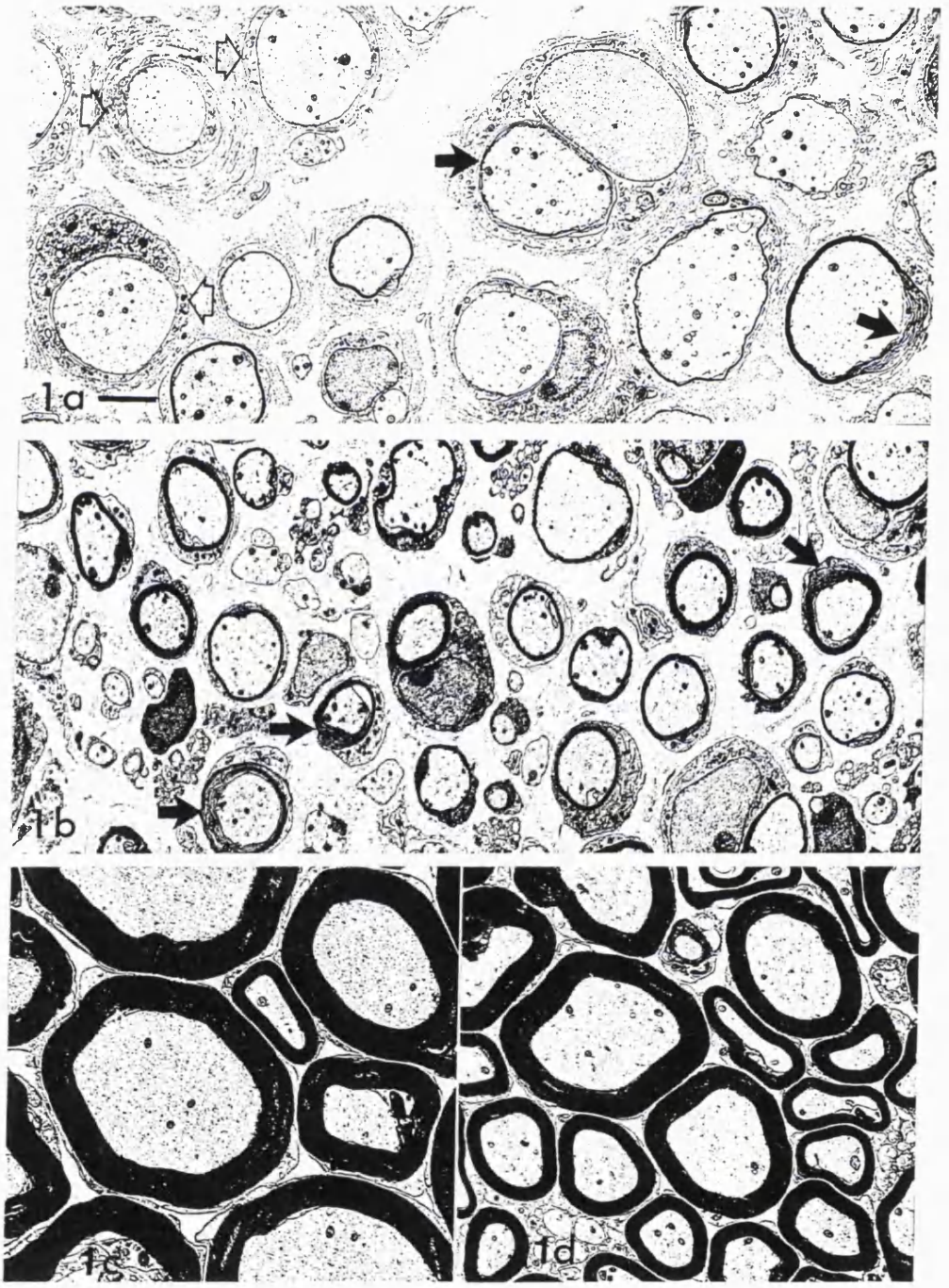

Fig. 1. (*a*) Ventral root of a 3 mo *Tr*^{J} animal. Axons of a size that would normally be myelinated (see Fig. 1*c*) are completely devoid of myelin (open arrows). Others are surrounded by myelin which is inappropriately thin for the size of the axon. Where myelin is present it is commonly uncompacted (filled arrows). (*b*) Dorsal root from the same 3 mo *Tr*^{J} animal as (*a*). Fibres are surrounded by more myelin than those in the ventral root. Myelin is uncompacted (filled arrows). (*c*) Ventral root 3 mo unaffected animal. (*d*) Dorsal root 3 mo unaffected animal. Bar, 3 μm (applies to all panels).

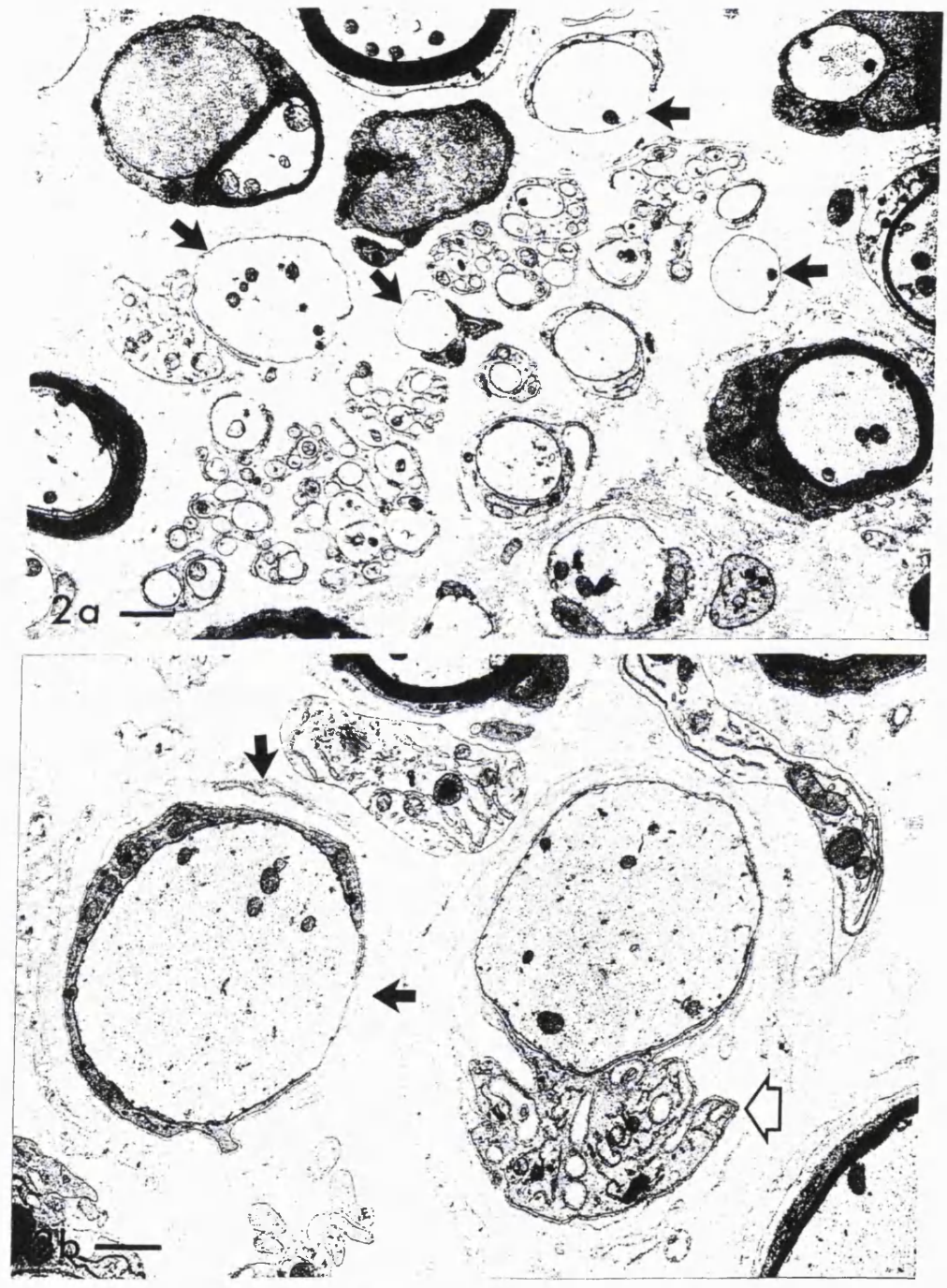

Fig. 2. (*a*) Dorsal root of a 3 mo *Tr*$^{+}$ animal. Many fibres are incompletely surrounded by Schwann cell cytoplasm (filled arrows). (*b*) Dorsal root of a 3 mo *Tr*$^{+}$ animal. Schwann cell processes project into the endoneurium (open arrow). Paired redundant basement membranes (filled arrows), one with a small amount of remaining cytoplasm, are considered to be indicative of the Schwann cell extending processes and then withdrawing them. Bars, 1 μm.

light microscope level. In these cases the axon was measured and the fibres assigned a g ratio of 1. Ultrathin sections were contrasted with lead citrate and methanolic uranyl acetate for electron microscopy. The proportion of fibres incompletely surrounded by Schwann cell cytoplasm was counted in nonoverlapping electron micrographs. At least 200 fibres from each dorsal and ventral root were counted. Sections were taken from pairs of dorsal and ventral roots immediately proximal to the dorsal root ganglia.

RESULTS

Clinical

Affected Tr^{J} animals developed a neuropathy that could be detected in the most severely affected animals at between 4 and 6 wk of age. The disorder primarily affected the hind limbs, resulting in an abnormal gait with splaying of the hind limbs, muscle wasting and weakness. The severity varied between animals; in some mildly affected animals gait abnormalites were not detectable until several months of age. Convulsions, which were described as a feature in the *Tr* mouse (Braverman, 1953), were not observed.

Morphology

The sciatic nerve, dorsal and ventral roots and dorsal root ganglia were examined by light and electron microscopy. The most obvious features were a lack of myelin and an increased number of Schwann cell nuclei, as previously reported for Trembler mice (Ayers & Anderson, 1973; Low & McLeod, 1975; Aguayo et al. 1977; Perkins et al. 1981). Myelination was most severely affected in the ventral roots and both posterior and anterior roots were more severely affected than the sciatic nerve (Fig. 1). Only minor structural changes were seen in the dorsal root ganglion cells. There was no evidence of active demyelination at any of the sites sampled and Schwann cell mitoses were not encountered.

In the spinal roots examined, myelin was very thin and in many fibres consisted of only 1 or 2 turns. Myelin was often uncompacted, especially near the nodes of Ranvier. Sections of severely affected roots showed axons incompletely surrounded by Schwann cell cytoplasm (Fig. 2). The proportion of fibres incompletely surrounded by Schwann cell cytoplasm was not significantly different between the dorsal and ventral roots (mean and standard deviation $29 \pm 4\%$ and $25 \pm 7\%$ respectively). Supernumerary Schwann cells unassociated with axons were not seen and concentric Schwann cell proliferation producing 'classic' onion bulbs was not evident. Instead many 'basal laminal onion bulbs' consisting of concentric or sectorial arrays of cell processes were frequent (Figs 2*b*, 3*a*). Several previously unreported abnormalities for the Tr^{J} mouse were observed. Terminal loops of the myelin sheaths were occasionally found turning outwards into the extracellular space instead of terminating on the axon (Fig. 3*b*). Schwann cell nuclei were often not located at the centre of the internode as is usually the case but were found very close to one end of the internode, often over the terminal loops (Fig. 3*c*, *d*). The incidence of this increased with the severity of the neuropathy. The cytoplasm of Schwann cells in Tr^{J} animals tended to be concentrated in the perinuclear region with an attenuated layer extending on either side towards the nodes of Ranvier. Their nuclei had abnormally rounded profiles. Exuberant protrusions of Schwann cell cytoplasm into the endoneurium was also a feature of the Tr^{J} animals (Fig. 2*b*).

Morphometry

The number of Schwann cell nuclei in cross sections of dorsal and ventral roots was 4–5 times higher in the spinal roots both in 3 and 12-mo-old Tr^{J} animals when compared with age matched controls. There was no alteration with age in the number of nuclei either in control or Tr^{J} animals (Table 1). Total fascicular area was not significantly affected either by strain or age (Table 2). In the ventral roots there was no difference in fibre density between Tr^{J} and controls, although both demonstrated a significant age related decrease in density. In the dorsal roots, however, there was a significant decrease in fibre density in Tr^{J} animals when compared with age matched controls.

Myelin thickness

In Tr^{J} animals a large proportion of axons (40–60%) were either devoid of myelin or surrounded by myelin too thin to be measured at the light microscopic level (Table 3). Myelination was most severely affected in the ventral roots of 12 mo animals where 60–65% of fibres had myelin that was considered too thin to quantify accurately (less than 5 turns of myelin).The dorsal roots were significantly less affected than the ventral with only 40–50% of fibres falling into this category ($P < 0.01$). This dorsal/ventral root difference was not significant in the 3 mo animals. In the remaining fibres with measurable myelin, Tr^{J} animals had a higher proportion of fibres with

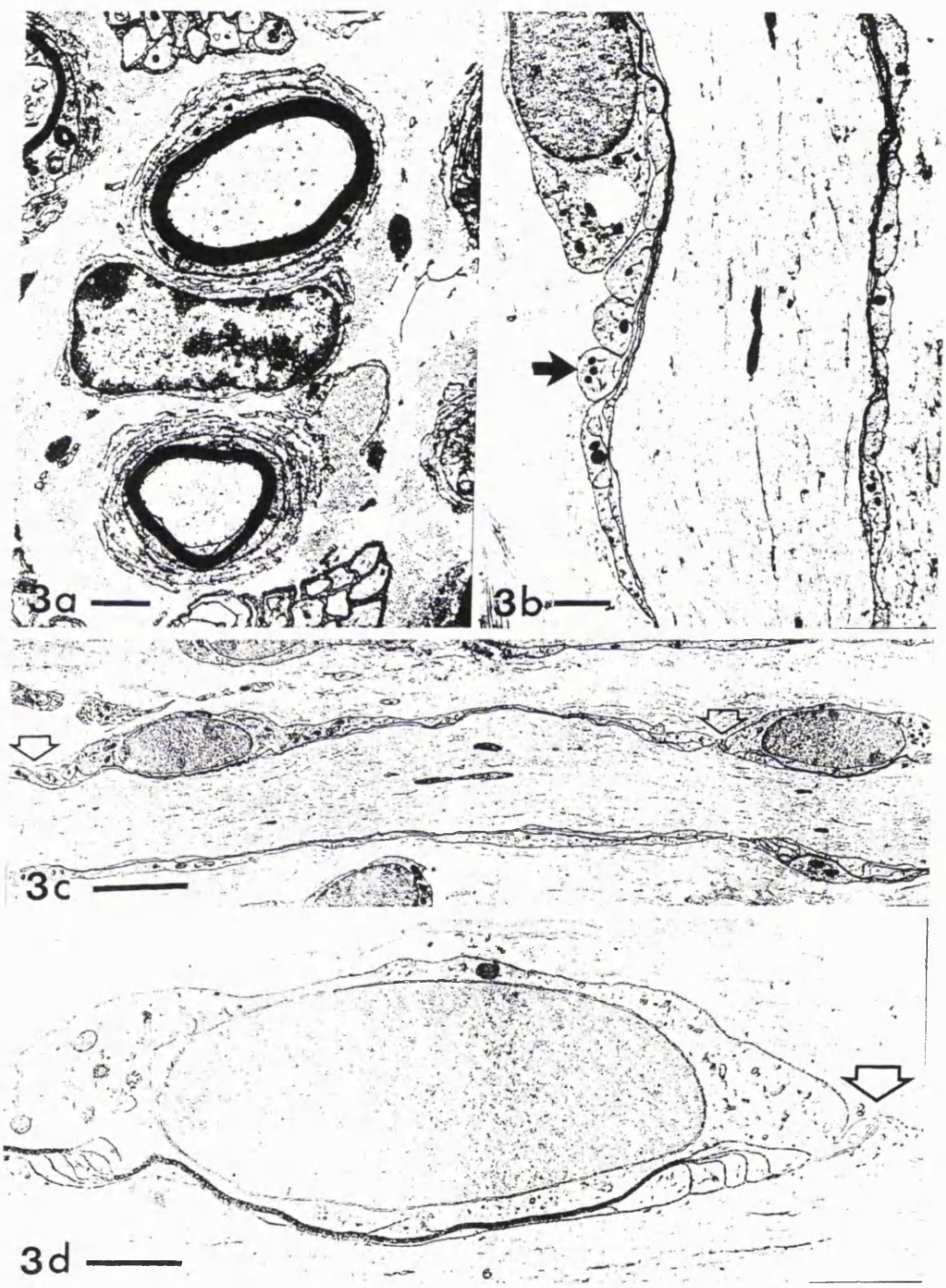

Fig. 3. (*a*) Fibres encircled by layers of redundant basal lamina. Sciatic nerve 12 mo Tr^{J}. Bar, 1 μm. (*b*) Terminal myelin loops turning outwards from the axon (arrow). Bar, 2 μm. (*c*) Schwann cell nuclei placed at the ends of the internode, close to the nodes of Ranvier (arrows). Bar, 5 μm. (*d*) Nucleus located over a node of Ranvier (arrow). Bar, 1 μm.

Table 1. *Numbers of Schwann cell nuclei and nerve fibre density in Tr^J mice*

	Schwann cell nuclei*				Density**			
	Ventral root		Dorsal root		Ventral root		Dorsal root	
Age	3 mo	12 mo	3 mo	12 mo	3 mo	12 mo	3 mo	12 mo
Tr^J	166	125	255	202	19854	12647	28152	23983
($n = 6$)	(25)	(23)	(38)	(20)	(730)	(611)	(1790)	(904)
Control	35	47	60	53	16777	13303	39151	35531
(n = 7)	(5)	(5)	(9)	(8)	(1685)	(943)	(1735)	(3322)
Mann–Whitney U-test	$P < 0.01$	$P < 0.05$	$P < 0.01$	$P < 0.01$			$P < 0.05$	$P < 0.01$

* Numbers per fascicle: means (S.E.M.); ** fibres per mm^2: means (S.E.M.).

Table 2. *Fascicle area in spinal roots (mm^2)*

	Fascicle area Ventral root		Dorsal root	
Age	3 mo	12 mo	3 mo	12 mo
Tr^J	35519	50539	41931	15151
($n = 6$)	(3288)	(9052)	(4432)	(1072)
Control	43166	74526	34244	34173
(n = 7)	(7060)	(14361)	(5179)	(4333)
Mann–Whitney U-test				

* Means (S.E.M.).

inappropriately thin myelin (g ratio > 0.8) (Table 3). The ventral roots were more severely affected (20–26%) than the dorsal (4–6%) both in 3 and 12 mo animals ($P = 0.004$ and $P = 0.04$).

Fibre and axon sizes

Both in the dorsal and ventral roots of Tr^J animals at both ages there was a significant increase in the proportion of small fibres and a concomitant decrease in the proportion of large fibres (Fig. 4*a*, *b*). Axon diameters followed the same pattern as fibre diameters with an increased proportion of small and a decreased proportion of large fibres (Fig. 4*c*, *d*). In the ventral roots of Tr^J animals both fibre and axon diameters increased with age.

DISCUSSION

The dominant features of the Tr^J neuropathy are a myelination deficit, an increased number of Schwann cells and a failure of the Schwann cells to ensheath the axons fully. Myelination was most severely affected in the ventral roots both in the 3 and 12 mo animals. The dorsal roots were significantly less affected and the sciatic nerve less so again. Of the fibres with measurable myelin Tr^J animals had a significantly higher proportion in which myelin was inappropriately thin for the size of the axon (g ratio > 0.8). In terms of nerve fibre pathology the phenotype of Tr^J appears very similar to that seen with the equivalent point mutation in man (Gabreëls-Festen et al. 1995, cases 14–16; personal communication) in which the mean number of fibres in the sural nerve with a g ratio of 1.0 ranged from 72% to 80%.

Fibre density was significantly reduced in the dorsal roots both in the 3 and 12 mo Tr^J animals when compared with controls. As there was no alteration in fascicular area this indicates axonal loss; this has not previously been reported either in *Tr* or Tr^J. This decrease in density was limited to the dorsal roots, but

Table 3. *Myelination of dorsal and ventral spinal root fibres in Tr^J mice (percentages)*

	Fibres lacking measureable myelin*				Hypomyelinated fibres (g ratio > 0.8)*			
	Ventral root		Dorsal root		Ventral root		Dorsal root	
Age	3 mo	12 mo	3 mo	12 mo	3 mo	12 mo	3 mo	12 mo
Tr^J	65.5	60	52.5	40.5	18.4	26.1	6.6	3.8
(n = 6)	(5.7)	(1.7)	(4.0)	(4.3)	(4.0)	(1.6)	(1.9)	(0.7)
Control	0.04	0.04	0.27	0.06	0.39	11.0	0.33	0.02
(n = 7)	(0.01)	(0.01)	(0.08)	(0.05)	(0.21)	(2.7)	(0.15)	(0.02)
Mann–Whitney U-test	$P < 0.005$	$P < 0.005$	$P < 0.005$	$P < 0.005$	$P < 0.005$	$P < 0.005$	$P < 0.005$	$P < 0.005$

* Means (S.E.M.).

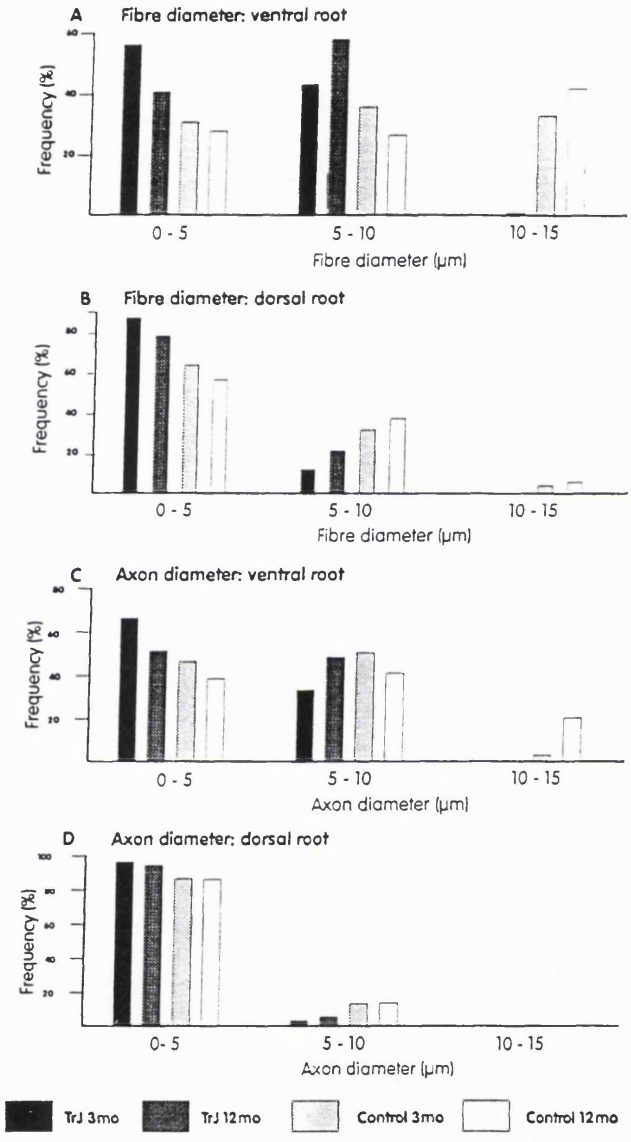

Fig. 4. Bar diagrams of distribution of fibre and axon diameters in ventral and dorsal roots of 3 and 12 mo Tr^J and control mice.

whether loss of motor fibres occurs more peripherally to explain the muscle wasting was not established. Axonal loss was not related to the degree of myelination or to the lack of ensheathment of axons by Schwann cells. The number of Schwann cell nuclei was 3–5 times higher in Tr^J than in age matched control animals and did not alter with age.

Axonal loss has not been sought in the dorsal roots of *Tr* animals; it is known not to occur in the L4 ventral root or in the ulnar nerve (Perkins et al. 1981). The cause for such axonal loss is uncertain, as it is in other neuropathies characterised by primary demyelination. Recently Hyman Friedman et al. (1996) have described abnormalities of growth factor expression by Schwann cells in Tr^J mice and have raised the possibility that this may impair axonal support by these cells, resulting in axonal atrophy. As the distribution of PMP22 is not known to differ

significantly between the dorsal and ventral roots, it is difficult to suggest a mechanism whereby the dorsal roots should be more susceptible to axonal loss than the ventral, or why myelination should be more affected in the ventral roots. Although the *Tr* and Tr^{J} mutations are essentially similar, demonstrating largely the same features, they are not identical. Tr^{J} animals tend to be less severely affected than *Tr*. In the sciatic nerves of Tr^{J} almost all axons in a one-to-one Schwann cell relationship are surrounded by at least a few turns of myelin. In contrast, in the *Tr* mouse nerve many axons do not progress from a stage of single ensheathment (promyelination) to myelination but remain completely devoid of myelin and often incompletely surrounded by Schwann cell cytoplasm. This lack of ensheathment is rare in the sciatic nerves of Tr^{J} animals but is commonly seen (25%) in the more severely affected spinal roots. There was very little evidence in Tr^{J} either of active demyelination or of cycles of demyelination/remyelination leading to concentric proliferation of Schwann cells around nerve fibres with the formation of hypertrophic or 'classic' onion bulbs. In contrast, basal laminal onion bulbs were more common. These layers of collapsed basement membrane have been suggested as indicating that the Schwann cells become reactive, extend cytoplasmic processes and then withdraw them (Ayers & Anderson, 1975). Schwann cell protrusions were evident in the present material (see Fig. 2*b*). The occasional sectorial distribution of the empty basal laminal layers, i.e. affecting only a part of the circumference of the fibre (Fig. 2*b*) would favour this explanation. An alternative explanation would be ongoing Schwann cell proliferation with loss of the redundant supernumerary Schwann cells. Against this explanation is the lack of morphological evidence of cell death.

The appearances in the Tr^{J} mouse thus differ from those in HMSN Ia in man, due to chromosome 17p11.2 duplication, in which classic onion bulbs are observed. However, in HMSN Ia these take several years to develop (Gabreëls-Festen & Gabreëls, 1993). The appearance in Tr^{J} resemble more closely the examples of congenital hypomyelination neuropathy in man in which basal laminal onion bulbs are prominent (Guzzetta et al. 1982). In the *Tr* mouse, Perkins et al. (1981) showed that Schwann cell proliferation continues throughout the life of the animals. One explanation would be that ongoing demyelination leads to Schwann cell division followed by proliferation and remyelination with an excess of proliferated cells that accumulate circumferentially around the axons thus producing the onion bulb, as originally suggested for human hypertrophic neuropathy (Thomas & Lascelles, 1967). Our results in Tr^{J} have shown that the number of Schwann cell nuclei is increased compared with control animals. As redundant supernumerary Schwann cells were not a feature of the neuropathy and fibre numbers were not increased, this indicates shorter Schwann cell territories along the length of the axons. Comparison of the counts of Schwann cell nuclei in the spinal roots between 3 and 12 mo animals in the present study indicated no significant changes. This suggests either a stable cell population or a balance between cell proliferation and death. We have not yet examined cell proliferation, but no mitosis or examples of cell death were encountered, nor was active demyelination observed. Whether continuing Schwann cell proliferation plays a role in the genesis of the neuropathy in the Tr^{J} mouse is therefore uncertain.

It is tempting to speculate on the possible role of the L2/HNK-1 epitope in this disorder. In at least 2 members (PMP22 and CL20) in their family of proteins the L2/HNK epitope is associated with the glycosylation site on the highly conserved 1st transmembrane domain (Snipes et al. 1993; Marvin et al. 1995). The HNK-1 epitope characterises a large family of recognition molecules and is thought to serve as a ligand for adhesion (Kunemund et al. 1988; Griffith et al. 1992). L2/HNK-1 is known to be expressed in developing peripheral nerve where it is thought to be involved in Schwann cell–axon interactions (Martini & Schachner, 1986; Martini et al. 1994). L2/HNK-1 is involved in cell/cell and cell/laminin interactions and antibodies directed against it are capable of functionally blocking neural adhesion to laminin in the presence of heparin (Keilhauer et al. 1985; Kunemund et al. 1988; Hall et al. 1993). It is likely that PMP22 is the major L2/HNK-1 expressing glycoprotein in peripheral nerve (Snipes et al. 1993) and in the light of the ultrastructural abnormalities found in the Tr^{J} mouse it seems plausible that altered interaction of a mutated protein and the carbohydrate moiety may be involved.

ACKNOWLEDGEMENTS

Financial support from the Wellcome, Leverhulme and John and Barbara Attenborough Trusts is gratefully acknowledged. The electron microscope was provided by the Muscular Dystrophy Group of Great Britain.

REFERENCES

Adlkofer K, Martini R, Aguzzi A, Zielasek J, Toyka KV, Suter U (1995) Hypermyelination and demyelinating peripheral

neuropathy in PMP-22 deficient mice. *Nature Genetics* **11**, 274–280.

AGUAYO AJ, ATTIWELL M, TRECARTEN J, PERKINS S, BRAY GM (1977) Abnormal myelination in transplanted Trembler mouse Schwann cells. *Nature* **265**, 73–75.

AYERS MM, ANDERSON RM (1973) Onion bulb neuropathy in the Trembler mouse: a model of hypertrophic interstitial neuropathy (Dejerine-Sottas) in man. *Acta Neuropathologica* **25**, 54–70.

AYERS MM, ANDERSON RM (1975) Development of onion bulb neuropathy in the Trembler mouse. Comparison with normal nerve maturation. *Acta Neuropathologica* **32**, 43–59.

BAECHNER D, LIEHR T, HAMEISTER H, ALTENBERGER H, GREHL H, SUTER U et al. (1995) Widespread expression of the peripheral myelin protein-22 (pmp22) in neural and non-neural tissues during murine development. *Journal of Neuroscience Research* **42**, 733–741.

BOSSE F, ZOIDL G, WILMS S, GILLEN CP, KUHN HG, MULLER HW (1994) Differential expression of two mRNA species indicates a dual function of peripheral myelin protein PMP22 in cell growth and myelination. *Journal of Neuroscience Research* **37**, 529–537.

FALCONER DS (1951) Two new mutants, 'Trembler' and 'Reeler' with neurological actions in the house mouse (*Mus musculus* L.): an investigation. *Journal of Genetics* **50**, 192–201.

GABREËLS-FESTEN AAWM, BOLHUIS PA, HOOGENDIJK JE, VALENTIJN LJ, ESHUIS EJHM, GABREËLS FJM (1995) Charcot-Marie-Tooth disease type 1A: morphological phenotype of the 17p duplication versus PMP22 point mutations. *Acta Neuropathologica* **90**, 645–649.

GABREËLS-FESTEN A, GABREËLS F (1993) Hereditary demyelinating motor and sensory neuropathy. *Brain Pathology* **3**, 135–146.

GRIFFITH LS, SCHMITZ B, SCHACHNER M (1992) L2/HNK-1 carbohydrate and protein-protein interactions mediate the homophilic binding of the neural adhesion molecule PO. *Journal of Neuroscience Research* **33**, 639–648.

GUZZETTA F, FERRIÈRE G, LYON G (1982) Congenital hypomyelination polyneuropathy. Pathological findings compared with polyneuropathies starting later in life. *Brain* **105**, 391–416.

HALL H, LIU L, SCHACHNER M, SCHMITZ B (1993) L2/HNK-1 carbohydrate mediates the adhesion of neural cells to laminin. *European Journal of Neuroscience* **5**, 34–42.

HANEY C, SNIPES GJ, SHOOTER EM, SUTER U, GARCIA CA, GRIFFIN JW et al. (1996) Ultrastructural distribution of PMP22 in Charcot-Marie-Tooth disease type 1A. *Journal of Neuropathology and Experimental Neurology* **55**, 290–299.

HENRY EW, COWEN JS, SIDMAN RL (1983) Comparison of Trembler and Trembler-J mouse phenotypes: varying severity of peripheral hypomyelination. *Journal of Neuropathology and Experimental Neurology* **42**, 688–706.

HYMAN FRIEDMAN HC, JELSMA TN, BRAY GM, AGUAYO AJ (1996) A distinct pattern of trophic factor expression in myelin-deficient nerves of Trembler mice: implications for trophic support by Schwann cells. *Journal of Neuroscience* **16**, 5344–5350.

KEILHAUER G, FAISSNER A, SCHACHNER M (1985) Differential inhibition of neurone-neurone, neurone-astrocyte and astrocyte-astrocyte adhesion by L1, L2, and N-CAM antibodies. *Nature* **316**, 728–730.

KUMAR NM, JARVIS LJ, TENBROEK E, LOUIS CF (1993) Cloning and expression of a major rat lens membrane protein MP20. *Experimental Eye Research* **56**, 35–43.

KUNEMUND V, JUNGALWALA F, FISSCHER G, CHOU DKH, KEILHAUER G, SCHACHNER M (1988) The L2/HNK-1 carbohydrate of neural cell adhesion molecules is involved in cell interactions. *Journal of Cell Biology* **106**, 213–223.

LOW PA (1976*a*) Hereditary hypertrophic neuropathy in the Trembler mouse. Part 1. Histopathological studies: light microscopy. *Journal of the Neurological Sciences* **30**, 327–341.

LOW PA (1976*b*) Hereditary hypertrophic neuropathy in the Trembler mouse. Part 2. Histopathological studies: electron microscopy. *Journal of the Neurological Sciences* **30**, 343–368.

LOW PA (1977) The evolution of 'onion bulbs' in the hereditary hypertrophic neuropathy of the Trembler mouse. *Neuropathology and Applied Neurobiology* **3**, 81–92.

LOW PA, MCLEOD JG (1975) Hereditary demyelinating neuropathy in the Trembler mouse. *Journal of the Neurological Sciences* **26**, 565–574.

MANFIOLETTI G, RUARO ME, DEL SAL G, PHILIPSON L, SCHNEIDER C (1990) A growth arrest-specific (gas) gene codes for a membrane protein. *Molecular and Cellular Biology* **10**, 2924–2930.

MARTINI R, SCHACHNER M (1986) Immunoelectron microscopic localisation of neural cell adhesion molecules (L1, N-CAM, and MAG) and their shared carbohydrate epitope and myelin basic protein in developing sciatic nerve. *Journal of Cell Biology* **103**, 2439–2448.

MARTINI R, SCHACHNER M, BRUSHART TM (1994) The L2/HNK-1 carbohydrate is preferentially expressed by previously motor axon-associated Schwann cells in reinnervated peripheral nerves. *Journal of Neuroscience* **14**, 7180–7191.

MARVIN KW, FUJIMOTO W, JETTEN AM (1995) Identification and characterisation of a novel squamous cell-associated gene related to PMP22. *Journal of Biological Chemistry* **270**, 28910–28916.

PERKINS CS, AGUAYO AJ, BRAY GM (1981) Schwann cell multiplication in Trembler mice. *Neuropathology and Applied Neurobiology* **7**, 115–126.

SIDMAN RL, COWEN JS, EICHER EM (1979) Inherited muscle and nerve diseases in mice: a tabulation with commentary. *Annals of the New York Academy of Sciences* **317**, 497–505.

SNIPES GJ, SUTER U, WELCHER AA, SHOOTER EM (1992) Characterization of a novel peripheral nervous system myelin protein (PMP-22/SR13). *Journal of Cell Biology* **117**, 225–238.

SNIPES GJ, SUTER U, SHOOTER EM (1993) Human peripheral myelin protein-22 carries the L2/HNK-1 carbohydrate adhesion epitope. *Journal of Neurochemistry* **61**, 1961–1964.

SPREYER P, KUHN G, HANEMANN CO, GILLEN C, SCHALAL H, KUHN R et al. (1991) Axon-regulated expression of a Schwann cell transcript that is homologous to a 'growth arrest-specific' gene. *EMBO Journal* **10**, 3661–3668.

SUTER U, MOSKOW JJ, WELCHER AA, SNIPES JG, KOSARAS B, SIDMAN RL et al. (1992*a*) A leucine to proline mutation in the putative first transmembrane domain of the 22-kDa peripheral myelin protein in the Trembler-J mouse. *Proceedings of the National Academy of Sciences of the USA* **89**, 4382–4386.

SUTER U, WELCHER AA, ÖZCELIK T, SNIPES GJ, KOSARAS B, FRANCKE U et al. (1992*b*) Trembler mouse carries a point mutation in a myelin gene. *Nature* **356**, 241–244.

SUTER U, SNIPES GJ, SCHOENER-SCOTT R, WELCHER AA, PAREEK S, LUPSKI JR et al. (1994) Regulation of tissue-specific expression of alternative peripheral myelin protein-22 (PMP22) gene transcripts by two promotors. *Journal of Biological Chemistry* **269**, 25795–25808.

TAYLOR V, WELCHER AA, AMGEN EST PROGRAM, SUTER U (1995) Epithelial membrane protein-1, peripheral myelin protein 22, and lens membrane protein 20 define a novel gene family. *Journal of Biological Chemistry* **270**, 28824–28833.

THOMAS PK, LASCELLES RG (1967) Hypertrophic neuropathy. *Quarterly Journal of Medicine* **36**, 223–238.

WELCHER A, SUTER U, DE LEON M, SNIPES GJ, SHOOTER EM (1991) A myelin protein is encoded by the homologue of a growth arrest-specific gene. *Proceedings of the National Academy of Sciences of the USA* **88**, 7195–7199.

ZOIDL G, BLASS-KAMPMANN S, D'URSO D, SCHMALENBACH C, MULLER HW (1995) Retroviral-mediated gene transfer of the peripheral myelin protein PMP22 in Schwann cells: modulation of cell growth. *EMBO Journal* **14**, 1122–1128.

Human Molecular Genetics, 1998, Vol. 7, No. 3 449–458

Correlation between varying levels of PMP22 expression and the degree of demyelination and reduction in nerve conduction velocity in transgenic mice

C. Huxley[1,*], E. Passage[2], A. M. Robertson[4], B. Youl[4], S. Huston[1], A. Manson[1], D. Sabéran-Djoniedi[2], D. Figarella-Branger[3], J. F. Pellissier[3], P. K. Thomas[4] and M. Fontés[2,*]

[1]Imperial College School of Medicine at St Mary's, London W2 1PG, UK, [2]INSERM U406, Faculté de Médecine de la Timone, BP 24, 13385 Marseille cedex 5, France, [3]Laboratoire de Pathologie Neuro-musculaire, Équipe DGRT N0866, Faculté de Médecine de la Timone, 13351 Marseille cedex 5, France and [4]Royal Free Hospital School of Medicine, London NW3 2PF, UK

Received October 1, 1997; Revised and Accepted December 12, 1997

Charcot-Marie-Tooth disease type 1A is most commonly caused by a duplication of a 1.5 Mb region of chromosome 17 which includes the peripheral myelin protein 22 gene (*PMP22*). Over-expression of this gene leads to a hypomyelinating/demyelinating neuropathy and to severely reduced nerve conduction velocity. Previous mouse and rat models have had relatively high levels of expression of the mouse or human *PMP22* gene leading to severe demyelination. Here we describe five lines of transgenic mice carrying increasing copies of the human *PMP22* gene (one to seven) and expressing increasing levels of the transgene. From histological and electrophysiological observations there appears to be a threshold below which expression of PMP22 has virtually no effect; below a ratio of human/mouse mRNA expression of ~0.8, little effect is observed. Between a ratio of 0.8 and 1.5, histological and nerve conduction velocity abnormalities are observed, but there are no behavioural signs of neuropathy. An expression ratio >1.5 leads to a severe neuropathy. A second observation concerns the histology of the different lines; the level of expression does not affect the type of demyelination, but influences the severity of involvement.

INTRODUCTION

The hereditary demyelinating neuropathies are a genetically complex group of disorders of which the commonest form is type 1A Charcot-Marie-Tooth disease (CMT1A) otherwise known as type Ia hereditary motor and sensory neuropathy (HMSN Ia). It is characterized by an onset in childhood and results in widespread demyelination and later axonal loss, associated with severely reduced nerve conduction velocity. It is caused by over-expression or point mutations in the gene for the peripheral myelin protein 22 (PMP22)[for a review, see (1)].

PMP22 is found in compact myelin in peripheral nerve where it makes up ~2–5% of the total myelin proteins (2). Thus PMP22 is not one of the major structural proteins of myelin, such as P0 which makes up ~50% of the myelin proteins, and its role in myelin is not known. It is also expressed in many other cells of the body, though at much lower levels than in Schwann cells, and was actually first identified as a gene which is switched on in growth-arrested fibroblasts. This has led to the suggestion that it has a role in Schwann cell differentiation and division. *In vitro*, over-expression of PMP22 in Schwann cells reduces cell growth and delays transition from G0/G1 to the S phase of the cell cycle (3), while in NIH-3T3 fibroblasts over-expression causes an apoptotic-like phenotype (4).

The commonest cause of CMT1A is over-expression of PMP22 usually due to a duplication of a 1.5 Mb region on chromosome 17p11.2, including the *PMP22* gene [for a review see (1)]. This usually occurs by unequal crossing over between two copies of a repeated sequence (5), most frequently during male meiosis (6) although it can also be of maternal origin (7). The repeated sequence has been determined to be 24 011 bp in length (8,9) and the hotspot of recombination within these repeats occurs near a region with very high homology to the Drosophila Mariner element (10). *De novo* duplication events have been found in nine out of 10 sporadic cases (11) indicating that it is a relatively common occurrence possibly stimulated by double-stranded breaks at the Mariner-like element. The patients with this over-expression have slowed nerve conduction velocity and a hypertrophic demyelination characterized by abnormally thick

*To whom correspondence should be addressed. M. Fontés: Tel: +33 91 78 44 77; Fax: +33 91 80 43 19; C. Huxley: Tel: +44 171 594 3771; Fax: +44 171 706 3272; Email: c.huxley@ic.ac.uk

myelin on intact nerve fibres, demyelination and remyelination, and numerous onion bulbs characteristic of cycles of demyelination and remyelination [for a review, see (12)].

Patients heterozygous for point mutations in the *PMP22* gene have been reported with slow nerve conduction and demyelination (13–18). Some of these mutations cause CMT1A with later onset and intermediate nerve conduction velocities (13,15) while others cause a more severe demyelination with earlier onset and very slow nerve conduction sometimes referred to as the Dejerine-Sottas syndrome (14,16–18). There are two mouse mutants which have dominantly acting point mutations in the *Pmp22* gene. Trembler (*Tr*) is a dominant mutation causing severe hypomyelination and continuing Schwann cell proliferation throughout life (19). Trembler-J (*Tr^J*) has a mutation which corresponds to one found in a human CMT1A family (13). It is semidominant with some gene dosage effect. Homozygotes are very severely affected with peripheral myelin deficiency and early death at postnatal day 17 or 18 (20).

DNA changes which cause null mutations in the *PMP22* gene, such as a 2 bp frameshifting deletion (21) or the complete deletions due to the reciprocal of the CMT duplication event (22,23), in the heterozygous condition give the human disease hereditary neuropathy with liability to pressure palsies (HNPP). This is characterized by a less severe reduction in nerve conduction velocity and by focal myelin thickenings termed tomacula. Clearly the point mutations in *PMP22* which cause prominent demyelination (see above), as opposed to the less severe demyelination with tomacula seen in HNPP, are not acting as haplo-insufficient null mutations but as dominantly acting mutations. Humans homozygous for null mutations have not been reported.

Three animal models with over-expression have been reported. A rat carrying about three copies of the mouse *Pmp22* gene on a cosmid has quite severe demyelination and slowed nerve conduction. The homozygote is more severely affected with virtually no myelin in the peripheral nervous system (24). Mice with seven copies of the human gene have a severe demyelination (25) while mice with 16 or more copies of the mouse gene have very severe demyelination (26). In this paper we report a series of transgenic mouse lines with different copy numbers of the *PMP22* gene with correlation to the levels of expression. We have related the level of expression in the different lines with the observed histology and electrophysiology.

RESULTS

Transgenic mice expressing different levels of human PMP22

The YAC 49G7 (27,25) contains the 40 kb human *PMP22* gene as well as ~300 kb of upstream and ~100 kb of downstream sequences (Fig. 1A). This YAC DNA was gel purified and used for pronuclear injection giving rise to six transgenic lines called C1, C2, C16, C22, C58 and C61. One of the lines, C22, showed a dominant phenotype of weakness and progressive paralysis of the hind legs which we have already described (25). Heterozygotes of the other lines do not show an abnormal phenotype.

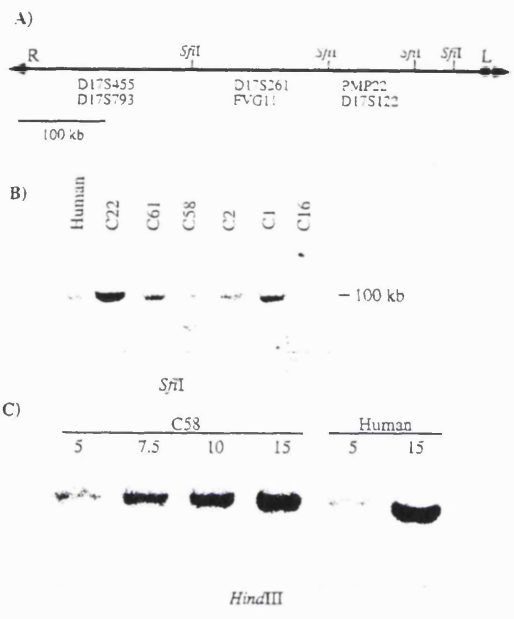

Figure 1. Analysis of the DNA in the transgenics. (**A**) Map of the YAC showing the *SfiI* sites and the approximate positions of various markers and the *PMP22* gene. (**B**) Intactness of the YAC transgene. Genomic DNA from human cells for each of the six transgenic lines as indicated above each lane was digested with *SfiI*, separated by pulsed field gel electrophoresis and hybridized with the human *PMP22* cDNA probe. (**C**) Determination of the copy number of the YAC transgenes; 5–15 μg of genomic DNA from human cells or from the C58 line (as indicated above the lanes) was cut with *Hin*dIII and hybridized with a human *PMP22* exon 2 probe.

However, C61 homozygotes have a clear weakness and paralysis similar to C22. Homozygotes of C1 and C58 homozygotes look normal but do not breed well while C2 and C16 homozygotes do not show an abnormal phenotype. C22 mice have never bred to give homozygotes for this line although four pairs have been together for 6 months. The mouse lines and phenotypes are summarized in Table 1.

The lines were analysed for six markers located in the YAC including the left and right arms of the YAC, the markers D17S122, FVG11 and D17S261 and the *PMP22* gene itself (Fig. 1A, Table 2). Only C22 and C61 contain all six markers. Intactness of the region around the transgene was further analysed by digestion with *SfiI* which gives an ~100 kb fragment spanning the *PMP22* gene in the YAC (Fig. 1A and B). All the lines except C16 showed the intact *SfiI* fragment indicating that they contain the intact gene and surrounding DNA. C16 only showed a smaller fragment indicating that the YAC is deleted and this line was not analysed further.

Table 1. Summary of mice

Mouse genotype	Copy no.	Ratio human/ mouse mRNA	MCV[a] (m/s)	Histology	Visible phenotype
Wild type	0	–	38	normal	none
C2 het	1	0.4	nd	normal	none
C2 hom	2	0.8	41	normal	none
C1 het	2	0.5	46	normal	none
C58 het	2	0.6	49	normal	none
C1 hom	4	1.3	26	mild demyelination	don't mate well
C58 hom	4	nd	21	mild demyelination	don't mate well
C61 het	4	1.0	25	mild demyelination	none
C22 het	7	1.6	4	demyelination	peripheral neuropathy
C61 hom	8	nd	4	demyelination	peripheral neuropathy
C22 hom	14	–	–	–	never produced

[a]Averages from Table 3.

Table 2. Transgene intactness

Line	Left arm	PMP22	D17S122	FVG11	D17S261	Right arm
C1	+	+	+	+	+	–
C2	+	+	+	+	–	+
C16	+	+	–	+	–	+
C22	+	+	+	+	+	+
C58	+	+	+	+	+	–
C61	+	+	+	+	+	+

The copy numbers of the YAC transgenes were determined by digestion with *Hin*dIII, followed by hybridization with the *PMP22* exon 2 probe. An example of this is shown for the line C58 which clearly has a copy number of two (Fig. 1C). The copy numbers in the lines are; one in C2, two in C1 and C58, four in C61 and seven in C22 (Table 1). Interestingly, the line with the highest copy number, C22 (seven copies), is the only one showing a dominant phenotype while C61 with four copies only shows the phenotype in the homozygous state (eight copies) (see Table 1).

The lines were also analysed by FISH and found to have different integrations of YAC DNA into a mouse chromosome as shown for C1, C2, C61 and C22 in Figure 2. The C1 integration is into chromosome 7, C2 into chromosome 1, C22 into chromosome 12, C58 into chromosome 15 and C61 into chromosome 10. Thus the lines have different integration sites and integration does not seem to occur preferentially in a particular region of the chromosomes such as centromeres, telomeres, heterochromatin or euchromatin.

Level of expression of the human *PMP22* transgenes

The level of expression of the human *PMP22* transgenes was determined relative to the level of mouse *Pmp22* mRNA in sciatic nerves of the mice. Two primers were used which amplify both the mouse and human cDNAs equally. The product was then cut with either *Taq*I, which cuts the human cDNA, or *Alu*I, which cuts the mouse cDNA, and the products quantified (25). RNA from a single mouse was analysed four times starting with different cDNA reactions and the average taken. One mouse was analysed for each genotype except C58 homozygote and C61 homozygote and the results are shown in Table 1.

The level of human transgene expression relative to the mouse mRNA is plotted against the transgene copy number in Figure 3A. The level of expression is roughly proportional to the copy number of the YAC transgene irrespective of the different positions of integration in the different lines. However, the expression of each transgene copy is only about half that of each mouse gene and the mice with four copies of the transgene have approximately the same amount of human as mouse mRNA.

Electrophysiology

Nerve conduction was examined under terminal anaesthesia. Conduction velocity was measured in the tibial division of the sciatic nerve, together with the distal motor and F wave latencies. The results are given in Tables 1 and 3 and Figures 3 and 4. Seven wild-type mice were found to have an average motor nerve conduction velocity (MCV) of 38.2 ± 6.3 m/s and an average distal motor latency (DML) of 0.82 ± 0.1 ms (Table 3, Fig. 4A).

Nine C22 heterozygotes were measured (Table 3, Fig. 4E). In three, no response to nerve stimulation could be recorded. The others had an average MCV of 3.7 ± 2.2 m/s which is very slow and an average DML of 4.3 ± 1.6 ms which is much greater than normal. The mice analysed ranged from 30 to 336 days of age but the MCVs and DMLs did not seem to correlate with age and the 30-day-old mouse had one of the slowest MCV recordings (Table 3). Similarly the three males did not appear to be different from the six females analysed (Table 3). In these animals with severely reduced motor conduction velocity, or in which no response to nerve stimulation could be obtained, denervation of the muscle was confirmed by the recording of spontaneous fibrillation potentials and myotonic runs on needle movement.

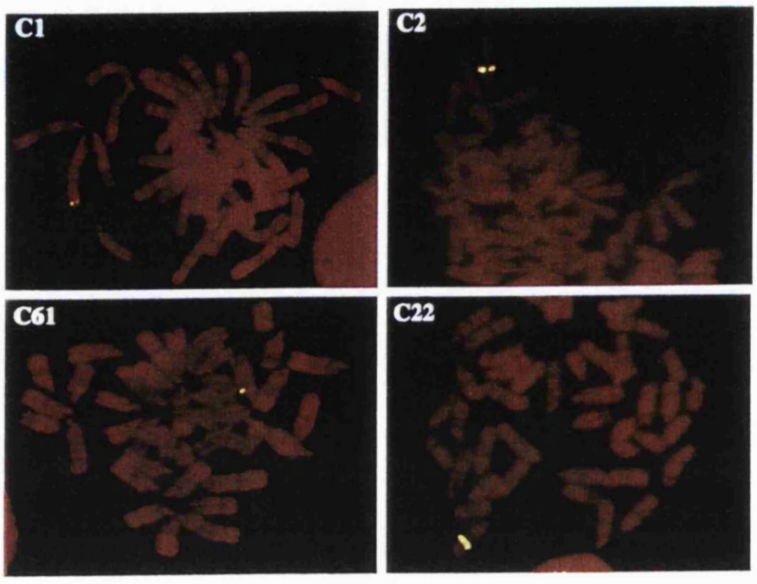

Figure 2. FISH analysis of the transgenic lines C1, C2, C61 and C22 showing the different integration sites.

Table 3. Motor nerve conduction velocity and distal motor latency

Genotype	Copy no.	Age (days)	Sex	Right MCV (m/s)	Left MCV (m/s)	Right DML (ms)	Left DML (ms)
Wild type	0	30	F	34.1	25.0	0.66	0.85
Wild type	0	83	F	35.9	38.2	0.80	0.95
Wild type	0	83	F	34.4	34.7	0.74	0.75
Wild type	0	140	F	40.0	39.0	0.73	0.90
Wild type	0	320	F	47.0	49.0	0.88	1.04
Wild type	0	52	M	37.3	–	0.77	–
Wild type	0	211	M	36.2	46.0	0.68	0.96
C22 het	7	30	F	NR	1.7	NR	5.6
C22 het	7	30	F	NR	NR	NR	NR
C22 het	7	83	F	1.4	3.4	5.02	3.36
C22 het	7	83	F	NR	NR	NR	NR
C22 het	7	118	F	7.3	7.0	2.81	3.56
C22 het	7	336	F	NR	NR	8.0	2.74
C22 het	7	52	M	3.0	2.6	4.40	4.50
C22 het	7	140	M	NR	NR	NR	NR
C22 het	7	211	M	3.4	NR	3.4	NR
C61 hom	8	299	F	5.1	3.4	1.57	1.74
C61 het	4	214	F	24.0	26.0	1.19	1.08
C1 hom	4	305	F	28.0	24.0	0.84	1.50
C1 het	2	233	F	45.0	47.0	0.73	1.00
C58 hom	4	305	M	21.0	21.0	1.21	1.74
C58 het	2	221	F	46.0	51.0	0.84	0.94
C2 hom	2	139	M	44.0	37.0	0.89	0.88

MCV, motor nerve conduction velocity.
DML, distal motor latency.
NR, no response to stimulation.

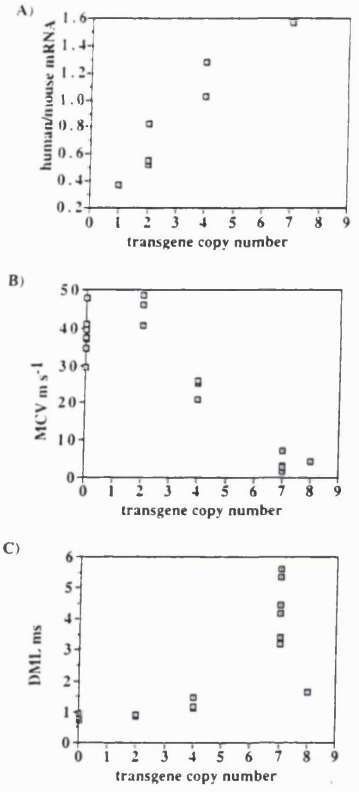

Figure 3. (**A**) Graph of the ratio of human:mouse *PMP22* mRNA against transgene copy number taken from Table 1. The points correspond to the following mice: one copy, a C2 heterozygote; two copies, a C1 heterozygote, a C2 homozygote and a C58 heterozygote; four copies, a C1 homozygote and a C61 heterozygote; and seven copies, a C22 heterozygote. (**B**) Graph of motor nerve conduction velocity (MCV in m/s) against transgene copy number taken from Table 3. Each point corresponds to one mouse for which the average of the left and right sides has been taken. Zero copies, seven wild-type mice; two copies, a C2 homozygote, a C1 heterozygote and a C58 heterozygote; four copies, a C1 homozygote, a C58 homozygote and a C61 heterozygote; seven copies, nine C22 heterozygous mice; eight copies, a C61 homozygote. (**C**) Graph of distal motor latency (DML in ms) against transgene copy number. Data are from the same mice as in (B) and are taken from Table 3.

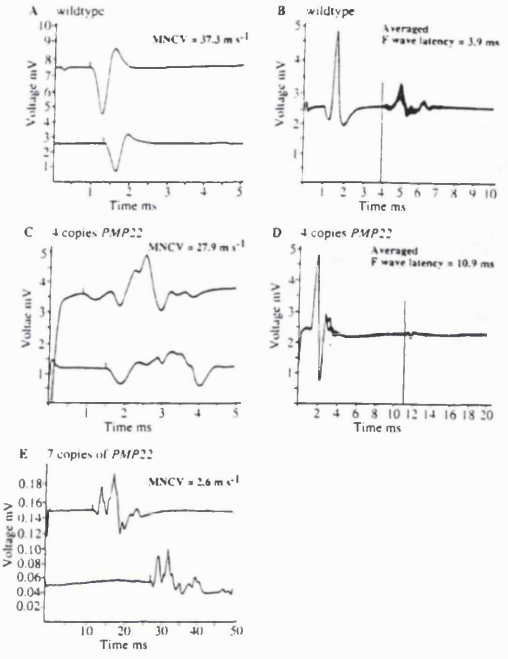

Figure 4. Traces of electrophysiological measurements. (**A**) Determination of motor nerve conduction velocity for a wild-type mouse. (**B**) Ten superimposed traces showing the F wave latency for a wild-type mouse. (**C**) Traces showing the motor nerve conduction velocity for a C1 homozygote mouse with four copies of the human transgene. (**D**) Ten superimposed traces showing the F wave latency for a C58 homozygote mouse with four copies of the human transgene. (**E**) Traces showing the MCV of a C22 mouse with seven copies of the human transgene. In each case, distal stimulation was at the ankle, proximal stimulation at the sciatic notch and recording was from the first interosseous space. In (A), (C) and (E) the vertical marks indicate the start of the evoked response. In (B) and (D) the vertical cursor indicates the start of the F wave.

For the other lines, a single mouse of each genotype was investigated and measurements were taken on both sides (Tables 1 and 3, Figs 3 and 4). A C2 homozygous mouse, a C1 heterozygote and a C58 heterozygote all had motor conduction velocities and distal motor latencies in the normal range (MCV > 35 m/s, DML < 1 ms). A C1 homozygote, a C58 homozygote and a C61 heterozygote all had intermediate values (MCV 20–30 m/s, DML 1–2 ms). Finally, a C61 homozygote had a MCV of 4.3 m/s which is as slow as the C22 mice. The DML for this mouse was 1.7 ms which is surprisingly low for the slow MCV and may be an artefact.

In the later experiments, F wave latency with ankle stimulation was also recorded. Mean F wave latency for five normal animals was 3.80 ms (Fig. 4B). For animals with moderately reduced motor conduction velocity it was 11.25 ms (mean for three animals)(Fig. 4D); responses were undetectable for the severely affected animals.

Histology

Comparison of sections of sciatic nerves from the same mice as used for the nerve conduction studies showed different degrees of severity of demyelination depending on the genotype. C22 heterozygous and C61 homozygous mice showed severe demyelination affecting most of the large axons (Fig. 5A). C1 homozygotes, C58 homozygotes and C61 heterozygotes all had intermediate degrees of demyelination (Fig. 5B), while C2 homozygotes, C1 heterozygotes and C58 heterozygotes showed only occasional demyelination of degenerating fibres (Fig. 5C).

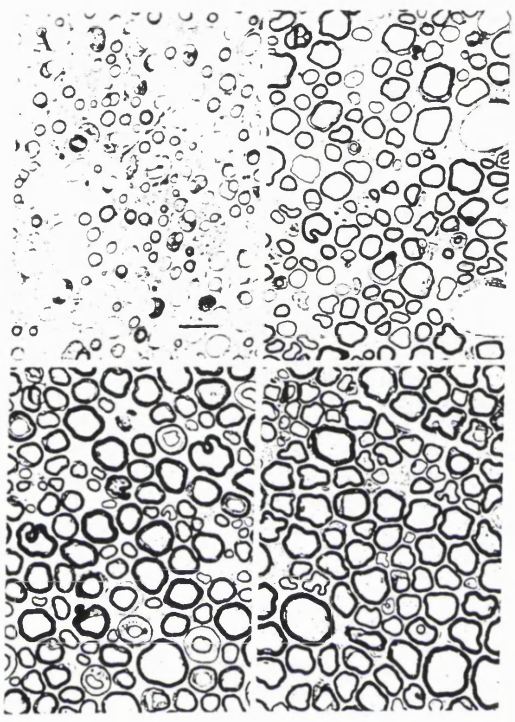

Figure 5. Transverse sections of the sciatic nerves of mice with different copy numbers of the human transgene. Scale bar = 10 μm, applies for all panels. (**A**) C22 heterozygote (seven copies). Nerves showed severe demyelination with most of the large axons being surrounded either by very few turns of myelin or none at all. (**B**) C61 heterozygote (four copies). Some thinly myelinated fibres are present. (**C**) C2 homozygote (two copies). Degenerating or demyelinated fibres were rare. (**D**) Control sciatic nerve.

Examination of a variety of nerves by light microscopy showed different levels of demyelination. When different fascicles of a nerve and plexus were considered, such as the median nerve and brachial plexus, they could have quite different levels of demyelination (Fig. 6A–D). In other nerve specimens, for instance the sciatic nerve, there were patches of demyelinated fibres and patches of myelinated fibres (Fig. 6E).

Electronmicroscopic examination of the nerves of mice of different genotypes showed that they all had a similar pattern of demyelination although different numbers of fibres were affected. Features included uncompacted myelin characteristically on the outsides of the myelin sheaths of medium sized axons (Fig. 7A), demyelination of large axons with reduplicated basal lamina (basal lamina onion bulbs)(Fig. 7B), completely demyelinated large axons (Fig. 7C), and macrophages indicating the occurrence of active demyelination (Fig. 7D).

DISCUSSION

In this paper we report the generation of transgenic mice carrying one, two, four, seven or eight copies of the human *PMP22* gene carried on a YAC, and their associated phenotypes. In lines with different integration sites but the same number of copies, the level of expression of human versus mouse mRNA is very similar indicating that the position of integration of the gene is not affecting the level of expression. The level of expression of human mRNA is also roughly proportional to the copy number of the transgene. Thus the expression appears to be position independent and copy number dependent as expected for a gene surrounded by a large region of genomic DNA. However, each transgene only gives about half as much expression as each single mouse gene which could be due to the transgenes being of human origin and thus not functioning completely efficiently in the mouse environment. The integrations at different loci also indicate that the observed phenotypes are not due to disruptions of genes on integration.

Exploration of the different lines, heterozygotes as well as homozygotes, has led to the following observations. In mice with one or two copies of the transgene, there was no detectable phenotype abnormality, the mice bred well, only minor histological abnormalities were present and motor nerve conduction was also normal. These mice expressed about half as much human as mouse messenger RNA which is equivalent to the mice having one extra copy of the *PMP22* gene. One might therefore expect to see a phenotype comparable with human CMT1A whereas in fact an abnormal phenotype is not detectable. Possibly, over-expression of the human gene is not affecting the mice to the same extent as over-expression of the human gene affects humans. Alternatively, clinical signs appear during the first and second decades of life in humans, mainly related to loss of axons. This aspect would make the comparison of relatively young mice with older humans inappropriate.

In mice with four copies of the gene there was slightly more human than mouse mRNA, equivalent in level of expression to two extra copies of the mouse gene. There is no overt weakness or paralysis, although they do not move as smoothly as wild-type and the C1 and C58 homozygotes did not mate well. However, there was considerable demyelination in the peripheral nerves of these mice. Also the motor nerve conduction velocities, distal motor latencies and F wave latencies were intermediate between the normal and the severely affected mice. The phenotype is roughly equivalent to early CMT1A in terms of slowed nerve conduction, the degree of demyelination and slight physical disability, but the hypermyelination (28) is not reproduced.

In mice with seven or eight copies there was ~1.5 times as much human as mouse mRNA. There is a severe phenotype of weakness and progressive paralysis of the rear legs as described previously for the C22 line (25). These mice also had severe demyelination of the peripheral nerves and very slow nerve conduction velocities and prolonged distal motor latencies.

One of the most striking features is the high degree of correlation between the number of YAC copies, the level of expression and the phenotypes in different lines. Two examples are particularly illustrative. C1 heterozygotes (two copies) have no abnormal phenotype. C1 homozygotes (four copies) have a mild demyelination and intermediate nerve conduction velocity. C61 heterozygotes (four copies) present the same mild demyelination and intermediate nerve conduction velocity as C1

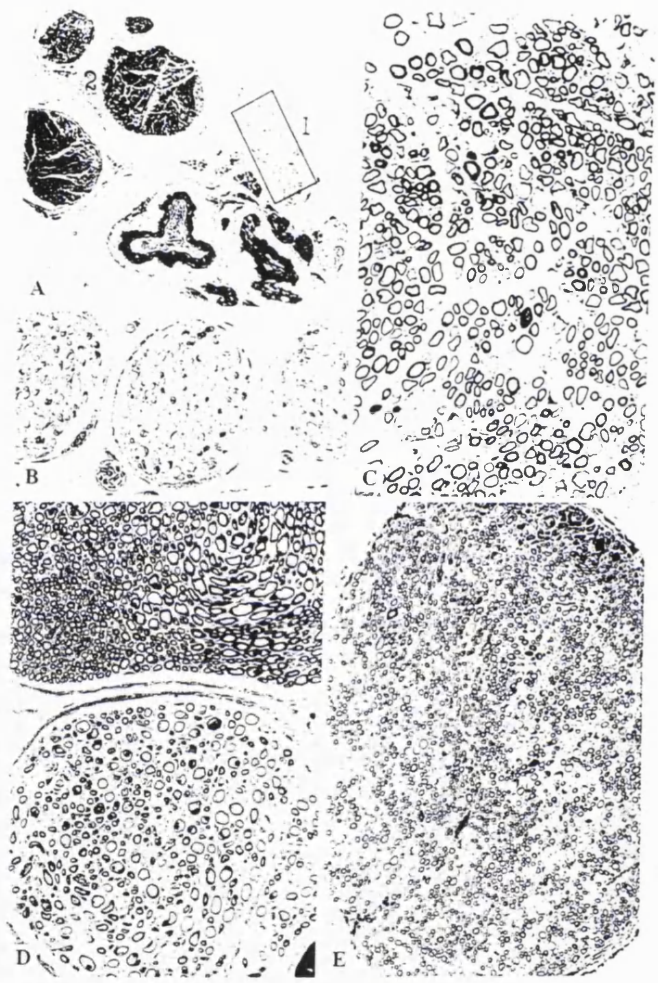

Figure 6. Light microscopy of various nerves from a C61 homozygote mouse. (**A**) Transverse semithin sections showing different fascicles with various levels of demyelination in the brachial plexus. (**B**) fascicles with demyelinated fibres corresponding to box 1, and (**C**) fascicle with intermingled demyelinated and hypomyelinated fibres corresponding to box 2. (**D**) Different degrees of demyelination in contiguous fascicles of the median nerve. (**E**) Patches of demyelinated and myelinated fibres in the sciatic nerve. PPD stain. (A) ×80, (B) ×270, (C) ×675, (D) ×270, (E) ×135.

homozygotes (same number of YAC copies and same level of transgene expression). However, these lines do not present any overt disability. Finally, C61 bred to homozygosity (eight copies) has a severe peripheral neuropathy similar to C22 heterozygotes (seven copies).

One question about our mice is whether the human transgene is acting in the same way that over-expression of the mouse gene would, or whether it is acting more like a point mutation in the *PMP22* gene due to differences between the mouse and human proteins. The published rat model with three copies of the mouse gene has a visibly abnormal phenotype and corresponds to a condition somewhat milder than our severe class (24). The nerve histology is quite different with the rats having extensive onion bulbs at 6 months of age while our mice have rare basal lamina onion bulbs. This could either be due to the fact that we have a mouse rather than a rat model or that we have over-expressed the human rather than the mouse gene. There is also a published mouse model with 16 or more copies of the mouse *Pmp22* gene which has almost no peripheral myelin (26). This is clearly more severe than our mice with seven or eight copies of the human gene which have an appreciable amount of myelin. Unfortunately, as the mice with the mouse *Pmp22* transgene are much more

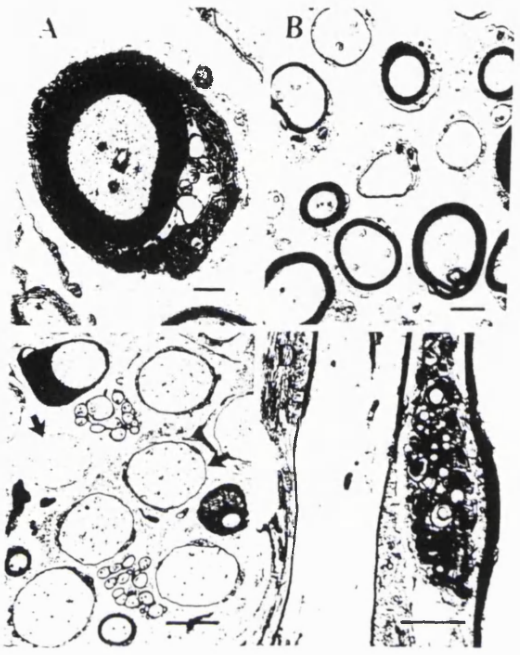

Figure 7. Electron micrographs from the sciatic nerve of a severely affected C61 homozygote mouse. (**A**) Uncompacted myelin characteristically on the outside of the myelin sheath of medium sized axons. Scale bar = 1 μm. (**B**) Hypomyelination of large axons with reduplicated basal lamina (centre). Scale bar = 2 μm. (**C**) Thin myelin or a complete lack of myelin around large axons which are often incompletely surrounded by Schwann cell cytoplasm (arrows). Scale bar = 2 μm. (**D**) Macrophage indicating active demyelination or fibre degeneration. Scale bar = 2 μm.

severely affected than our mice with the human transgene, a comparison of the histologies does not address the question of whether the mouse and human transgenes are acting by the same mechanism.

An important observation is that there appears to be a threshold level of expression under which there is almost no effect on the histology and nerve conduction velocity. Thus, mice expressing up to 0.8 times as much human as mouse mRNA are barely affected while as soon as the expression is >~1:1 the demyelination gets rapidly worse. CMT1A patients with a 17p11.2 duplication present with variable degrees of severity, including asymptomatic carriers. This has led authors to suggest the existence of modifier genes (29). However, a report about twins with variable degrees of expression of the disorder (30), makes the hypothesis of modifier genes, strongly affecting the phenotype, unlikely. From our data, we would suggest that the over-expression in humans is close to the threshold, and that variations in severity among patients could be due to individual variations in the expression of PMP22, which place the patient on one or other side of the threshold. As the relationship between over-expression and phenotypes seems not to be linear, small variations of expression of PMP22 can have a strong effect on the phenotype. If this holds true for humans, it suggests that a partial correction of the over-expression in patients could have a strong effect on the pathology, and that it will not be necessary to totally suppress the over-expression to benefit patients.

The other important points raised by our work concern the histology of the different lines. The histological findings indicate that over-expression of the *PMP22* gene does not prevent the association of Schwann cells with axons and initiation of myelination but that with increased expression of the gene the Schwann cells become incapable of maintaining myelination, in particular on larger axons. The variation in the degree of demyelination both within a nerve fascicle and between fascicles is of interest, perhaps suggesting differential vulnerability of different functional classes of nerve fibres. This requires further study. As the level of expression increases, the number of axons affected and the amount of demyelination increases but the process of demyelination (thin or absent myelin on the larger axons, decompaction of the outside of the myelin sheath and some basal lamina onion bulbs) remains the same. This indicates that it is the same mechanism acting in all the mice but with different severity.

The different lines we have constructed represent a unique tool to test different approaches to correct the phenotype. This is particularly true as the different lines have been bred now up to the eighth generation, without any variation in the expression of the transgene, or expression of the various phenotypes.

MATERIALS AND METHODS

Generation of transgenic mice

The intact YAC DNA was prepared as described previously (31,25). Transgenic mice were generated by pronuclear injection using standard techniques (32). Mice used for the generation of transgenics and for all subsequent crosses were C57BL/6J × CBA/Ca F1. Homozygotes were identified by crossing to wild-type mice.

DNA analysis and FISH

Mouse DNA was extracted from cultured fibroblasts using standard procedures both as low-molecular-weight DNA for analysis of copy number and as high-molecular-weight DNA in agarose blocks. Blocks were digested overnight with 20 U of *Sfi*I. Pulsed field gel electrophoresis was performed on a BioRad CHEF DRII with a pulse time of 10–45 s over 33 h at 160 V. Gels were blotted on PALL membranes in 10 × SSC overnight. The probe was labelled using random priming and stringent washes were performed at 0.1 × SSC at 65°C. The signal was imaged and quantitated with a phosphorimager. The *PMP22* exon 2 probe does cross-hybridize with the mouse gene but the sizes of the *Hin*dIII and *Sfi*I fragments differ between mouse and human DNA.

For FISH analysis, Alu-PCR products from the YAC 49G7 were synthesized and labelled as described elsewhere (33). One hundred ng of labelled probe was pre-annealed to 20-fold excess of Cot1 DNA for 20 min at 37°C and then precipitated in ethanol and centrifuged. The pellet was resuspended in 10 μl and hybridized to denatured chromosome spreads at 37°C overnight in 50% formamide. The probe sequences were detected with

avidin-FITC (Sigma). Slides were examined on a Zeiss Axiophot microscope equipped with a 3 CCD camera.

RNA analysis

Sciatic nerves were dissected from both legs of a mouse, snap frozen in liquid nitrogen and stored at –80°C for up to 3 weeks. Poly(A)$^+$ RNA was extracted using the Invitrogen Micro-Fast Track kit according to the manufacturer's instructions. cDNA synthesis was carried out using the Invitrogen cDNA cycle kit. In order to quantify the level of human transgene mRNA in relation to mouse mRNA, the cDNA was amplified using two primers: 5′-GTC TCC AC$^C/_G$ ATC GTC AGC CAA TG-3′ (starts at position 249 of accession D11428) and 5′-CTC ATC ACG CAC AGA CCA GCA AG-3′ (starts at position 523 of accession D11428) which are homologous to both the mouse and the human cDNAs and amplify across an intron. The 275 bp human product cuts with *Taq*I to give two fragments of 154 and 121 bp while the mouse product cuts with *Alu*I to give fragments of 198 and 77 bp. Amplification for 24–32 cycles of PCR was found to give the same ratio of human to mouse product, so 30 cycles was used for quantification. ^{33}P was incorporated during the PCR and the 2% agarose gel was dried and quantitated using a Phosphorimager (Molecular Dynamics, 'Imagequant' program).

Histology

The nerves were fixed either with 2.5% glutaraldehyde and postfixed in 1% osmium tetroxide (Fig. 7A and B) or in 1% paraformaldehyde/1% glutaraldehyde in 0.1 M PIPES [piperazine-*N*,*N*′-bis(2-ethanesulfonic acid)] buffer at pH 7.4 with postfixation in 1% osmium tetroxide in the same buffer plus 2% sucrose, 3% sodium iodate and 1.5% potassium ferricyanide (Figs 5 and 7C and D). The specimens were embedded in resin after dehydration through graded concentrations of ethanol. Semithin sections were stained with haematoxylin-phloxin-saffron and paraphenylene diamine (PDD) (Fig. 6). Ultrathin sections for electron microscopy were contrasted with lead citrate and methanolic uranyl acetate (Figs 5 and 7).

Electrophysiological recordings

Electromyographic measurements were carried out under terminal anaesthesia. Terminal anaesthesia was achieved by intraperitoneal injection of between 0.15 and 0.5 ml of a 1 in 10 dilution of Sagatal. The severely demyelinated mice (C22 line) were more sensitive to Sagatal: they became anaesthetized with less and occasionally died rapidly. Recordings were obtained via a fine concentric needle electrode inserted into the muscles of the first interosseous space of the hind foot employing a Medelec Saphire IL electromyograph. The sciatic nerve at the sciatic notch and the tibial nerve at the ankle were stimulated via fine stainless steel electrodes, the anode being inserted in the midline sacral region. Latency measurements were made by an electronic cursor on the oscilloscope screen. The tracings were also stored photographically. For the calculation of motor nerve conduction velocity between the proximal and distal recording sites, measurements of interelectrode distance were made on the skin with calipers with the leg in the fully extended position used for the recordings. In initial experiments, the accuracy of the surface measurement was verified by the injection of India ink through needles inserted at the sites of the stimulating electrodes. Throughout the recording the temperature of the limb was maintained at 38 ± 0.5°C using an electrically heated plate to which the animal was strapped by adhesive tape, and by a lamp above the animal.

ACKNOWLEDGEMENTS

We thank Dr Feuerstein for his help in mouse dissection and Gail Baker in genotyping. This work has been supported by AFM (Association Française contre les Myopathies) and the Wellcome, Leverhulme and Philip and Barbara Attenborough Trusts.

REFERENCES

1. Harding, A.E. (1995) From the syndrome of Charcot, Marie and Tooth to disorders of peripheral myelin proteins. *Brain*, **118**, 809–818.
2. Snipes, G.J. and Suter, U. (1995) Molecular anatomy and genetics of myelin proteins in the peripheral nervous system. *J. Anat.*, **186**, 483–494.
3. Zoidl, G., Blass-Kampmann, S., D'Urso, D., Schmalenbach, C. and Müller, H.W. (1995) Retroviral-mediated gene transfer of the peripheral myelin protein PMP22 in Schwann cells: modulation of cell growth. *EMBO J.*, **14**, 1122–1128.
4. Fabbretti, E., Edomi, P., Brancolini, C. and Schneider, C. (1995) Apoptotic phenotype induced by overexpression of wild-type gas3/PMP22: its relation to the demyelinating peripheral neuropathy CMT1A. *Genes Dev.*, **9**, 1846–1856.
5. Pentao, L., Wise, C.A., Chinault, A.C., Patel, P.I. and Lupski, J.R. (1992) Charcot-Marie-Tooth type 1A duplication apears to arise from recombination at repeat sequences flanking the 1.5 Mb monomer unit. *Nature Genet.*, **2**, 292–300.
6. Palau, F., Löfgren, A., De Jonghe, P., Bort, S., Nelis, E., Sevilla, T., Martin, J.-J., Vilchez, J., Prieto, F. and Van Broeckhoven, C. (1993) Origin of the de novo duplication in Charcot-Marie-Tooth disease type 1A: unequal nonsister chromatid exchange during spermatogenesis. *Hum. Mol. Genet.*, **2**, 2031–2035.
7. LeGuern, E., Gouider, R., Ravise, N., Lopes, J., Tardieu, S., Gugenheim, M., Abbas, N., Bouche, P., Agid, Y. and Brice, A. (1996) A de novo case of hereditary neuropathy with liability to pressure palsies (HNPP) of maternal origin: a new mechanism for deletion in 17p11.2? *Hum. Mol. Genet.*, **5**, 103–106.
8. Kiyosawa, H., Lensch, M.W. and Chance, P.F. (1995) Analysis of the CMT1A-REP repeat: mapping crossover breakpoints in CMT1A and HNPP. *Hum. Mol. Genet.*, **4**, 2327–2334.
9. Reiter, L.T., Murakami, T., Koeuth, T., Gibbs, R.A. and Lupski, J.R. (1997) The human COX10 gene is disrupted during homologous recombination between the 24 kb proximal and distal CMT1A-REPs. *Hum. Mol. Genet.*, **6**, 1595–1603.
10. Reiter, L.T., Murakami, T., Koeuth, T., Pentao, L., Muzny, D.M., Gibbs, R.A. and Lupski, J.R. (1996) A recombination hotspot responsible for two inherited peripheral neuropathies is located near a mariner transposon-like element. *Nature Genet.*, **12**, 288–296.
11. Hoogendijk, J.E., Hensels, G.W., Gabreëls-Festen, A.A.W.M., Gabreëls, F.J.M., Janssen, E.A.M., de Jonghe, P., Martin, J.-J., van Broeckhoven, C., Valentijn, L.J., Baas, F., de Visser, M. and Bolhuis, P.A. (1992) De-novo mutation in hereditary motor and sensory neuropathy type 1. *Lancet*, **339**, 1081–1082.
12. Thomas, P.K., King, R.H.M., Small, J.R. and Robertson, A.M. (1996) The pathology of Charcot-Marie-Tooth disease and related disorders. *Neuropathol. Appl. Neurobiol.*, **22**, 269–284.
13. Valentijn, L.J., Baas, F., Wolterman, R.A., Hoogendijk, J.E., van den Bosch, N.H.A., Zorn, I., Gabreëls-Festen, A.A.W.M., de Visser, M. and Bolhuis, P.A. (1992) Identical point mutations of PMP-22 in trembler-J mouse and Charcot-Marie-Tooth disease type 1A. *Nature Genet.*, **2**, 288–290.
14. Roa, B.B., Dyck, P.J., Marks, H.G., Chance, P.F. and Lupski, J.R. (1993) Dejerine-Sottas syndrome associated with point mutation in the peripheral myelin protein 22 (PMP22) gene. *Nature Genet.*, **5**, 269–273.
15. Roa, B.B., Garcia, C.A., Suter, U., Kulpa, D.A., Wise, C.A., Mueller, J., Welcher, A.A., Snipes, G.J., Shooter, E.M., Patel, P.I. and Lupski, J.R. (1993) Charcot-Marie-Tooth disease type 1A association with a spontaneous point mutation in the PMP22 gene. *N. Engl. J. Med.*, **329**, 96–101.
16. Ionasescu, V.V., Ionasescu, R., Searby, C. and Neuhring, R. (1995) Dejerine-Sottas disease with de novo dominant point mutation of PMP22 gene. *Neurology*, **45**, 1766–1767.

17. Valentijn, L.J., Ouvrier, R.A., van den Bosch, N.H., Bolhuis, P.A., Baas, F. and Nicholson, G.A. (1995) Dejerine-Sottas neuropathy is associated with a de novo PMP22 mutation. *Hum. Mutat.*, **5**, 76–80.
18. Tyson, J., Ellis, D., Fairbrother, U., King, R.H.M., Muntow, F., Jacobs, J., Malcolm, S., Harding, A.E. and Thomas, P.K. (1997) Hereditary demyelinating neuropathies of infancy. A genetically complex syndrome. *Brain*, **120**, 47–63.
19. Suter, U., Welcher, A.A., Ozcelik, T., Snipes, G.J., Kosaras, B., Francke, U., Billings-Gagliardi, S., Sidman, R.L. and Shooter, E.M. (1992) Trembler mouse carries a point mutation in a myelin gene. *Nature*, **356**, 241–244.
20. Suter, U., Moskow, J.J., Welcher, A.A., Snipes, G.J., Kosaras, B., Sidman, R.L., Buchberg, A.M. and Shooter, E.M. (1992) A leucine-to-proline mutation in the putative first transmembrane domain of the 22-kDa peripheral myelin protein in the trembler-J mouse. *Proc. Natl Acad. Sci. USA*, **89**, 4382–4386.
21. Nicholson, G.A., Valentijn, L.J., Cherryson, A.K., Kennerson, M.L., Bragg, T.L., DeKroon, R.M., Ross, D.A., Pollard, J.D., Mcleod, J.G., Bolhuis, P.A. and Baas, F. (1994) A frame shift mutation in the PMP22 gene in hereditary neuropathy with liability to pressure palsies. *Nature Genet.*, **6**, 263–266.
22. Chance, P.F., Alderson, M.K., Leppig, K.A., Lensch, M.W., Matsunami, N., Smith, B., Swanson, P.D., Odelberg, S.J., Disteche, C.M. and Bird, T.D. (1993) DNA deletion associated with hereditary neuropathy with liability to pressure palsies. *Cell*, **72**, 143–151.
23. Chance, P.F., Abbas, N., Lensch, M.W., Pentao, L., Roa, B.B., Patel, P.I. and Lupski, J.R. (1994) Two autosomal dominant neuropathies result from reciprocal DNA duplication/deletion of a region on chromosome 17. *Hum. Mol. Genet.*, **3**, 223–228.
24. Sereda, M., Griffiths, I., Pühlhofer, A., Stewart, H., Rossner, M.J., Zimmermann, F., Magyar, J.P., Schneider, A., Hund, E., Meinck, H.-M., Suter, U. and Nave, K.-A. (1996) A transgenic rat model of Charcot-Marie-Tooth Disease. *Neuron*, **16**, 1049–1060.
25. Huxley, C., Passage, E., Manson, A., Putzu, G., Figarella-Branger, D., Pellissier, J.F. and Fontés, M. (1996) Construction of a mouse model of Charcot-Marie-Tooth disease type 1A by pronuclear injection of human YAC DNA. *Hum. Mol. Genet.*, **5**, 563–569.
26. Magyar, J.P., Martini, R., Ruelicke, T., Aguzzi, A., Adlkofer, K., Dembic, Z., Zielasek, J., Toyka, K.V. and Suter, U. (1996) Impaired differentiation of Schwann cells in transgenic mice with increased PMP22 gene dosage. *J. Neurosci.*, **16**, 5351–5360.
27. Chevillard, C., Le Paslier, D., Passage, E., Ougen, P., Billault, A., Boyer, S., Mazan, S., Bachellerie, J.P., Vignal, A., Cohen, D. and Fontes, M. (1993) Relationship between Charcot-Marie-Tooth 1A and Smith-Magenis regions. snU3 may be a candidate gene for the Smith-Magenis syndrome. *Hum. Mol. Genet.*, **2**, 1235–1243.
28. Gabreels-Festen, A.A.W.M., Bolhuis, P.A., Hoogendijk, J.E., Valentijn, L.J., Eshuis, E.J.H.M. and Gabreels, F.J.M. (1995) Charcot-Marie-Tooth disease type 1A: morphological phenotype of the 17p duplication versus PMP22 point mutations. *Acta Neuropathol.*, **90**, 645–649.
29. Thomas, P.K., Marques Jr, W., Davis, M.B., Sweeney, M.G., King, R.H.M., Bradley, J.L., Muddle, J.R., Tyson, J., Malcolm, S. and Harding, A.E. (1997) The phenotypic manifestations of chromosome 17 duplication. *Brain*, **120**, 465–478.
30. Garcia, C.A., Malamut, R.E., England, J.D., Parry, G.S., Liu, P. and Lupski, J.R. (1995) Clinical variability in two pairs of identical twins with the Charcot-Marie-Tooth disease type 1A duplication. *Neurology*, **45**, 2090–2093.
31. Gnirke, A., Huxley, C., Peterson, K. and Olson, M.V. (1993) Microinjection of intact 200- to 500-kb fragments of YAC DNA into mammalian cells. *Genomics*, **15**, 659–667.
32. Hogan, B., Costantini, F. and Lacy, E. (1986) *Manipulating the Mouse Embryo*. Cold Spring Harbor Laboratory Press, Cold Spring Harbor, NY.
33. Lengauer, C., Green, E.D. and Cremer, T. (1992) Fluorescence in situ hybridization of YAC clones after Alu-PCR amplification. *Genomics*, **13**, 826–828.

Development of early postnatal peripheral nerve abnormalities in Trembler-J and PMP22 transgenic mice

A. M. ROBERTSON[1], C. HUXLEY[2], R. H. M. KING[2] AND P. K. THOMAS[1]

[1] Royal Free and University College Medical School and [2] Imperial College School of Medicine, London, UK

(Accepted 20 April 1998)

ABSTRACT

Mutations in the gene for peripheral myelin protein 22 (*PMP22*) are associated with peripheral neuropathy in mice and humans. Although PMP22 is strongly expressed in peripheral nerves and is localised largely to the myelin sheath, a dual role has been suggested as 2 differentially expressed promoters have been found. In this study we compared the initial stages of postnatal development in transgenic mouse models which have, in addition to the murine *pmp22* gene, 7 (C22) and 4 (C61) copies of the human *PMP22* gene and homozygous and heterozygous Trembler-J (Tr^J) mice, which have a point mutation in the *pmp22* gene. The number of axons that were singly ensheathed by Schwann cells was the same in all groups indicating that PMP22 does not function in the initial ensheathment and separation of axons. At both P4 and P12 all mutants had an increased proportion of fibres that were incompletely surrounded by Schwann cell cytoplasm indicating that this step is disrupted in PMP22 mutants. C22 and homozygous Tr^J animals could be distinguished by differences in the Schwann cell morphology at the initiation of myelination. In homozygous Tr^J animals the Schwann cell cytoplasm had failed to make a full turn around the axon whereas in the C22 strain most fibres had formed a mesaxon. It is concluded that PMP22 functions in the initiation of myelination and most likely involves the ensheathment of the axon by the Schwann cell, and the extension of this cell along the axon. Abnormalities may result from a failure of differentiation but more probably from defective interactions between the axon and the Schwann cell.

Key words: Myelination; Schwann cells; Charcot-Marie-Tooth disease; hereditary motor and sensory neuropathy.

INTRODUCTION

Mutations in the gene for peripheral myelin protein 22 (PMP22) are associated with peripheral neuropathy in mice and humans (Lupski et al. 1991; Raeymaekers et al. 1991; Suter et al. 1992*a*). PMP22 is a 22 kDa glycoprotein which is localised mainly in the myelin sheath of peripheral nerve, although it is also found in plasma membranes of the Schwann cells that surround the axons of unmyelinated fibres (Snipes et al. 1992; Haney et al. 1996). Representing less than 5% of total myelin protein, PMP22 is unlikely to play a structural role in myelin but its function is not yet clear.

A dual role for PMP22 has been suggested on the basis that 2 differentially expressed tissue specific PMP22 promoters have been found. Promoter 1 is preferentially expressed in myelinating Schwann cells and promoter 2 in tissues that do not form myelin (Bosse et al. 1994; Suter et al. 1994). PMP22 is a member of a small family of proteins most of which are expressed in epithelial cells (CL20, EMP-1, EMP-2, EMP-3, MP20) (Kumar et al. 1993; Marvin et al. 1995; Taylor et al. 1995; Bolin et al. 1997). Observations on epithelial cell lines suggest that these proteins are involved in cell–cell interactions, including roles both in the switch from proliferation to differentiation and in the maintenance of the differentiated state (Taylor et al. 1995). EMP-3 (HNMP-1), which has the highest amino acid homology to PMP22 (44%), is transiently expressed by Schwann cells during sciatic nerve myelination. The EMP-3 protein itself is axon associated and is thought to play a role

Correspondence to Dr A. M. Robertson, Clinical Neurosciences, Royal Free and University College Medical School, Royal Free Campus, Rowland Hill Street, London NW3 2PF, UK.
Tel.: +44 171 830 2408; fax: +44 171 431 1577.

in axon-Schwann cell interactions (Bolin et al. 1997). It has been speculated that promoter 1 for *PMP22* has been acquired specifically during evolution to allow high level expression in myelinating Schwann cells. This additional function is likely to coexist alongside the retained original function (Naef & Suter 1998).

PMP22 mutations are associated with 3 different disease phenotypes in humans. The most common human disorder involving PMP22, Charcot-Marie-Tooth disease 1A (CMT1A) or hereditary motor and sensory neuropathy 1a (HMSN1a), is associated with a 1.5 Mb duplication on chromosome 17p11.2–12, leading to the presence of an extra copy of the *PMP22* gene (Lupski et al. 1991; Raeymaekers et al. 1991). This duplication produces a peripheral neuropathy which generally presents in the first decade of life and typically results in distally accentuated muscle wasting and weakness. Histologically it is characterised by hypermyelination (Gabreëls-Festen et al. 1995) followed by demyelination and myelinated nerve fibre loss, and the development of onion bulbs (indicative of repeated cycles of demyelination and remyelination). In older patients hypermyelination is succeeded by hypomyelination (Thomas et al. 1997). A deletion of this same 17p11.2–12 region causes hereditary neuropathy with liability to pressure palsies (HNPP) (Chance et al. 1993; Tyson et al. 1996). The most characteristic pathological feature of HNPP is the presence of tomacula (sausage-shaped enlargements in the myelin sheath) (Madrid & Bradley 1975). The reciprocal disorders HNPP and CMT1A are thought to be the result of unequal crossing over at meiosis. Point mutations in the *PMP22* gene are also associated with a Charcot-Marie-Tooth like phenotype but with a hypomyelinating/demyelinating neuropathy (Gabreëls-Festen et al. 1995) or with a more severe childhood onset neuropathy, Dejerine-Sottas disease (DSD). As most CMT1A patients have 3 copies of the *PMP22* gene and HNPP patients have only 1, a gene dosage effect has been proposed as a mechanism for both diseases (Schenone et al. 1997). This is supported by observations which have shown that PMP22 protein expression is increased in CMT1A patients and reduced in HNPP patients as compared with patients with normal *PMP22* gene copy number (Vallat et al. 1996; Gabriel et al 1997).

Mutations in the mouse *pmp22* gene are responsible for the peripheral nerve abnormalites in the Trembler murine mutants *Tr*, *Tr*^{J} and *Tr-Ncnp* (Suh et al. 1997; Suter et al. 1992*a*, *b*). A Dutch kindred has the same Leu16Pro mutation as is found in the *Tr*^{J} mouse (Valentijn et al. 1992). Pathologically the human phenotype is more severe than the murine, with the human mutation resulting in a DSD phenotype and a reduction in myelinated fibre density of 80% (Gabreëls-Festen et al. 1995). In the *Tr*^{J} mouse the reduction in the proportion of myelinated fibres is a more modest 20% (Robertson et al. 1997).

We have recently reported the generation of transgenic mice carrying increasing copy numbers of the human *PMP22* gene and expressing increasing levels of the transgene (Huxley et al. 1996, 1998). Increased expression of PMP22 does not result in a steady worsening of phenotype but instead there appears to be a threshold level of PMP22 expression. Below a level which equates to 2 additional copies of *PMP22* there was no detectable effect. At around 4 additional copies of *PMP22* a degree of hypomyelination was found in older mice with some electrophysiological deficit but no behavioural signs. Above 7 additional copies of *PMP22* the mice had a severe dysmyelinating neuropathy affecting more than 40% of fibres in adult mice. These mice had a severe phenotype with a progressive paralysis of the rear legs, resulting in abnormal gait with splaying of the hindlimbs. Although different numbers of fibres were affected in the mildly and severely affected groups, the type of lesion was similar. Both showed demyelination of large axons and uncompacted myelin, usually on the outer aspects of the myelin sheath.

In this study we have compared the initial stages of postnatal development of the sciatic nerves of transgenic mice with 7 (C22) and 4 (C61) copies of the human *PMP22* gene with both homozygous and heterozygous Trembler-J mice (*Tr*^{J}), which have a point mutation in the *pmp22* gene.

MATERIALS AND METHODS

Tr^{J} animals were originally obtained from the Jackson Laboratories, Bar Harbor, Maine, USA, and are now maintained in a colony at the Royal Free and University College Medical School, London. Transgenic animals were generated by pronuclear injection of YAC 49G7 DNA, which contains the 40 kb human *PMP22* gene. The determination of copy numbers and the level of expression of the human *PMP22* transgenes have previously been described (Huxley et al. 1998). The animals are maintained at Imperial College School of Medicine, London. Transgenic line C22 is now designated TgN (PMP22) C22C1h and line C61 is designated TgN (PMP22) C61C1h following the international guidelines for naming transgenics.

Animals were killed by cervical dislocation, the sciatic nerve was fixed in situ for 20 min (1%

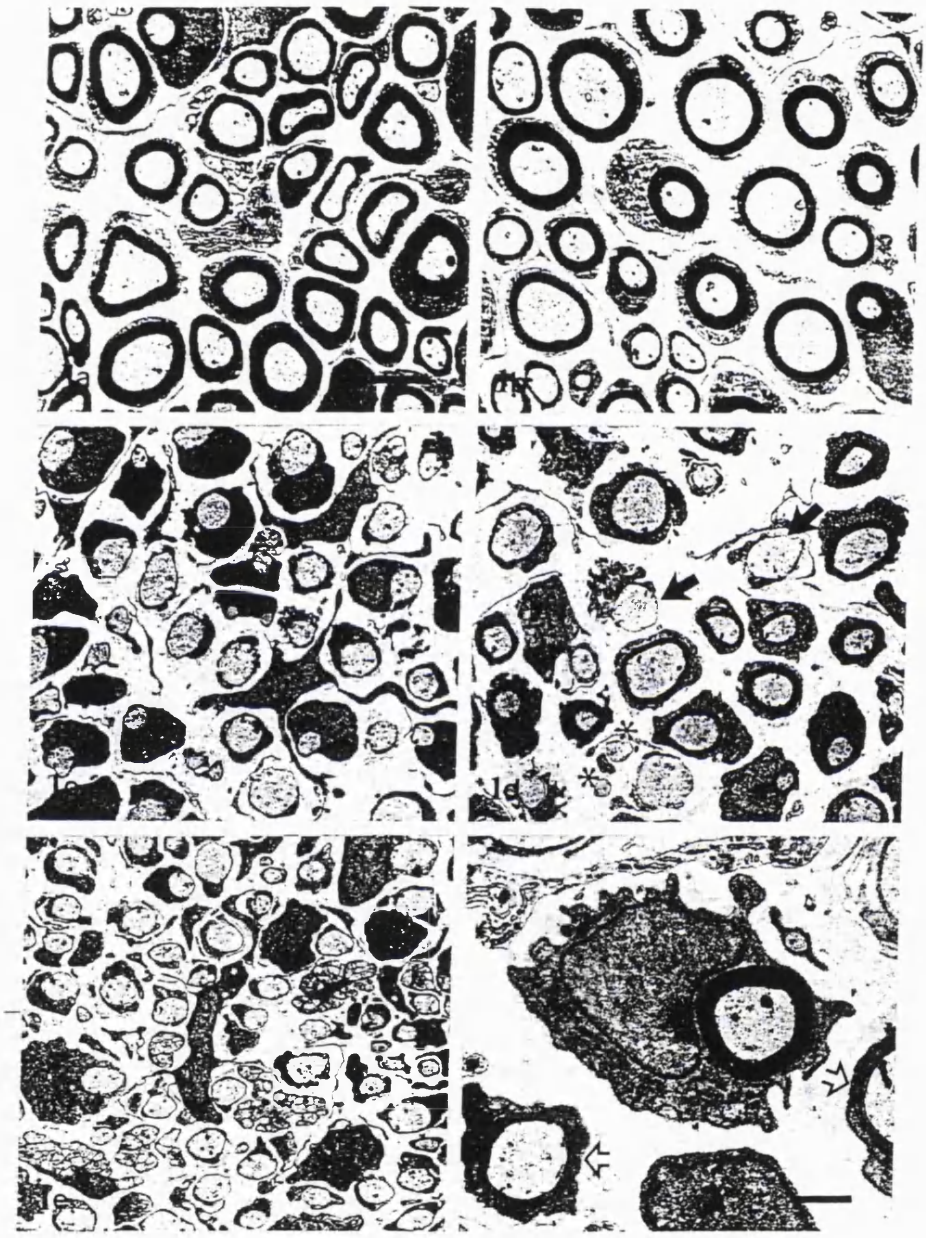

Fig. 1. Electron micrographs of the sciatic nerve of P10–12 animals. (*a*) Control; bar (and for *b–e*), 2·5 μm. (*b*) 4 copies of *PMP22* (C61); (*c*) 7 copies of *PMP22* (C22); (*d*) *Tr*^{J} heterozygote. Incompletely surrounded axons (arrow). Naked axons (asterisk). (*e*) *Tr*^{J} homozygote. (*f*) *Tr*^{J} heterozygote. Schwann cell cytoplasm with an irregular outline. Such irregular outlines as were commonly seen in heterozygotes and permitted them to be distinguished from C61 and control animals as early as P4. Uncompacted myelin (open arrrow). Bar, 1 μm.

paraformaldehyde, 1% glutaraldehyde in 0·1 M PIPES buffer) and then removed and placed in fresh fixative overnight. Samples were processed for electron microscopy as previously described (Robertson et al. 1997). Sections examined were taken from the midthigh level of the sciatic nerve.

Table 1. *Total number of singly ensheathed fibres*

	Control	4 copies (C61)	7 copies (C22)	Tr^J het	Tr^J hom
P4	643 ± 20	629 ± 62	657 ± 25	538 ± 98	761 ± 68

Mean ± S.E.M. (n = 6)

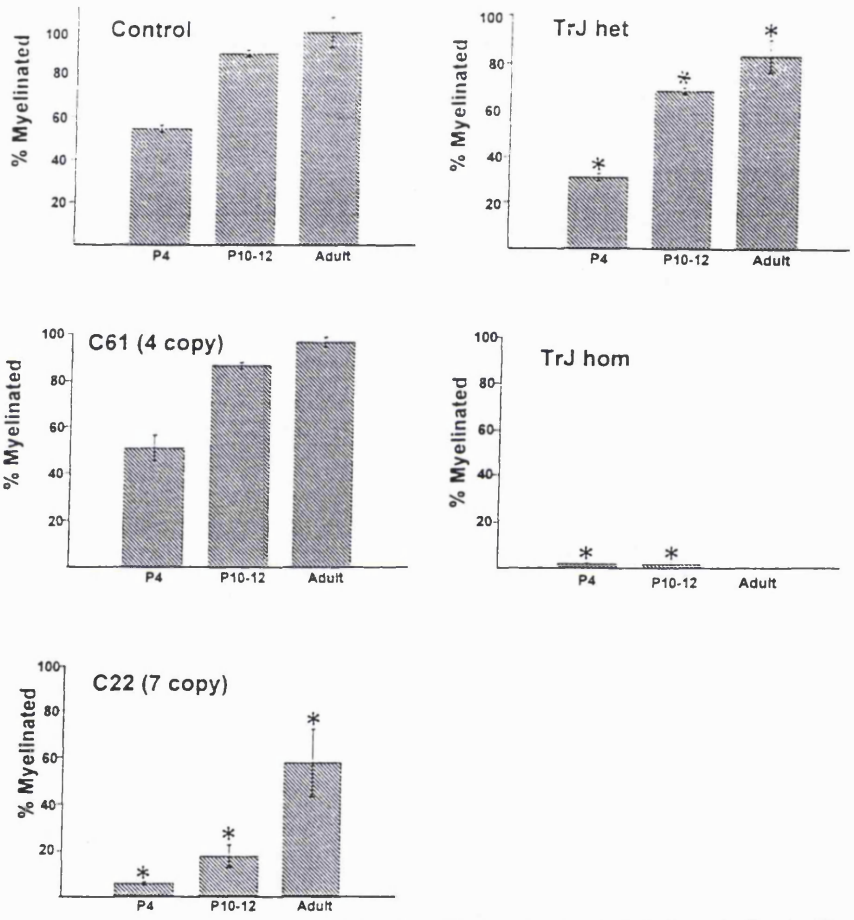

Fig. 2. Percentage of singly ensheathed fibres that were myelinated at the different ages examined. *Indicates significantly different from control at the same age.

In young animals at postnatal day 4 (P4) and P10–12, fibres were counted at a magnification of ×7000 using a Zeiss 902C electron microscope. Counts were taken from nonoverlapping fields; a total area of 0.63 mm² was analysed. Promyelin fibres were defined as those which had separated from axon bundles and were associated with a single Schwann cell. In adult animals the counts were performed on a Zeiss Axiophot microscope; an entire fascicle was counted. All statistics were calculated using the Mann-Whitney U test at a significance level of 5%.

RESULTS

On examination of semithin sections at P4 and P12, affected C22 (7 copies of *PMP22*) (Fig. 1*c*) and homozygous Tr^J animals (Fig. 1*e*) were easily

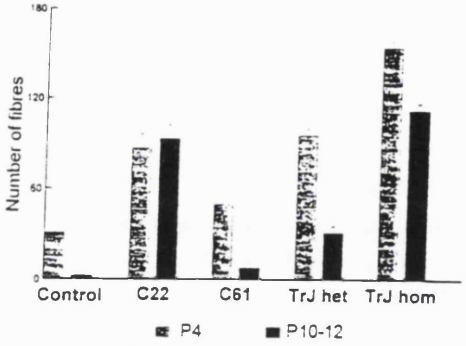

Fig. 3. Number of fibres incompletely surrounded by Schwann cell cytoplasm.

recognised as they had markedly decreased numbers of myelinated fibres. In heterozygous *Tr'* animals (Fig. 1*d*), the decrease in myelinated fibres was more difficult to judge visually, particularly at P4, but they also could be distinguished from controls and C61 animals by the presence of many fibres with irregular contours of Schwann cell cytoplasm (Fig. 1*f*). The C61 strain (Fig. 1*b*) could not be distinguished morphologically from controls either at P4 or P12 although by 6 wk a small subgroup of the larger myelinated fibres had become hypomyelinated. See (Huxley et al. 1998).

In *Tr'* mice and in both transgenic strains the process of axon separation from fetal bundles into a 1:1 relationship with individual Schwann cells appeared to proceed normally. At P4 there was no difference in the total number of singly ensheathed fibres in the different strains (Table 1). No abnormality was noted in unmyelinated fibre bundles.

The number of myelinated fibres was decreased at all ages in C22 (7 copies) and both heterozygous and homozygous *Tr'* animals, while C61 (4 copies) were not significantly different from the controls (Fig. 2). Homozygous *Tr'* animals were the most severely affected with less than 2% of the singly ensheathed axons being myelinated and these animals developed very little myelin before their death around weaning at P21 (Fig. 2). The proportion of myelinated fibres increased with age in control, C61 (4 copies), heterozygous *Tr'* and to a lesser extent C22 animals. However, C22 (7 copies) mice remained very poorly myelinated, with fewer than 60% of axons being myelinated in adult animals.

Both at P4 and P12, heterozygous and homozygous *Tr'* and the 2 transgenic strains had an increased number of fibres that were incompletely surrounded by Schwann cell cytoplasm. In C22 animals this number did not alter during development but in all the other strains the number decreased with age (Fig. 3). It is interesting to note that the only feature in which C61 mice differed from control animals at these ages is the inability of the Schwann cell to surround a fibre completely.

An increased number of Schwann cells is a feature of most neuropathies and this was also found in the mouse models (Table 2). At P4 the C22 (7 copies) mutants already had a significantly higher number of Schwann cells per 100 axons than controls. By P12 *Tr'* heterozygotes and *Tr'* homozygotes also had significantly increased numbers of Schwann cells. Between P4 and P12 the number of Schwann cells per 100 axons decreased in control and the mildly affected C61 strains as myelination progressed. In the more severe mutants the number of Schwann cells increased significantly (Table 2). When comparing early postnatal (P12) and adult values the number of Schwann cells decreased by half in control and C61 in which almost all the singly ensheathed fibres were myelinated. Schwann cells decreased to a much lesser extent in the poorly myelinated C22 animals and in *Tr'* heterozygote nerves the number of Schwann cells did not alter from early postnatal values.

The 2 most affected strains (*Tr'*/*Tr'* and C22) could be distinguished morphologically from each other by P10–12. Schwann cell cytoplasm in the promyelin fibres of *Tr'*/*Tr'* animals failed to complete

Table 2. Number of Schwann cell nuclei per 100 axons

	Strain				
	Control	4 copies (C61)	7 copies (C22)	*Tr'* het	*Tr'* hom
P4	10.5 ± 0.5	10.7 ± 1.1	13.3 ± 0.6†	12.0 ± 0.6	11.6 ± 0.5
P12	7.4 ± 0.5*	8.2 ± 0.4*	19.5 ± 1.8*†	15.7 ± 0.6*†	13.3 ± 0.5*
Adult	4.4 ± 0.4ψ	5.4 ± 0.5ψ	12.3 ± 0.9ψ†	13.9 ± 0.8†	

Mean ± S.E.M.. (n = 6) *Significantly different from P4 , ψSignificantly different from P12.
† Significantly different from control at the same age.

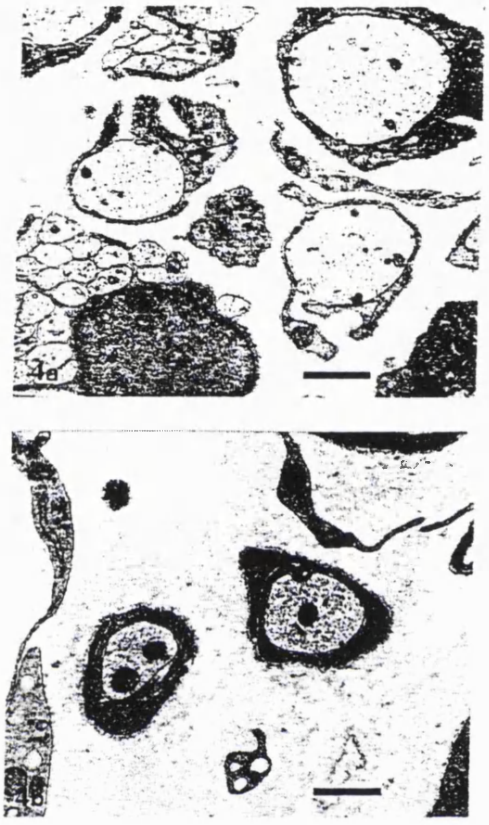

Fig. 4. (*a*) Fibres from a *Tr*^{J} homozygote animal in which the Schwann cell cytoplasm fails to complete a full turn around the axon.P10–12. (*b*) Fibres from a 7 copy (C22) animal in which the Schwann cell cytoplasm has completed a full turn around the axon.P10–12 Bar, 1 μm.

a full turn around the axon (Fig. 4*a*), whereas in C22 animals many had progressed so that a short mesaxon had been formed (Fig. 4*b*).

DISCUSSION

This study shows that the axons initially separate normally into a 1:1 relationship with individual Schwann cells both in mice which overexpress the *PMP22* gene and in those with a point mutation in the *pmp*22 gene. In all the mutants analysed there is a high proportion of fibres that are incompletely surrounded by Schwann cell cytoplasm. This suggests that the first abnormality and, by implication, the first function of PMP22 predates myelin formation and involves the attachment and extension of the Schwann cell around the axon. This is related specifically to axons that are destined to myelinate and is not a general feature of mutant Schwann cells. There was no evidence of abnormalities in the relationship of unmyelinated axons and Schwann cells.

A similar scenario of delayed myelination, following the establishment of normal 1:1 ratios of Schwann cells to axons, has been observed in 10 d old mice which overexpress the mouse pmp22 protein (Magyar et al. 1996) and in 5 wk rats overexpressing the mouse pmp22 protein (Serada et al 1996). Similarly, in 4 d mice lacking all pmp22 expression, the nonmyelinated axons were associated with prospective myelinating Schwann cells in a 1:1 ratio, but only 19%, in comparison to 60% in wild type rats, of the larger calibre axons were ensheathed by compact myelin. This is in contrast to in vitro data from neurons cocultured with Schwann cells which had been genetically modified with retroviruses to over or under-express PMP22 (D'Urso et al. 1997). Here, over and under expression of PMP22 was found to have virtually no effect on the early stages of myelination and membrane compaction. In view of the consistent observations in all mouse and rat models with over and under expression of *pmp*22 and expression of mutant *pmp*22, it seems that *pmp22* has an important role in the initiation of myelination in vivo after the association of Schwann cells with axons.

In addition the 2 most severely affected strains (C22 transgenic and *Tr*^{J} homozygotes) could be distinguished from each other by differences in the initial ensheathment of axons. In homozygous *Tr*^{J} animals the 2 apposing edges of Schwann cell cytoplasm failed to overlap but in the C22 strain there was usually a small overlap of Schwann cell membranes and initial mesaxon formation. This suggests that PMP22 is involved either in mesaxon formation, i.e. the contact between the apposing edges of the Schwann cell surrounding the axon, or in the guidance/recognition processes involved in the spiralling of Schwann cell membranes to form the myelin sheath.

Two features of this early developmental morphology can be produced by interrupting Schwann cell differentiation with the thymidine analogue, 5-bromodeoxyuridine (BrdU). Following treatment of demyelinated nerve with BrdU, Hall & Gregson (1977) reported an increased number of promyelinated fibres with cytoplasm that was irregular in outline. These are morphologically very similar to the irregular fibres characteristic of *Tr*^{J} heterozygote animals. Additionally many cells possessed pseudopodial processes, a feature also commonly found in both heterozygous and homozygous *Tr*^{J} nerves.

These results raise 2 possible interpretations, firstly that the mutant phenotype results from a failure of the differentiation process or secondly that it results from disrupted Schwann cell/ Schwann cell or Schwann cell/axon interactions. If the Schwann cells fail to differentiate fully into their myelinating phenotype, they are unlikely to be capable of responding appropriately to axonal signals to myelinate. During the differentiation process Schwann cells cease proliferation and grow both longitudinally (internode length) and radially (myelin sheath thickness). An inability of mutant Schwann cells to surround axons and subsequently to produce a spiral ensheathment around them to form myelin may be seen as a manifestation of failed differentiation. Alternatively, if PMP22 functions in mediating the interaction between cell types, it is possible that differentiation failure itself is secondary to defective cell interactions. In a previous study we proposed that adult *Tr*^{J} animals exhibited abnormalities that were consistent either with defective Schwann cell/axon or Schwann cell/extracellular matrix interactions (Robertson et al. 1997). Axonal contact is known to be a prerequisite for the initiation of myelination. If the Schwann cell only partially surrounds the axon, the signal may be insufficient to produce differentiation and myelination. Similarly, Schwann cells in culture only cease to divide and commence myelin formation when they are in contact with the extracellular matrix (De Vries. 1993). In this study the only feature that distinguished the C61 (4 copy) strain from controls was the increased number of fibres that were not surrounded by Schwann cell cytoplasm. This leads us to conclude that the axon/Schwann cell interaction is more likely to be the site of abnormality than Schwann cell/extracellular matrix interaction. In either of these 2 scenarios the lack of myelination in these PMP22 related disorders can be seen as a secondary feature. This is largely overcome with time in most of the models, shown by improvement in the degree of myelination from P10–12 to adult.

Comparative observations on the severity of associated axonal loss will be of interest in the C61 strain, which is relatively unaffected during the early stages of development. A small proportion of larger fibres (7%) become hypomyelinated in adult mice suggesting that a moderate overexpression of PMP22 leads to myelin instability later in life (data not shown).

The early growth response 2 gene (EGR2), also known as Krox-20, may be involved in the regulation of cell proliferation. It is part of a multigene family encoding Cys2-His2 type zinc finger proteins (Joseph et al. 1988; Ragnnekar et al. 1990). It is expressed in Schwann cells before the onset of myelination (Topilko et al. 1994) and *egr2* knock-out mice exhibit a failure of myelination in the peripheral nerves. The Schwann cells wrap their cytoplasmic processes only one and a half turns around the axon and fail to lay down myelin (Topilko et al. 1994). The Schwann cells express the early myelin marker, myelin associated glycoprotein (MAG), but not later myelin gene products including myelin protein zero (MPZ). *Egr2* is therefore likely to control a set of genes necessary for the completion of myelination. Its loss produces a more profound structural deficit than the PMP22 related disorders investigated in this present study. However the stage of arrest with the margins of the Schwann cell just overlapping around the axons is almost identical to that observed in the C22 mice with overexpression of PMP22. This suggests that egr2 and PMP22 are involved in a very similar stage of Schwann cell differentiation.

From the present results, the increased Schwann cell numbers found in adult *Tr*^{J} heterozygote and C22 animals appear to arise mainly from a failure in the normal maturational decrease in density per unit length (or cross sectional area) of nerve related to the cessation of mitosis after myelination and the progressive increase in Schwann cell length during development. This differs from the situation seen in the *Tr* mutant where Schwann cell numbers increase steadily with age and are associated with ongoing demyelination (Perkins et al. 1981). The absence of continuous Schwann cell proliferation suggests that C22 and *Tr*^{J} mutants are primarily dysmyelinating and not demyelinating. If demyelination subsequently takes place in the animals we have studied this would be expected to result in Schwann cell proliferation. Schwann cell proliferation usually preceeds the onset of myelination and the protracted length of the myelination period, during which elongation of nerves related to increase in limb length will have occurred, may result in the increase in Schwann cell number seen in *Tr*^{J} heterozygote and C22 transgenic animals between P4 and P12. An increase in Schwann cell number was also seen in the krox-20 mutant mice, again showing the similarities of these 2 models.

The transgenic PMP22 mice were developed in a endeavour to replicate the human disease, CMT1A, which is most commonly the result of the possession of an extra copy of the *PMP22* gene because of a segmental duplication on chromosome 17p11.2. It is evident from the present study and our previous observations (Huxley et al. 1998) that the morphological changes that are found resemble more

closely those in the *Tr*^{J} mouse than the human disorder. As already discussed, CMT1A related to a chromosome 17p11.2 duplication is probably the result of overexpression of the *PMP22* gene (Vallat et al. 1996). The transgenes may however be exerting a dominant negative effect, possibly because they are of human origin. The effect of introducing additional copies of the murine *pmp22* gene into the genome will therefore be of interest.

ACKNOWLEDGEMENTS

The authors are grateful to Action Research for financial support and to the Wellcome trust for a grant to enable the establishment of the Trembler-J mouse colony.

REFERENCES

BOLIN LM, MCNEIL T, LUCIAN LA, DEVAUX B, FRANZ-BACON K, GORMAN DM et al. (1997) HNMP-1: A novel hematopoietic and neural membrane protein differentially regulated in neural development and injury. *Journal of Neuroscience* **17**, 5493–5502.

BOSSE F, ZOIDL G, WILMS S, GILLEN CP, KUHN HG, MÜLLER HW (1994) Differential expression of two mRNA species indicates a dual function of peripheral myelin protein PMP22 in cell growth and myelination. *Journal of Neuroscience Research* **37**, 529–537.

CHANCE PF, ALDERSON MK, LEPPIG KA, LENSCH MW, MATSUNAMI N, SMITH B et al. (1993) DNA deletion associated with hereditary neuropathy with liability to pressure palsies. *Cell* **72**, 143–151.

D'URSO D, SCHMALENBACH C, ZOIDL G, PRIOR R, MÜLLER HW (1997) Studies on the effects of altered PMP22 expression during myelination in vitro. *Journal of Neuroscience Research* **48**, 31–42.

DE VRIES GH. (1993). Schwann cell proliferation. In *Peripheral Neuropathy* (ed. Dyck PJ, Thomas PK, Griffin JW, Low PA, Poduslo JF), pp. 290–298. Philadelphia: W. B. Saunders.

GABREËLS-FESTEN AAWM, BOLHUIS PA, HOOGENDIJK JE, VALENTIJN LJ, ESHUIS EJHM, GABREËLS FJM (1995) Charcot-Marie-Tooth disease type 1A: morphological phenotype of the 17p duplication versus PMP22 point mutations. *Acta Neuropathologica* **90**, 645–649.

GABRIEL JM, ERNE B, PAREYSON D, SGHIRLANZONI A, TARONI F, STECK AJ (1997) Gene dosage effects in hereditary peripheral neuropathy-expression of peripheral myelin protein 22 in Charcot-Marie-Tooth disease type 1A and hereditary neuropathy with liability to pressure palsies nerve biopsies. *Neurology* **49**, 1635–1640.

HALL SM, GREGSON, NA (1978) The effect of 5-bromodeoxyuridine on remyelination in the peripheral nervous system of the mouse. *Neuropathology and Applied Neurobiology* **4**, 117–127.

HANEY C, SNIPES GJ, SHOOTER EM, SUTER U, GARCIA CA, GRIFFIN JW et al. (1996) Ultrastructural distribution of PMP22 in Charcot-Marie-Tooth disease type 1A. *Journal of Neuropathology and Experimental Neurology* **55**, 290–299.

HUXLEY C, PASSAGE E, MANSON A, PUTZU G, FIGARELLA-BRANGER D, PELLISSIER JF et al. (1996) Construction of a mouse model of Charcot-Marie-Tooth disease type 1A by pronuclear injection of human YAC DNA. *Human Molecular Genetics* **5**, 563–569.

HUXLEY C, PASSAGE E, ROBERTSON AM, YOUL B, HUSTON S, MANSON A et al. (1998) Correlation between varying levels of PMP22 expression and the degree of demyelination and reduction in nerve conduction velocity in transgenic mice. *Human Molecular Genetics* **7**, 449–458.

JOSEPH LJ, LEBEAU MM, JAMIESON GA, ACHARYA S, SHOWS TB, ROWLEY JD et al. (1988) Molecular-cloning, sequencing, and mapping of EGR2, a human early growth-response gene encoding a protein with 'zinc-binding finger' structure. *Proceedings of the National Academy of Sciences of the USA* **85**, 7164–7168.

KUMAR NM, JARVIS LJ, TENBROEK E, LOUIS CF (1993) Cloning and expression of a major rat lens membrane protein, MP20. *Experimental Eye Research* **56**, 35–43.

LUPSKI JR, DE OCA-LUNA LM, SLAUGENHAUPT S, PENTAO L, GUZZETTA V, TRASK BJ et al. (1991) DNA duplication associated with Charcot-Marie-Tooth disease type 1A. *Cell* **66**, 219–232.

MADRID R, BRADLEY WG (1975) The pathology of neuropathies with focal thickening of the myelin sheath (Tomaculous neuropathy). Studies on the formation of the abnormal myelin sheath. *Journal of the Neurological Sciences* **25**, 415–448.

MAGYAR JP, MARTINI R, RUELICKE T, AGUZZI A, ADLKOFER K, DEMBIC Z et al. (1996) Impaired differentiation of Schwann cells in transgenic mice with increased PMP22 gene dosage. *Journal of Neuroscience* **16**, 5351–5360.

MARVIN KW, FUJIMOTO W, JETTEN AM (1995) Identification and characterisation of a novel squamous cell-associated gene related to PMP22. *Journal of Biological Chemistry* **270**, 28910–28916.

NAEF R, SUTER U (1998) Many facets of the peripheral myelin protein PMP22 in myelination and disease. *Microscopy Research and Technique* **41**, 359–371.

PERKINS CS, AGUAYO AJ, BRAY GM (1981) Schwann cell multiplication in Trembler mice. *Neuropathology and Applied Neurobiology* **7**, 115–126.

RAEYMAEKERS P, TIMMERMAN V, NELIS E, DE JONGHE P, HOOGENDIJK JE (1991) Duplication in chromosome 17p11.2 in Charcot-Marie-Tooth neuropathy type 1a (CMT1a). *Neuromuscular Disorders*. **1**, 93–97.

RAGNEKAR VM, APLIN AC, SUKHATME VP (1990) The serum and TPA responsive promoter and intron-exon structure of EGR2, a human early growth response gene encoding a zinc finger protein. *Nucleic Acids Research* **18**, 2749–2759.

ROBERTSON AM, KING RHM, MUDDLE JR, THOMAS PK (1997) Abnormal Schwann cell/axon interactions in the Trembler-J mouse. *Journal of Anatomy* **190**, 423–432.

SCHENONE A, NOBBIO L, MANDICH P, BELLONE E, ABBRUZZESE M, AYMAR F et al. (1997) Underexpression of messenger RNA for peripheral myelin protein 22 in hereditary neuropathy with liability to pressure palsies. *Neurology* **48**, 445–449.

SERADA M, GRIFFITHS I, PÜHLHOFER HS, STEWART H, ROSSNER MJ, ZIMMERMAN F et al. (1997) A transgenic rat model of Charcot-Marie-Tooth disease. *Neuron* **16**, 1049–1060.

SNIPES GJ, SUTER U, WELCHER AA, SHOOTER EM (1992) Characterization of a novel peripheral nervous system myelin protein (PMP-22/SR13). *Journal of Cell Biology* **117**, 225–238.

SUH J-G, ICHIHARA N, SAIGOH K, NAKABAYASHI O, YAMANISHI T, TANAKA K et al. (1997) An in-frame deletion in peripheral myelin protein-22 gene causes hypomyelination and cell death of the Schwann cells in the new *TREMBLER* mutant mice. *Neuroscience* **79**, 735–744.

SUTER U, MOSKOW J, WELCHER A, SNIPES J, KOSARAS B, SIDMAN R et al. (1992*a*) A leucine to proline mutation in the putative first transmembrane domain of the 22-kDa peripheral myelin protein in the Trembler-J mouse. *Proceedings of the National Academy of Sciences of the USA* **89**, 4382–4386.

SUTER U, WELCHER AA, ÖZCELIK T, SNIPES GJ,

KOSARAS B, FRANCKE U et al. (1992b) *Trembler* mouse carries a point mutation in a myelin gene. *Nature* **356**, 241–244.

SUTER U, SNIPES GJ, SCHOENER-SCOTT R, WELCHER AA, PAREEK S, LUPSKI JR et al. (1994) Regulation of tissue-specific expression of alternative peripheral myelin protein-22 (PMP22) gene transcripts by two promoters. *Journal of Biological Chemistry* **269**, 25795–25808.

TAYLOR V, WELCHER AA, AMGEN EST PROGRAM, SUTER U (1995) Epithelial membrane protein-1, peripheral myelin protein 22, and lens membrane protein 20 define a novel gene family. *Journal of Biological Chemistry* **270**, 28824–28833.

THOMAS PK, MARQUES JR W, DAVIS MB, SWEENEY MG, KING RHM, BRADLEY JL et al. (1997) The phenotypic manifestations of chromosome 17p11.2 duplication. *Brain* **120**, 465–478.

TOPILKO P, SCHNEIDER-MAUNOURY S, LEVI G, BARON-VAN EVERCOOREN A, CHENNOUFI AB, SEITANIDOU T et al. (1994) Krox-20 controls myelination in the peripheral nervous system. *Nature* **371**, 796–799.

TYSON J, MALCOLM S, THOMAS PK, HARDING AE (1996) Deletions of chromosome 17p11.2 in multifocal neuropathies. *Annals of Neurology* **39**, 180–186.

VALENTIJN LJ, BAAS F, WOLTERMAN RA, HOOGENDIJK JE, BOSCH NHA, ZORN I et al. (1992) Identical point mutations of PMP-22 in Trembler-J mouse and Charcot-Marie-Tooth disease type 1A. *Nature Genetics* **2**, 288–291.

VALLAT JM, SINDOU P, PREUX PM, TABARAUD F, MILOR AM, COURATIER P et al. (1996) Ultrastructural PMP22 expression in inherited demyelinating neuropathies. *Annals of Neurology* **39**, 813–817.